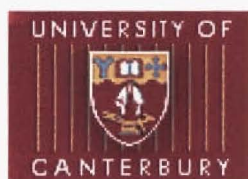


CONFORMATIONALLY RESTRICTED PEPTIDOMIMETICS

A thesis
submitted in partial fulfillment
of the requirements for the Degree
of
Doctor of Philosophy in Chemistry
in the University of Canterbury
by
Barnaby C. H. May



University of Canterbury

2000

QD
431
.M466
2000

CONTENTS

<i>Acknowledgements</i>	<i>i</i>
<i>Abstract</i>	<i>ii</i>
<i>Abbreviations</i>	<i>v</i>
CHAPTER ONE-INTRODUCTION	
1.0. Peptidomimetics	2
1.1. Peptidomimetic Enzyme Inhibitors	3
1.2. Conformational Restriction	4
1.2.1. Modifications of the Peptide Backbone	5
1.2.2. Modifications to Amino Acid Side-Chains	6
1.2.3. Conformationally-Stabilising Rings	7
1.2.4. Macrocyclic Peptidomimetics	7
1.2.5. <i>Cis</i> - Amide Bond Mimics	10
1.2.6. <i>Trans</i> - Amide Bond Mimics	15
1.3. The Tetrazole Ring as a Rigid <i>Cis</i> - Amide Bond Mimic	15
1.4. Work Described in this Thesis	20
1.5. References	23
CHAPTER TWO-DESIGN OF THE TETRAZOLE-BASED ISOSTERES	
2.1. HIV and AIDS	29
2.2. HIV Protease	29
2.3. HIVp Inhibitors	32
2.4. Binding Mode of HIVp Inhibitors	36
2.5. Design Features of the Tetrazole-Based Isosteres	37
2.6. Conclusion	39
2.7. References	41

CHAPTER THREE-SYNTHESIS OF 3-AMINO-2-HYDROXY-4-PHENYLBUTANOIC ACID	
3.1. Introduction	43
3.2. Synthesis by Functionalisation of <i>N-Z-L</i> -Phenylalaninal	48
3.3. Synthesis by Aminohydroxylation of (<i>E</i>)-4-Phenyl-2-butenic Acid Methyl Ester	52
3.4. Synthesis by Enolate Hydroxylation of <i>N-Z-L</i> -Homophenylalanine Methyl Ester	55
3.5. Conclusion	58
3.6. References	60
CHAPTER FOUR-STEREOCHEMICAL ASSIGNMENT OF TETRAZOLE-BASED INHIBITORS	
4.1. Introduction	64
4.2. Synthesis of the Tetrazole-Based Reference Compounds	67
4.3. NMR Studies on the Tetrazole-Based Reference Compounds	77
4.4. Conclusion	84
4.5. References	86
CHAPTER FIVE-SYNTHESIS AND BIOLOGICAL ACTIVITY OF α -METHYLENE TETRAZOLE-BASED INHIBITORS	
5.1. Introduction	89
5.2. Synthesis of the α -Methylene Tetrazole-Based Dipeptide Mimic	90
5.3. Solid-State Structure of the α -Methylene Tetrazole-Based Dipeptide Mimic	92
5.4. Elongation of the α -Methylene Tetrazole-Based Dipeptide Mimic	94
5.5. Biological Activity of the α -Methylene Tetrazole-Based Inhibitors	100
5.6. Conclusion	105
5.7. References	106
CHAPTER SIX-SYNTHESIS OF THE α -KETO TETRAZOLE ISOSTERE	
6.1. Introduction	109

6.2. Functionalisation of Tetrazole-Based Dipeptide Mimics	111
6.3. Synthesis of the α -Keto Tetrazole Isostere by Direct Alkylation of the Tetrazole Heterocycle	118
6.4. Conclusion	127
6.5. References	128
 CHAPTER SEVEN-SOLID STATE STRUCTURES OF TETRAZOLE-BASED DIPEPTIDE MIMICS	
7.1. Introduction	131
7.2. Solid State Structures of 1,5-Disubstituted Tetrazole-Based Dipeptide Mimics	131
7.3. Solid State Structure of 2,5- <i>N-Z-L</i> -Phenylalanine-[COCN ₄]-glycine Benzyl Ester	137
7.4. Conclusion	139
7.5. References	141
 CHAPTER EIGHT-FUTURE WORK	
8.1. HIVp Inhibitors	143
8.2. Targeting Medicinally Important Receptors	144
 CHAPTER NINE-EXPERIMENTAL	
9.1. General Methods and Experimental Procedures	146
9.2. Synthesis of 3-Amino-2-hydroxy-4-phenylbutanoic Acid	
9.2.1. Synthesis by Functionalisation of <i>N-Z-L</i> -Phenylalaninal	151
9.2.2. Preparation of (2 <i>R</i> ,3 <i>S</i>) and (2 <i>S</i> ,3 <i>S</i>)-AHPBA	158
9.2.3 Synthesis by Aminohydroxylation	159
9.2.4. Synthesis by Enolate Hydroxylation	161
9.3. Stereochemical Assignment of Tetrazole-Based Inhibitors	
9.3.1. Synthesis of the <i>L</i> -Alanine Derivatives	167
9.3.2. Synthesis of the <i>D</i> -Alanine Derivatives	171
9.4. Synthesis of α -Methylene Tetrazole-Based Inhibitors	176
9.5. Synthesis of the α -Keto Tetrazole Isostere	

9.5.1. Functionalisation of Tetrazole-Based Dipeptide Mimics	188
9.5.2. Synthesis of the α -Keto Tetrazole Isostere by Direct Alkylation of the Tetrazole Heterocycle	196
9.6. Solid-State Structures of Tetrazole-Based Dipeptide Mimics	204
9.7. References	206

ACKNOWLEDGEMENTS

Thank you to Associate Professor Andrew Abell and the Peptidomimetic Group, past and present members, for their support, supervision and encouragement. Thank you to Bruce Clark for mass spectroscopy, Professor Ward Robinson and Dr. Peter Steel for X-ray crystallographic determinations. Thank you to the workshop, stores, glassblowing and electrical technicians for their patience and assistance.

Thank you to my parents, Helen and Mike May, and siblings, Joe and Emily, who made this thesis possible through their love and support. Thank you to my friends who have helped me through the years with kind words and social reflection.

ABSTRACT

Peptidomimetic compounds are becoming increasingly important as medicinal agents. This thesis describes the design and synthesis of a novel class of non-hydrolysable peptidomimetic isosteres, the tetrazole-based amide bond isosteres. These new structural mimics have been developed for incorporation into enzyme inhibitors and biological probes where a non-hydrolysable *cis*-amide bond mimic is required.

Chapter one provides a general outline of conformational restriction and how this concept has been advantageously applied to the design of bioactive peptidomimetics. Conformational restriction, when used to pre-organise peptidomimetic ligands into a desired bioactive conformation, gives ligands that bind to target receptors with a greater affinity. The tetrazole heterocycle has obvious structural similarities to the *cis*-conformation of the amide bond and has been used to lock amide bonds in an equivalent conformation. Hence, the 1,5-disubstituted tetrazole ring is a popular constrained, planar *cis*-amide bond mimic and its use as such is reviewed in chapter one.

Chapter two outlines the design of the tetrazole-based isosteres, the α -methylene tetrazole (2.5.1),[†] α -hydroxymethylene tetrazole (2.5.2), and α -keto tetrazole isostere (2.5.3). The tetrazole-based isosteres incorporate the design features of a non-hydrolysable amide bond isostere and the conformational restriction of the 1,5-disubstituted tetrazole ring, to generate the first examples of non-hydrolysable tetrazole-based *cis*-amide bond mimics.

Chapter three reviews the synthesis of *N*-Z-(2*RS*,3*S*)-3-amino-2-hydroxy-4-phenylbutanoic acid [*N*-Z-AHPBA, 3.1.1], a key amide bond isostere used in potent protease inhibitors and a synthetic building block of the α -hydroxymethylene tetrazole isostere (2.5.2). We have investigated the synthesis of 3.1.1 by functionalisation of *N*-Z-*L*-phenylalaninal, 3.2.3. Due to shortcomings in this published procedure we have developed a new, generally applicable synthesis of this important amide bond isostere by

[†] Compound numbering is based on chapter number, eg. 2.5.1 represents compound 1 of Chapter 2.5.

hydroxylation of an enolate derived from methyl (3*S*)-*N*-Z-3-amino-4-phenylbutanoate (3.4.2) with the oxodiperoxymolybdenum (pyridine) (hexamethyl phosphoric triamide) complex (MoOPH).

Chapter four describes the synthesis and spectral analysis of diastereomeric tetrazole-based compounds. We have synthesised two series of α -methylene tetrazole-based compounds, 4.1.4a-4.1.7a and 4.1.4b-4.1.7b, derived from *L*-alanine and *D*-alanine, respectively. We have used this analysis to establish trends in the ^1H and ^{13}C NMR of the diastereomeric series as an aid to the assignment of configuration of tetrazole-based ligands. We have also been able to monitor epimerisation of the C6 stereocentre adjacent to the tetrazole by ^1H NMR under the conditions of peptide coupling.

Chapter five outlines the synthesis of (2*S*)-1-(benzyl ethanoate)-5-[2-(*N*-benzyloxycarbonylamino)-3-phenylpropane]-tetrazole,[†] 5.2.1, an α -methylene tetrazole-based dipeptide mimic. We have incorporated 5.2.1 into extended substrate sequences of HIVp and tested these compounds for *in vitro* activity against HIVp. The modestly potent HIVp inhibitors 5.4.1, 5.4.2, and 5.4.3 represent a step-wise elongation of the *C*-terminal, and gave IC₅₀ values against HIVp of 94 μM , 47 μM and 18 μM , respectively.

Chapter six describes the synthesis of the α -keto tetrazole isostere, 2.5.3, by direct alkylation of (1*RS*,2*S*)-5-[2-(*N*-*tert*-butyloxycarbonylamino)-1-hydroxyl-3-phenylpropane]-1*H*-tetrazole, 6.3.13, with benzyl bromoacetate, followed by a TEMPO oxidation. The desired 1,5-disubstituted dipeptide mimic, (2*S*)-1-(benzyl ethanoate)-5-[2-(*N*-*tert*-butyloxycarbonylamino)-1-oxo-3-phenylpropane]-tetrazole, 6.3.16, was isolated from the 2,5-disubstituted dipeptide mimic, (2*S*)-2-(benzyl ethanoate)-5-[2-(*N*-*tert*-butyloxycarbonylamino)-1-oxo-3-phenylpropane]-tetrazole, 6.3.17. This outlines a new and generally applicable synthesis of the tetrazole-based isosteres.

Chapter seven describes the solid state structures of three tetrazole-based dipeptide mimics. The α -methylene tetrazole based isostere has been observed in the X-ray structure of the dipeptide mimic, (2*S*)-1-(benzyl ethanoate)-5-[2-(*N*-

[†] Naming of tetrazole-based compounds is non-IUPAC and follows Zabrocki *et al.* *J. Am. Chem. Soc.* **1988**, *110*, 5875.

benzyloxycarbonylamino)-3-phenylpropane]-tetrazole 5.2.1, and the cyclic tetrazolodiazepine analogue, *cyclo*-{[(2*S*)-5-(2-amino-3-phenylpropane)-1-ethanamide]tetrazole}, 7.2.1. These are the first examples of the solid state structure of the α -methylene tetrazole isostere. We have also observed the solid state structure of the 2,5-disubstituted tetrazole, (2*S*)-2-(Benzyl ethanoate)-5-[2-(*N*-*tert*-butyloxycarbonylamino)-1-oxo-3-phenylpropane]-tetrazole, 6.3.17.

ABBREVIATIONS

aa	amino acid
AA	asymmetric aminohydroxylation
AHPBA	3-amino-2-hydroxy-4-phenylbutanoic acid
Ala	alanine
Asn	asparagine
Bn	benzyl
Boc	<i>tert</i> -butyloxycarbonyl
BOP	benzotriazo-1-yltris(dimethylamino)phosphonium hexafluorophosphate
d	doublet
DCC	dicyclohexylcarbodiimide
DIPEA	<i>N,N</i> -diisopropyl- <i>N</i> -ethylamine
DMF	<i>N,N</i> -dimethylformamide
EDCI	1-(3-dimethylaminopropyl)-3-ethylcarbodiimide hydrochloride
ee	enantiomeric excess
EI MS	electron impact mass spectroscopy
eq.	equivalents
ES MS	electrospray mass spectroscopy
FAB MS	fast atom bombardment mass spectroscopy
Fmoc	(9 <i>H</i>)-fluorenylmethyloxycarbonyl
Gly	glycine
HIV	Human Immunodeficiency Virus
HIVp	HIV protease
h	hours
HOBt	<i>N</i> -hydroxybenzotriazole
hPhe	homophenylalanine (3-amino-4-phenylbutanoic acid)
HPLC	high pressure liquid chromatography
Ile	isoleucine
KHMDS	potassium hexamethyldisilazide
LiHMDS	lithium hexamethyldisilazide
m	multiplet
min	minutes
MoOPH	oxodiperoxymolybdenum(pyridine)(hexamethylphosphoric triamide)
NaHMDS	sodium hexamethyldisilazide
Pg	protecting group
Phe	phenylalanine

PLC	plate layer chromatography
q	quartet
QC	2-quinolinylcarbonyl
rt	room temperature
s	singlet
THF	tetrahydrofuran
TLC	thin layer chromatography
Ts	tosyl
Val	valine
Z	benzyloxycarbonyl

CHAPTER ONE
INTRODUCTION

1.0 PEPTIDOMIMETICS

A peptidomimetic is a compound that incorporates secondary structural features analogous to a naturally occurring peptide, thus enabling it to mimic the biological function of the parent peptide.^{1,2,3,4} Peptidomimetics have become increasingly important in the development of therapeutic agents due to their ability to resist enzymatic degradation and hydrolysis,⁵ while displaying enhanced bioavailability and bioselectivity. The advantageous therapeutic profile of peptidomimetic compounds has made this class of compounds an attractive synthetic target and encouraged their isolation as natural products.⁶

Modern advances in the development of peptidomimetics as medicinal agents, and as biological probes, have been attributed primarily to the development of two key areas of modern drug discovery. First, the synthetic technology that is combinatorial chemistry,⁷ which allows the generation of vast libraries of organic compounds, in conjunction with the hardware for mass screening of these libraries to identify new lead compounds.⁸ The advent of solid phase organic chemistry has been critical to the preparation of these compound libraries, which range from those purely peptidic in nature to libraries of non-peptidic mimetics. The activity of lead compounds, identified through mass-screening, can in turn be optimised by structural and functional variation of the original peptidomimetic platform. Mass screening can also be used to identify lead compounds derived from libraries of natural products, which in turn can undergo refinement through investigation of the structure-activity relationship.

The second key development in the rise in popularity of peptidomimetic agents has been the development of modern chemical tools that allow the structural biologist to 'visualise' target receptors and native peptides. With this technology comes an understanding of the topochemical, conformational, and electronic properties of native peptide ligands, or correspondingly, the receptors. By combining modern nuclear magnetic resonance (NMR) spectroscopy, computer modelling and the data from X-ray structural analysis of peptides it has become possible to design tailor-made peptidomimetic compounds.

The pharmacophore* which can be obtained with this technology is considered to be a 'blue-print' for biological activity against the target receptor. The pharmacophore maps the structural and functional requirements that are necessary for favourable interactions to occur between the peptidomimetic compound and the target receptor. If a peptidomimetic compound can match this blue-print then there is a high chance that it will be able to displace the native peptide from the receptor. Armed with this information, the synthetic chemist can undertake a *rational-based* approach to the design and synthesis of peptidomimetic compounds which take into account the steric and functional requirements for interaction with the target receptor. Compound libraries are often analysed at this stage *in compuo* for compounds which match the requirements of a derived pharmacophore, thus reducing synthetic expenditure.

A large number of peptidomimetic compounds have proven to be successful as therapeutic agents, or have been utilised as probes to determine the structure or biological function of receptors and proteins.

1.1. PEPTIDOMIMETIC ENZYME INHIBITORS

Enzymes catalyse molecular transformations in many physiological processes. It is possible, in some instances, to block or inhibit the action of the enzyme, so that it is unable to perform its usual physiological role. This concept has been utilised in the development of medicinal agents. Drugs which inhibit an enzyme are used to treat disease where the catalytic action of a specific enzyme leads to the diseased state.

The native enzyme substrate is a rational starting point in inhibitor design, as its structural and electronic features specify structural requirements of target peptidomimetic inhibitors. The native substrate generally has high specificity and affinity for an enzyme and as such it can be used as a pharmacophore for inhibitor design. Many naturally occurring enzyme inhibitors are peptidic in nature. Unfortunately, peptides themselves make poor enzyme inhibitors due to their low metabolic stability and poor bioavailability.

* A pharmacophore maps the structural and electronic features of a bioactive compound.

Peptides are susceptible to enzymatic hydrolysis in the gastrointestinal tract and serum and are rapidly excreted through the liver and kidneys. Due to their relatively high molecular mass and lack of specific transport system they are not readily absorbed after oral ingestion.

A logical extension in rational drug design is to convert the three dimensional structural information contained in a native peptide substrate into a smaller non-peptidic compound. Such peptidomimetic compounds would be expected to retain the favourable selectivity of the native peptide whilst showing improved pharmacological properties. Researchers have successfully designed potent peptidomimetic enzyme inhibitors using this idea in conjunction with structural information regarding enzyme topography. There is an increasing number of peptidomimetic inhibitors being presented in current literature that contain one or more of the conformationally restricting motifs discussed in the next section. Conformational constraint is used in the pre-organisation of inhibitor peptidomimetics into bioactive conformations. This technique has been proven to give potent, selective, and proteolytically stable enzyme inhibitors.

1.2. CONFORMATIONAL RESTRICTION

A stretched out or randomly orientated protein is generally devoid of biological activity. Protein function is achieved through the spatial arrangement of the peptide backbone, which in turn is defined by the amino acid sequence. *Conformation defines biological activity*. This highlights an important concept applicable to peptidomimetic research. Enhanced biological activity can be achieved by mimicking the biologically active conformation of the native substrate. Additional structural elements can be incorporated into peptidomimetic design to force rigidity and achieve the desired bioactive conformation. These rigid structural features ensure the correct positioning of specific functionalities in order to optimise hydrogen bonding, electrostatic and hydrophobic interactions between the peptidomimetic ligand and the receptor.

To this effect, peptidomimetic ligands can be designed to be *preorganised* into a bioactive conformation by the inclusion of rigid structural elements. Rigid peptidomimetic analogues pay a lower entropy cost upon binding to the target receptor,

and therefore should bind more avidly, assuming a preorganised placement of pharmacophoric residues.

What follows is a discussion of some of the design strategies employed to force rigidity in peptidomimetic compounds.

1.2.1. MODIFICATIONS OF THE PEPTIDE BACKBONE

Modification of the peptide backbone refers to the generally isosteric[†] or isoelectronic exchange of units in the peptide chain, and the introduction of additional fragments. Some of the more general replacements are outlined on Table 1.2.1.1.

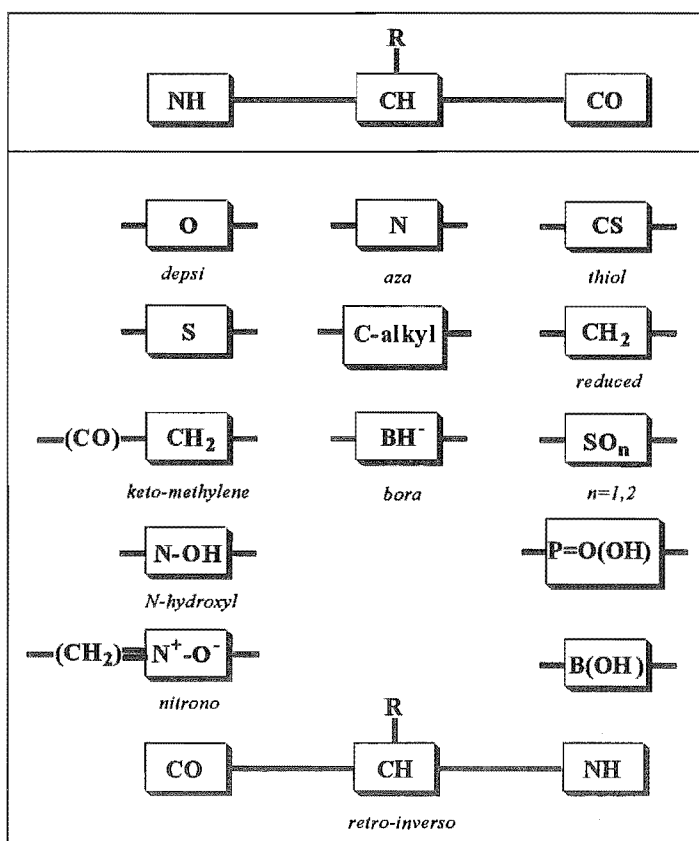
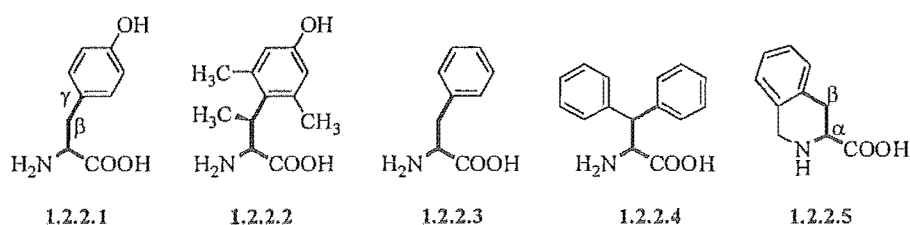


Table 1.2.1.1. General modifications to the peptide backbone

Conformational restriction is imparted from these modifications by electronic and steric effects of the backbone replacements. Backbone modifications lower the peptide character of the ligand, thereby increasing proteolytic stability, whilst retaining favourable properties of the parent peptide.

1.2.2. MODIFICATIONS TO AMINO ACID SIDE-CHAINS

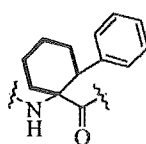
A well established method of incorporating conformational restriction into peptidomimetics is through the modification of naturally occurring amino acid side chains. Conformational restriction is possible by introducing sterically demanding groups so as to limit free rotation of the amino acid residue. Modification of the tyrosine, **1.2.2.1**, side chain by introducing methyl groups in the 2',6', and β -positions hinders free rotation about the $C^\beta-C^\gamma$ bond restricting the analogue, **1.2.2.2**, to a preferred conformation.⁹ Phenylalanine (**1.2.2.3**) derivative, **1.2.2.4**, has been incorporated into potent peptidomimetic ligands of the angiotension II receptor as a constrained phenylalanine mimic.¹⁰ Compound **1.2.2.5** is a phenylalanine analogue that is conformationally constrained, so that the dihedral angle about the $C^\alpha-C^\beta$ bond has a very narrow range. This unnatural amino acid, **1.2.2.5**, has been incorporated into various opioid antagonists.¹¹



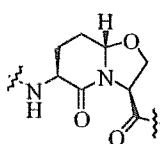
[†] Used to compare structural elements of a similar volume.

1.2.3. CONFORMATIONALLY-STABILISING RINGS

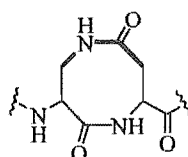
The conformation of ligands can be fixed by the introduction of short and long-range cyclisations within the peptidomimetic backbone.¹² The bridging can occur within a single amino-acid residue (eg. 1.2.3.1),¹³ or may involve several amino acid residues (eg. 1.2.3.2).¹⁴ In general the bridging unit will link two side chains (eg. 1.2.3.3),¹⁵ or a side chain bridged to the backbone (eg. 1.2.3.4),¹⁶ or between two backbone units (eg. 1.2.3.5).¹⁷



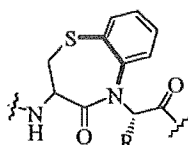
1.2.3.1



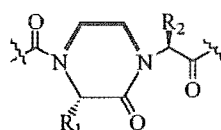
1.2.3.2



1.2.3.3



1.2.3.4

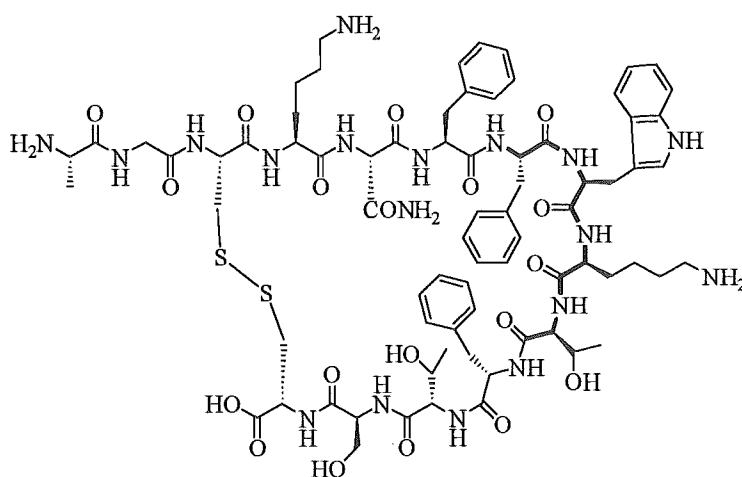
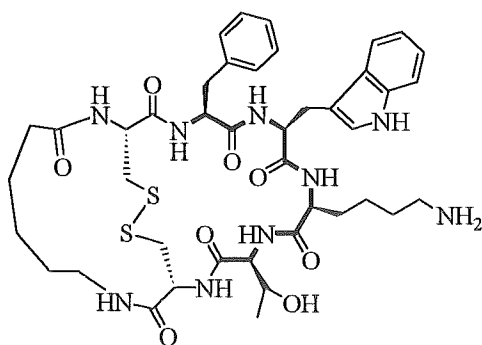


1.2.3.5

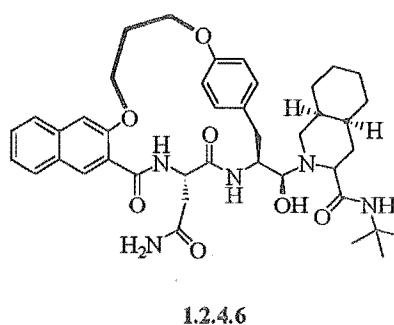
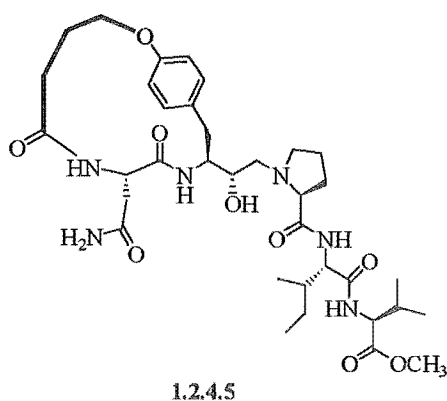
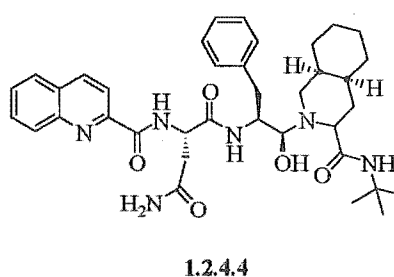
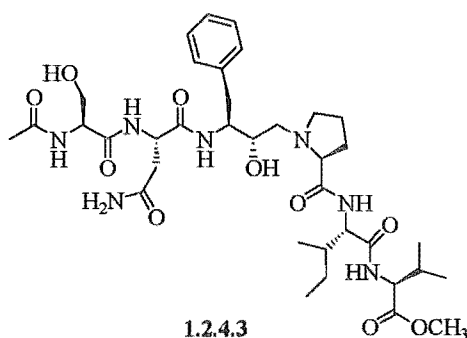
1.2.4. MACROCYCLIC PEPTIDOMIMETICS

Many biologically active macrocyclic peptides are found in nature. Their biological activity, in contrast to their acyclic counterparts, is due in part to the inherent conformational restriction provided by a cyclic system. The relatively restricted conformation of the macrocyclic peptides can offer enhanced binding selectivity with receptors as the availability, and orientation of peptide side-chains is constrained within a macrocyclic ligand. As with all constrained peptidomimetics, the macrocyclic motif offers an entropic advantage over an acyclic peptide, as the bioactive conformation of the constrained peptide is reached from a smaller population of random conformers. Somatostatin (1.2.4.1) is a macrocyclic peptide hormone,¹⁸ formed in the hypothalamus, that regulates the release of growth-hormone. It also acts in the pancreas, preventing the release of glucagon and insulin, leading to a lowering of blood glucose concentrations.

The regulatory action of somatostatin is due to interaction of the macrocyclic loop with a receptor site. Structure-activity studies and conformational probing has led to the rational design and synthesis of a variety of simplified peptidomimetic somatostatin analogues, including **1.2.4.2**,^{18,19,20} which shows similar potency to the parent peptide, **1.2.4.1**. The activity of the mimic is attributed to the conserved cyclic array (shown in bold, **1.2.4.1** and **1.2.4.2**), which forms a peptide recognition epitope, or loop, and leads to receptor recognition.

**1.2.4.1****1.2.4.2**

The notion of macrocyclic peptidomimetic inhibitors has also been successfully applied to the inhibition of HIV protease (HIVp),²¹ a key proteolytic enzyme in the replicative cycle of HIV (see Chapter 2.2). This proteolytic enzyme selectively recognises and cleaves extended substrate conformations. Structural information derived from the X-ray structure of HIVp-inhibitor complexes has enabled researchers to design and synthesise existing HIVp inhibitors that are constrained within a macrocyclic array. HIVp inhibitors 1.2.4.3,²² and 1.2.4.4²³ have been incorporated into cyclic analogues 1.2.4.5 and 1.2.4.6.²⁴ The *N*-terminal macrocycles of these new HIVp inhibitors (shown in bold 1.2.4.5 and 1.2.4.6) were designed to link residues that are spatially close when bound to the active site of HIVp. Researchers have also been able to generate *C*-terminal macrocyclic replacements,²⁵ and bicyclic hexapeptide analogues.²⁶ This has resulted in cyclic arrays that constrain segments of the peptidomimetic inhibitor in a bioactive conformation.



X-ray structure analysis of the macrocyclic inhibitors have shown that their conformation closely mimics that of the HIVp-bound conformation of the extended substrate inhibitors, 1.2.4.3 and 1.2.4.4. This structural mimicry leads to functional mimicry, since it has been shown that the macrocyclic analogues, 1.2.4.5 and 1.2.4.6, are potent inhibitors of HIVp. These compounds have a high binding affinity and an enhanced pharmacological profile in comparison to their acyclic counterparts, 1.2.4.3 and 1.2.4.4. The macrocyclic linkage reduces the susceptibility to proteolytic cleavage and increases the lipophilicity of 1.2.4.5 and 1.2.4.6, thus increasing their antiviral activity *in vivo*.

1.2.5. CIS- AMIDE BOND MIMICS

Pauling L. and Corey R. (1930) did pioneering work with X-ray crystallographic studies on the structure of amino acids and peptides. One of their significant findings was that the peptide unit was planar and rigid, such that the hydrogen of the substituted nitrogen is nearly always *trans*- to the carbonyl oxygen. This has been attributed to the partial double bond character of the amide bond. Delocalisation of the nitrogen electrons limits free rotation about the amide bond, and consequently limits the rate of interconversion between the *cis*- and *trans*- coplanar forms (Figure 1.2.5.1).[†]

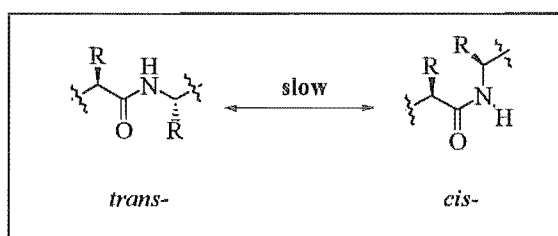


Figure 1.2.5.1. Geometry of the amide bond.

[†] *Cis*- and *trans*- nomenclature reflects the relative conformation of the peptide backbone, where oxygen has no priority.

The conformation of the amide bond is of crucial importance to the binding mode of an extended ligand to a receptor. In a normal amide bond the *trans*- conformation is energetically favoured over the *cis*- conformation by approximately 10 kcal mol^{-1} , due to less steric congestion between adjacent amino acid side chains. Extended peptide ligands are often seen bound to a receptor with a preference for either the *cis*- or *trans*- conformations. In some cases ligand binding will occur with a *cis*- conformation, even though this is energetically disfavoured in the unbound extended conformation.

L-Proline is the most common naturally occurring *N*-alkylated amino acid. The amide bond preceding proline in a linear peptide sequence will adopt a *cis*- conformation in a large number of cases (see Figure 1.2.5.2). As a result, Xaa[§]-*cis*-proline amides are seen in 10-30% of short propyl peptides, while a further 6% of Xaa-proline amide bonds in peptides are known to adopt the *cis*- conformation.²⁷ X-Ray data for a number of proline containing bioactive peptides reveals that the unbound ligands adopt a *cis*- conformation in 10% of examples studied.

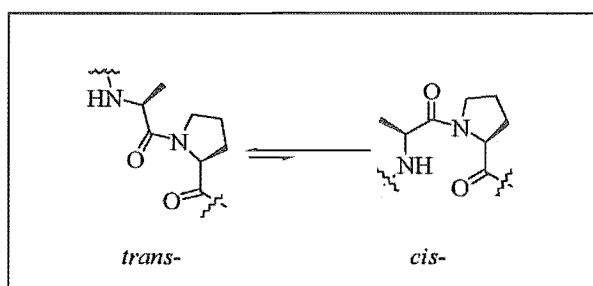
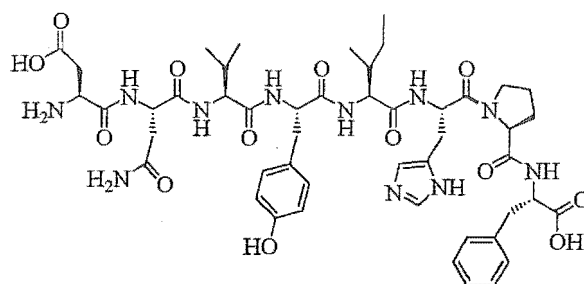


Figure 1.2.5.2. The *cis-trans*- proline equilibrium.

In the angiotension II analogue, 1.2.5.1, *cis-trans*-propyl isomerism has been observed by NMR,²⁸ and the conformational preference for *cis*- or *trans*-proline correlated with biological activity. The result obtained suggest that the peptidomimetic analogue binds in a *cis*-proline conformation to the receptor, and the histidine-*cis*-proline (shown in bold, 1.2.5.1) conformation is responsible for the observed activity.

[§] Where Xaa is any amino acid.



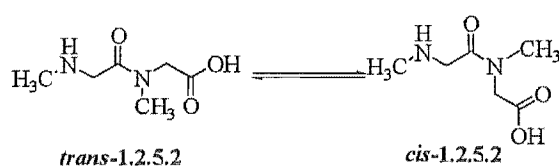
1.2.5.1

On the time scale of protein folding thermal *cis-trans*-propyl interconversion (Figure 1.2.5.2) is slow, leading to slow steps in the protein folding, of propyl peptides. This limits the use of a proline amide as a *cis*- amide bond mimic as it cannot be considered preorganised into the required *cis*- conformation. This fact, and the hydrolytic instability of the proline amide bond, disfavors the use of the proline residue in conformationally restricted peptidomimetics. For the design of constrained ligands and biological probes it is obviously advantageous to have access to *cis*- residue mimics. In response, peptidomimetic chemists have developed a series of *cis*- amide bond surrogates which have been successfully used in this application.

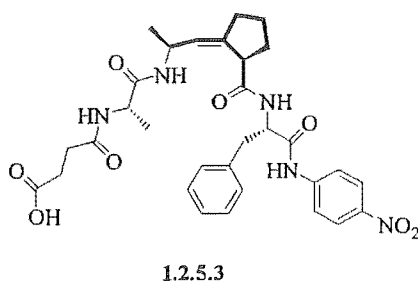
Although a *cis*- olefin would be a logical mimic for the *cis*- amide bond, the synthesis of such dipeptide analogues has proved extremely difficult because of the propensity of the *cis*- β,γ -unsaturated carbonyl system to isomerise to the energetically favoured *trans*- α,β -unsaturated carbonyl system, even under the relatively mild conditions of peptide synthesis.²⁹ Many *cis*- amide bond mimics have been presented in the literature as alternatives to the *cis*-olefin analogue,³⁰ and some of these will be discussed here.

Many *N*-alkylated amides are found in naturally occurring bioactive peptides,⁶ and others have been synthesised as constituents of conformationally constrained peptidomimetics. The energy difference between *cis*- and *trans*- conformations of *N*-alkylated amides is small, as both conformers have similar 1,4-steric interactions. The energetic accessibility of the *cis*- conformation is reflected in the binding modes of many *N*-alkylated peptidomimetics, which have shown a preference for the *cis*- conformation

for recognition and binding to a receptor. *N*-Methylated amino acids are found in naturally occurring bioactive peptidomimetics and many have been shown to bind in a *cis*- conformation. Conformation calculations and NMR studies on the *N*-methylated dipeptide, **1.2.5.2**, revealed that the *cis*- isomer is only 0.6 kcalmol⁻¹ higher in energy than the corresponding *trans*- isomer.³¹ The energetic accessibility of the *cis*- conformation to *N*-alkylated amides has made this conformational constraint a popular *cis*- amide bond mimic.

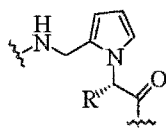


The peptidyl-propyl isomerase inhibitor, **1.2.5.3**, has been synthesised as an aid to understand the mechanistic action of the isomerase enzyme.³² It has been shown from an X-ray structure of the enzyme-ligand complex that the isomerase substrate binds the active site in a *cis*- conformation.³³ A *cis*-alkene proline mimic (**1.2.5.3**, shown in bold) has been developed and subsequently incorporated into an isomerase substrate sequence.

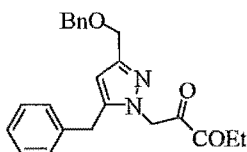


The *cis*- amide bond can also be mimicked by constraining the amide bond within a heterocyclic ring. The synthesis of the 1,2-disubstituted pyrrole-based dipeptide analogue, **1.2.5.4**, has been developed in our laboratories, as a generally applicable *cis*-amide bond surrogate.³⁴ Duncia *et al.* have synthesised trisubstituted pyrazoles (**1.2.5.5**), 1,2,4-triazoles (**1.2.5.6**) as *cis*- amide mimics, and incorporated these into peptidomimetic

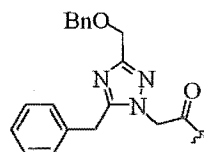
boronate inhibitors of thrombin.³⁵ de Luca *et al.* have prepared 1,3-disubstituted (1.2.5.7) and 1,5-disubstituted (1.2.5.8) pyrazolyl rings as peptidomimetic building blocks.³⁶ The synthesis allows for the regio- and stereoselective synthesis of substituted pyrazoles as analogues of the *cis*- amide bond. Somatostatin (1.2.4.1)¹⁸ analogues have been synthesised with a variety of conformational constraints to force the recognition epitope (see Chapter 1.2.5). The disulphide linked *cis*- amide analogue, 1.2.5.9, was shown to retain high potency.³⁷ van Binst *et al.* prepared the *ortho*-substituted benzene ring (1.2.5.10) to replace the proline-phenylalanine dipeptide in a cyclic somatostatin analogue.³⁸ Branalt *et al.*³⁹ have used a similar *ortho*-substituted benzene as a *cis*- amide mimic in potent HIVp inhibitors. Abell *et al.*⁴⁰ have used the ring closing metathesis reaction⁴¹ to prepare a generally applicable *cis*- phenylalanine analogue, 1.2.5.11. The solid state structure of analogue, 1.2.5.11, revealed that the residue possessed a rigid *cis*- conformation. Another popular *cis*- amide mimic is the *cis*- epoxide, 1.2.5.12. A variety of peptidomimetic examples exist in current literature that have used the *cis*- epoxide to produce *pseudo*-C₂ symmetric,⁴² and asymmetric inhibitors of HIVp.⁴³



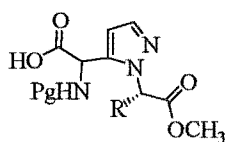
1.2.5.4



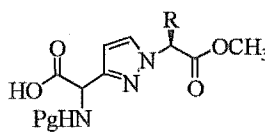
1.2.5.5



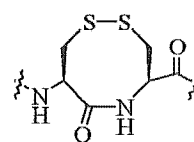
1.2.5.6



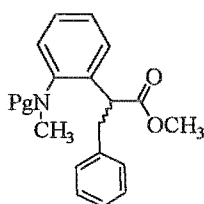
1.2.5.7



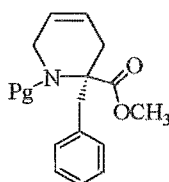
1.2.5.8



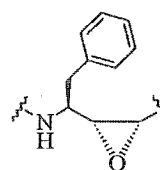
1.2.5.9



1.2.5.10



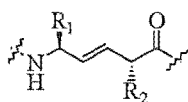
1.2.5.11



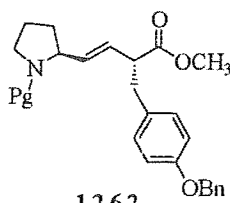
1.2.5.12

1.2.6. TRANS- AMIDE BOND MIMICS

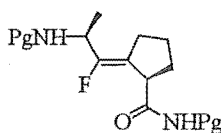
Another important constraint incorporated into peptidomimetics is the *trans*-amide bond mimic. The substitution of a *trans*-amide bond mimic for a dipeptidyl unit in peptidomimetic ligands has produced bioactive compounds that have been used to probe conformational requirements of receptor recognition and binding. The *trans*-double bond isostere, 1.2.6.1, has been used in numerous peptidomimetic ligands.⁴⁴ The similarity of 1.2.6.1 to the *trans*-amide bond was recognised early on in the development of *trans*-amide mimics. A number of novel synthetic procedures have been developed to incorporate side chain residues (R_1 and R_2) into the isostere 1.2.6.1 with stereocontrol.⁴⁵ The *E*-alkene isostere, 1.2.6.1, has been incorporated into the *C*-terminal of the potent neurotensin binder, 1.2.6.2.⁴⁶ The fluorinated analogue of 1.2.6.1 [(*Z*)-fluoro alkene], has been incorporated into the dipeptidyl protease IV inhibitor, 1.2.6.3.^{47,48} A *trans*-alkene proline mimic has been incorporated into the tripeptide mimic, 1.2.6.4, which has shown modest inhibitory activity against the peptidyl-propyl isomerase enzyme.



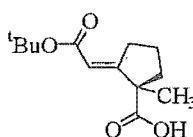
1.2.6.1



1.2.6.2



1.2.6.3

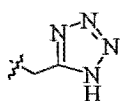


1.2.6.4

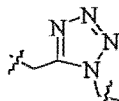
1.3. THE TETRAZOLE RING AS A RIGID CIS- AMIDE BOND MIMIC

There are many examples in the literature of the tetrazole ring being used in medicinal agents.⁴⁹ The tetrazole function is metabolically stable and has an acid strength similar to aliphatic carboxylic acids. This close proximity in acidic character has inspired

the syntheses of the (1*H*)-tetrazole ring, 1.3.1, as a carboxylic mimic in medicinal therapeutics.⁵⁰

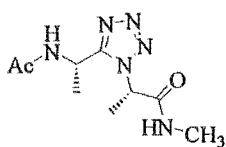


1.3.1

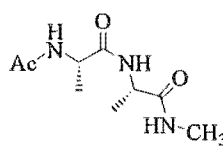


1.3.2

Marshall *et al.*⁵¹ originally proposed the 1,5-disubstituted tetrazole, 1.3.2, as a *cis*-amide bond surrogate to lock a dipeptide analogue in an equivalent conformation. To study the amount of geometric and steric similarity between the 1,5-disubstituted tetrazole ring and the *cis*-amide bond, Marshall *et al.* determined the conformational mimicry index based on solid state structure of 1.3.3.⁵² The conformational mimicry index is a measure of the orientations available to the analogue 1.3.3, which are in turn available to the parent dipeptide, 1.3.4. For the tetrazole surrogate the conformational index is 88%. As the receptor bound conformation of a target peptide is not always known, such statistical arguments for the suitability of analogues are useful. During these studies it was also shown that tetrazole 1.3.3 had more conformational freedom than the parent dipeptide, 1.3.4. This has been attributed to the increased valence angle between the C^α-C=N of the tetrazole compared with the C^α-C=O of the *cis*-amide bond. Marshall *et al.*⁵² concluded that the tetrazole ring is an excellent mimic of the *cis*-amide bond and recognised its potential to probe the binding mode of bioactive ligands.



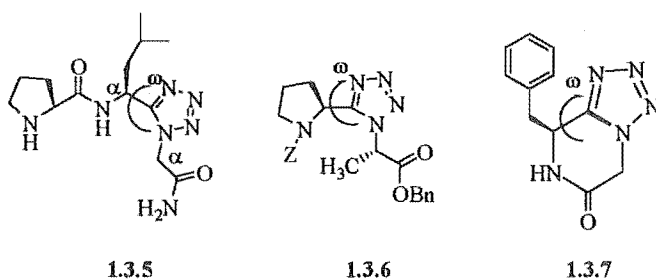
1.3.3



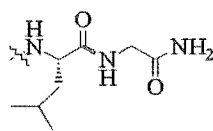
1.3.4

Yu *et al.*⁵³ reported a synthesis of 1,5-disubstituted tetrazoles based on the direct modification of peptide amide bonds with phosphorous pentachloride and hydrazoic acid. Subsequently, Marshall *et al.*^{52,54} reported the stereoselective synthesis of a tetrazole dipeptide mimic by the simple addition of quinoline to the phosphorous pentachloride reaction.

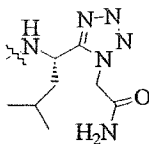
Several tetrazole dipeptide analogues have been synthesised and their solid state structures characterised by X-ray diffraction. All of these show a remarkable resemblance to the *cis*- amide bond in their orientation of the peptide backbone and adjacent amino acid side chains. The tetrazole ring represents a good geometrical mimic, with bond angles and lengths reasonably close to the *cis*- amide conformer. In linear tetrazole dipeptides (eg. 1.3.5 and 1.3.6) the critical C^α---C^α separation between adjacent residues is only 0.3 angstrom greater than that typical of a *cis*- amide bond. This small variation is the result of a larger bond angle at the C^α-C=N bond, itself a consequence of the increased steric bulk of the tetrazole moiety. The tetrazole does not offer the unique arrangement of adjacent hydrogen-donor and acceptor found in the amide bond. However, the tetrazole ring and its 1,5-substituents adopt an essentially planar arrangement, such that the torsion angle, ω , approximates zero in all three solid state examples presented to date (1.3.5⁵⁵ $\omega=7.2^\circ$, 1.3.6⁵⁶ $\omega=4.8^\circ$, 1.3.7⁵² $\omega=2.9^\circ$). The results of these structural determinations illustrate the rigidity of the tetrazole ring when it is incorporated into a peptide backbone. In addition, it is clear that there is a high degree of geometric similarity with linear structures containing the *cis*- amide bond.



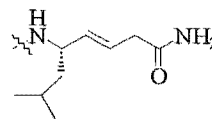
The tetrazole amide surrogate has been incorporated into oxytocin (1.3.8) analogues to replace the leucine-glycine amide bond (shown in bold, 1.3.8).⁵⁷ Analogues were synthesised to determine the favoured binding mode, *cis*- or *trans*-, of the leucine-glycine amide bond to the receptor. A comparison of the biological activity of the tetrazole analogue, 1.3.9, with the corresponding *trans*- olefin analogue, 1.3.10, suggests that the *trans*-leucine-glycine conformation (eg. 1.3.10) is favoured for binding of oxytocin analogues.



1.3.8

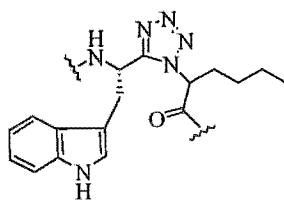


1.3.9

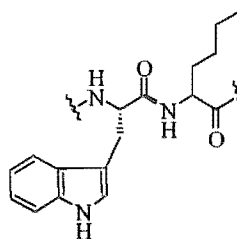


1.3.10

Bradykinin mimics⁵⁸ incorporating a tetrazole constraint are reported to give reduced bioactivity relative to the parent peptide, indicating that the *trans*-amide was the active form or that the steric bulk of the tetrazole ring restricted favourable ligand binding.⁵⁹ Hruby *et al.*^{60,61} synthesised a tetrazole-based mimic, 1.3.11, of a cholecystokinin pentapeptide, 1.3.12, to probe the importance of the conformation at the tryptophan-norleucine amide bond (shown in bond, 1.3.12). It had been suggested that the *cis*-conformation about this amide bond is responsible for conferring high affinity and selectivity against the cholecystokinin receptor. However, the tetrazole analogue, 1.3.11, showed reduced activity relative to the parent peptide.



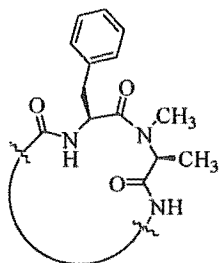
1.3.11



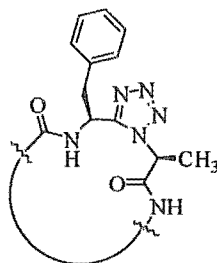
1.3.12

A tetrazole surrogate has also been incorporated into the somatostatin analogue, 1.3.14, as a replacement for the phenylalanine-*N*-methyl-alanine amide bond of the potent somatostatin analogue, 1.3.13.^{62,63} NMR studies showed a close similarity between the conformation of the tetrazole analogue, 1.3.14, and the active somatostatin analogue, 1.3.13. The tetrazole analogue showed slightly reduced biological activity, which led the researchers to conclude that it is the *cis*-amide bond that exists in the biologically active

conformation of the somatostatin analogue, 1.3.13. The slight decrease in activity may represent the increased steric bulk of the tetrazole ring within the active site of the somatostatin receptor.

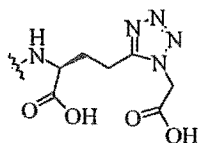


1.3.13

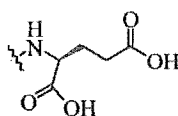


1.3.14

The thymidylate synthase inhibitor, 1.3.15, was synthesised with a tetrazole mimic on the glutamate side chain in an attempt to stabilise the glutamyl bond to enzymatic hydrolysis.⁶⁴ The inhibitory potency of the tetrazole derivative was broadly similar to the parent compound, 1.3.16.



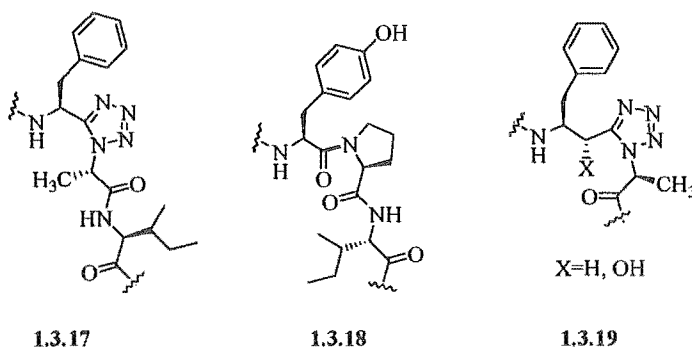
1.3.15



1.3.16

Garofalo *et al.*⁶⁵ incorporated the tetrazole surrogate into 1.3.17, which was derived from the heptapeptide substrate of HIVp, 1.3.18. They were interested in determining whether the *cis*-proline amide bond (shown in bold, 1.3.18), which had been shown to exist in 30% of available conformers of the native substrate, 1.3.18, was important in HIVp recognition. Molecular modeling showed a positive correlation between the *cis*-proline amide bond of 1.3.18, and the tetrazole *cis*-amide mimic, 1.3.17. However, the tetrazole analogue was found not to inhibit HIVp. This may reflect the increased steric bulk of the tetrazole ring which, in turn, may prevent effective binding to the active site of HIVp. Abell *et al.*⁶⁶ have synthesised four conformationally constrained

tetrazole analogues (1.3.19) of the potent HIVp inhibitor (1.2.4.3).²⁰ This early study on tetrazole-based peptidomimetics forms the basis of much of the work presented in this thesis.



The above examples illustrate the general application of the tetrazole ring as a *cis*-amide bond mimic. The ability of the tetrazole ring to spatially mimic the *cis*-amide bond and its metabolic stability have endeared this heterocycle to peptidomimetic research as a rigid, constrained *cis*-amide bond mimic.

1.4. WORK DESCRIBED IN THIS THESIS

Chapter two of this thesis describes the design of the tetrazole-based amide bond isosteres. This novel class of conformationally restricted, non-hydrolysable isosteres has been designed around the bioactive conformation of the potent HIVp inhibitor JG-365, 1.2.4.3. This chapter discusses the specificity and selectivity of the aspartic protease HIVp, and also discusses important structural and electronic features of successful HIVp inhibitors. The novel class of tetrazole-based isosteres, which includes the α -methylene (2.5.1), α -hydroxymethylene (2.5.2), and the α -keto tetrazole (2.5.3), isosteres are the first examples of non-hydrolysable amide bond isosteres to incorporate conformational restriction from a 1,5-disubstituted tetrazole ring.

Chapter three describes the synthesis of *N*-Z-(2*RS*,3*S*)-3-amino-2-hydroxy-4-phenylbutanoic acid, (*N*-Z-AHPBA, 3.1.1) which has been incorporated into numerous protease inhibitors as an amide bond isostere and which is a key synthetic component of the α -hydroxymethylene tetrazole isostere (2.5.2). Different synthetic methodologies

have been investigated for the synthesis of 3.1.1, and a new generally applicable synthetic method has been developed during the course of this investigation.

Chapter four describes an investigation into the configuration of tetrazole-based ligands which have been synthesised to incorporate the α -methylene tetrazole isostere (2.5.1). To aid the stereochemical assignment of tetrazole-based HIVp inhibitors, diastereomeric tetrazole-based ligands have been synthesised and trends established in the ^1H and ^{13}C NMR spectra of the compounds. This work has also allowed us to monitor epimerisation of stereocentres adjacent to the tetrazole heterocycle under the conditions of peptide coupling.

Chapter five describes the synthesis of HIVp inhibitors that contain the α -methylene tetrazole-based isostere, 2.5.1. A step-wise elongation of the C-terminal of a tetrazole-based dipeptide mimic has generated three tetrazole-based HIVp inhibitors of modest potency. We have been able to observe the solid state structure of the α -methylene tetrazole isostere and have compared this to the bioactive conformation of JG-365 (1.3.4.3) which formed the basis of our isostere design. The tetrazole-based inhibitors have also given us insight into the preferential binding mode of the tetrazole-based isostere and the optimisation of inhibitor potency through filling the $\text{S}_3\text{-S}_3'$ subsites of HIVp.

Chapter six describes the synthesis of the α -keto tetrazole isostere, 2.5.3. Two approaches have been taken to the synthesis of this isostere, direct introduction of the α -keto functionality to an appropriate α -methylene tetrazole-based dipeptide mimic and by direct alkylation of a (1*H*)- α -keto tetrazole. Problems encountered with the first approach have led us to develop a more efficient synthesis of tetrazole-based dipeptide mimics and this has been applied to the synthesis of the α -keto tetrazole isostere, 2.5.3.

Chapter seven describes the solid state structures of three tetrazole-based dipeptide mimics. The 1,5-disubstituted tetrazole-based dipeptides, 5.4.1, and the cyclic analogue, 7.2.1, are the first examples of the α -methylene tetrazole isostere for which X-ray structures exist. Compound 7.2.1, belongs to a medically important class of compounds, the tetrazolodiazepines, of which no X-ray structures exist. The third X-ray

structure is of the 2,5-disubstituted tetrazole-based dipeptide, 6.3.17, a regioisomer of the α -keto tetrazole isostere, 2.5.3.

1.5. REFERENCES

- 1 Gante, J. *Angew. Chem. Int. Ed. Engl.* **1994**, *33*, 1699.
- 2 Kahn, M. *Synlett* **1993**, 821.
- 3 Olsen, G. L.; Bolin, D. R.; Bonner, M. P.; Bos, M.; Cook, C. M.; Fry, D. C.; Graves, B. J.; Hatada, M.; Hill, D. E.; Kahn, M.; Madison, V. S.; Rusiecki, V. K.; Sarabu, R.; Sepinwall, J.; Vincent, G. P.; Voss, M. E. *J. Med. Chem.* **1993**, *36*, 3039.
- 4 Giannis, A.; Kolter, T. *Angew. Chem. Int. Ed. Engl.* **1993**, *32*, 1244.
- 5 Goodman, M.; Ro, S. In, *Burgers Medicinal Chemistry and Drug Design*. Eds. Wolff, M. E. Wiley Interscience **1995**, *1*, 803.
- 6 Fusetani, N.; Matsunaga, S. *Chem. Rev.* **1993**, *93*, 1793.
- 7 Dorner, B.; Houghten, R. A.; In, *Advances in Amino Acid Mimics and Peptidomimetics*. Eds. Abell, A. D. JAI Press **1997**, *1*, 109.
- 8 Sweetman, P. M.; Price, C. H.; Ferkany, J. W. In, *Burgers Medicinal Chemistry and Drug Design*. Eds. Wolff, M. E. Wiley Interscience **1995**, *1*, 697.
- 9 Jaio, D.; Russell, K. C.; Hurby, V. J. *Tetrahedron* **1993**, *49*, 3511
- 10 Hsieh, K-H.; La Hann, T. R.; Speth, R. C. *J. Med. Chem.* **1989**, *32*, 898.
- 11 Kazmierski, W.; Hrub, V. J. *Tetrahedron* **1988**, *44*, 697.
- 12 Toniolo, C. *Int. J. Peptide Protein Res.* **1990**, *35*, 287.
- 13 Cativiela, C. C.; Diaz de Villegas, M. D.; Avenoza, A.; Peregrina, J. M. *Tetrahedron* **1993**, *49*, 10987.
- 14 Tamura, S. Y.; Goldman, E. A.; Brunck, T. K.; Ripkah, W. C.; Semple, J. E. *Bioorg. Med. Chem. Lett.* **1997**, *7*, 331.
- 15 Rone, R.; Manesis, N.; Hassan, M.; Goodman, M.; Hagler, D.H.; Kitsen, D. H.; Roberts, V. A. *Tetrahedron* **1988**, *44*, 895.
- 16 Gante, J.; Weitzel, R. *Tetrahedron Lett.* **1988**, *29*, 3853.
- 17 Di Maio, J.; Bellau, B. *J. Chem. Soc. Perkins Trans. 1* **1989**, 1687.
- 18 Burgus, R.; Ling, N.; Butcher, M.; Guillemin, R. *Proc. Natl. Acad. Sci. USA* **1973**, *70*, 684.

- ¹⁹ Veber, D. F.; Holly, F.; Paleveda, W. J.; Nutt, R. F.; Bergstrand, S. J.; Torchiana, M.; Glitzer, M. S.; Saperstein, R.; Hirshmann, R. *Proc. Natl. Acad. Sci. USA* **1978**, *75*, 2636.
- ²⁰ Veber, D. F.; Freidinger, R. M.; Perlow, D. S.; Paleveda, W. J.; Holly, F.; Strachan, R. G.; Nutt, R.; Arison, B. H.; Homnic, C.; Randall, W. C.; Glitzer, M. S.; Saperstein, R.; Hirshmann, R. *Nature* **1981**, *292*, 55.
- ²¹ Kempf, D. J.; Sham, H. L. *Curr. Pharma. Design* **1996**, *2*, 225.
- ²² Swain A. L.; Miller, M. M.; Green, J.; Rich, D. H.; Schneider, J.; Kent, S. B. H.; Wlodawer, A. *J. Med. Chem.* **1990**, *33*, 1285.
- ²³ Roberts, N. A.; Martin, J. A.; Kinchington, D.; Broadhurst, A. V.; Craig, J. C. *Science* **1990**, *248*, 358.
- ²⁴ Reid, R. C.; Fairlie, D. P. In, *Advances in Amino Acid Mimics and Peptidomimetics*. Eds. Abell, A. D. JAI Press: Stamford **1997**, *1*, 77.
- ²⁵ March, D. R.; Abbenante, G.; Bergmann, D. A.; Brinkworth, R. I.; Wickramasinghe, W.; Begun, J.; Martin, J. L.; Fairlie, D. P. *J. Am. Chem. Soc.* **1996**, *118*, 3375.
- ²⁶ Reid, R. C.; March, D. R.; Dooley, M. J.; Bergman, D. A.; Abbenante, G.; Fairlie, D. P. *J. Am. Chem. Soc.* **1996**, *118*, 8511.
- ²⁷ Stewart, D. E.; Sarkar, A.; Wampler, J. E. *J. Mol. Biol.* **1990**, *214*, 2654.
- ²⁸ Liakopoulou-Kyriakides, M.; Glardy, R. E. *Biochemistry* **1975**, *14*, 4953.
- ²⁹ Hann, M. M.; Sammes, P. G.; Kennewell, P. D.; Taylor, J. B. *J. Chem. Soc. Perkin Trans. 1* **1982**, 307.
- ³⁰ Etzkorn, F. A.; Travins, J. M.; Hart, S. A. In, *Advances in Amino Acid Mimics and Peptidomimetics*. Eds. Abell, A. D. JAI Press: Stamford **1999**, *2*, 125.
- ³¹ Howard, J. C.; Momany, F. A.; Andreatta, R. H.; Scheraga, H. A. *Macromolecules* **1973**, *6*, 535.
- ³² Hart, S. A.; Etzkorn, F. A. *J. Org. Chem.* **1999**, *64*, 2998.
- ³³ Ke, H.; Mayrose, D.; Cao, W. *Proc. Natl. Acad. Sci. USA* **1993**, *90*, 3324. Konno, M.; Ito, M.; Hayano, T.; Takahashi, N. *J. Mol. Biol.* **1996**, *256*, 897.
- ³⁴ Abell, A. D.; Hault, D. A.; Jamieson, E. J. *Tetrahedron Lett.* **1992**, *33*, 5831.

- 35 Duncia, J. V.; Santella, J. B.; Higley, C. A.; Van Atten, M. K.; Weber, P. C.; Alexander, R. S.; Kettner, R. A.; Pruitt, J. R.; Liauw, A. Y.; Quan, M. L.; Knabb, R. M.; Wexler, R. R. *Bioorg. Med. Chem. Lett.* **1998**, *154*, 515.
- 36 de Luca, L.; Falorni, M.; Giacomelli, G.; Porcheddu, A. *Tetrahedron Lett.* **1999**, *40*, 8701.
- 37 Brady, S. F.; Paleveda, W. J.; Arison, B. H.; Saperstein, R.; Brady, E. J.; Raynor, K.; Reisine, T.; Veber, D. F.; Freidinger, R. M. *Tetrahedron* **1993**, *49*, 3449.
- 38 vander Elst, P.; van den Berg, E.; Pepermans, H.; vander Auwera, L.; Zeeuws, R.; Tourwe, D.; van Binst, G. *Int. J. Peptide Protein Res.* **1987**, 318. Elseviers, M.; Auwera, V. D.; Pepermans, H.; Tourwe, D.; van Binst, G. *Biochem. Biophys. Res. Commun.* **1988**, *154*, 515. Elst, P. V.; Gondol, D.; Wynants, C.; Tourwe, D.; van Binst, G. *Int. J. Peptide Protein Res.* **1987**, *29*, 331.
- 39 Branalt, J.; Kvarnstrom, I.; Classon, B.; Samuelsson, B.; Nillroth, U.; Danielson, H.; Karlen, A.; Hallberg, A. *Tetrahedron Lett.* **1997**, *38*, 3483.
- 40 Abell, A. D.; Gardiner, J.; Phillips, A. J.; Robinson, W. T. *Tetrahedron Lett.* **1998**, *39*, 9563.
- 41 Miller, S. J.; Blackwell, H. E.; Grubbs, R. H. *J. Am. Chem. Soc.* **1996**, *118*, 9606.
- 42 Park, C.; Koh, J. S.; Son, Y. C.; Choi, H.; Lee, C. S.; Choy, N.; Moon, K. Y.; Jung, W. H.; Kim, S. C.; Yoon, H. *Bioorg. Med. Chem. Lett.* **1995**, *5*, 1843. Abell, A. D.; Hoult, D. A.; Bergman, D. A.; Fairlie, D. P. *Bioorg. Med. Chem. Lett.* **1997**, *7*, 2853.
- 43 Grant, S. K.; Moore, M. L.; Fakhoury, S. A.; Tomaszek, T. A.; Meek, T. D. *Bioorg. Med. Chem. Lett.* **1992**, *2*, 1441. Lee, C. S.; Choy, N.; Park, C.; Choi, H.; Son, Y. C.; Kim, S.; Ok, J. H.; Yoon, H.; Kim, S. C. *Bioorg. Med. Chem. Lett.* **1996**, *6*, 589.
- 44 Hann, M. M.; Sammes, P. G.; Kennewell, P. D.; Taylor, J. B. *J. Chem. Soc. Chem. Commun.* **1980**, 234. Cox, M. T.; Heaton, D. W.; Horbury, J. *J. Chem. Soc. Chem. Commun.* **1980**, 799. Cox, M. T.; Cormey, J. J.; Hayward, C. F.; Petter, N. *J. Chem. Soc. Chem. Commun.* **1980**, 800. Bol, K.; Liskamp, R. M. J. *Tetrahedron* **1992**, *48*, 6425.

- 45 Spaltenstein, A.; Carpino, P. A.; Mikaye, F.; Hopkins, P. B. *Tetrahedron Lett.* **1986**, *27*, 2095. Kempf, D. J.; Wang, X. C.; Spanton, S. G. *Int. J. Peptide Protein Res.* **1991**, *38*, 237. Fujii, N.; Habashita, H.; Shigemori, N.; Otaka, A.; Ibuka, T.; Tanaka, M.; Yamamoto, Y. *Tetrahedron Lett.* **1991**, *32*, 4969. Ibuka, T.; Habashita, H.; Otaka, A.; Fujii, N.; Oguchi, T.; Uyehara, T.; Yamamoto, Y. *J. Org. Chem.* **1991**, *56*, 4370. Ikuda, T.; Habashita, H.; Funakoshi, S.; Fujii, N.; Oguchi, Y.; Uyehara, T.; Yamamoto, Y. *Angew. Chem. Int. Ed. Engl.* **1990**, *29*, 801.
- 46 Christos, T. E.; Arvanitis, A.; Cain, G. A.; Johnson, A. L.; Pottorf, R. S.; Tam, S. W.; Schmidt, W. K. *Bioorg. Med. Chem. Lett.* **1993**, *3*, 1035.
- 47 Lin, J.; Toxcano, P. J.; Welsh, J. T. *Proc. Natl. Acad. Sci. USA* **1998**, *95*, 14020.
- 48 Welsh, J. T.; Lin, J. *Tetrahedron* **1996**, *52*, 291.
- 49 Sigh, H.; Chawla, A. S.; Kapoor, V. K.; Paul, D.; Malhotra, R. K. *Pro. Med. Chem.* **1980**, *17*. Wittenberger, S. *J. Org. Prep. Proced. Int.* **1994**, *26*, 499.
- 50 Butler, R. N. *Adv. Heterocycl. Chem.* **1977**, *21*, 323.
- 51 Marshall, G. R.; Humblet, C.; van Opdenbosch, N.; Zabrocki, J. In, *Peptides: Synthesis, Structure, Function; Proceedings of the Seventh American Peptide Symposium*. Eds. Rich, D. H.; Gross, E. Pierce Chemical: Rockford Il, **1981**, 669.
- 52 Zabrocki, J.; Smith, G. D.; Dunbar, J. B.; Iijima, H.; Marsahll, G. R. *J. Am. Chem. Soc.* **1988**, *110*, 5875.
- 53 Yu, K-L.; Johnson, R. L. *J. Org. Chem.* **1987**, *52*, 2051.
- 54 Marshall, G. R. In, *The Chemical Regulation of Biological Mechanisms*. Eds. Creighton, A. M.; Turner, S. The Royal Society of Chemistry, Burlington House: London **1982**, 279.
- 55 Valle, G.; Crisma, M.; Yu, K-L.; Toniolo, C.; Misha, R. K.; Johnson, R. L. *Coll. Czech. Chem. Commun.* **1988**, *53*, 2863.
- 56 Smith, G. D.; Zabrocki, J.; Flak, T. A.; Marshall, G. R. *Int. J. Peptide Protein Res.* **1991**, *37*, 191.
- 57 Lebl, M.; Slaninova, J.; Johnson, R. L. *Int. J. Peptide Protein Res.* **1989**, *33*, 16.

- ⁵⁸ Zabrocki, J.; Dunbar, J. B.; Marshall, K. W.; Toth, M. V.; Marshall, G. R. *J. Org. Chem.* **1992**, *57*, 202.
- ⁵⁹ London, R. E.; Stewart, J. M.; Williams, R.; Cann, J. R. *J. Am. Chem. Soc.* **1979**, *101*, 2455.
- ⁶⁰ Boteju, L.; Hruby, V. J. *Tetrahedron Lett.* **1993**, *34*, 1757.
- ⁶¹ Boteju, L. W.; Zalewska, T.; Yamamura, H. I.; Hruby, V. J. *Bioorg. Med. Chem. Lett.* **1993**, *3*, 2011.
- ⁶² Zabrocki, J.; Slomczynska, U.; Marshall, G. R. In, *Peptides: Chemistry and Biology; Proceedings of the 11th American Peptide Symposium*. Eds. Rivier, J. E.; Marshall, G. R. ESCOM: Leiden **1990**, 195.
- ⁶³ Beuson, D. D.; Zabrocki, J.; Slomczynska, U.; Head, R. D.; Kao, J. L-F.; Marshall, G. R. *Biopolymers* **1995**, *36*, 181.
- ⁶⁴ Bavetsias, V.; Bisset, G. M. F.; Kimbell, R.; Boyle, F. T.; Jackman, A. L. *Tetrahedron* **1997**, *53*, 13383.
- ⁶⁵ Garofalo, A.; Tarnus, C.; Remy, J-M.; Leppik, R.; Piriou, F.; Harris, B.; Pelton, J. T. In, *Peptides: Chemistry and Biology; Proceedings of the 11th American Peptide Symposium*. Eds. Rivier, J. E.; Marshall, G. R. ESCOM: Leiden **1990**, 833.
- ⁶⁶ Abell, A. D.; Foulds, G. J. *J. Chem. Soc. Perkins. Trans 1* **1997**, 2475.

CHAPTER TWO
DESIGN OF THE TETRAZOLE-BASED
ISOSTERES

2.1. HIV AND AIDS

Since the onset of the Acquired Immune Deficiency Syndrome (AIDS) epidemic 15 years ago, the causative agent, the Human Immunodeficiency Virus (HIV), has infected more than 47 million people in the world. With more than 2.2 million deaths in 1998, AIDS has now become the fourth leading cause of mortality and its negative impact on global health is set to increase.¹ An enormous amount of research has focused on the development of therapeutic agents to treat HIV. Until recent years AIDS has been an inevitably fatal and incurable disease. The advent of HIV protease inhibitors, administered in combination with the more established HIV reverse transcriptase inhibitors, such as AZT and 3TC, has enabled HIV positive patients to manage their disease. Unfortunately this combination therapy is not a cure, although it has been shown to reduce viral load, an indication of the level of infection to a manageable level.

2.2. HIV PROTEASE

HIV protease (HIVp) is a virally-encoded enzyme necessary for the assembly and maturation of infectious virions.² HIVp is specifically responsible for the post-translational processing of viral polypeptides encoded by the viral *gag* and *pol* genes. Proteolytic cleavage of the polypeptides by HIVp yields protein fragments which are required for structural elements of the infectious virions. Inactivation of HIVp by a single mutation of the catalytic aspartate 25 (Asp25) residue results in non-infectious virions and implicates HIVp as a key enzyme in the replication of HIV.² This observation led researchers to target the inhibition of HIVp as a viable strategy for the treatment of HIV infection.

HIVp belongs to the class of aspartic proteases that includes the well characterised proteolytic enzymes renin and pepsin. Considerable effort has been directed towards developing renin inhibitors as hypertensive drugs, based on knowledge of the catalytic action of aspartic proteases. This collective information proved invaluable in providing an understanding of the catalytic mechanism of HIVp and in the development of early HIVp inhibitors.

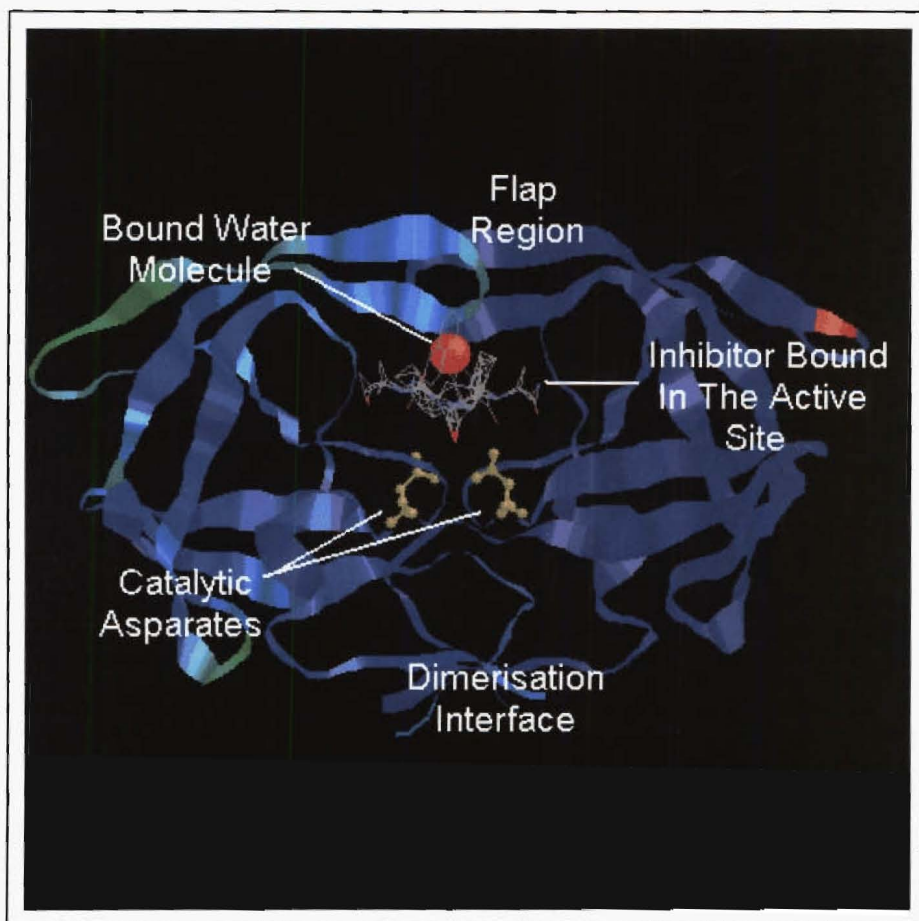


Figure 2.2.1. HIVp complexed with the inhibitor, acetyl pepstatin.

HIVp is an unusual proteolytic enzyme in that it cleaves phenylalanine-proline and tyrosine-proline amide bonds. The amide bonds of proline residues are not usually susceptible to enzymatic hydrolysis by other mammalian endopeptidases. The rational design of HIVp inhibitors has been greatly aided by the availability of solid-state crystal structures of HIVp in its native form,³ and in inhibitor-HIVp complexes (eg. Figure 2.2.1).⁴ These structures reveal that HIVp is a homodimer comprising two identically folded polypeptides of ninety-nine amino acid residues. The monomeric polypeptides interact non-covalently along a dimerisation zone, marked by a C_2 symmetric axis (running through the vertical plane as shown in Figure 2.2.1). Two conformationally

flexible flaps are able to close around the substrate and 'lock' the substrate in the hydrophobic binding cleft.

Two key catalytic aspartate residues (Asp 25) are centered at the base of a cylindrical substrate binding cleft (Figure 2.2.1). One residue acts as a base (Figure 2.2.2), initiating nucleophilic attack on the scissile amide bond of the substrate by a bound water molecule (see Figure 2.2.1). The other aspartate residue acts as an acid, stabilising the carbonyl oxygen of the tetrahedral intermediate (Figure 2.2.2).

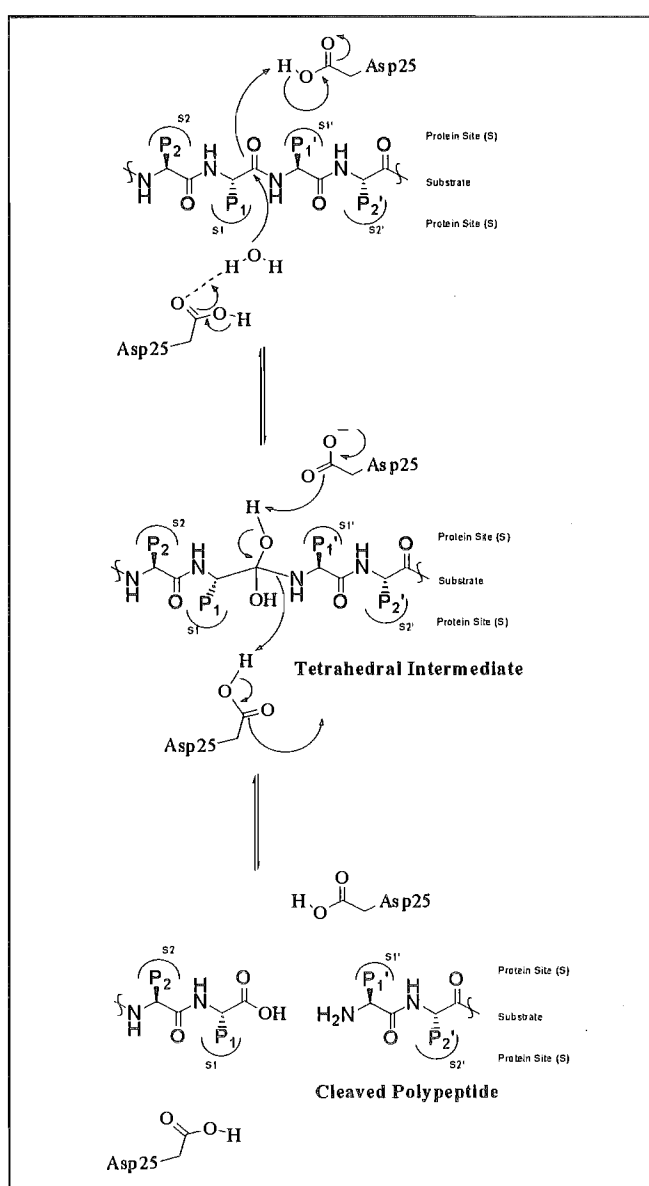


Figure 2.2.2. Amide bond hydrolysis by the proteolytic enzyme, HIVp.

2.3. HIVP INHIBITORS

To date the U.S. Food and Drug Administration (FDA) has approved four HIVp inhibitors for clinical use (Figure 2.3.1). The number of available HIVp inhibitors is set to grow in an effort to offset viral resistance and a need to provide a more comprehensive array of inhibitors for combination therapy.

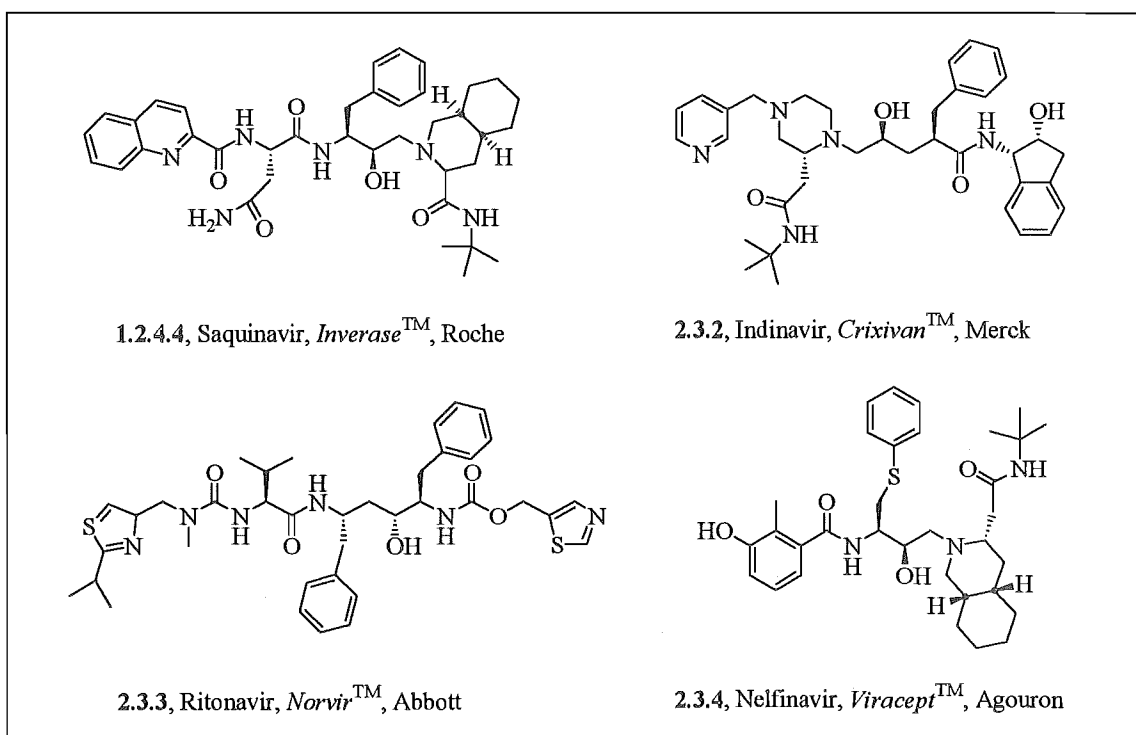
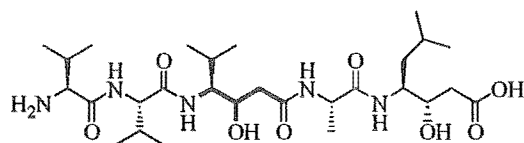


Figure 2.3.1. FDA approved HIVp inhibitors.

An examination of the clinically available HIVp inhibitors (Figure 2.3.1) reveals some common design features which have been refined in the development of these potent HIVp inhibitors. A classic strategy in the design of peptidomimetic protease inhibitors is the incorporation of a non-hydrolysable amide bond isostere into the natural enzyme substrate at the P₁-P₁' (notation of Schechter⁵) cleavage site. The idea of using such isosteres was developed from the naturally occurring peptidomimetic compound pepstatin (2.3.5), a potent mechanism-based inhibitor of aspartic protease.⁶ Pepstatin contains the amide bond isostere, statine (shown in bold 2.3.5), which mimics the *sp*³

hydroxymethylene tetrahedral intermediate formed during normal amide bond hydrolysis (see Figure 2.2.2).



2.3.5

It is now well established that enzymes bind more favorably to ligands resembling the tetrahedral intermediate of an enzyme catalysed reaction than to ligands resembling the substrate.² The application of tetrahedral intermediate mimicry has been used in the design of approved HIVp inhibitors by the incorporation of the hydroxymethylene isostere between the P₁-P₁' residues (Figure 2.3.1).² A variety of isosteric replacements have been presented in the literature (Figure 2.3.2) and incorporated into HIVp inhibitors of varying potency.

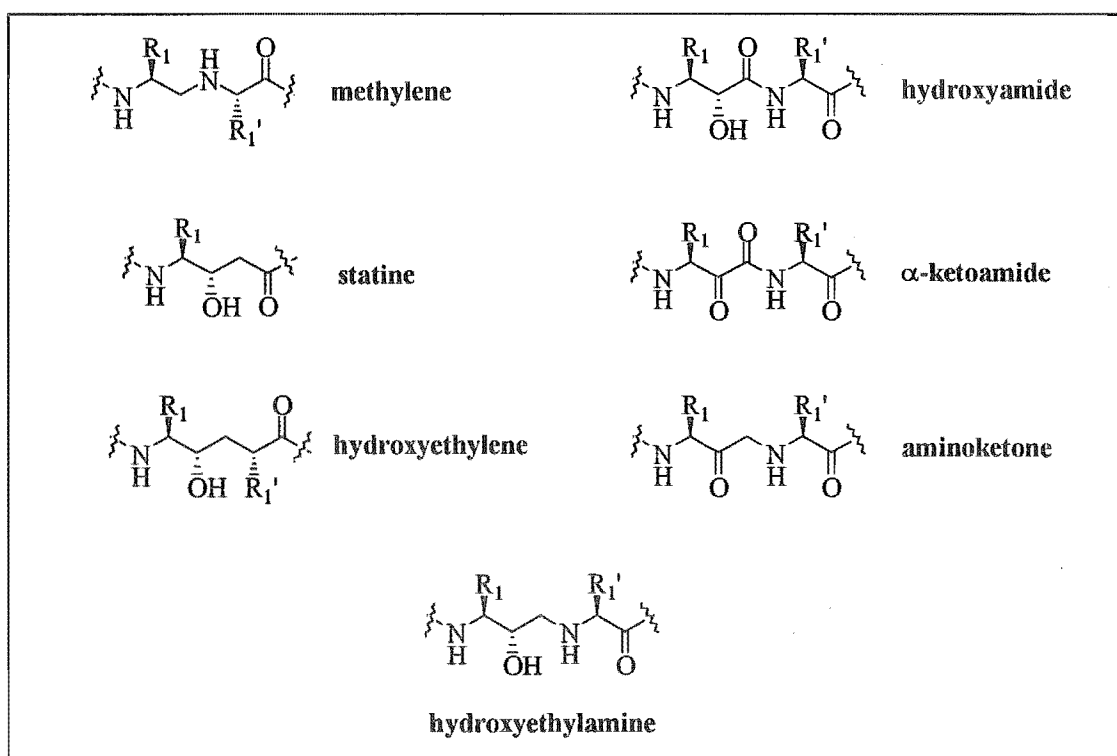
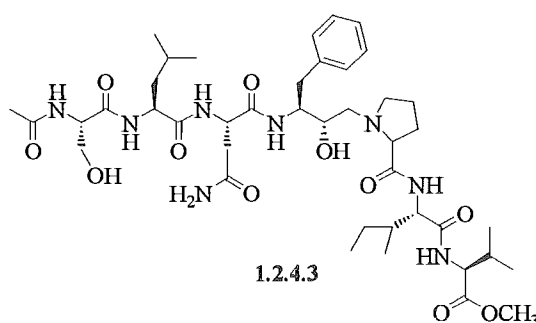


Figure 2.3.2. Non-hydrolysable amide bond isosteres.

Potent and selective HIVp inhibition is possible by mimicking the tyrosine-proline or phenylalanine-proline (P_1 - P_1') cleavage site that is unique to retroviral proteases. Since this cleavage site is rare in mammalian endopeptidases such inhibitors have a selective advantage for HIVp and are not readily degraded by other proteolytic enzymes. Incorporation of the hydroxyethylamine isostere into the minimum substrate sequence (S_4 - S_4') required for HIVp recognition gave the potent HIVp inhibitor, JG-365 (1.2.4.3),⁷ where phenylalanine and proline occupy the S_1 and S_1' subsites, respectively.



JG-365 is a potent inhibitor *in vitro* but failed to inhibit HIVp in cellular assays, possibly due to its largely peptidic character which would limit its ability to penetrate cell membranes. Smaller inhibitors (eg. Figure 2.3.1) that occupy only four or five positions in the active site (S_3 - S_2') were designed to display reduced peptide character and are more potent in cellular assays. These inhibitors (Figure 2.3.1) still retain the phenylalanine residue at P_1 for enzyme recognition and a sterically demanding residue at P_1' to maximise interaction with the S_1' subsite.

Wlodawer *et al.*⁸ extracted the structures of twelve HIVp inhibitors from solid state HIVp-inhibitor complexes and superimposed these structures to illustrate the HIVp binding cleft (Figure 2.3.3). It can be seen from this that the conformationally flexible inhibitors adopt a common conformation on binding with the enzyme cleft. The structural superimposition defines the S_4 - S_4' subsites of the cleft and the shape and binding properties of the cleft. Potent inhibitors have been generated by optimising binding interaction between inhibitor residues (P_4 - P_4'), and individual subsites (S_4 - S_4'), of the catalytic cleft.

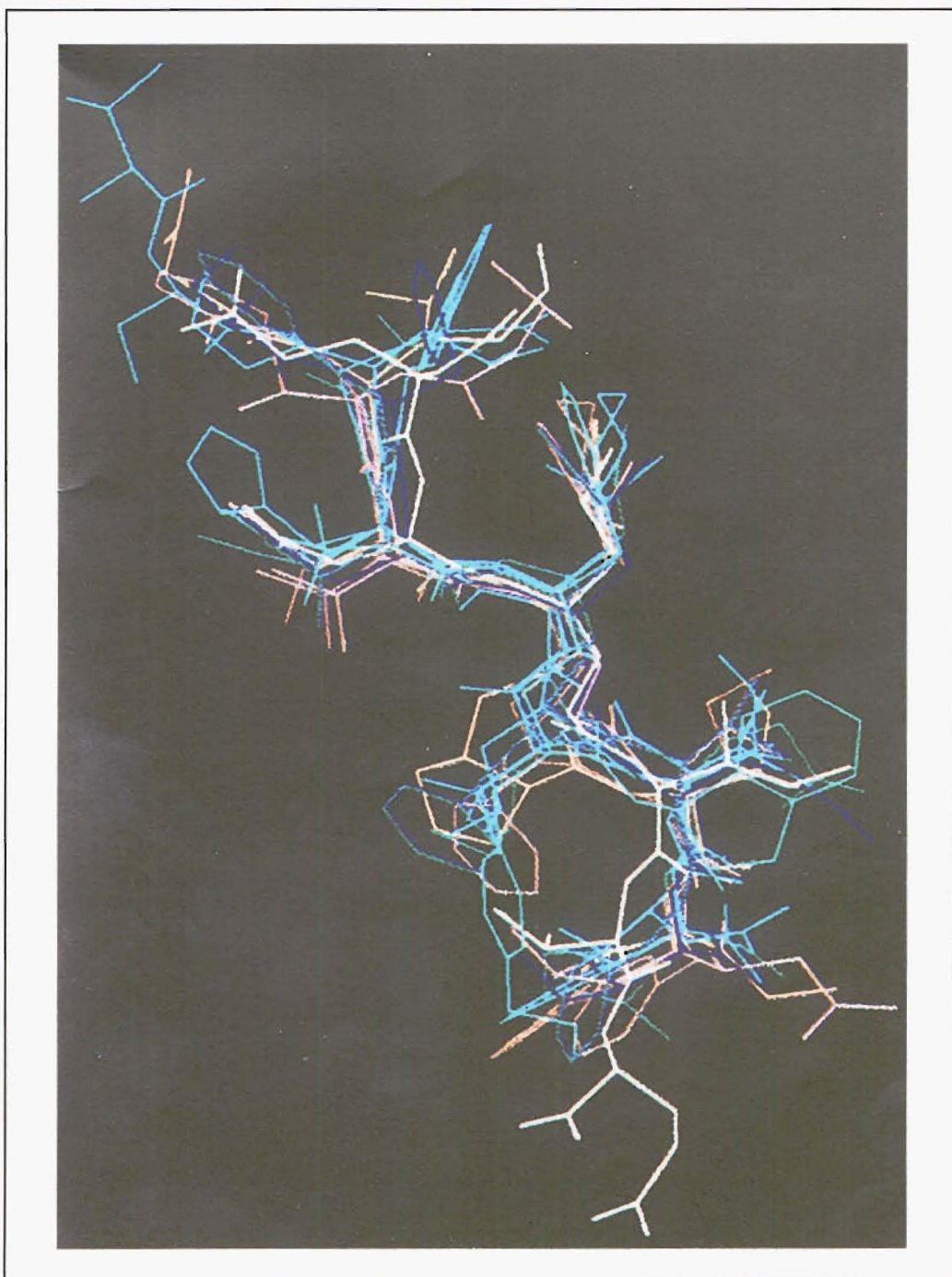


Figure 2.3.3. A superimposition of twelve HIVp inhibitors.

2.4. BINDING MODE OF HIVP INHIBITORS

Two distinct binding modes are observed in the solid state structures determined for HIVp-inhibitor complexes of JG-365 (1.2.4.3), and Saquinavir (1.2.4.4).⁹ JG-365 (1.2.4.3) binds to the active site of HIVp with a pseudo *cis*- conformation about the C-C bond adjacent to the proline residue. The torsion angle (indicated by a broad arrow, Figure 2.4.1) about this bond is 11°, implying an essentially planar conformation. The ligand binds in an extended conformation, with the isoleucine-valine residues (P₂'-P₃'), occupying the S₂'-S₃' subsites as expected. The binding mode favours a (3*S*)-configuration of the central hydroxymethylene tetrahedral intermediate mimic. The corresponding (3*R*)-OH epimer shows greatly reduced activity as this configuration places the central hydroxyl group out of range for a favourable interaction with the catalytic aspartate residues.

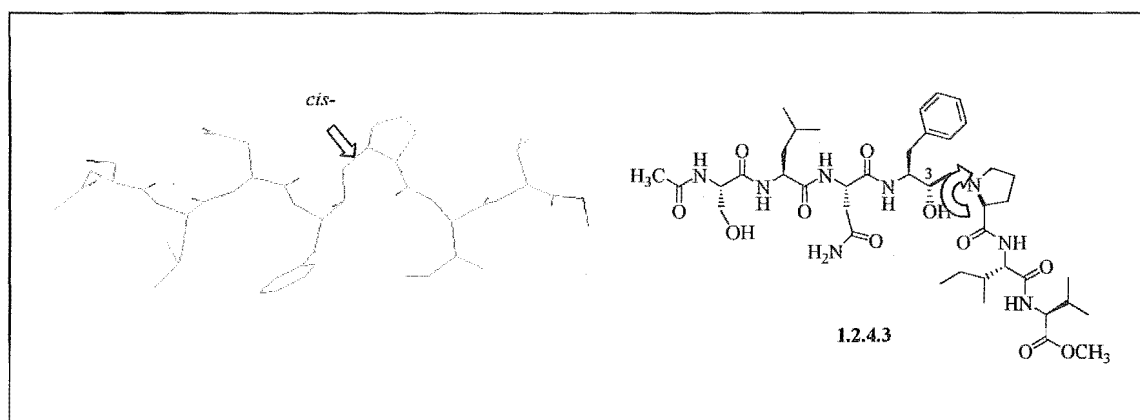


Figure 2.4.1. JG-365 (1.2.4.3) extracted from the HIVp active site, shown bound in a pseudo *cis*-conformation (left). The torsion angle (shown in bold) of the bound inhibitor is essentially planar (right).

Analysis of the solid state bound conformation of Saquinavir (1.2.4.4) shows a distinctly different binding mode from JG-365. It may be expected that the bulky *tert*-butyl C-terminal of Saquinavir (1.2.4.4) would fill the binding cleft in an extended conformation. However, the solid state structure (Figure 2.4.2) reveals that the *tert*-butyl group specifically twists to fill the S₂' subsite, with the large decahydroisoquinoline (Diq)

ring occupying the entire S_1' subsite, with some interaction with the S_3' . The binding of the *tert*-butyl group to the S_2' subsite twists the backbone and places the C-C bond adjacent to the Diq ring in a pseudo *trans*- conformation. The *trans*- binding mode shows a clear preference for the (3*R*)-OH configuration for interaction between the central hydroxyl and the catalytic aspartate residues. The corresponding (3*S*)-OH configuration shows greatly reduced activity, in direct contrast to the configurational preference of JG-365.

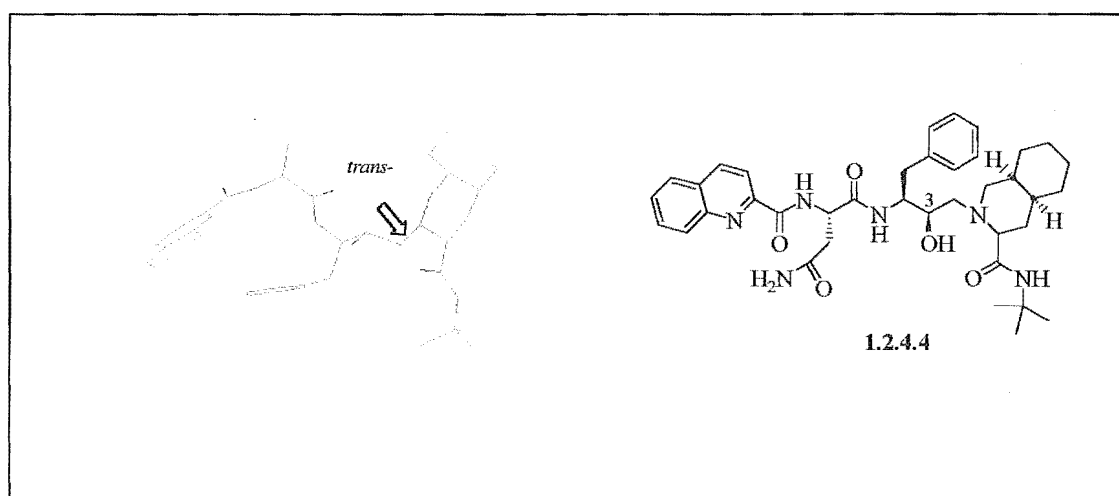


Figure 2.4.2. Saquinavir (1.2.4.4) extracted from the HIVp active site, shown bound in a pseudo *trans*-conformation (left).

2.5. DESIGN FEATURES OF THE TETRAZOLE-BASED ISOSTERES

We have designed a series of isosteric replacements that are conformationally constrained to force the pseudo *cis*- binding mode observed in JG-365 (1.2.4.3).¹⁰ The 1,5-disubstituted tetrazole ring has been used as a conformationally constrained *cis*-amide bond mimic to probe the preferential binding mode of a variety of peptidomimetic ligands (see Introduction 1.3). Our idea was to use the tetrazole ring as a rigid *cis*-amide bond mimic in the design of a generally applicable isosteric replacement, for incorporation into HIVp inhibitors and for use as a conformational probe. Our tetrazole-based isosteres are the first example of the tetrazole heterocycle being incorporated into a

non-hydrolysable amide bond isostere. Our design considerations are outlined in Figure 2.5.1.

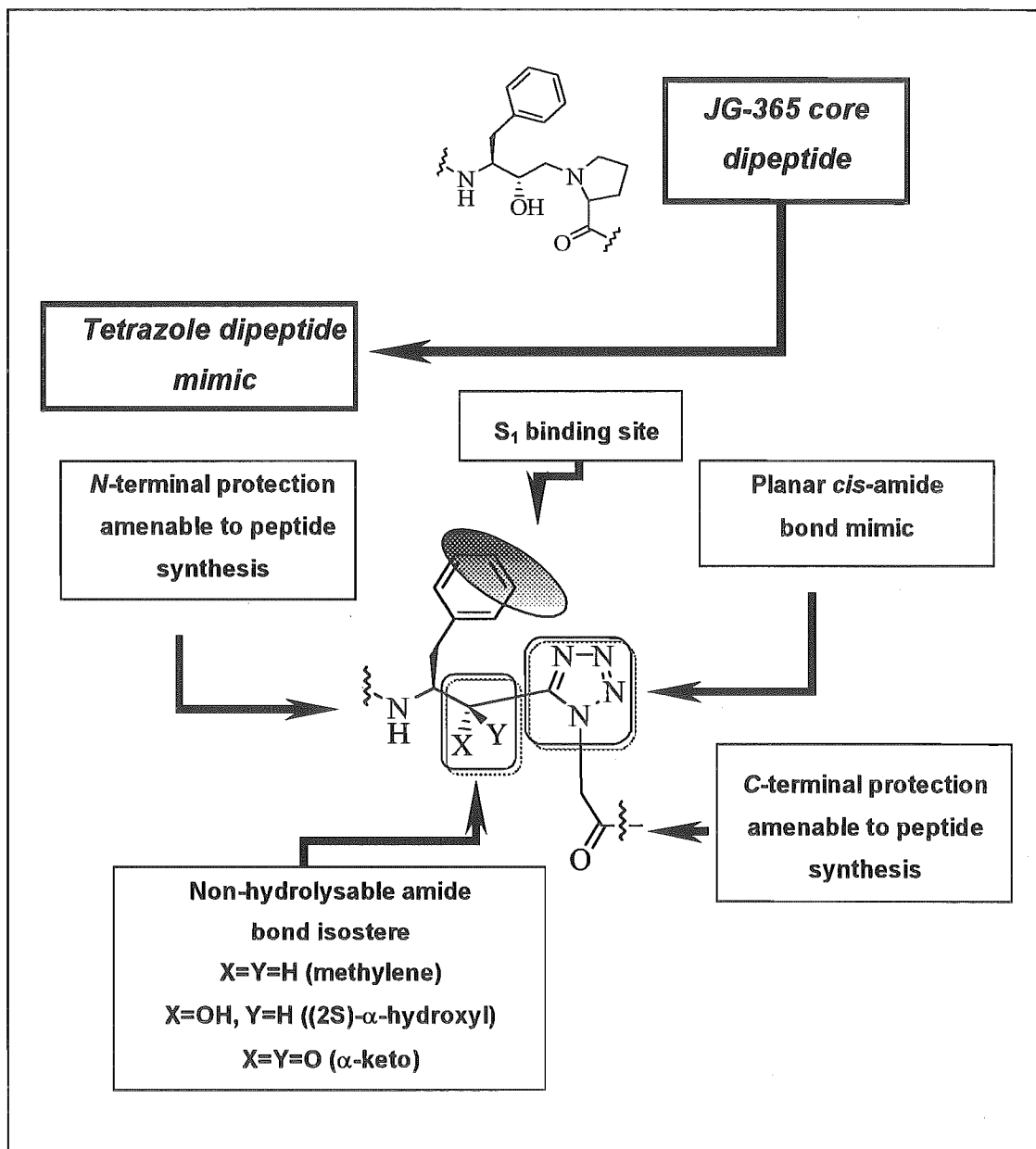


Figure 2.5.1. Design features of the tetrazole-based dipeptide mimic.

The target isosteres (Figure 2.5.2) use a 1,5-disubstituted tetrazole ring to provide a rigid, planar, *cis*- amide bond mimic to pre-organise the ligand into a conformation designed to approximate the bioactive conformation of JG-365. The design of the tetrazole-based dipeptide mimics also incorporate a non-hydrolysable amide bond isostere (see Chapter 2.3) adjacent to the tetrazole heterocycle. The α -methylene [CH_2CN_4] (2.5.1), α -hydroxymethylene [CHOHCN_4] (2.5.2), and α -keto isosteres [COCN_4] (2.5.3) (see Figure 2.5.2) have been included, based on the proven potency of these isosteric replacements in HIVp inhibitors. A phenylalanine residue has been incorporated at P_1 for selective recognition by HIVp. The isosteres are generally applicable to the design of peptidomimetics by selection of suitable natural or unnatural sidechains, incorporated through elongation of the *C*- and *N*-terminals. This requires a protecting strategy that is amenable to peptide synthesis.

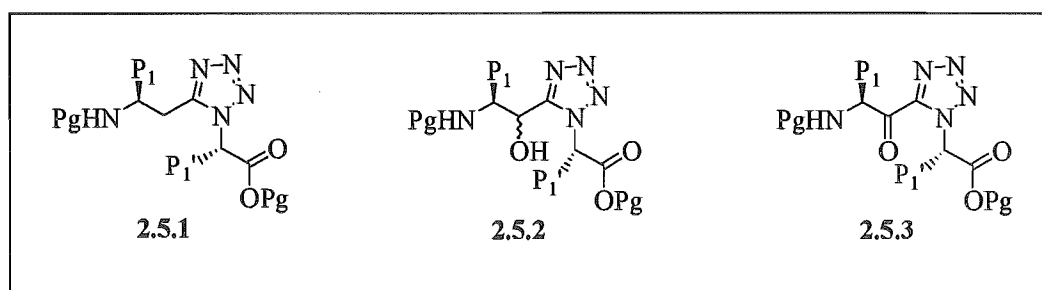


Figure 2.5.2. The target tetrazole-based isosteres.

2.6. CONCLUSION

The tetrazole-based isosteres have been designed as generally applicable mimics of the *cis*- amide bond. The design of the isosteres, 2.5.1-2.5.3, was based on the observed binding mode of the potent HIVp inhibitor, JG-365, and brings together the principles of ligand pre-organisation through conformational restriction and non-hydrolysable amide bond isosteres. The tetrazole-based isosteres (Figure 2.5.2) are the first example of non-hydrolysable amide bond isosteres that incorporate conformational restraint from a tetrazole heterocycle. We have incorporated this mimic into inhibitors of

HIVp, and foresee it as an important conformational probe to investigate the binding preference of peptidomimetic ligands.

The body of this thesis deals with the development of synthetic routes to the tetrazole-based dipeptides and incorporation of the mimic into HIVp inhibitors. Work has also focused on addressing stereochemical problems encountered in earlier work on the synthesis of tetrazole-based HIVp inhibitors.¹⁰

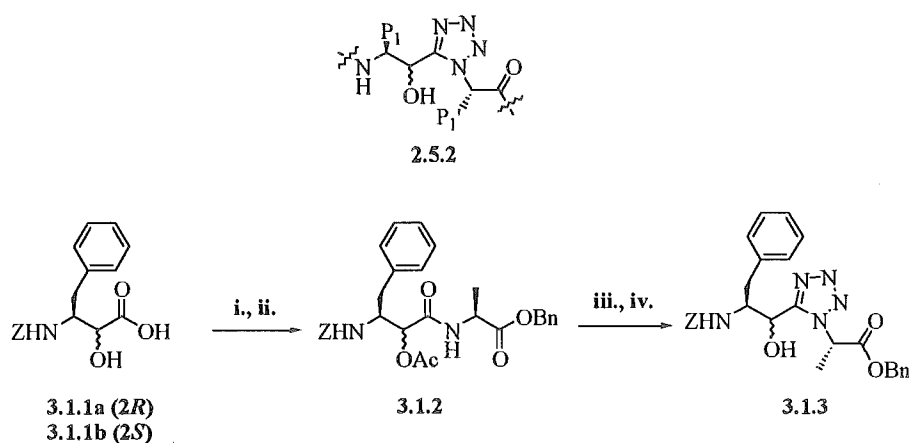
2.7. REFERENCES

- ¹ World Health Organisation, 1999, webpage <http://www.who.int/emc/diseases/hiv>.
- ² Huff, J. R. *J. Med. Chem.* **1991**, *34*, 2305.
- ³ Wlodawer, A.; Miller, M.; Jaskoski, M.; Sathyanarayana, B. K.; Baldwin, E.; Weber, I. T.; Selk, L. M.; Claeson, L.; Schneider, J.; Kent, S. B. H. *Science* **1989**, *245*, 616.
- ⁴ Miller, M.; Schneider, J.; Sathyanarayana, B. K.; Toth, M. V.; Marshall, G. R.; Clawson, L.; Selk, L.; Kent, S. B. H.; Wlodawer, A. *Science* **1989**, *246*, 1149.
- ⁵ Schechter, I.; Bergman, A. *Biochem. Biophys. Res. Commun.* **1967**, *27*, 157.
Schechter, I.; Bergman, A. *Biochem. Biophys. Res. Commun.* **1968**, *32*, 898.
- ⁶ Umezawa, H.; Aoyagi, T.; Morishima, H.; Matsuzaki, M.; Hamada, M.; Takeguchi, T. *J. Antibiot.* **1970**, *23*, 259.
- ⁷ Norbeck, D. W.; Kern, E.; Hayashi, S.; Rosenbrook, W.; Sham, H.; Herrin, T.; Plattner, J. J.; Erickson, J.; Clement, J.; Swanson, N.; Shipkowitz, N.; Hardy, D.; Marsh, K.; Arnett, G.; Shannon, W.; Broder, S.; Mitsuya, H. *J. Med. Chem.* **1990**, *33*, 1285.
- ⁸ Sathyanarayana, B. K.; Wlodawer, A. *Current Science* **1993**, *65*, 835.
- ⁹ Rich, D. H.; Sun, C-Q.; Prasad, J. N. V. N.; Pathiasseril, A.; Toth, M. V.; Marshall, G. R.; Clare, M.; Mueller, R. A.; Houseman, K. *J. Med. Chem.* **1991**, *34*, 1225. Krohn, A.; Redshaw, S.; Ritchie, J. C.; Graves, B. J.; Hatada, M. H. *J. Med. Chem.* **1991**, *34*, 3340.
- ¹⁰ Abell, A. D.; Foulds, G. J. *J. Chem. Soc. Perkins. Trans 1* **1997**, 2475. Foulds, G. J. Ph.D thesis, *Biologically Active Peptide Analogues*, University of Canterbury, **1996**.

CHAPTER THREE
SYNTHESIS OF 3-AMINO-2-HYDROXY-4-
PHENYLBUTANOIC ACID

3.1. INTRODUCTION

In previous work on tetrazole-based peptidomimetics the α -hydroxymethylene tetrazole isostere [CHOHCN₄] (2.5.2) has been synthesised by incorporation of the α -hydroxy acid, 3-amino-2-hydroxy-4-phenylbutanoic acid [(2*RS*,3*S*)-AHPBA] (3.1.1), into the tetrazole-based dipeptide mimic, 3.1.3, according to Scheme 3.1.1.¹

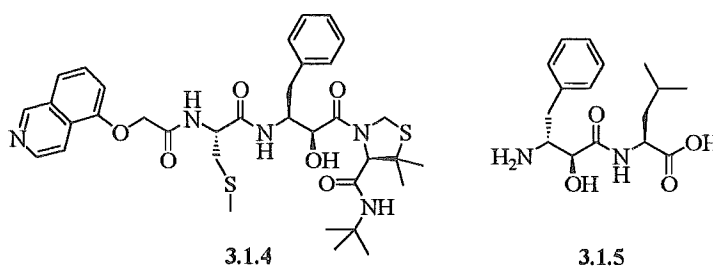


Scheme 3.1.1. Reagents and conditions; **i.** *L*-Ala OBn.HCl, DCC, HOBT, Et₃N, rt; **ii.** Ac₂O, pyridine, rt; **iii.** PCl₅, Quinoline, HN₃, rt; **iv.** K₂CO₃, rt.

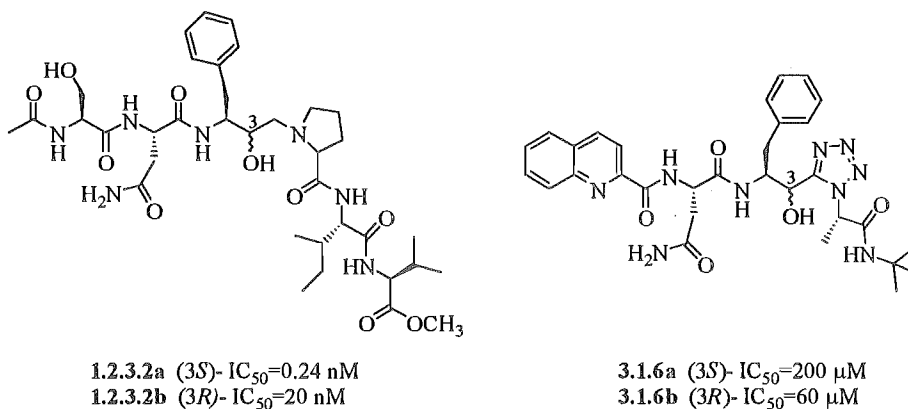
Chiral 3-amino-2-hydroxy acids (eg. 3.1.1) are also of considerable importance being crucial components of many medicinally useful molecules such as taxol,² immunological response modifiers,³ and several small peptides possessing antihypertensive activity.⁴ Many examples exist in the literature where 3-amino-2-hydroxy acids have been incorporated into short peptide sequences to produce potent protease inhibitors.⁵ As part of this current study we have investigated the synthesis of AHPBA and developed an improved method for the synthesis of this important amide bond isostere.

We have designed the tetrazole-based isostere, 2.5.2, to incorporate the α -hydroxy functional motif as this motif has been shown to mimic the tetrahedral intermediate of a hydrolysing amide bond under protease catalysis, and as such has been shown to increase the potency of protease inhibitors (see Chapter 2.3.).^{6,7} Mimoto *et al.*⁸ have used (2*RS*,3*S*)-3-amino-2-hydroxy-4-phenylbutanoic acid, 3.1.1 [(2*RS*,3*S*)-AHPBA]

in the synthesis of a potent HIVp inhibitor, 3.1.4 ($IC_{50}=2.3$ nM), which is based around the non-hydrolysable hydroxyethylamide isostere. The α -hydroxy amino acid, 3.1.1, is also a component of the naturally occurring low molecular weight peptidomimetic enzyme inhibitor, Bestatin (3.1.5).⁹ Bestatin is a potent inhibitor of leucine aminopeptidase and aminopeptidase B. Bestatin has reported antitumor and antimicrobial properties, associated with its ability to inhibit cell surface aminopeptidases.

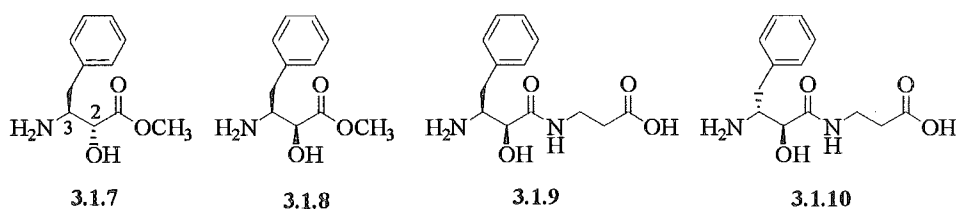


There is often a marked difference in biological activity between epimeric α -hydroxy peptidomimetics due to the stereospecific nature of a receptor. A receptor often requires the interacting ligand to have complimentary stereochemistry for potent binding to occur. The stereochemistry of the hydroxyethylamine isostere is important for tight binding of HIVp inhibitors to the catalytic cleft of HIVp (see Discussion 2.4). For example, JG-365 (1.2.3.2a $IC_{50}=0.24$ nM) is an order of magnitude more potent than its hydroxyethylamine epimer, 1.2.3.2b ($IC_{50}=20$ nM), due to a more favourable interaction of the hydroxyl oxygen with the catalytic aspartate residues. A similar activity dependency is seen by a comparison of the activity of the α -hydroxymethylene tetrazole-based HIVp inhibitors, 3.1.6a and 3.1.6b, where the (3*R*)-epimer (3.1.6a $IC_{50}=60$ μ M) is



an order of magnitude more potent against HIVp than the (3*S*)-epimer (3.1.6b IC_{50} =200 μ M).

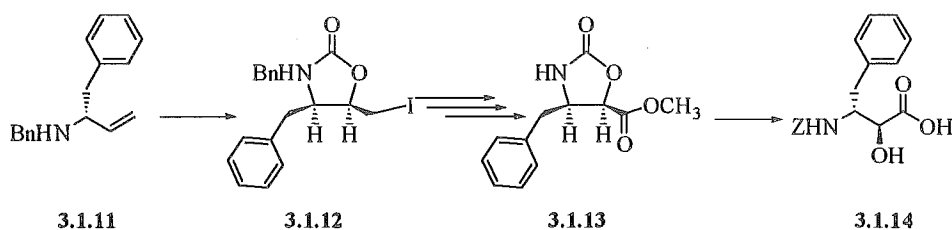
Leukotriene A_4 hydrolase inhibitors have also been synthesised that are based around AHPBA. Yuan *et al.*¹⁰ showed that the stereochemistry of both the C2 and C3 centres have a direct bearing on the relative potency of the hydrolase inhibitors, 3.1.7-3.1.10. (2*R*,3*S*)-AHPBA methyl ester (IC_{50} >0.5 mM) (3.1.7), was an order of magnitude less potent than its C2 epimer, (2*S*,3*S*)-AHPBA methyl ester (IC_{50} =50 μ M) (3.1.8), against leukotriene A_4 hydrolase. Control of the C3 stereochemistry is important for mimicking either the natural *L*-phenylalanine residue, or as is sometimes required the unnatural *D*-phenylalanine residue. The dipeptide (2*S*,3*S*)-AHPBA-Gly-OH (3.1.9) has the same C3 stereochemistry as naturally occurring *L*-phenylalanine and was shown to be a more potent hydrolase inhibitor than its C3 epimer, 3.1.10.



The obvious importance of AHPBA for the preparation of peptidomimetic compounds is reflected in the variety of synthetic procedures which have been published for the synthesis of this α -hydroxy amino acid. The essential problem in the synthesis of AHPBA is the construction of the desired diastereomeric C2, C3 portion, which has been shown to have a direct bearing on the activity of the derived peptidomimetic ligands (see examples above). A variety of strategies have been developed to overcome this synthetic challenge. What follows is a brief discussion of some of these synthetic methods that have been presented in the literature.

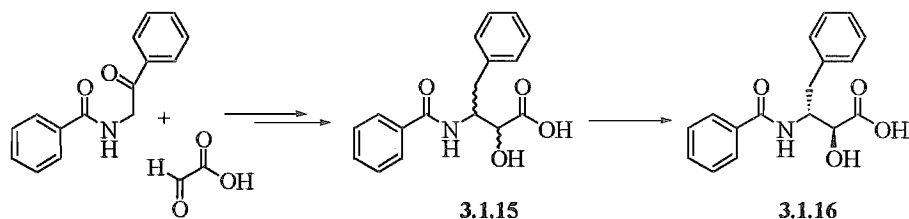
Kobayashi *et al.*¹¹ prepared *N*-Z-(2*S*,3*R*)-AHPBA, 3.1.14, by the iodocyclocarbamation of the allylamine, 3.1.11, which was derived from *N*-protected *D*-phenylalanine (Scheme 3.1.2). The configuration of the C2 and C3 stereocentres was introduced during formation of the key iodocyclocarbamate intermediate, 3.1.13. This

compound then underwent a series of functional group interconversions to yield the oxazolidone, **3.1.13**, which was ring opened by alkaline hydrolysis and the free amine reprotected to give **3.1.14**.



Scheme 3.1.2. Preparation of *N*-Z-(2*S*,3*R*)-AHPBA by the iodocyclocarbamation of an allylamine.

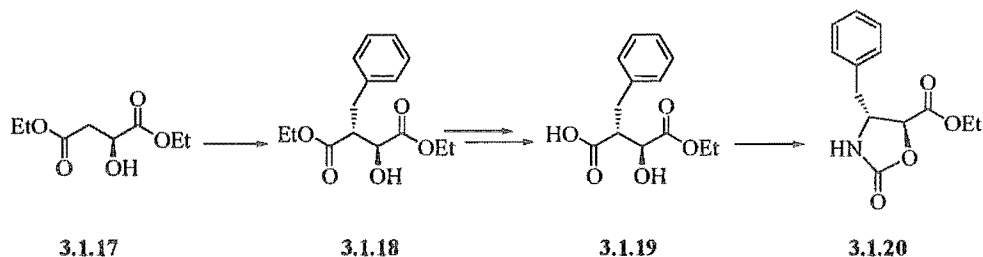
Nishizawa *et al.*¹² have developed a non-stereoselective synthesis of AHPBA through condensation of *N*-acyl- α -aminoacetophenone and glyoxylic acid, followed by catalytic hydrogenation and resolution of the racemic product, **3.1.15**, by salt formation with *S*-(-)- α -methylbenzylamine (Scheme 3.1.3). Diastereomerically pure (2*S*,3*R*)-AHPBA was obtained following acidic cleavage of the *N*-acyl protected **3.1.16**.



Scheme 3.1.3. Preparation of *N*-acyl-(2*S*,3*R*)-AHPBA by condensation of *N*-acyl- α -aminoacetophenone and glyoxylic acid.

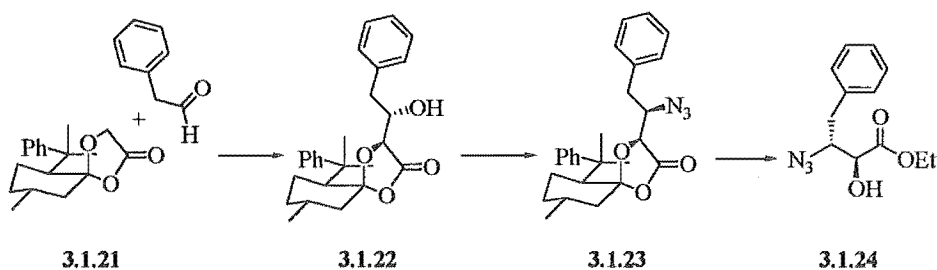
(*S*)-Malate diethyl ester, **3.1.17**, has been used as a precursor of defined C2 stereochemistry in the synthesis of (2*S*,3*R*)-AHPBA.¹³ The phenyl side chain was introduced stereoselectively by direct alkylation of the C3 carbon of **3.1.17** (Scheme 3.1.4). Selective saponification of the C4 ester of **3.1.18** according to the procedure of Miller,¹⁴ gave the required C4 acid, **3.1.19**. A subsequent Curtius rearrangement of the mono-acid gave an intermediate isocyanate, which was trapped by reaction with the C2

hydroxyl. The synthesis of (2*S*,3*R*)-AHPBA was completed by saponification of the oxazolidone, 3.1.20, formed during Curtius rearrangement.



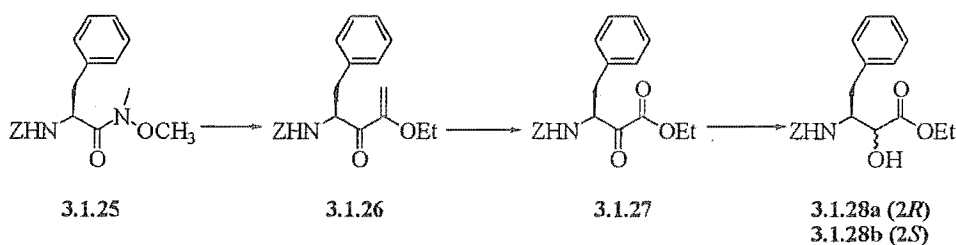
Scheme 3.1.4. Preparation of (2*S*,3*R*)-AHPBA by direct alkylation of (*S*)-malate diethyl ester.

Pearson and Hines¹⁵ reacted phenyl acetaldehyde with a spirocyclic 1,3-dioxolan-4-one, 3.1.21, to give stereoselectively, the aldol adduct, 3.1.22, with the desired C3 stereochemistry (Scheme 3.1.5). The *anti*-aldol adduct, 3.1.22, was then converted to the azide, 3.1.23, via a Mitsunobu interconversion and the chiral auxiliary removed with ethanolic HCl to give the azide ethyl ester, 3.1.24. Finally, catalytic hydrogenation of the azide, 3.1.24, gave the desired (2*S*,3*R*)-AHPBA ethyl ester.



Scheme 3.1.5. Preparation of (2*S*,3*R*)-AHPBA ethyl ester by alkylation of spirocyclic 1,3-dioxolan-4-one.

Angelastro *et al.*¹⁶ prepared the AHPBA isostere for incorporation into HIVp inhibitors by ozonolysis and reduction of peptidyl α -ethoxy vinyl ketones (Scheme 3.1.6). The vinyl ethyl ester, 3.1.26, was prepared by reacting *N*-Z-*L*-phenylalanine Weinreb amide, 3.1.25, with (α -ethoxyvinyl)magnesium bromide in the presence of *tert*-butyl lithium. Ozonolysis of 3.1.26 gave the α -keto ethyl ester, 3.1.27, which was subsequently reduced with sodium borohydride to give the desired *N*-Z-(2*R**S*,3*S*)-AHPBA ethyl esters, 3.1.28, as a mixture of C2 epimers (4:3, 3.1.28a:3.1.28b).



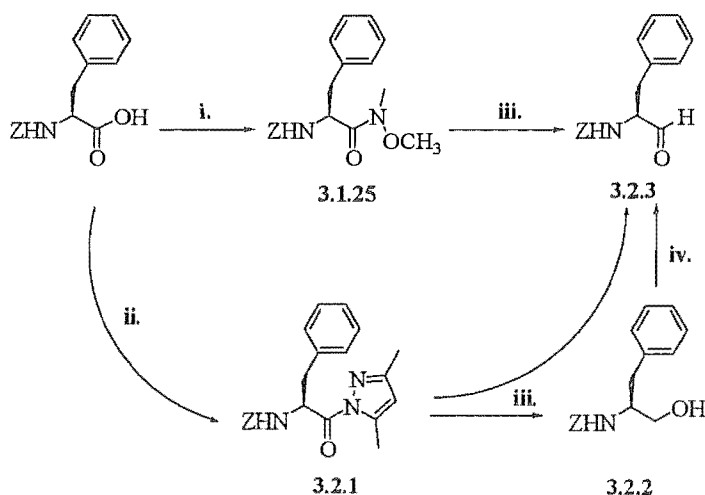
Scheme 3.1.6. Preparation of *N-Z*-(2*RS*,3*S*)AHPBA ethyl esters by ozonolysis and reduction of α -ethoxy vinyl ketones.

Many other synthetic methods have been reported for the preparation of AHPBA, **3.1.1**, some of which include the cycloaddition of an imine and benzoylketene,¹⁷ and the ring opening of aziridine diols.¹⁸ The examples above have been included to illustrate the range of synthetic methods that are available for the stereoselective and non-stereoselective synthesis of AHPBA. Some of these published methods are synthetically challenging and in this current work we have investigated the synthesis of AHPBA, with the aim of developing a convenient preparation of this important α -hydroxy acid.

3.2. SYNTHESIS BY FUNCTIONALISATION OF *N-Z-L*-PHENYLALANINAL

The most cited procedure for the preparation of **3.1.1**, and a procedure that we have investigated in this thesis, involves formation of cyanohydrins from an α -amino aldehyde, followed by acidic hydrolysis.^{19,20} We have prepared the key *N*-protected aldehyde **3.2.3** by two different synthetic routes (Scheme 3.2.1). In the first method, we prepared the aldehyde, **3.2.3** from *N-Z-L*-phenylalanine, via a reduction with lithium aluminium hydride of either **3.1.25**, or **3.2.1**. A BOP mediated coupling of Weinreb amine hydrochloride (*O,N*-dimethylhydroxylamine hydrochloride),²¹ gave Weinreb amide **3.1.25** in 86% yield. Similarly, a DCC mediated coupling of 3,5-dimethylpyrazole to *N-Z-L*-phenylalanine, gave **3.2.1**, in 85% yield. Reduction of **3.1.25** with lithium aluminium hydride, at $-50\text{ }^{\circ}\text{C}$, for fifteen minutes gave the desired aldehyde, **3.2.3** in 77% yield. However, a similar reduction of **3.2.1** gave a mixture of the aldehyde, **3.2.3**, and the primary alcohol, **3.2.2**, in 49% and 29% yields, respectively. The alcohol, **3.2.2** was formed by further reduction of the aldehyde, **3.2.3**, in the presence of excess lithium

aluminium hydride. The alcohol was re-oxidised to the desired aldehyde with Dess-Martin periodinane.²²



Scheme 3.2.1. Reagents and conditions: **i.** BOP, Et₃N, *O,N*-dimethylhydroxylamine, rt; **ii.** 3,5-dimethylpyrazole, DCC, -10 °C, 1 h, rt, 2d; **iii.** LiAlH₄, -50 °C, 15 min, -50-0 °C over 20 min; **iv.** Dess-Martin periodinane, rt, 1 h.

The addition of a nucleophile to 3.2.3 can occur with 1,2-asymmetric induction to give an excess of one of the two possible epimeric cyanohydrin products (3.2.4a or 3.2.4b) (Scheme 3.2.2).²³ Two strategies have been developed to exert stereocontrol on the addition of a nucleophile to chiral aldehydes such as 3.2.3 (Figure 3.2.1). The first of these methods occurs by the stereoselective attack of a bulky nucleophile according to electronic and steric factors in the presence of a non-chelating reagent, according to Cram's rules.²⁴ The second strategy proceeds with chelation control and requires the use of a Lewis acid to form an intermediate chelate, which reacts with a bulky nucleophile from the least hindered face. Generally the two methods lead to opposite diastereomeric products.

Herranz *et al.*²⁵ investigated the chelation and non-chelation controlled attack of trimethylsilylcyanide (TMSCN) on *N-Z-D*-phenylalaninal ((2*R*)-epimer of 3.2.3). They reported that under chelation control, in the presence of tin tetrachloride, the *syn/anti*-

diastereoisomeric ratio (3.2.4a:3.2.4b) was unaffected. Under non-chelation control, a predominance of the *syn*- product was observed. The steric bulk of the amine protecting group is also important in effecting non-chelation control.²⁶ The bulky *N,N*-dibenzylamino aldehydes form almost exclusively the non-chelation controlled adducts.²⁷

We anticipated that non-chelation controlled addition of TMS-CN to 3.2.3 would give a (2*R*,3*S*)-cyanohydrin, 3.2.4a (Scheme 3.2.2) stereoselectively. Treatment of the aldehyde, 3.2.3, with TMS-CN according to the method of Herranz *et al.*²⁵ gave low yields of both diastereomeric cyanohydrins, 3.2.4a and 3.2.4b. As an alternative the aldehyde 3.2.3 was reacted directly with potassium cyanide under non-chelation control in ethyl acetate-water to give the cyanohydrin C2-epimers, 3.2.4a and 3.2.4b (1:1 mixture by ¹H NMR), in 74% combined yield (Scheme 3.2.2).

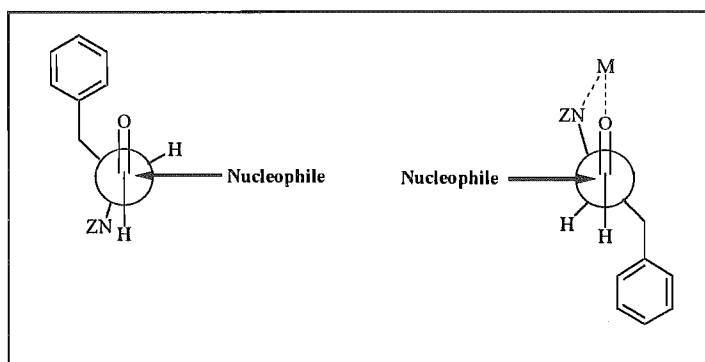
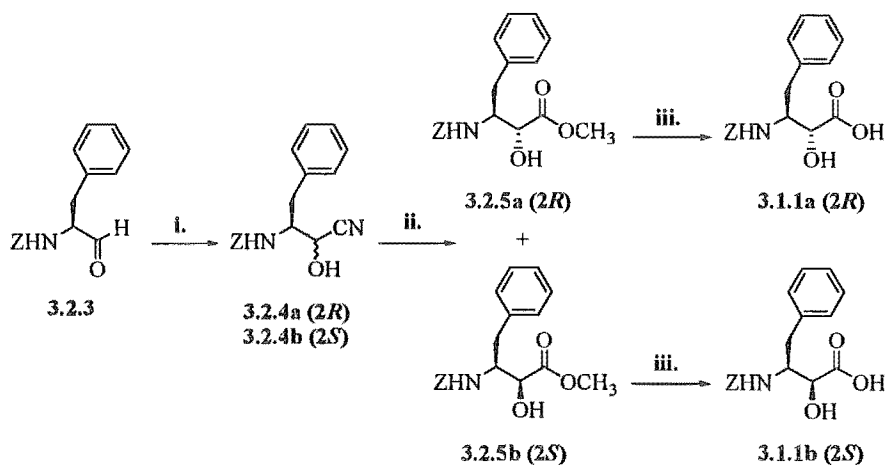


Figure 3.2.1. Non-chelation controlled attack (left), and chelation controlled attack (right) of 3.2.3.

The mixture of epimeric cyanohydrins, (3.2.4a and 3.2.4b), was directly transformed into the corresponding α -hydroxy amino esters, 3.2.5a and 3.2.5b by treatment with dry methanolic hydrogen chloride, followed by an *in situ* hydrolysis of the imidate hydrochloride intermediates (Scheme 3.2.2). The product methyl esters, 3.2.5a, and 3.2.5b, were separated by flash column chromatography, and further purified by a single recrystallisation. The less polar (2*R*,3*S*)-AHPBA methyl ester, 3.2.5a, (27% yield), eluted prior to (2*S*,3*S*)-AHPBA methyl ester, 3.2.5b (30% yield). The methyl esters were identified by comparison of their ¹H NMR spectra with that of the enantiomeric literature compounds,²⁵ derived from *N-Z-D*-phenylalanine.

Alkaline hydrolysis of methyl ester **3.2.5a** with sodium hydroxide in methanol-water for 2 hours, to give the corresponding acid, **3.1.1a**, in 88% yield (Scheme 3.2.2). Similarly, methyl ester **3.2.5b** was hydrolysed to give acid, **3.1.1b**, in 88% yield.



Scheme 3.2.2. Reagents and conditions: **i.** KCN, EtOAc, water, rt; **ii.** MeOH/H₂O, HCl(g), 5 °C, 24 h; **iii.** NaOH, MeOH/H₂O, rt, 2h.

Overall we have found this procedure for the preparation of *N-Z-AHPBA* to be highly variable. Formation of the primary alcohol, **3.2.2** was difficult to avoid in the preparation of the key aldehyde, **3.2.3**, and required further purification and re-oxidation to produce the desired aldehyde (Scheme 3.2.1). Formation of the epimeric cyanohydrins did not occur reliably and in some instances no product cyanohydrin could be detected in the reaction mixture. With this in mind we thought it would be beneficial to develop a new synthetic route to *N-Z-AHPBA* that was synthetically reliable, made use of readily available intermediates and that lacked the complexity of some of the existing procedures.

3.3. SYNTHESIS BY AMINOHYDROXYLATION OF (*E*)-4-PHENYL-2-BUTENOIC ACID METHYL ESTER

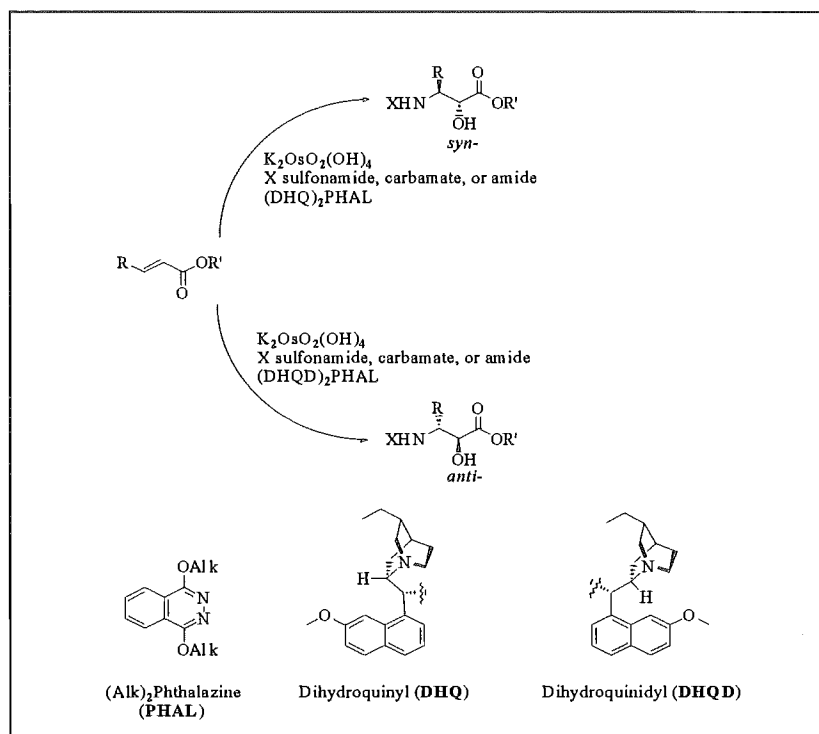


Figure 3.3.1. Osmium catalysed asymmetric aminohydroxylation (AA) of α,β -unsaturated esters.

The Sharpless asymmetric aminohydroxylation (AA) reaction has received considerable attention as a method of synthesising chiral compounds with the aminohydroxy functionality.²⁸ The utility of the AA reaction has been refined with the development of new ligands and reaction conditions to give improved regioselectivity, chemoselectivity and stereoselectivity. This reaction utilises the masked 1,2-functional group relationship of olefins to achieve a 1,2-functionalisation by face selective oxidation (Figure 3.3.1). The reaction employs osmium to catalyse the suprafacial addition of a nitrogen atom, from an appropriate nitrogen source (X) and an oxygen atom from water, to the double bond. The nitrogen atom is added preferentially to the center distal to the most electron withdrawing group. Three types of enantiomerically enriched *N*-protected hydroxyamines can be prepared depending on the choice of the stoichiometric nitrogen

source, X: *N*-sulphonamides, *N*-carbamates, and *N*-carboxamides. Enantioselectivity is induced by the cinchona alkaloid ligands, dihydroquinidine (DHQD), and dihydroquinine (DHQ), developed for the asymmetric dihydroxylation (AD) system.²⁹ The cinchona ligands dictate enantiofacial selectivity, which can be predicted using the mnemonic device from the AD system (Figure 3.2.2).

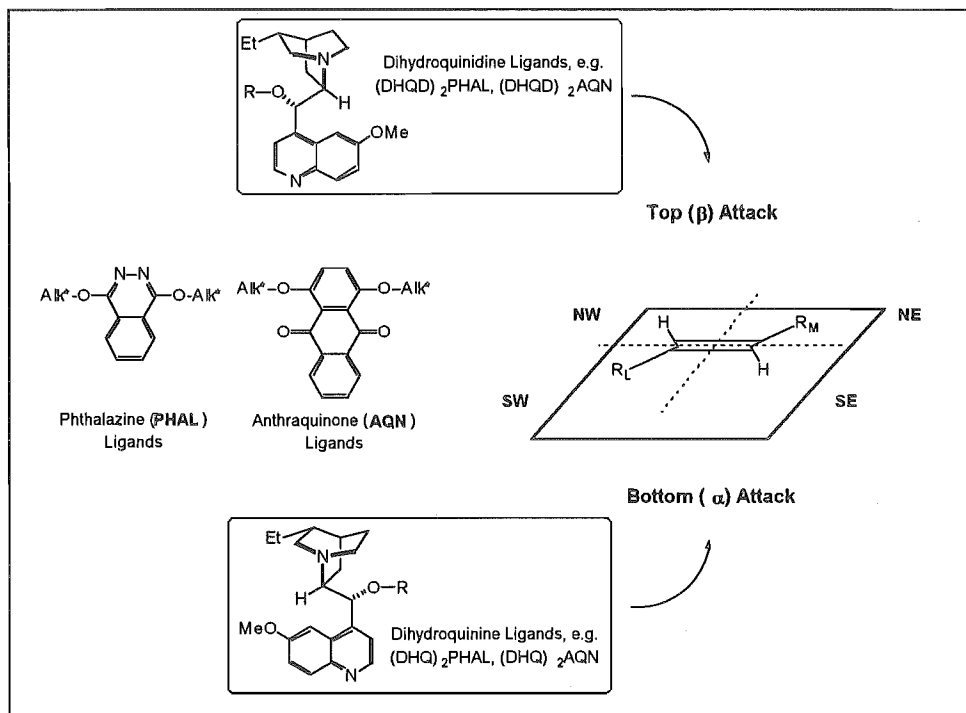
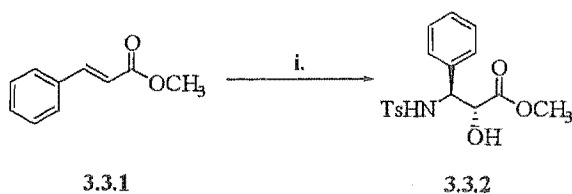


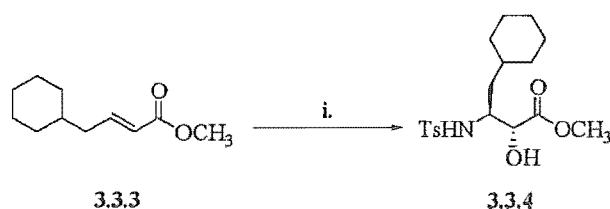
Figure 3.2.2. Mnemonic device for the prediction of face selectivity.

Sharpless *et al.* have applied the AA reaction to the synthesis of *N*-protected (2*R*,3*S*)-3-amino-2-hydroxy-3-phenylbutanoic acid (3.3.2), which was further elaborated to give the C13 side chain of Taxol.³⁰ The commercially available methyl cinnamate, 3.3.1, was subjected to the catalytic AA process using (DHQ)₂PHAL ligand in the presence of Chloramine T hydrate (Scheme 3.3.1). The *N*-sulphamide protected (2*R*,3*S*)-hydroxyamine methyl ester, 3.3.2, was obtained in 69% yield and 82% enantiomeric purity (ee).



Scheme 3.3.1. Reagents and conditions: **i.** (DHQ)₂PHAL, K₂OsO₂(OH)₄, TsNCINa₃H₂O, rt, *t*-BuOH/H₂O.

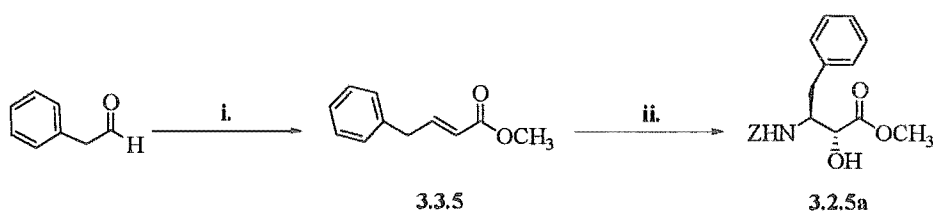
Sudalai and Upadhy³¹ have applied the Sharpless AA reaction to the synthesis of cyclohexylnorstatine [(2*R*,3*S*)-3-amino-4-cyclohexyl-2-hydroxybutyric acid, **3.3.4**], a key *C*-terminal moiety of potent renin inhibitors.³² Catalytic asymmetric aminohydroxylation of olefin, **3.3.3**, using OsO₄, (DHQ)₂PHAL and Chloramine T hydrate, (Scheme 3.3.2) as the nitrogen source, gave the *N*-sulphonamide protected ester, **3.3.4**, in 60% yield and 96% ee.



Scheme 3.3.2. Reagents and conditions: **i.** (DHQ)₂PHAL, K₂OsO₂(OH)₄, TsNCINa₃H₂O, rt, *t*-BuOH/H₂O.

We have extended this work by preparing the aryl olefin, **3.3.5**, and subjecting it to the Sharpless AA reaction to prepare 3-amino-2-hydroxy methyl ester, **3.2.5a**. The aryl olefin, **3.3.5** (Scheme 3.3.3), substrate for the Sharpless aminohydroxylation, was prepared by standard Wittig-Horner chemistry.³³ Phenylacetaldehyde was reacted with the stabilised ylide, methyl (triphenylphosphoranylidene) acetate, at room temperature, to give **3.3.5**, as a mixture of *cis*- and *trans*- olefins (1:9 by ¹H NMR). Flash column chromatography of the isomeric mixture gave the desired *trans*-**3.3.5** in 54% yield. The aryl olefin, **3.3.5**, was reacted in the presence of benzyl carbamate, as the nitrogen source, catalytic K₂OsO₄(OH)₄ and the (DHQ)₂PHAL ligand, according to the procedure of

Sharpless.³⁰ Flash column chromatography of the reaction mixture gave *N-Z*-protected (2*R*,3*S*)-AHPBA methyl ester, **3.2.5a**, in <5% yield, contaminated with benzyl carbamate. We were unable to optimise the reaction any further and considered a different strategy for the synthesis of AHPBA.



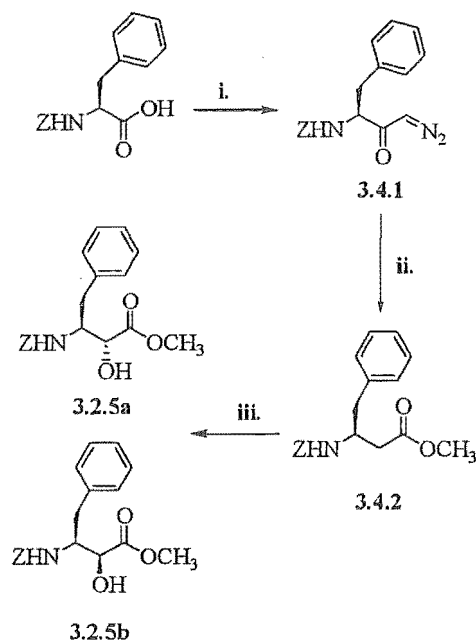
Scheme 3.3.3. Reagents and conditions: i. $\text{Ph}_3\text{PCHCOOCH}_3$, rt; ii. $(\text{DHQ})_2\text{PHAL}$, $\text{K}_2\text{OsO}_2(\text{OH})_4$, benzyl carbamate, rt, $\text{CH}_3\text{CN}/\text{H}_2\text{O}$.

3.4. SYNTHESIS BY ENOLATE HYDROXYLATION OF *N-Z-L*-HOMOPHENYLALANINE METHYL ESTER

Introduction of the α -hydroxy functionality can be achieved by direct hydroxylation of an appropriate enolate by the oxodiperoxymolybdenum (pyridine) (hexamethyl phosphoric triamide) complex (MoOPH).³⁴ The MoOPH complex has been employed in the synthesis of the C13 taxol side chain, **3.3.2** (Scheme 3.3.1) [(2*R*,3*S*)-3-amino-2-hydroxyl-3-phenylpropanoic acid], by direct oxidation of an enolate derived from *N*-protected *L*-homophenylglycine methyl ester.³⁵ In consideration of this method, we concluded that a similar approach could be used for the synthesis of AHPBA, **3.1.1**,³⁶ and turned our attention to the preparation of the required β -amino acid methyl ester, **3.4.2**.

Diazoketone **3.4.1** (Scheme 3.4.1) was obtained in high yield (75%) from *N-Z-L*-phenylalanine by treatment of the mixed anhydride with diazomethane, according to the established procedure of Plucinska *et al.*³⁷ Compound **3.4.1** was subjected to a Wolff rearrangement, catalysed by silver benzoate, in the presence of methanol, to give *N-Z-L*-homophenylalanine methyl ester, **3.4.2** in 83% yield.³⁸ Similarly, the benzyl ester of *N-Z*-

L-homophenylalanine was synthesised by using benzyl alcohol as the trapping nucleophile during Wolff rearrangement of diazoketone 3.4.1, to give *N-Z-L*-homophenylalanine benzyl ester in 83% yield. Wolff rearrangement of diazoketones with a chiral centre adjacent to a carbonyl group is shown to proceed with retention of configuration (see Chapter 4.2).³⁹



Scheme 3.4.1. Reagents and conditions: i. EtOCOCl, NEt₃, THF/ether, CH₂N₂, -15 °C, 18h; ii. PhCOOAg, CH₃OH, NEt₃, THF, rt, 1h; iii. KHMDS, THF, MoOPH, -78°C, 3h.

Hydroxylation of 3.4.2 (Scheme 3.4.1) was examined in anticipation of delivery of oxygen by the MoOPH complex.⁴⁰ Reaction of the potassium enolate derivative of 3.4.2 (KHMDS, 6 eq., -78 °C to -25 °C) with MoOPH (1.5 eq.) was carried out at -60 °C to give methyl esters, 3.2.5a and 3.2.5b (53:47 *syn/anti* mixture by ¹H NMR) (Scheme 3.4.1). Column chromatography of the crude reaction mixture gave *N-Z-(2R,3S)*-AHPBA methyl ester (3.2.5a), and *N-Z-(2S,3S)*-AHPBA methyl ester (3.2.5b) in 35% and 32% yield respectively, based on recovered starting material. A single recrystallisation gave pure samples of the methyl esters, the diastereomeric purity of which was determined to be >95% by ¹H NMR.

In the course of developing this method we investigated optimising the stereoselectivity and yield of the hydroxylation reaction. There was only slight variation in the *syn/anti*-selectivity and yield between the bases KHMDS, NaHMDS and LiHMDS. Best *syn*-selectivity was obtained with potassium as the counterion (KHMDS). This result can be rationalised according to Davies *et al.*⁴¹ by considering the reacting potassium enolate existing as an equilibrium mixture of a chelated eight-membered ring (I), or six-membered ring (II) (Figure 3.4.1), which are preferentially attacked by the electrophilic MoOPH complex at the *Si* and *Re* faces respectively. The eight-membered ring (I) is favoured when potassium acts as the counterion and is attacked at the less hindered face of the enolate, resulting in a predominance of the *syn*-hydroxylated product, (2*R*,3*S*)-AHPBA methyl ester, 3.2.5a.

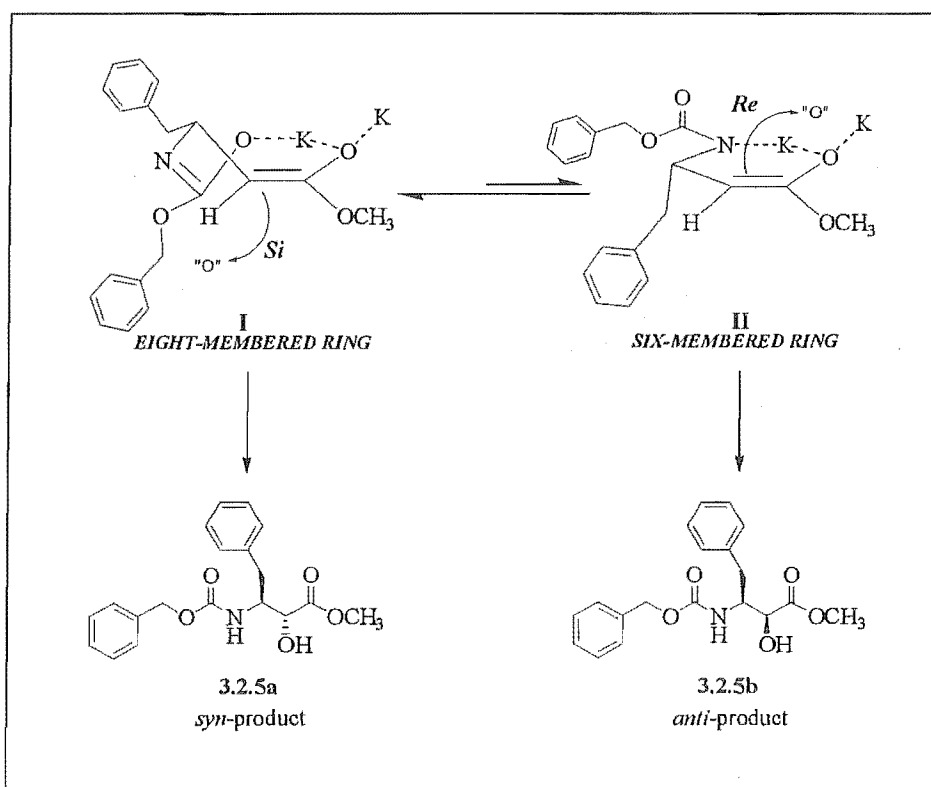


Figure 3.4.1. Rationalising the *syn*-stereoselectivity of the enolate hydroxylation.

Variations in temperature, (-40 °C, -60 °C), and time of the reaction, (3-5 h), had little impact on the *syn*-selectivity or yield of the product methyl esters, 3.2.5a and

3.2.5b. *N-Z-L*-Homophenylalanine benzyl ester was untouched by the same reaction conditions (KHMDS, 6 eq., -78 °C to -25 °C, MoOPH 1.5 eq., -60 °C) presumably due to the steric constraints of the bulkier benzyl ester.

Hydrolysis of the methyl esters, **3.2.5a**, and **3.2.5b**, with sodium hydroxide followed the established procedure (Scheme 3.2.2) to give the free acids, **3.1.1a** and **3.1.1b**. Incorporation of the free acids into the appropriate substrate can be achieved simply through *C*-terminal elongation, *N-Z*-deprotection and *N*-terminal elongation, to furnish the desired ligand incorporating the hydroxyethylamide isostere.

The method developed here provides a convenient synthesis of *N-Z*-(*2R,3S*)-AHPBA (**3.1.1a**) and *N-Z*-(*2S,3S*)-AHPBA (**3.1.1b**), in 36% overall yield from commercially available *N-Z-L*-phenylalanine. Standard synthetic methods were employed for the synthesis of an enolisable substrate to which the C2 hydroxyl functionality could be directly introduced by the MoOPH complex. Practically this method was found superior in simplicity and efficiency to those methods already published.

3.5. CONCLUSION

The α -hydroxy amino acid, (*2RS,3S*)-AHPBA, (**3.1.1**) is an important component of many protease inhibitors, where it is used as a non-hydrolysable amide bond isostere. The importance of this compound is reflected in the variety of methods that exist in the literature for the preparation of (*2RS,3S*)-AHPBA. The available methods for forming the diastereomeric C2 and C3 centres vary in synthetic complexity and practicality.

We have synthesised (*2RS,3S*)-AHPBA by functionalisation of *N-Z-L*-phenylalaninal and found this method to be highly variable, with several steps being non-reproducible. In an effort to develop new synthetic strategies for the synthesis of (*2RS,3S*)-AHPBA we have investigated the Sharpless AA reaction and enolate hydroxylation by the MoOPH complex. The Sharpless AA methodology proved to be low yielding and suffered from reagent contamination. Direct introduction of the α -

hydroxy functionality by the MoOPH complex has been developed as a simple and reliable method for the synthesis of (2*RS*,3*S*)-AHPBA, 3.1.1.

3.6. REFERENCES

- ¹ Abell, A. D.; Foulds, G. *J. Chem. Soc. Perkin 1* **1997**, 2475.
- ² Guenard, D.; Gueritte-Voegelein, F.; Potier, P. *Acc. Chem. Res.* **1993**, *26*, 160.
- ³ Suda, H.; Takita, T.; Aoyagi, T.; Umezawa, H. *J. Antibiotics* **1976**, *26*, 100.
- ⁴ For examples see; Okino, T.; Matsuda, H.; Murakami, M.; Yamaguchi, K. *Tetrahedron Lett.* **1993**, *34*, 501. Iizuka, K.; Kamijo, T.; Harada, H.; Akahane, K.; Kubota, T.; Umeyama, H.; Kiso, Y. *J. Chem. Soc. Chem. Commun.* **1989**, 1678.
- ⁵ Babine, R. E.; Bender, S. L. *Chem. Rev.* **1997**, *97*, 1359.
- ⁶ Gante, J. *Angew. Chem. Int. Ed. Engl.* **1994**, *33*, 1699.
- ⁷ Huff, J. R. *J. Med. Chem.* **1991**, *34*, 2305.
- ⁸ Mimoto, T.; Imai, J.; Kisanuki, S.; Enomoto, H.; Hattori, N.; Akaji, K.; Kiso, Y. *Chem. Pharm. Bull.* **1992**, *40*, 2251.
- ⁹ Herranz, R.; Castro-Pichel, J.; Vinuesa, S.; Garcia-Lopez, M. T. *J. Org. Chem.* **1990**, *55*, 2232 (and references herein).
- ¹⁰ Yuan W.; Munoz, B.; Wong, C-H.; Haeggstrom, J. Z.; Wetterholm, A.; Samuelson, B. *J. Med. Chem.* **1993**, *36*, 211.
- ¹¹ Kobayashi, S.; Isobe, T.; Ohno, M. *Tetrahedron Lett.* **1984**, *25*, 5079.
- ¹² Nishizawa, R.; Saino, T.; Suzuki, M.; Fujii, T.; Shirai, T.; Aoyagi, T.; Umezawa, H. *J. Antibiotics* **1983**, *36*, 695.
- ¹³ Norman, B. H.; Morris, M. L. *Tetrahedron Lett.* **1992**, *33*, 6803.
- ¹⁴ Miller, M. J.; Bajwa, J. S.; Mattingly, P. G.; Peterson, K. *J. Org. Chem.* **1982**, *47*, 4928.
- ¹⁵ Pearson, W. H.; Hines, J. V. *J. Org. Chem.* **1989**, *54*, 4235.
- ¹⁶ Angelastro, M. R.; Peet, N. P.; Philippe, B. *J. Org. Chem.* **1989**, *54*, 3913. Slee, D. H.; Laslo, K. L.; Elder, J. H.; Ollman, I. R.; Gustchina, A.; Kervinen, J.; Zdanov, A.; Wlodawer, A.; Wong, C-H. *J. Am. Chem. Soc.* **1995**, *117*, 11867.

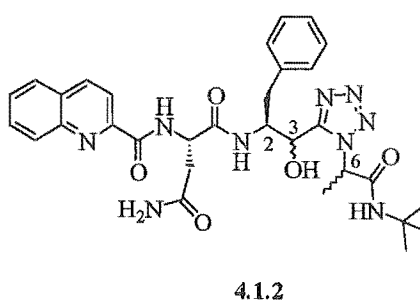
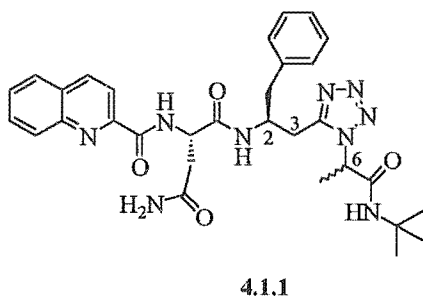
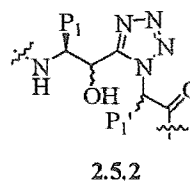
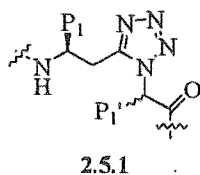
- ¹⁷ Kobayashi, Y.; Takemoto, Y.; Ito, Y.; Terashima, S. *Tetrahedron Lett.* **1990**, *31*, 3031. Palomo, C.; Arrieta, A.; Cossio, F. P.; Aizpurua, J. M.; Mielgo, A.; Aurrekoetxea, N. *Tetrahedron Lett.* **1990**, *31*, 6429.
- ¹⁸ Kang, S. H.; Ryu, D. H. *Bioorg. Med. Chem. Lett.* **1995**, *5*, 2959.
- ¹⁹ Nishizawa, R.; Saino, T. *J. Med. Chem.* **1977**, *20*, 510. Herranz, R.; Castro-Pichel, J.; Vinuesa, S.; Garcia-lopez, M. T. *J. Chem. Soc. Chem. Commun.* **1989**, 938. Matsuda, F.; Matsumoto, T.; Ohsaki, M.; Ito, Y.; Terashima, S. *Chem. Lett.* **1990**, 723. Iizuka, K.; Kamijo, T.; Harada, H.; Akahane, K.; Umeyama, H.; Ishida, T.; Kiso, Y. *J. Med. Chem.* **1990**, *33*, 2707. Yuan, W.; Munoz, B.; Wong, C-H.; Haeggstrom, J. Z.; Wetterholm, A.; Samuelsson, B. *J. Med. Chem.* **1993**, *36*, 211.
- ²⁰ Herranz, R.; Castro-Pichel, J.; Garcia-Lopez, T. *Synthesis* **1989**, 703.
- ²¹ Goel, O. P.; Krolla, U. *Org. Syn.* **1987**, *19*, 75.
- ²² Dess, D. B.; Martin, J. C. *J. Org. Chem.* **1983**, *48*, 4155. Ireland, R. E.; Liu, L. *J. Org. Chem.* **1993**, *58*, 2899.
- ²³ Reetz, M. T. *Angew. Chem. Int. Ed. Engl.* **1984**, *23*, 556.
- ²⁴ Morrison, J. D.; Mosher, H. S. In, *Asymmetric Organic Reactions*, Prentice-Hall: Englewood Cliffs **1971**.
- ²⁵ Herranz, R.; Castro-Pichel, J.; Vinuesa, S.; Garcia-Lopez, M. T. *J. Org. Chem.* **1990**, *55*, 2232.
- ²⁶ Reetz, M. T. *Pure Appl. Chem.* **1992**, *64*, 351.
- ²⁷ Reetz, M. T.; Drewes, M. W.; Harms, K.; Reif, W. *Tetrahedron Lett.* **1988**, *29*, 3295.
- ²⁸ Li, G.; Sharpless, B. *Acta Chem. Scand.* **1996**, *50*, 649. Becker, H.; Sharpless, K. B. *Angew. Chem. Int. Ed. Engl.* **1996**, *35*, 448. Li, G.; Chang, H-T.; Sharpless, K. B. *Angew. Chem. Int. Ed. Engl.* **1996**, *35*, 451. Li, G.; Angert, H. H.; Sharpless, K. B. *Angew. Chem. Int. Ed. Engl.* **1996**, *35*, 2813. Rudolf, J.; Sennhenn, P. C.; Vlaar, C. P.; Sharpless, K. B. *Angew. Chem. Int. Ed. Engl.* **1996**, *35*, 2810.
- ²⁹ Kolb, H. C.; Van Nieuwenhze, M. S.; Sharpless, K. B. *Chem. Rev.* **1994**, *94*, 2483.

- 30 Li, G.; Sharpless, K. B. *Acta Chem. Scand.* **1996**, *50*, 649.
- 31 Upadhyaya, T. T.; Sudalai, A. *Tetrahedron: Asymmetry* **1997**, *8*, 3685.
- 32 Iiuka, K.; Kamijo, T.; Harada, H.; Akahane, K.; Kubota, T.; Umeyama, H.; Kiso, Y. *J. Chem. Soc. Chem. Commun.* **1989**, 1678.
- 33 Hoult, D. A. *The Design and Synthesis of Conformationally Restricted and Epoxide Based Peptidomimetics*. Ph.D. thesis, University of Canterbury, **1997**.
- 34 Vedejs, E. *J. Am. Chem. Soc.* **1974**, 5944. Vedejs, E.; Engler, D. A.; Telschow, J. *E. J. Org. Chem.* **1978**, *43*, 188.
- 35 Hanessian, S.; Sanceau, J-Y. *Can. J. Chem.* **1996**, *74*, 621.
- 36 May, B. C. H.; Abell, A. D. *Syn. Commun.* **1999**, *29*, 2515.
- 37 Plucinska, K.; Liberek, B. *Tetrahedron* **1987**, *43*, 3509.
- 38 Podlech, J.; Seebach, D. *Angew. Chem. Int. Ed. Eng.* **1995**, *107*, 507.
- 39 Wiberg, K. B.; Hutton, T. W. *J. Am. Chem. Soc.* **1956**, *78*, 1640.
- 40 Sardina, F. J.; Paz, M. M.; Fernandez-Margia, E.; de Boer, R. F.; Alvarez, M. P. *Tetrahedron Lett.* **1992**, *33*, 4637. Jefford, C. W.; Wang, J. B.; Lu, Z-H. *Tetrahedron Lett.* **1993**, *34*, 7557. Gamboni, R.; Waespe-Sarcevic, N.; Tamm, C. *Tetrahedron Lett.* **1985**, *26*, 203.
- 41 Davis, F. A.; Reddy, R. T.; Reddy, R. E. *J. Org. Chem.* **1992**, *57*, 6387.

CHAPTER FOUR
STEREOCHEMICAL ASSIGNMENT OF
TETRAZOLE-BASED INHIBITORS

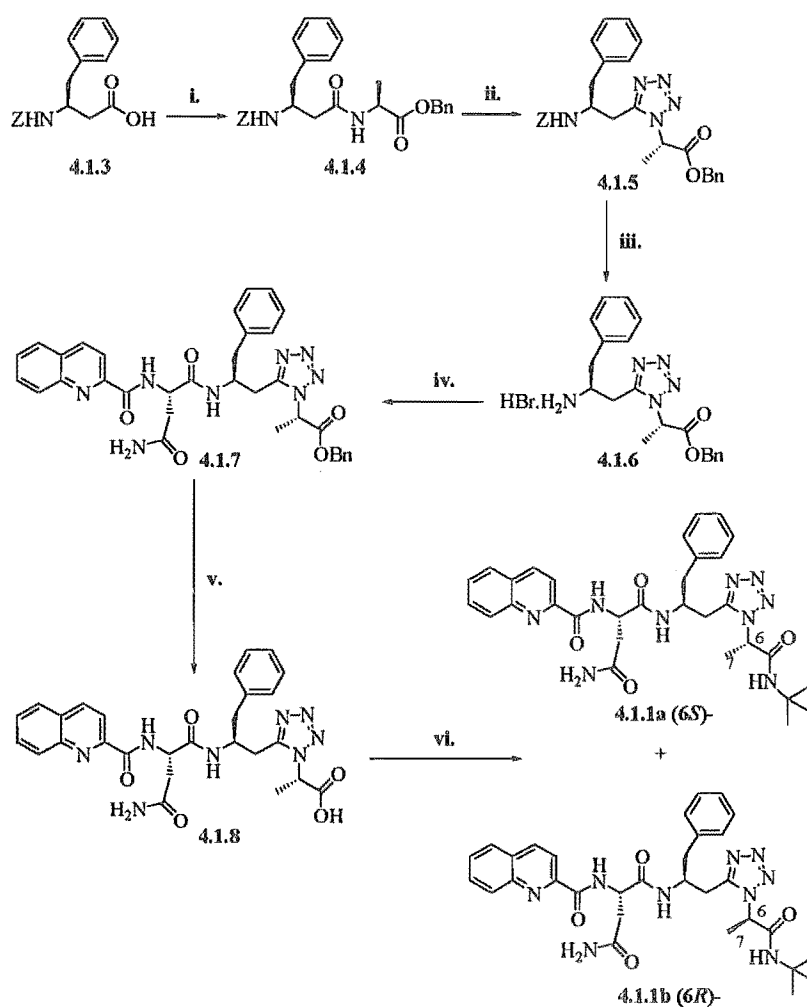
4.1. INTRODUCTION

Foulds *et al.*¹ prepared modestly potent HIVp inhibitors, 4.1.1 and 4.1.2, which incorporated the tetrazole-based *cis*- amide bond mimic (see Chapter 2.5). Inhibitor 4.1.1 incorporated the non-hydrolysable α -methylene tetrazole isostere, 2.5.1, while 4.1.2 was based around the α -hydroxymethylene tetrazole isostere, 2.5.2 (see Chapter 2.5).



Inhibitor 4.1.1 was prepared by Foulds *et al.*¹ as a 1:1 (by ¹H NMR) mixture of C6 epimers, 4.1.1a and 4.1.1b, according to Scheme 4.1.1. The core α -methylene tetrazole-based dipeptide mimic 4.1.5, was synthesised from the corresponding dipeptide, 4.1.4, by the method of Zabrocki *et al.*² Following *N*-Z-deprotection, the *N*-terminal was elongated by a BOP mediated coupling of the amine hydrobromide, 4.1.6, and *N*-(2-quinolinylcarbonyl)-*L*-asparagine to give the protected tripeptide, 4.1.7. The free acid, 4.1.8, was coupled to *tert*-butyl amine with BOP reagent in the presence of triethylamine. This final coupling step, in the preparation of 4.1.1, resulted in epimerisation at C6, to give a mixture of diastereomers, 4.1.1a and 4.1.1b (1:1 by ¹H NMR). The epimeric C6 inhibitors were separated by HPLC, and their C6 stereochemistry was assigned by ¹H NMR spectroscopy. Foulds *et al.*¹ based this stereochemical assignment on trends seen in the chemical shifts of the Ala- β -H₃ resonance of the synthetic intermediates leading to the target inhibitors 4.1.1a and 4.1.1b (Scheme 4.1.1). The Ala- β -H₃ resonances of the

(6*S*)- intermediates (Scheme 4.1.1) 4.1.5, 4.1.6, 4.1.7, 4.1.8 were δ 1.88, 1.89, 1.88, 1.91 respectively. The C6 configuration of tetrazole 4.1.1a, was assigned as (6*S*)- (the same configuration as natural *L*-alanine) as the observed Ala- β - H_3 resonance of 4.1.1a gave a similar shift to the (6*S*)- intermediates, 4.1.5-4.1.8, at δ 1.92.[†] Tetrazole 4.1.1b gave an Ala- β - H_3 resonance at δ 1.74, and was according assigned as the (6*R*)-configuration (the same configuration as unnatural *D*-alanine).[†]



Scheme 4.1.1. Reagents and conditions: i. HCl-*L*-Ala-OBn, DCC, HOBT, Et₃N, rt 18 h; ii. PCl₅, 1.5 h, HN₃, rt, 2 d; iii. 30% HBr/acetic acid, rt; iv. QC-*L*-Asn-OH, BOP, Et₃N, rt; v. H₂, 10% Pd/C, 1 atm, rt; vi. *t*-butyl amine, BOP, Et₃N, rt.

[†] The Ala- β - H_3 ¹H NMR shift of 4.1.1a was obtained in CDCl₃/TFA, while 4.1.1b was obtained in CDCl₃/CD₃OD/TFA.¹

The synthesis of inhibitor 4.1.2 also resulted in epimerisation of the C6 stereocentre and the configuration of the C6 epimers of 4.1.2 was also based on the above premise. The synthesis of inhibitor 4.1.2 was further complicated by the additional stereocentre adjacent to the tetrazole ring at C3. Foulds *et al.*¹ showed that the basic coupling conditions used in the synthesis of 4.1.2 not only epimerised the C6 stereocentre, but also epimerised the C3 stereocentre. A stereochemical assignment of the C3 centres of 4.1.2 were made using the α -hydroxy methyl esters, 3.2.5a and 3.2.5b (see Chapter 3.2) as reference compounds.

We have undertaken a systematic study of the stereochemistry of the C6 stereocentre of these compounds in an effort to unambiguously assign the configuration of this stereocentre in inhibitors, 4.1.1a and 4.1.1b, and hence related compounds. We have synthesised a series of reference compounds with defined C6 stereochemistry to establish spectral trends, to aid in the assignment of the epimeric C6 tetrazole-based inhibitors. We have also been able to monitor epimerisation of the C6 stereocentre in intermediates in the synthesis of inhibitor 4.1.1.

4.2. SYNTHESIS OF TETRAZOLE-BASED REFERENCE COMPOUNDS

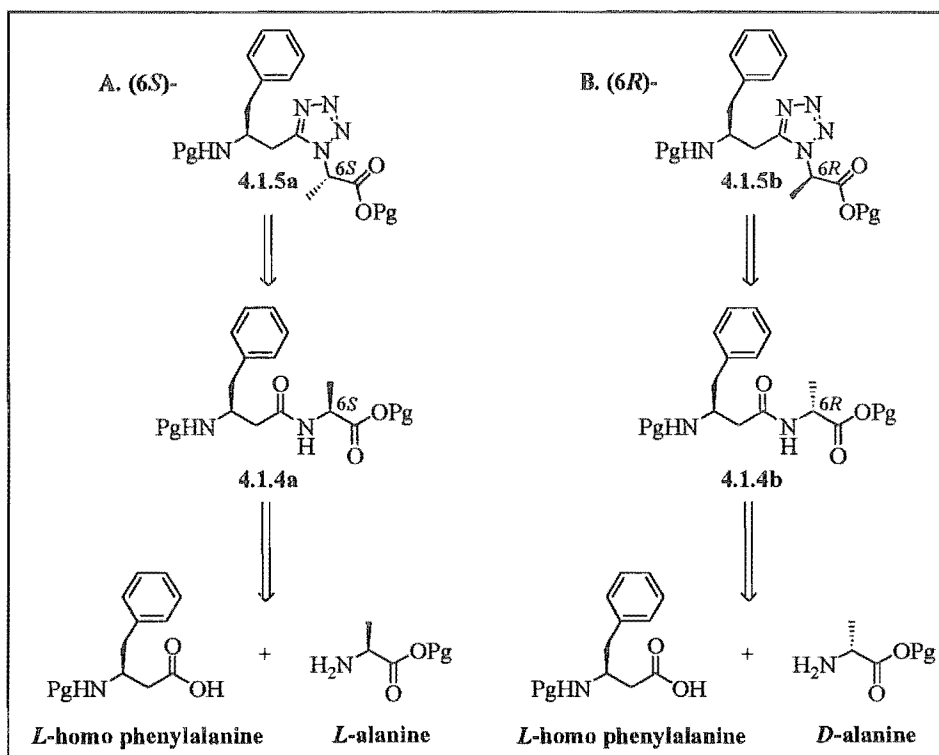


Figure 4.2.1. Retrosynthetic analysis of the target tetrazole-based dipeptide mimics 4.1.5a, and 4.1.5b.

A retrosynthetic analysis of the core tetrazole-based dipeptide mimics, 4.1.5a and 4.1.5b, with defined C6 stereochemistry is outlined in Figure 4.2.1. The stereochemistry of the C6 chiral centre was introduced from the corresponding alanine amino acid to give dipeptides, 4.1.4a [(6*S*)- derived from *L*-alanine] and 4.1.4b [(6*R*)- derived from *D*-alanine].

The tetrazole heterocycle (eg. 4.1.5 Figure 4.2.1) can be prepared from the corresponding amide (eg. 4.1.4 Figure 4.2.1) by reaction with phosphorous pentachloride (PCl_5), to give an imidoyl chloride intermediate, which is subsequently reacted *in situ* with hydrozoic acid (HN_3), according to the method of Zabrocki *et al.*² A protecting group strategy was chosen to reflect the requirements of the tetrazole forming reaction and be amenable to *N*- and *C*-terminal elongations, by standard peptide synthesis.

The inhibitors 4.1.1a and 4.1.1b (Scheme 4.1.1) have been synthesised to incorporate the non-hydrolysable α -methylene tetrazole isostere (2.5.1). This isostere is derived from the unnatural homologated amino acid, *L*-homophenylalanine, 4.1.3 (Figure 4.2.2). Arndt-Eistert homologation of an *N*-protected α -amino acid, via an α -diazoketone, is a widely used method for the preparation of enantiomerically pure β -amino acids such as 4.1.3 from relatively cheap α -amino acid starting materials. Two routes can be employed for the synthesis of *N*-protected *L*-homophenylalanine containing dipeptides, either; Arndt-Einstert homologation utilising a silver (I) catalysed rearrangement in the presence of water as the trapping nucleophile (Figure 4.2.2 I), to generate β -amino acids (eg. 4.1.3), which can subsequently be coupled; or a photochemical or silver (I) catalysed rearrangement in the presence of an amino acid, to generate the homologated *L*-amino acid, with comittant peptide coupling (eg. 4.1.4 Figure 4.2.2 III).^{3,4} Both methods require the synthesis of the α -diazoketone, 3.4.1 (Figure 4.2.2). Ketene rearrangement in the presence of an alcohol (R_2OH) can also be

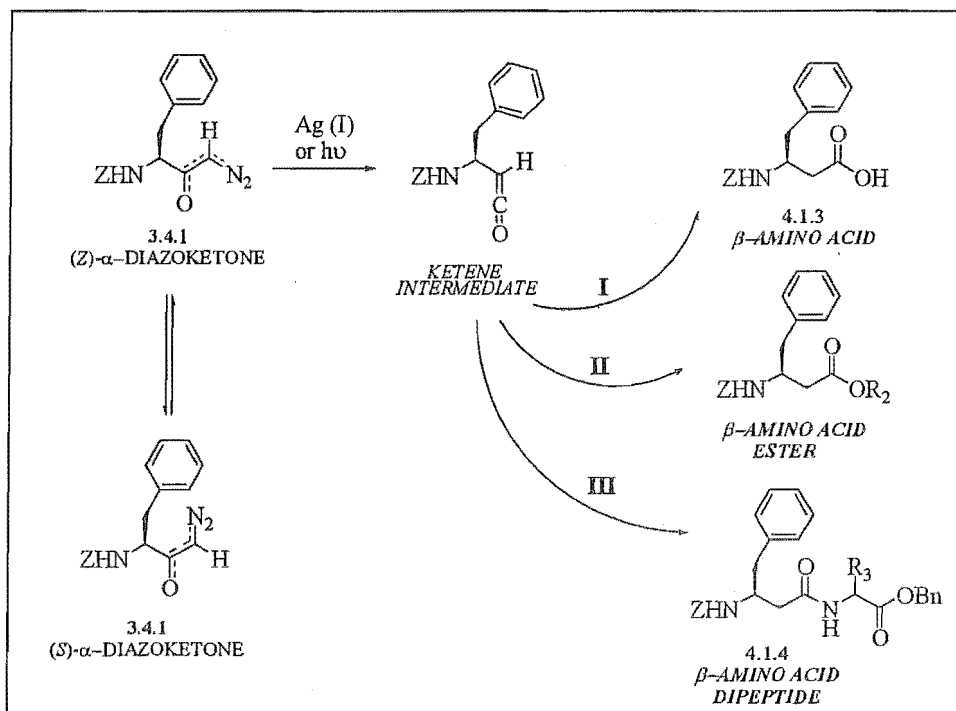


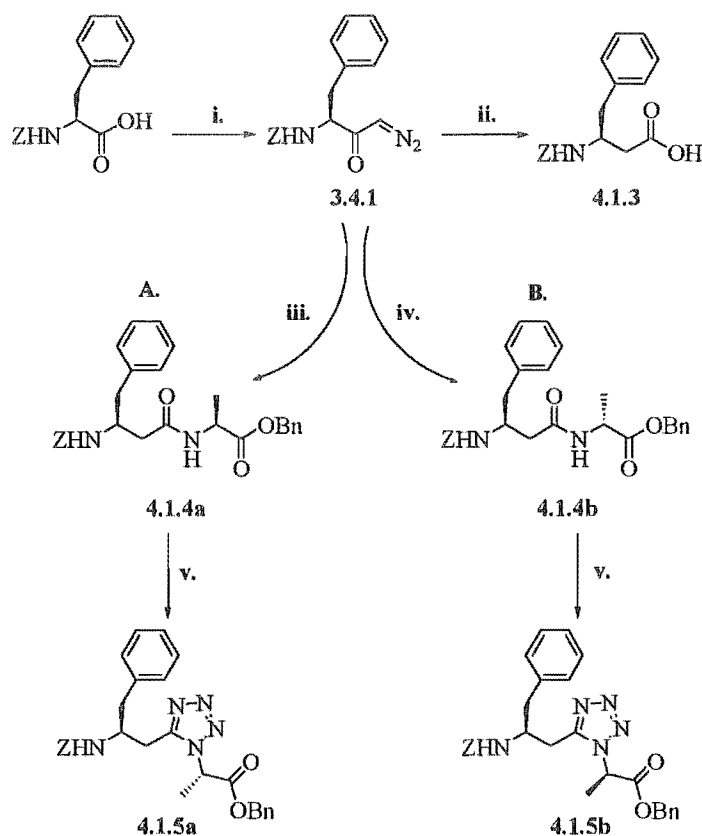
Figure 4.2.2. Wolff rearrangement of an α -diazoketone amino acid. $Ag(I)$ catalysed Arndt-Einstert homologation (I) in the presence of water; synthesis of β -amino acid esters by Wolff rearrangement in the presence of an alcohol (R_2OH) (II); photochemically catalysed Wolff rearrangement with comittant peptide coupling (III).

acid esters (Figure 4.2.2 II).

The Wolff rearrangement of α -diazoketones containing a chiral centre adjacent to the carbonyl occurs with retention of configuration.⁵ The rearrangement of α -diazoketones (Figure 4.2.2) proceeds via a ketene intermediate, with elimination of the nitrogen and alkyl group migration. Thermal initiation of the reaction is catalysed by metal ions such as silver (I), or the rearrangement can be photochemically catalysed. A concerted mechanism has been proposed for the ketene formation,⁶ from the (*Z*) form of the α -diazoketone (3.4.1 Figure 4.2.2), where the leaving group N_2 and migrating group are in an ideal antiperiplanar geometry. The ketene intermediate can then be trapped by a variety of nucleophiles (Figure 4.2.2 I-III).

The α -diazoketone 3.4.1 (Scheme 4.2.1), can be prepared via the acid chloride of the *L*-amino acid,⁷ however, attempts to form the acid chloride of *N-Z-L*-phenylalanine usually results in formation of the undesired cyclic *N*-carboxyanhydride.¹ We have used an alternative procedure for the preparation of *N-Z*-protected *L*-amino acid α -diazoketone, 3.4.1, via the corresponding mixed anhydride.⁸ Treatment of *N-Z-L*-phenylalanine with ethyl chloroformate and triethylamine (Scheme 4.2.1), followed by an *in situ* reaction of the mixed anhydride intermediate with diazomethane, gave the desired α -diazoketone, 3.4.1, in 70% yield.

The α -diazoketone, 3.4.1, was then dissolved in dioxane/water and heated in the presence of silver (I) oxide to give *N-Z-L*-homophenylalanine, 4.1.3, in 68% yield (Scheme 4.2.1). Foulds *et al.*¹ coupled the free acid, 4.1.3, to *L*-alanine benzyl ester to give the desired dipeptide intermediate, 4.1.4a (Scheme 4.1.1). We have used a more direct route to the dipeptide intermediates, by using a Wolff rearrangement of 3.4.1 with comittant peptide coupling (Figure 4.2.2 III), to furnish the dipeptides 4.1.4a and 4.1.4b. A solution of α -diazoketone, 3.4.1, and *L*-alanine benzyl ester in acetonitrile, was irradiated at 300 nm in the presence of triethylamine (Scheme 4.2.1 A). Following flash column chromatography, the dipeptide, 4.1.4a was isolated in 61% yield as a cream solid. Similarly, 3.4.1 was reacted photochemically with *D*-alanine benzyl ester (Scheme 4.2.1 B) to give dipeptide 4.1.4b, in 65% yield.



Scheme 4.2.1. Reagents and conditions: i. EtCOCl, Et₃N, -20 °C, 15 min, then, CH₂N₂, 5 °C, 18 h; ii. Ag₂O, Na₂CO₃, Na₂S₂O₃, 78-85 °C, 2 h; iii. HCl.L-Ala-OBn, Et₃N, 300 nm, rt, 24 h; iv. pTsOH.D-Ala-OBn, Et₃N, 300 nm, rt, 24 h. v. PCl₅, quinoline, HN₃, rt.

Having synthesised the key dipeptide intermediates, 4.1.4a and 4.1.4b, we focused on converting these protected dipeptides to the desired α -methylene tetrazole dipeptides, 4.1.5a and 4.1.5b (Scheme 4.2.1). Several methods for the conversion of amides into 1,5-disubstituted tetrazoles have been published in the literature and are summarised in Figure 4.2.3. Thomas⁹ synthesised simple 1,5-dialkyl tetrazoles by reacting the corresponding amide with trifluoromethanesulphonic anhydride, to form an imidoyl triflate, which was subsequently reacted *in situ* with sodium azide to furnish a 1,5-disubstituted tetrazole (Figure 4.2.3 A). Duncia *et al.*¹⁰ employed triphenylphosphine and diethyl azodicarboxylate to activate an amide toward reaction with trimethylsilyl

azide, to yield 1,5-disubstituted tetrazoles (Figure 4.2.3 B). Yu and Johnson¹¹ have studied the conversion of dipeptides to the corresponding 1,5-disubstituted tetrazoles. The reaction proceeded via an imidoyl chloride from reaction of the amide with phosphorous pentachloride. The imidoyl chloride was then reacted *in situ* with hydrazoic acid to give a 1,5-disubstituted tetrazole (Figure 4.2.3 C). Zabrocki *et al.*² have further extended the methodology of Yu and Johnson by adapting the synthesis to exert stereocontrol over the product tetrazoles by the simply addition of quinoline to the reaction mixture. We have used the method of Zabrocki *et al.*² for the synthesis of the tetrazole-based dipeptides, 4.1.5a and 4.1.5b (Scheme 4.2.1).

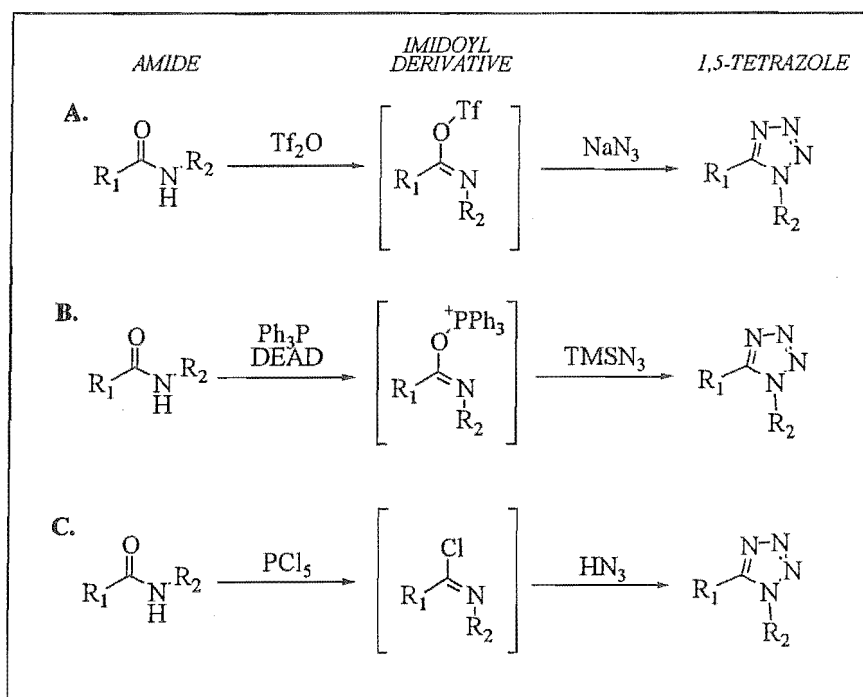


Figure 4.2.3. Methods for the preparation of 1,5-disubstituted tetrazoles from amides; A. trimethylsulphonic anhydride (Tf_2O), sodium azide;⁹ B. triphenylphosphine (Ph_3P), diethyl azodicarboxylate (DEAD), trimethylsilylazide (TMSN_3);¹⁰ C. phosphorous pentachloride (PCl_5), hydrazoic acid (HN_3).¹¹

Both Yu and Johnson¹¹ and Zabrocki *et al.*¹ reported that treatment of a protected dipeptide with phosphorous pentachloride and hydrazoic acid led to epimerisation of the

carbon centres adjacent to the tetrazole ring. The use of phosphorous pentachloride to convert the amide bond to the imidoyl chloride, leads to acid catalysed epimerisation at C2 by the proposed mechanism shown in Figure 4.2.4. A reversible elimination of the 2-H proton of 4.2.2 (Figure 4.2.4) to form the dipeptide ketene imine hydrochloride, 4.2.3, leads to scrambling of the C2 stereocentre. The 2-H proton is more acidic in the hydrochloride 4.2.2, than in 4.2.1, and therefore the simple addition of an organic base such as quinoline to the reaction when generating the imidoyl chloride, was shown to prevent the acid-catalysed epimerisation of the C2 stereocentre.

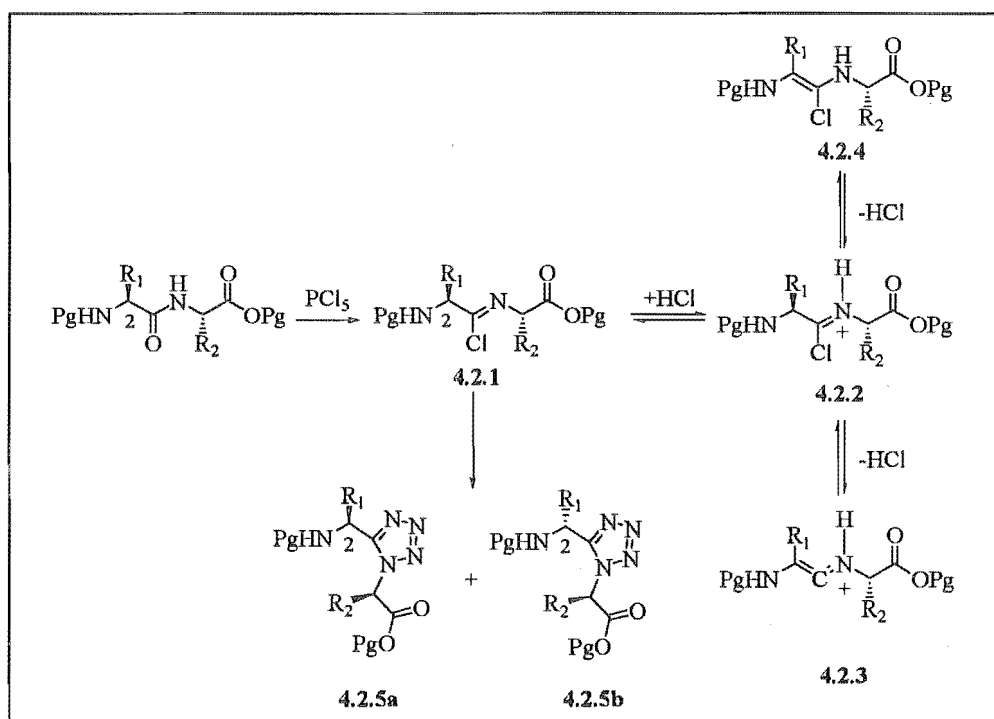


Figure 4.2.4. Acid catalysed epimerisation during tetrazole formation.²

The resulting tetrazole dipeptides (eg. 4.1.5a and 4.1.5b) are base sensitive and both the C3 and C6 stereocentres have been shown to epimerise in mildly basic conditions. Therefore the choice of acidolytic protecting groups is crucial to maintain the chiral integrity of these stereocentres. Zabrocki *et al.*² favoured the use of *N*-Z- and *N*-phthalyl protected dipeptides as the formation of the tetrazole was shown to favor aromatic *N*-terminal protection. Aromatic *C*-terminal protection was favoured over alkyl ester protection, with methyl ester protected dipeptides giving greatly reduced yields of

the corresponding tetrazoles.¹² Studies by Yu and Johnson¹¹ suggested that the yield of tetrazole was dependent not only on the choice of *N*- and *C*-terminal protection, but also the nature of the amino acid residues of the dipeptide. Dipeptides with bulky amino acid side-chains gave low yields of the tetrazole, probably due to unfavorable *cis*-1,4 steric interactions in the transition intermediates leading to the tetrazole product. Glycine containing dipeptides also gave low yields of the corresponding 1,5-disubstituted tetrazoles.

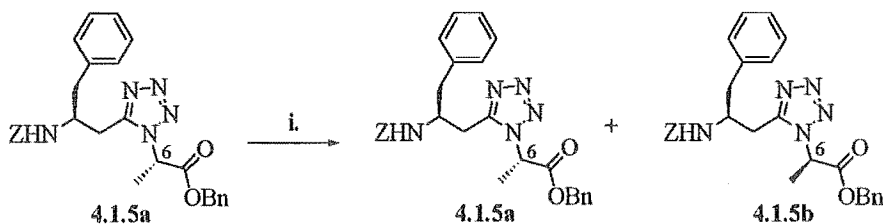
Boteju and Hruby¹² used a modified procedure to prepare tetrazoles containing bulky tryptophan residues. The modifications involved longer reaction times and the use of an additional portion of phosphorous pentachloride in the formation of the imidoyl chloride intermediate. With the longer reaction times higher yields were reportedly obtained, while the shorter reaction times reported by Zabrocki *et al.*² resulted in the recovery of a higher percentage of starting dipeptide.

For the preparation of tetrazoles 4.1.5a and 4.1.5b (Scheme 4.2.1) we have used *N*-*Z*-protection, and benzyl ester protection of the *C*-terminal, following the criteria outlined by Zabrocki *et al.*² Selective removal of *N*-*Z*-protection by reaction with hydrobromic acid in the presence of the acid stable benzyl ester, is part of an orthogonal protecting group strategy that is amenable to the synthesis of tetrazole dipeptides.

The conversion of the protected dipeptides 4.1.4a and 4.1.4b into the corresponding tetrazole-based dipeptides, 4.1.5a and 4.1.5b followed the modified method of Boteju and Hruby.¹² Quinoline was added to the reaction mixture even though there was no stereocentre adjacent to the amide bond at C3 in 4.1.4a, or 4.1.4b. The addition of base in the synthesis of tetrazoles via imidoyl chlorides is known to accelerate the reaction.¹³ This is supported by the work of Zabrocki *et al.*² which showed that the addition of quinoline to the reaction mixture not only prevented epimerisation of the C2 stereocentre (4.2.1 Figure 4.2.4), but also increased the yield of the reaction. The dipeptide, 4.1.4a was added slowly to a stirred chloroform solution of phosphorous pentachloride and quinoline (Scheme 4.2.1 A). After 1 hour an additional portion of phosphorous pentachloride was added. A total reaction time of 3.5 hours was allowed for conversion of the dipeptide to the imidoyl chloride. At this time a benzene or chloroform solution of hydrazoic acid was added and stirring continued for 48 hours. The tetrazole,

4.1.5a was purified, first by radial chromatography, then by reverse-phase HPLC to give 4.1.5a in 10% yield, as a single stereoisomer by ^1H NMR. Similarly, the dipeptide 4.1.4b was converted to the protected tetrazole, 4.1.5b (Scheme 4.2.1 B), and obtained in 15% yield following radial chromatography and reverse-phase HPLC.

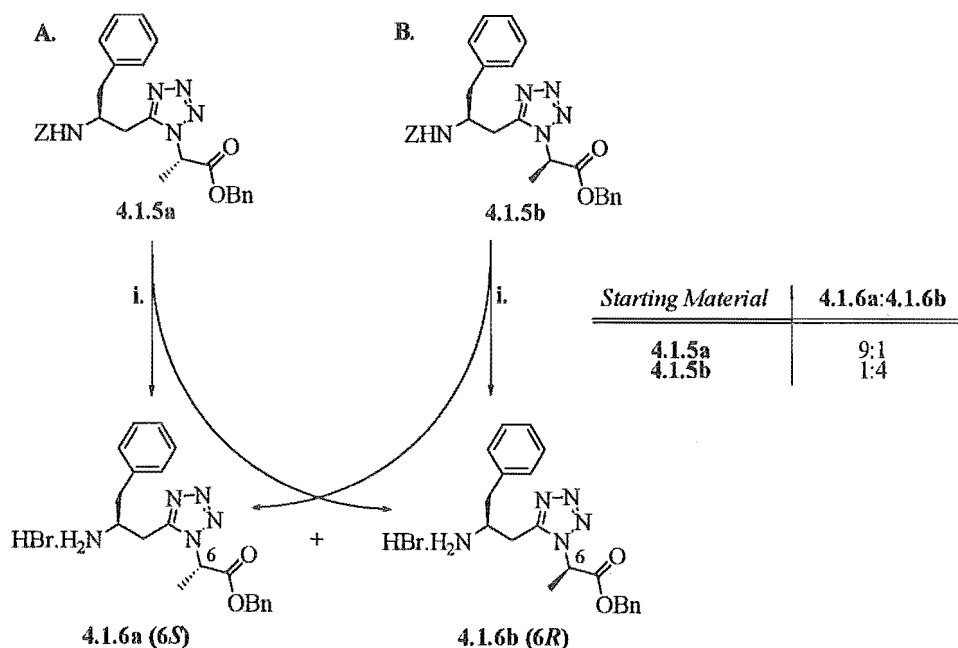
Zabrocki *et al.*² reported that the *C*-terminal stereocentre adjacent to the tetrazole ring readily undergoes epimerisation in the presence of triethylamine. We have epimerised tetrazole 4.1.5a to confirm the structure of the C6 epimer, 4.1.5b (Scheme 4.2.2). A sample of tetrazole 4.1.5a was dissolved in 10% triethylamine/ CDCl_3 , and epimerisation of the C6 stereocentre was monitored by ^1H NMR. After 48 hours at room temperature complete epimerisation of tetrazole 4.1.5a had occurred to give a mixture of diastereomeric tetrazoles, 4.1.5a and 4.1.5b (1:1 by ^1H NMR). The tetrazoles were separated by plate layer chromatography. Tetrazole 4.1.5a was collected from a higher R_f band in 17% yield, while tetrazole 4.1.5b ran as a lower R_f band and was obtained in 20% yield. The ^1H NMR and ^{13}C NMR of tetrazole 4.1.5b were identical to that obtained by direct synthesis from dipeptide 4.1.4b (Scheme 4.2.1).



Scheme 4.2.2. Reagents and conditions: i. Et_3N , CDCl_3 , rt, 48 h.

Having synthesised the key tetrazole-based dipeptide mimics, 4.1.5a and 4.1.5b, we focused on elongating the *N*-terminal of the dipeptides to generate reference compounds for spectral comparison with the tetrazole-based inhibitors, 4.1.1 and 4.1.2. Firstly, the preferential removal of the *N*-Z-protection in the presence of the benzyl ester *C*-terminal protecting group, was necessary to enable extension of the tetrazole dipeptides through coupling of the free amines. Acidic cleavage of the *N*-Z-protection with hydrobromic acid to give the deprotected dipeptides followed a well established deprotection method (Scheme 4.2.3).¹⁴ Tetrazole dipeptide, 4.1.5a, was dissolved in

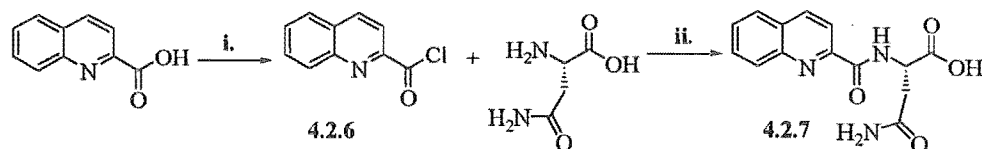
concentrated acetic acid and the solution treated with a 50% hydrobromic acid/acetic acid solution (Scheme 4.2.3 A). The reaction was stirred at room temperature for 30 minutes, then triturated with ether/petroleum ether. The hydromide salt was dried *in vacuo* for 24 hours to give the product dipeptide in 90% yield, as a mixture of C6 epimers, 4.1.6a and 4.1.6b (9:1 by ^1H NMR). The same deprotection protocol was used for tetrazole dipeptide, 4.1.5b, and gave an epimeric mixture of 4.1.6b and 4.1.6a (4:1 by ^1H NMR), in 89% yield (Scheme 4.2.3 B). In both cases the major isomer is assumed to have the same absolute C6 configuration as the starting material. The epimeric hydrobromides, 4.1.6a and 4.1.6b, were used without further purification.



Scheme 4.2.3. Reagents and conditions: i. CH_3COOH , 50% $\text{HBr}/\text{CH}_3\text{COOH}$, rt, 30 min.

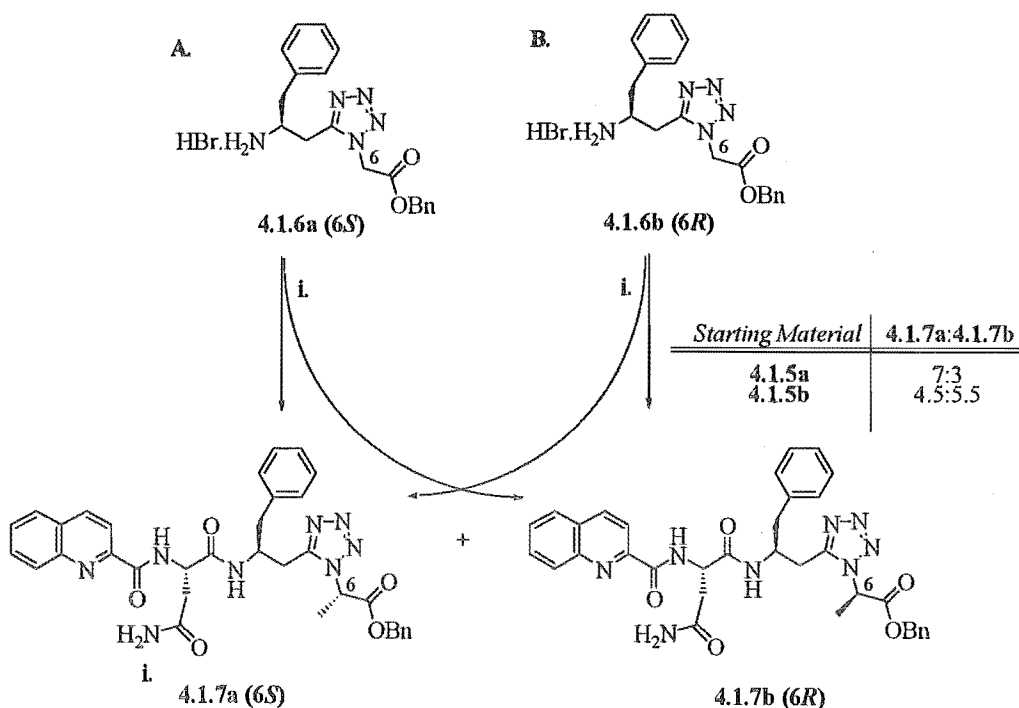
To model the original tetrazole-based HIVp inhibitors, 4.1.1 and 4.1.2, the amine hydrobromides, 4.1.6a and 4.1.6b, were elongated from the *N*-terminal by coupling to *N*-(2-quinolinylcarbonyl)-*L*-asparagine (QC-*L*-Asn-OH), 4.2.7 (Scheme 4.2.4). This *N*-protected *L*-amino acid was synthesised in a simple one-pot reaction of quinaldic acid chloride, using *L*-asparagine under modified Schotten-Baumann conditions,¹⁵ according to the procedure of Camp *et al.*¹⁶ Quinaldic acid chloride, 4.2.6, was prepared from the reaction of thionyl chloride with quinaldic acid in the presence of triethylamine (Scheme

4.2.4). The crude acid chloride, 4.2.6, was then reacted *in situ* with *L*-asparagine in the presence of potassium carbonate. Work-up and a single recrystallisation from ethanol gave the free acid, 4.2.7, in 40% yield.



Scheme 4.2.4. Reagents and conditions: i. thionyl chloride, Et₃N, rt, 3 h; ii. K₂CO₃, rt, 4 h.

The amine hydrobromide, 4.1.6a, as a mixture of C6 epimers (9:1 4.1.6a:4.1.6b, by ¹H NMR) was coupled to 4.2.7 by a standard BOP mediated coupling procedure in the presence of triethylamine (Scheme 4.2.5 A). The crude reaction product was purified by plate layer chromatography to give the protected tripeptide, 4.1.7, as a mixture of C6 epimers, 4.1.7a and 4.1.7b (7:3 by ¹H NMR). Similarly, hydrobromide 4.1.6b, as an epimeric mixture (4:1 4.1.6b:4.1.6a), was coupled to *N*-(2-quinolinylcarbonyl)-*L*-asparagine, 4.2.7 (Scheme 4.2.5 B). Purification of the crude protected tripeptide by plate layer chromatography gave the epimeric tripeptides, 4.1.7b and 4.1.7a (5.5:4.5 by ¹H



Scheme 4.2.5. Reagents and conditions: i. QC-*L*-Asn-OH (4.2.7), BOP, Et₃N, rt, 18 h.

NMR). In both cases it was assumed that the major isomer of the product mixtures had the same absolute configuration as the major isomer of the starting material.

Further elongation of the *C*-terminal was considered futile because of the known epimerisation at C6 that had occurred during the synthesis of inhibitors 4.1.1a and 4.1.1b (Scheme 4.1.1).¹ Based on these earlier results it would be expected, for example, that *C*-terminal deprotection, and subsequent coupling of 4.1.7a would give a 1:1 mixture of the coupled products, 4.1.1a and 4.1.1b (Scheme 4.1.1).

A spectral analysis of the epimeric reference compounds was undertaken to establish trends in the chemical shifts of the 6*S* and 6*R* compounds.

4.3. NMR STUDIES ON THE TETRAZOLE-BASED REFERENCE COMPOUNDS

The reference tetrazole compounds 4.1.4a-4.1.7a and 4.1.4b-4.1.7b were characterised by ¹H NMR and ¹³C NMR to establish differences in the NMR spectra between these epimeric reference compounds. Epimerisation of the C6 stereocentre was also detected by ¹H NMR in the synthesis of intermediate tetrazoles, 4.1.6 and 4.1.7.

Studies by Yu and Johnson¹¹ on the conversion of protected dipeptides to the corresponding tetrazole dipeptides showed characteristic differences between the ¹H and ¹³C NMR spectra of the starting dipeptide and the 1,5-disubstituted tetrazole product. We have noted similar spectral distinctions in the formation of tetrazoles 4.1.5a and 4.1.5b from the dipeptides, 4.1.4a and 4.1.4b. Typically the tetrazole products are less polar than the starting dipeptides and elute on silica at a higher R_f. The formation of the tetrazole ring was evidenced by the disappearance of the amide carbonyl carbon resonance (hPhe-CO) typically observed at δ 170 and the appearance of a new signal corresponding to the tetrazole (hPhe-CN₄) carbon at δ 150-155. The Ala-α-CH signal of the tetrazole product was shifted downfield in the order of 8-10 ppm, to around δ 56, in comparison with the Ala-α-CH signal of the dipeptide. Additionally, the Ala-α-CH₃ carbon resonance was shifted upfield 2-3 ppm to δ 16-17 in the tetrazole product. The methylene carbon signal, hPhe-α-CH₂, was shifted upfield in the order of 8-13 ppm. An example of the observed

changes in the ^{13}C NMR spectra is shown in Figure 4.3.1, where the key changes in the ^{13}C NMR resonances have been annotated by a broad arrow.

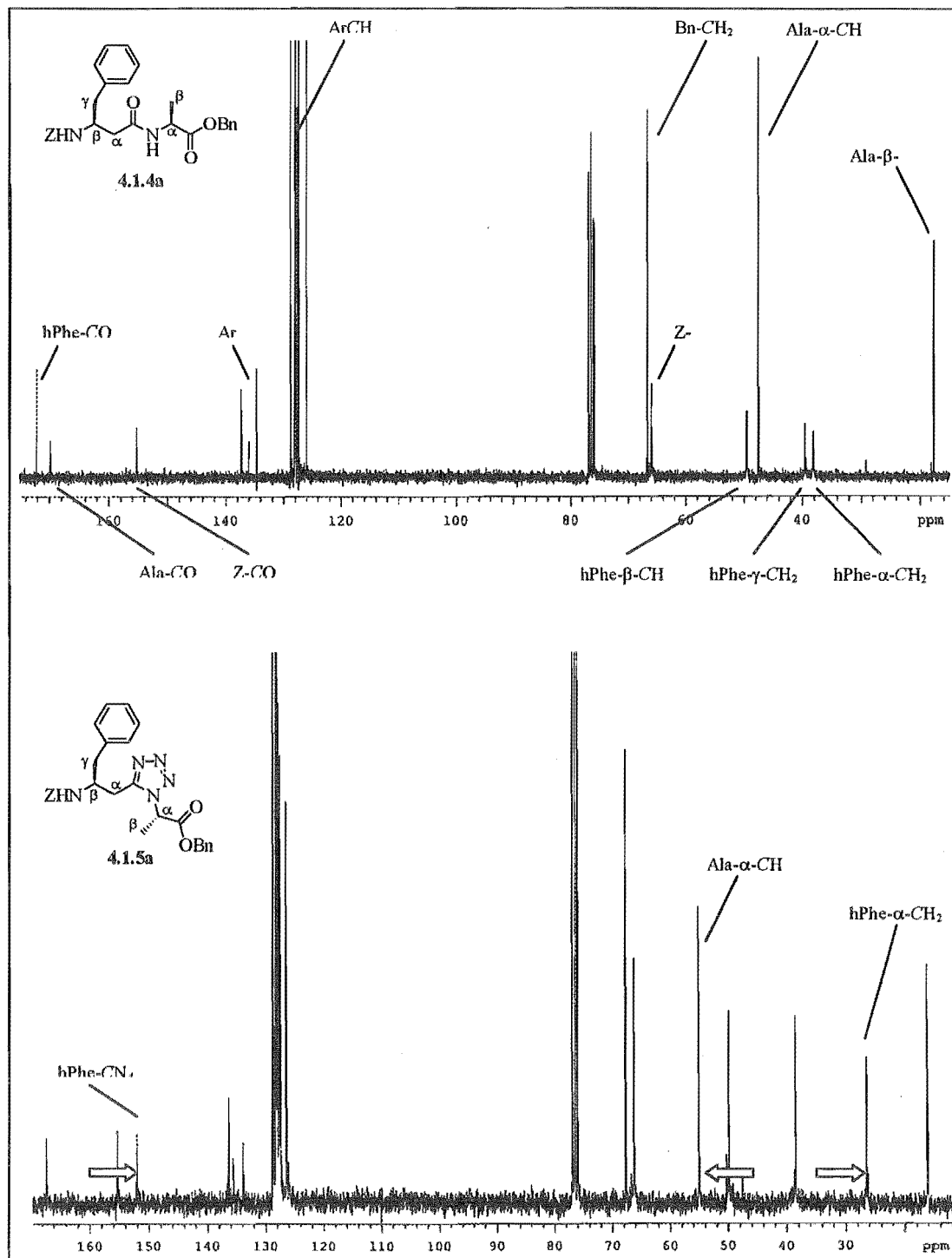


Figure 4.3.1. Representative ^{13}C NMR spectra for the dipeptide 4.1.4a, and the tetrazole dipeptide 4.1.5a, showing diagnostic shift differences between the two compounds.

The ^1H NMR spectrum of the dipeptide was also characteristically different to the ^1H NMR spectrum of the corresponding 1,5-disubstituted tetrazole. The Ala- $\beta\text{-H}_3$ and Ala- $\alpha\text{-H}$ signals were shifted downfield, 0.4-0.5 ppm and 0.4-0.6 ppm, respectively relative to the starting dipeptide. Likewise, the hPhe- $\alpha\text{-H}_2$ resonances were shifted downfield 0.5-1.0 ppm. An example of the observed ^1H NMR differences are annotated in Figure 4.3.2, as indicated by the broad arrows.

The resonance shifts are presumably associated with differences in the electron density between the amide bond and the tetrazole heterocycle (Figure 4.3.3). The N5 lone pair of electrons are delocalised throughout the heterocycle, thus it is relatively more electron deficient than the nitrogen of the amide bond. Correspondingly, the 6-CH carbon centre of the tetrazole shows ^1H and ^{13}C NMR signals that are shifted downfield relative to the starting dipeptide. The delocalisation of the N5 electrons also makes the hPhe- CN_4 carbon centre more electron rich relative to the carbonyl of the amide bond (hPhe-CO). The C3 carbon centre of the tetrazole shows ^1H and ^{13}C NMR resonances (hPhe- $\alpha\text{-CH}_2$) that are shifted up-field relative to the starting dipeptide to reflect this increase in electron density.

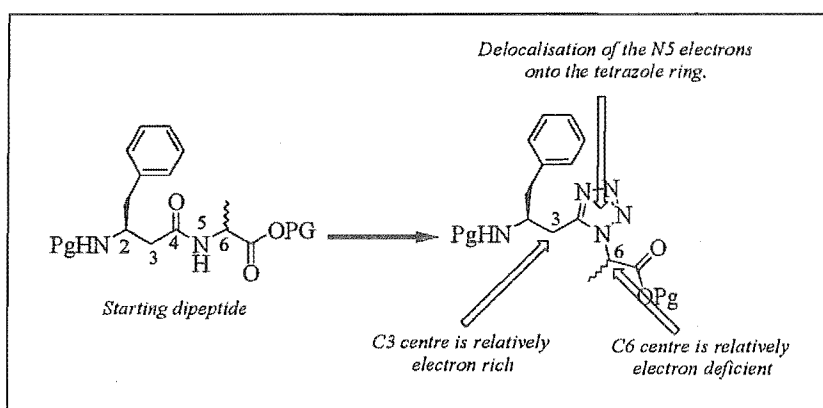


Figure 4.3.3. Rationalising the observed changes in the chemical shifts between the starting dipeptide, and the tetrazole-based dipeptide.

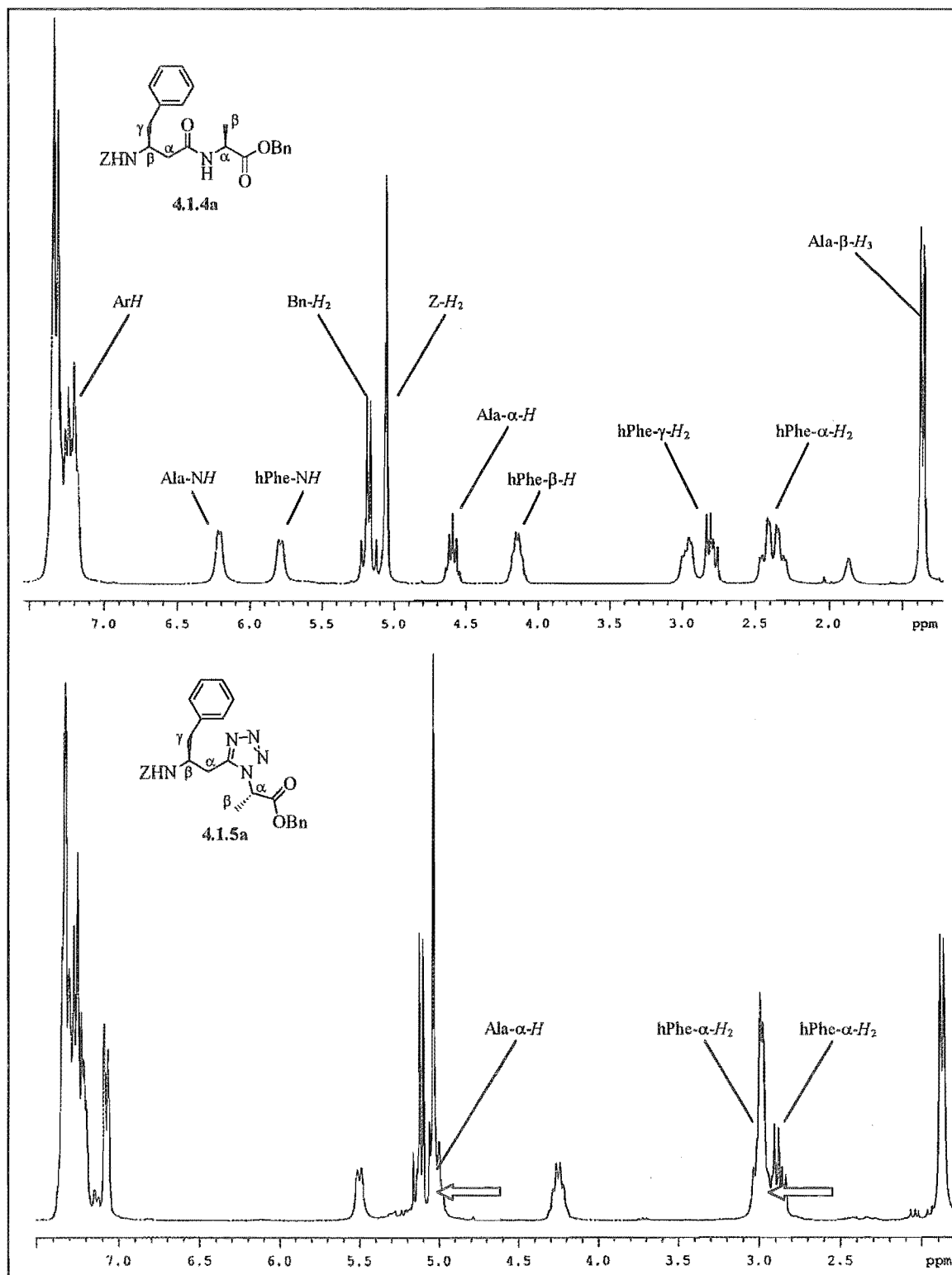


Figure 4.3.2. Representative ¹H NMR spectra for the dipeptide 4.1.4a, and the tetrazole dipeptide 4.1.5a, showing diagnostic shift differences between the two compounds.

We have synthesised two series (A and B) of tetrazole-based reference compounds with defined C6 configuration (Table 4.3.1) to investigate whether there are any distinguishable trends in the ^1H and ^{13}C NMR spectra of these compounds. It is thought that the observed trends in NMR spectra could be used to unambiguously assign the C6 configuration of other tetrazole-based peptidomimetics, (eg. 4.1.1 and 4.1.2). Compounds of series A (4.1.4a-4.1.7a Table 4.3.1) have defined (6*S*)-configuration derived from natural *L*-alanine, while the compounds of series B (4.1.4b-4.1.7b Table 4.3.1), have defined (6*R*)-configuration, derived from unnatural *D*-alanine.

Foulds *et al.*¹ assigned the C6 configuration of tetrazole-based inhibitors 4.1.1 and 4.1.2 on the assumption that the (6*S*) Ala- β - H_3 ^1H NMR resonances were in a characteristic downfield position (1.86-1.92 ppm) relative to the corresponding (6*R*)-configuration (see Chapter 4.1). At each stage of the synthesis of the reference tetrazole-based compounds a NMR comparison has been made between the diastereomeric compounds of series A and series B.[‡] We have compared the ^1H and ^{13}C NMR resonances of Ala- β - CH_3 and Ala- α - CH , and summarised these in Table 4.3.1.

[‡] For comparison between epimeric reference compounds (series A vs. series B) ^1H and ^{13}C NMR spectra were obtained in identical deuterated solvents (see Chapter 9.3).

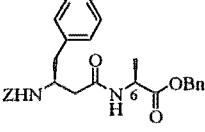
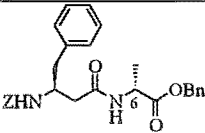
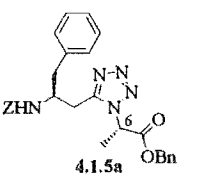
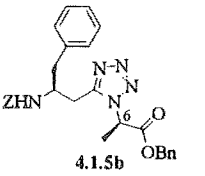
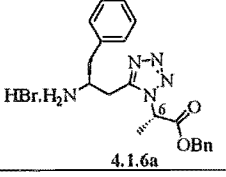
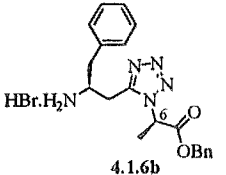
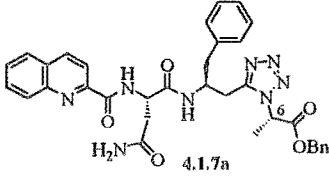
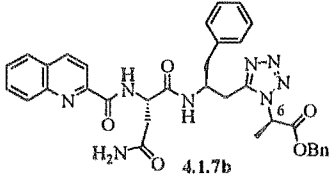
	Ala- β -H ₃	Ala- α -H	Ala- β -CH ₃	Ala- α -CH
 4.1.4a	1.36	4.59	18.01	48.05
 4.1.4b	1.39	4.60	18.15	48.09
 4.1.5a	1.87	5.00	16.80	55.92
 4.1.5b	1.87	5.15	16.66	55.53
 4.1.6a	1.89	5.67	16.81	57.43
 4.1.6b	1.91	5.69	16.96	57.55
 4.1.7a	1.92	5.21	16.25	55.49
 4.1.7b	1.97	5.37	16.33	55.54

Table 4.3.1. Comparison of the ¹H and ¹³C NMR resonances of the (6*S*)-, and (6*R*)-diastereomers.

Significant differences do not appear in the chemical shifts of the ^1H NMR signals of diastereomeric compounds of series A and series B. Reference compounds from series B with (6*R*)-configuration gave Ala- β - H_3 and Ala- α - H resonances that were typically downfield of the (6*S*)-epimer in the order of 0.01-0.03 ppm and 0.01-0.15 ppm, respectively. Differences in the ^{13}C NMR of related compounds were more diagnostic. Typically the compounds with (6*R*)-configuration (4.1.4b, 4.1.6b, 4.1.7b) gave Ala- β - CH_3 resonances downfield (0.10-0.15 ppm) compared to their (6*S*)-epimers. However, this trend was reversed for the protected tetrazoles, 4.1.5a and 4.1.5b, with the Ala- β - CH_3 resonance of 4.1.5a being downfield (0.15 ppm) of the corresponding resonance of 4.1.5b. This reversal in the trend was also seen in the Ala- α - CH resonance of 4.1.5a, being 0.41 ppm downfield of its (6*R*)-epimer, 4.1.5b. The Ala- α - CH resonances of the series B compounds were typically 0.02-0.12 ppm downfield of the series A (6*S*)-epimers.

The difference in NMR shifts between the diastereomeric reference compounds was very subtle and in some cases the shift difference was negligible. However, a trend is seen in the NMR resonances of the reference compounds. Tetrazoles with the (6*R*)-configuration (ie. 4.1.4b-4.1.7b), characteristically gave Ala- β - CH_3 and Ala- α - CH NMR resonances (^1H and ^{13}C) that were downfield of the corresponding (6*S*)-epimer (ie. 4.1.4a-4.1.7a).

During the synthesis of the reference tetrazole-based compounds we were able to monitor the extent of epimerisation of the C6 stereocentre under the reaction conditions used for the synthesis of inhibitor 4.1.1. Epimerisation of the C6 centre has been detected much earlier in this synthetic sequence than was reported by Foulds *et al.*,¹ who observed epimerisation at C6 only in the final coupling step in the preparation of inhibitor, 4.1.1 (Scheme 4.1.1). We have observed epimerisation of the C6 stereocentre during two key steps in the synthesis of the reference tetrazole-based compounds, as evidenced by the ^1H NMR spectra of the product mixtures (Figure 4.3.4). Detectable epimerisation of C6 occurred during *N*-Z-deprotection of tetrazoles, 4.1.5a and 4.1.5b. Treatment of 4.1.5a with 50% hydrobromic acid/acetic acid gave a 9:1 mixture (by ^1H NMR) of C6 epimers, 4.1.6a and 4.1.6b (Scheme 4.2.2). Similarly treatment of 4.1.5b under identical conditions resulted in a 1:4 mixture (by ^1H NMR) of 4.1.6a and 4.1.6b. Coupling of the

hydrobromide salts (4.1.6a and 4.1.6b), in the presence of triethylamine resulted in further epimerisation of the C6 centre (Scheme 4.2.3). The coupling of hydrobromide, 4.1.6a, with BOP reagent in the presence of triethylamine gave a 7:3 mixture (by ^1H NMR) of the diastereomeric protected tripeptides, 4.1.7a and 4.1.7b. Coupling of hydrobromide, 4.1.6b to *N*-(2-quinolinylcarbonyl)-*L*-asparagine, under the same reaction conditions gave a 5.5:4.5 mixture (by ^1H NMR) of diastereomers, 4.1.7b and 4.1.7a.

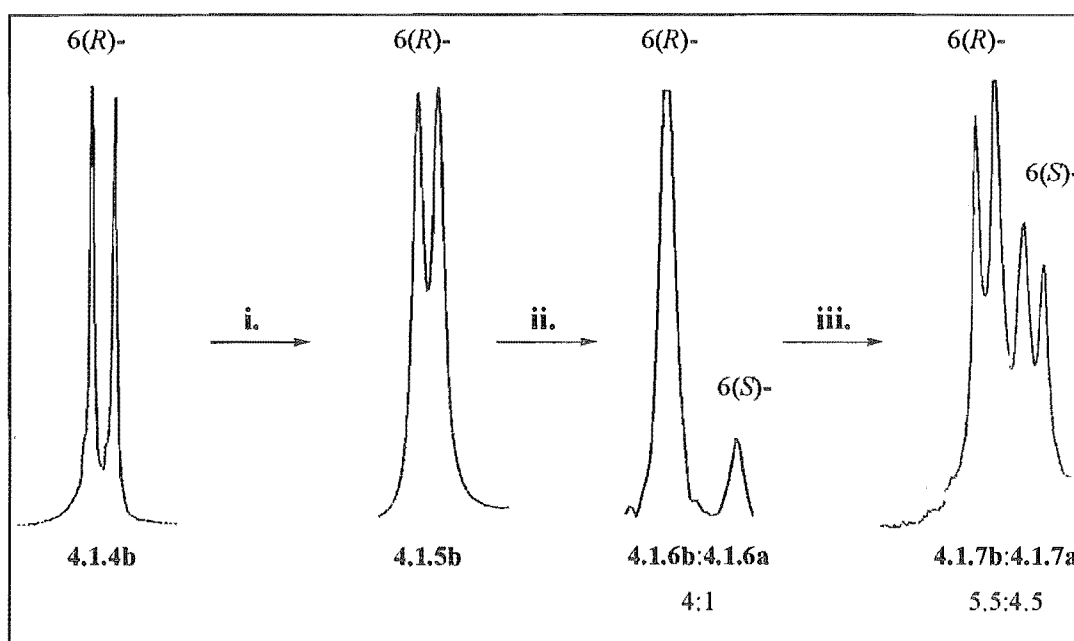


Figure 4.3.4. Ala- β - H_3 ^1H NMR resonance showing epimerisation of the C6 stereocentre. Reagents and conditions: i. PCl_5 , HN_3 , quinoline, rt, 2 d; ii. 50% HBr /acetic acid, rt, 30 min; iii. BOP, Et_3N , QC-*L*-Asn-OH, rt, 18 h.

4.4. CONCLUSION

The synthesis of the tetrazole-based reference compounds has allowed trends to be established in the relative ^1H and ^{13}C NMR chemical shifts of the diastereomeric tetrazole-based reference compounds. Although differences between the epimeric tetrazole-based reference compounds of series A and B were only subtle it can be seen that the reference compounds with a (6*R*)-configuration (series B) gave Ala- α -CH and Ala- β - CH_3 ^1H and ^{13}C NMR resonances that are typically downfield of the corresponding (6*S*)-epimers. The results obtained here are in contrast to the stereochemical assignment

tentatively made by Foulds *et al.*¹ of the tetrazole-based inhibitors, 4.1.1a and 4.1.1b. On the basis of the trends observed here the inhibitor, 4.1.1a, with (6*S*)-configuration, would give the observed Ala- β - H_3 resonance at δ 1.74. The (6*R*)-configuration of 4.1.1b would give the observed Ala- β - H_3 resonance downfield at δ 1.92. These trends will be useful in the stereochemical assignment of tetrazole-based peptidomimetics where the carbon centres adjacent to the tetrazole heterocycle are susceptible to epimerisation even under the conditions of peptide synthesis.

These results suggest the C6 stereocentre is highly susceptible to epimerisation in both acidic and basic conditions. In any future synthesis of tetrazole-based peptidomimetics careful consideration of the reaction conditions is needed to insure the chiral integrity of the stereocentres adjacent to the heterocycle.

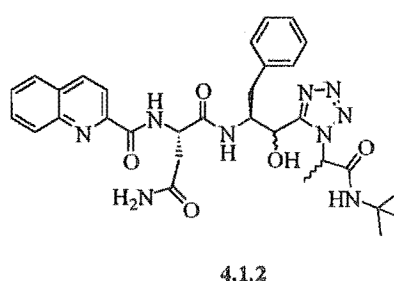
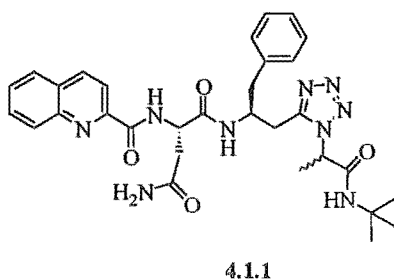
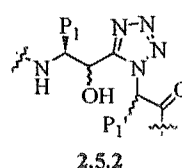
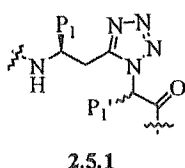
4.5. REFERENCES

- ¹ Foulds, G. J. *Biologically Active Peptide Analogues* Ph.D. thesis, University of Canterbury 1996. Abell, A. D.; Foulds, G. J. *Chem. Soc. Perkin 1* 1997, 2475.
- ² Zabrocki, J.; Dunbar, J. B.; Marshall, K. W.; Toth, M. V.; Marshall, G. R. *J. Org. Chem.* 1992, 57, 202.
- ³ Seebach, D.; Overhand, M.; Kuhnle, F. N. M.; Martinoni, B. *Helv. Chim. Acta.* 1996, 79, 913.
- ⁴ Bastiaans, H. M. M.; Alewijnse, A. E.; van der Baan, J. L.; Ottenheijm, H. C. J. *Tetrahedron Lett.* 1994, 41, 7659.
- ⁵ Wiberg, K. B.; Hutton, T. W. *J. Am. Chem. Soc.* 1956, 78, 1640.
- ⁶ Kaplan, F.; Meloy, G. K. *J. Am. Chem. Soc.* 1966, 88, 950. Kaplan, F.; Mitchell, M. L. *Tetrahedron Lett.* 1979, 759.
- ⁷ Chaturvedi, N. C.; Park, W. K.; Smeby, R. R.; Bumpus, F. M. *J. Med. Chem.* 1970, 13, 177.
- ⁸ Plucinska, K.; Liberek, B. *Tetrahedron* 1987, 43, 3509.
- ⁹ Thomas, E. W. *Synthesis* 1993, 767.
- ¹⁰ Duncia, J. V.; Pierce, M. E.; Santella, J. B. *J. Org. Chem.* 1991, 56, 2395.
- ¹¹ Yu, K-L.; Johnson, R. L. *J. Org. Chem.* 1987, 52, 2051.
- ¹² Boteju, L. W.; Hruby, V. J. *Tetrahedron Lett.* 1993, 34, 1757.
- ¹³ Butler, R. N. In, *Comprehensive Heterocyclic Chemistry*; Katritzky, A. R., Ed.; Pergamon Press: Oxford 1984, 5, 825.
- ¹⁴ Bodansky, M.; Bodansky, A. In, *The Practice of Peptide Synthesis*, Springer-Verlag: Berlin 1984, 165.
- ¹⁵ Schotten C. *Chem. Ber.* 1884, 17, 2544. Baumann, E. *Chem. Ber.* 1886, 19, 3218.
- ¹⁶ Camp, N. P.; Perrey, D. A.; Kinchington, D.; Hawkins, P. C. D.; Gani, H. *Bioorg. Med. Chem.* 1995, 3, 297.

CHAPTER FIVE
SYNTHESIS AND BIOLOGICAL ACTIVITY
OF α -METHYLENE TETRAZOLE-BASED
INHIBITORS

5.1. INTRODUCTION

In the design of peptidomimetic inhibitors it is generally recognised that the potency of inhibitors is greatly increased by elongation of the central isostere from the *N*- and *C*-terminals. It is possible to fill all the subsites (S) of the binding cleft by increasing the number of terminal residues (P) of the inhibitor. This leads to improved inhibitor activity as the interactions between the ligand and the enzyme binding cleft are increased. Although this approach has been used to develop potent inhibitors they generally display poor pharmacological properties *in vivo* due to their largely peptidic character. Potent protease inhibitors have been generated by simply replacing the central amide bond of a natural substrate with a non-hydrolysable isostere (eg. JG-365 1.2.4.3). In doing so the inhibitor retains the potent interactions that occur between the substrate residues and the subsites of the binding cleft. We have been interested in probing the effects of *C*-terminal elongations on the activity of HIVp inhibitors with a central tetrazole-based dipeptide mimic.



Foulds *et al.*² synthesised a series of tetrazole-based inhibitors (4.1.1 and 4.1.2) of HIVp which were capped on the *C*-terminal by *tert*-butylamine. HIVp inhibitors that incorporate a *tert*-butyl *C*-terminal (eg. Saquinavir 1.2.4.4) have been shown to bind to HIVp with a pseudo *trans*- conformation about the non-hydrolysable isostere (see Chapter 2.3).¹ The tetrazole-based inhibitors, 4.1.1 and 4.1.2, were synthesised to incorporate the α -methylene tetrazole (2.5.1) isostere and α -hydroxymethylene tetrazole

(2.5.2) isostere respectively.² These isosteric replacements have been designed (see Chapter 2.3) to preorganise the inhibitor ligands into a pseudo *cis*- conformation, as seen in the bioactive conformation of JG-365 (1.2.4.3). Due to the conflicting binding preferences of the *C*-terminal *tert*-butyl (pseudo *trans*-), and the tetrazole-based isostere (pseudo *cis*-), we postulated that the *tert*-butyl substituent of 4.1.1 and 4.1.2 has limited complementarity to the tetrazole-based *cis*- amide bond mimics, 2.5.1 and 2.5.2. The modest inhibitory potency (μM level) of 4.1.1 and 4.1.2 may in part be due to this unfavourable combination of structural elements.

We have been primarily concerned with investigating the trends in inhibition of HIVp associated with elongation of the *C*-terminal of the tetrazole-based dipeptide isostere. We have synthesised a series of modestly potent HIVp inhibitors based on the α -methylene tetrazole isostere [CH_2CN_4] 2.5.1, which have incorporated extended *C*-terminal substituents.

5.2. SYNTHESIS OF THE α -METHYLENE TETRAZOLE-BASED DIPEPTIDE MIMIC

We considered that *N-Z-L*-homophenylalanine- $[\text{CN}_4]$ -glycine benzyl ester, 5.2.1, (Figure 5.2.1) which incorporated the α -methylene tetrazole isostere, 2.5.1, would be an ideal tetrazole-based dipeptide mimic with which to probe the effects of *C*-terminal substitution. The problems associated with epimerisation of the carbon centres adjacent to the tetrazole ring (C3 and C6) (see Chapter 4.3) have been negated by the lack of substitution at these centres in 5.2.1 (Figure 5.2.1). The unnatural amino acid *L*-homophenylalanine (hPhe), 4.1.3, has been used to provide a non-hydrolysable α -methylene amide bond isostere in the dipeptide mimic, 5.2.1. A benzyl residue has been incorporated at P_1 as a mimic of phenylalanine for enzyme recognition and specificity. Incorporation of the glycine residue at P_1' (2.5.1 $\text{P}_1'=\text{H}$) reduces the complexity of the synthesis as epimerisation of methylene carbon (C6) under the conditions of peptide synthesis will not lead to the epimeric mixtures observed in the synthesis of inhibitor 4.1.1 and 4.1.2 (see Chapter 4.1).

A retrosynthetic analysis of the core α -methylene tetrazole dipeptide mimic,

5.2.1, is outlined in Figure 5.2.1. The tetrazole heterocycle was prepared from the corresponding amide, 5.2.2, by reaction with phosphorous pentachloride (PCl_5) and hydrozoic acid (HN_3), according to the modified method of Zabrocki *et al.*³ (see Chapter 4.2). A protecting group strategy was chosen to reflect the requirements of the tetrazole forming reaction and that is amenable to *N*- and *C*-terminal elongations by standard peptide synthesis. For this, *N*-Z-protection of the *N*-terminal amine and benzyl ester (Bn) protection of the *C*-terminal were chosen.

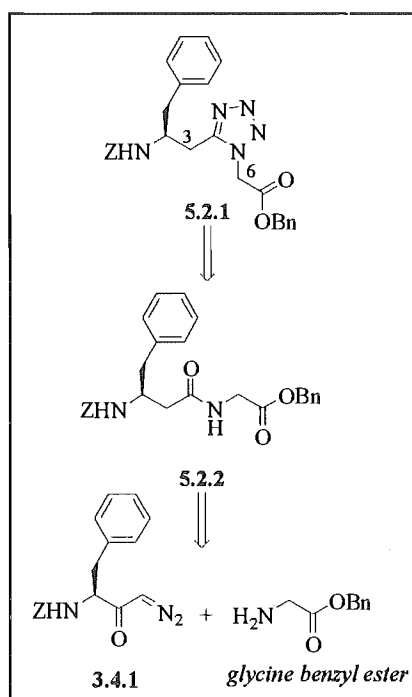
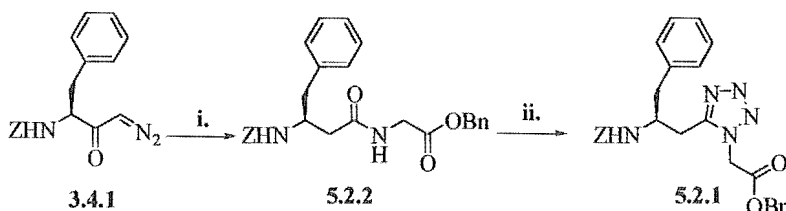


Figure 5.2.1. Retrosynthetic analysis of the target tetrazole-based dipeptide mimic, 5.2.1.

A Wolff rearrangement of the α -diazoketone, 3.4.1, with comittant peptide coupling (see Chapter 4.2) to glycine benzyl ester, was used to furnish the dipeptide intermediate, 5.2.2.⁴ Glycine benzyl ester hydrochloride was photochemically reacted with α -diazoketone, 3.4.1, in the presence of triethylamine (Scheme 5.2.1). Flash column chromatography of the crude reaction product gave the dipeptide, 5.2.2, in 85% yield. The dipeptide, 5.2.2, was then reacted with phosphorous pentachloride in the presence of quinoline according to the method of Zabrocki *et al.*³ After 3.5 hours at room temperature

the imidoyl chloride intermediate was reacted *in situ* with a benzene solution of hydrazoic acid. The crude tetrazole was separated from unreacted starting dipeptide, 5.2.2, by flash column chromatography and a single recrystallisation which then gave the desired tetrazole dipeptide mimic, 5.2.1, in 62% yield. The structure of the tetrazole-based dipeptide mimic, 5.2.1, was confirmed by a crystallographic structure determination by X-ray analysis.



Scheme 5.2.1. Reagents and conditions: i. HCl.Gly-OBn, 300 nm, Et₃N, rt, 18 h; ii. PCl₅, quinoline, HN₃, rt, 2 d.

5.3. SOLID-STATE STRUCTURE OF THE α -METHYLENE TETRAZOLE-BASED DIPEPTIDE MIMIC

Single crystals of *N-Z-L*-homophenylalanine-[CN₄]-glycine benzyl ester, 5.2.1, were grown from methanol by slow evaporation. The crystal structure of 5.2.1 (see Figure 5.3.1) was determined at 160(2) K and was satisfactorily refined. For a detailed discussion of the crystal structure of 5.2.1, see Chapter 7.2.

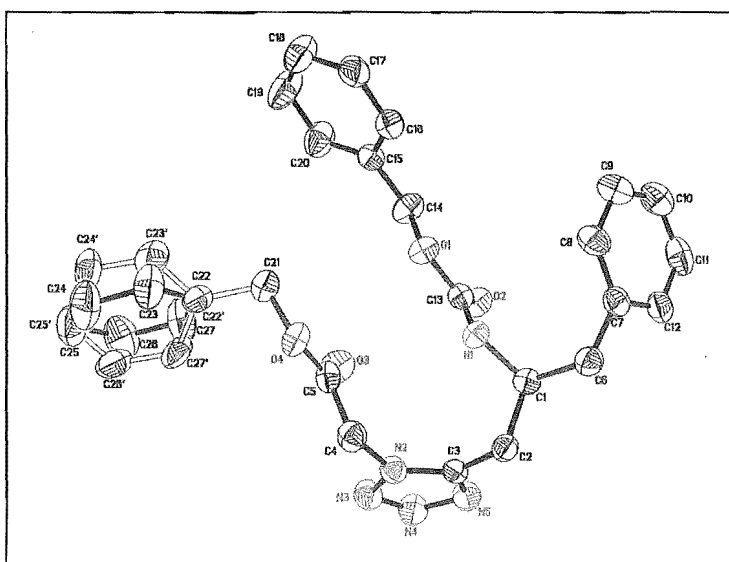


Figure 5.3.1. Solid state structure of α -methylene tetrazole dipeptide mimic, 5.2.1.

We have used the tetrazole-based dipeptide mimic, **5.2.1**, to preorganise inhibitor ligands synthesised in the current work into a conformation analogous to the bioactive conformation of JG-365 (**1.2.4.3**). The solid state structure of the α -methylene tetrazole dipeptide mimic, **5.2.1**, allows comparisons to be made between the design of the α -methylene tetrazole isostere, **2.5.1**, and the observed bioactive conformation of JG-365 (**1.2.4.3**).

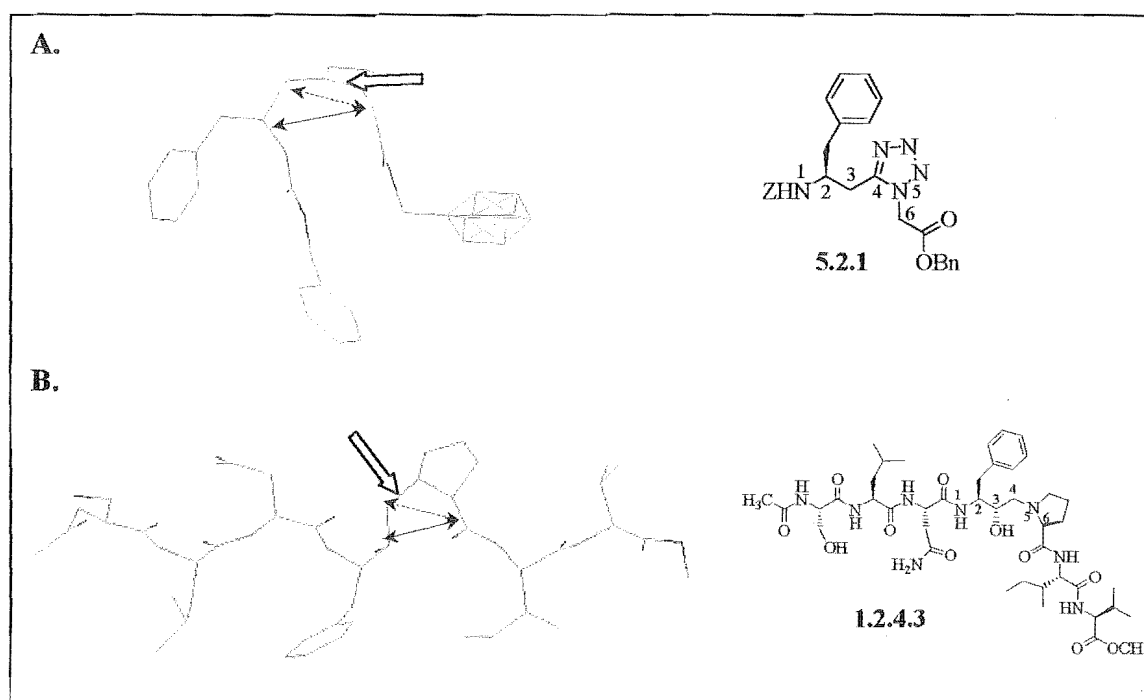


Figure 5.3.2. A. The solid state structure of the tetrazole-based dipeptide mimic, **5.2.1**; B. the solid state structure of JG-365 (**1.2.4.3**) bound to the active site of HIVp.

JG-365 binds to the active site of HIVp with a pronounced ‘kink’ characterised by the *cis*- conformation of the central C4-N5 bond of the non-hydrolysable isostere (indicated by the broad arrow, Figure 5.3.2 B). The tetrazole-based dipeptide mimic, **5.2.1**, is folded at the homophenylalanine-[CN₄]-glycine sequence. The solid state structure of **5.2.1** shows the tetrazole heterocycle forces a *cis*- conformation about the equivalent C4-N5 bond in the dipeptide mimic, **5.2.1** (shown by the broad arrow, Figure 5.3.2 A). The τ torsion angle, [C3-C4-N5-C6], at the homophenylalanine-glycine junction of **5.2.1** is forced by the tetrazole annular structure to be *cis*-, 13.1°. ⁵ This is a

good approximation of the ϖ torsion angle observed in the bound conformation of JG-365, where the ϖ torsion angle, [C3-C4-N5-C6], is essentially planar at 11.6°.

The correct positioning of the side chain residues, P₁ and P₁', of the α -methylene tetrazole isostere is important for favourable interactions to occur with the binding subsites, S₁ and S₁', of HIVp. The inter-residue distance, C2-C6 (shown by the solid arrow, Figure 5.3.2) of both JG-365 and 5.2.1 are similar being 4.31 Å and 3.88 Å, respectively. The distance between the P₁' residue (C6), and the central non-hydrolysable isostere (C3) in 5.2.1 (shown by the dotted arrow, Figure 5.3.2 A) is 3.19 Å, only slightly longer than in JG-365, being 2.96 Å. The increase in the C2-C6 and C3-C6 distances, may in part be due to the increased steric bulk of the tetrazole ring, which is reflected in an increased C4-N5-C6 bond angle (Figure 5.3.3) in 5.2.1.

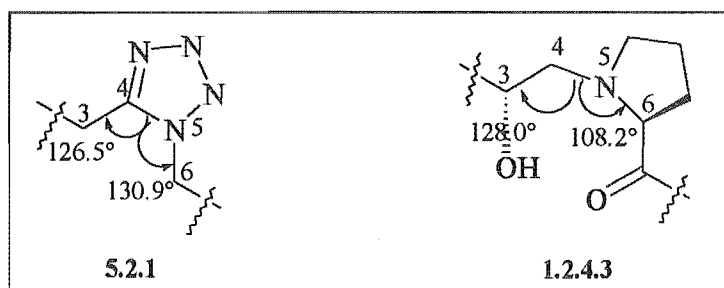


Figure 5.3.3. Bond angles, C3-C4-N5 and C4-N5-C6 for the tetrazole-based dipeptide mimic, 5.2.1, and JG-365, 1.2.4.3.

5.4. ELONGATION OF THE α -METHYLENE TETRAZOLE-BASED DIPEPTIDE MIMIC

Traditionally the activity of dipeptide isosteres has been enhanced by extension of the *N*- and *C*-terminals by incorporation of amino acid residues. Generally the *in vitro* potency of peptidomimetic inhibitors is increased as more subsites (S) of the binding cleft are filled by residues (P) of the inhibitor. Suitable P₃-P₃' residues have been chosen for this current series of HIVp inhibitors based on the optimisation of the known inhibitor JG-365 and the tetrazole based inhibitors, 4.1.1 and 4.1.2 (Table 5.4.1).

	P ₄	P ₃	P ₂	P ₁ -P ₁ '	P ₂ '	P ₃ '	P ₄ '	C3	IC ₅₀	
A. The hydroxyethylamine isostere (eg. JG-365, 2.3.1).										
1.			Z		O <i>t</i> Bu			R	6500nM	
2.		QC	Asn		O <i>t</i> Bu				R	23nM
3.	Ac	Leu	Asn		Ile	OCH ₃			RS	Ki 4520nM
4.	Ac	Leu	Asn		Ile	Val	OCH ₃		RS	Ki 21nM
B. The α-hydroxymethylene tetrazole isostere (eg. 4.1.2).										
5.			Z		OCH ₃			R	720 μ M	
6.		QC	Asn		NH <i>t</i> Bu				R	60 μ M
C. The α-methylene tetrazole isostere (eg. 4.1.1).										
7.		Z	Asn		NH <i>t</i> Bu			N/A	700 μ M	
8.		QC	Asn		NH <i>t</i> Bu				N/A	170 μ M

Table 5.4.1. HIVp activity with different *N*- and *C*-terminal substitutions of; **A.** the hydroxyethylamine isostere; **B.** the α -hydroxymethylene tetrazole isostere; **C.** the α -methylene tetrazole isostere.

The phenylalanine side chain is incorporated at P₁ in most, if not all, peptidomimetic HIVp inhibitors for selectivity and binding affinity with the hydrophobic S₁ subsite (see Chapter 2.3). Though the S₂ and S₂' subsites are mostly hydrophobic, both hydrophilic and hydrophobic residues can occupy these sites. Asparagine (Asn) has been shown to occupy the S₁ subsite and gives a dramatic improvement in activity when incorporated into the *N*-terminal of inhibitors that span P₁-P₁' (compare entries 1 and 2 Table 5.4.1).⁶ The S₃ subsite is large and less well defined than the S₂ and S₁ subsites. There is a clear preference for large aromatic residues at P₃ (entry 8 Table 5.4.1) over the smaller aromatic residues (entry 7 Table 5.4.1). The S₃ subsite will also accommodate a variety of natural amino acid residues (eg. entry 3 Table 5.4.1). Elongations of the *C*-

terminal fills the S_2' and S_3' subsites. Inhibitors that span the S_4 - S_2' (eg. entry 3 Table 5.4.1) display reduced activity over P_4 - P_3' inhibitors (eg. entry 4 Table 5.4.1). The S_4 and S_4' subsites are poorly defined and do not form an actual binding pocket.

The dipeptide mimic, **5.2.1**, was designed to incorporate a phenylalanine residue at P_1 , and a glycine residue at the P_1' binding site. The HIVp S_1' subsite binds hydrophobic P_1' residues of inhibitor ligands. A slight reduction in inhibitor potency has been noted when the S_1' subsite is left unfilled by inhibitors with a P_1' glycine residue.⁷ We have chosen the remaining P_3 - P_4' residues of our α -methylene tetrazole inhibitors based on the observed activity of known inhibitors (Table 5.4.1). Three inhibitors were targeted to investigate the effects of elongation of the *C*-terminal of **5.2.1** (Table 5.4.2). Each compound represents a step-wise increase in the *C*-terminal substitution.

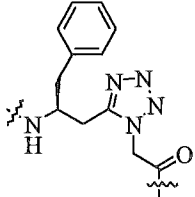
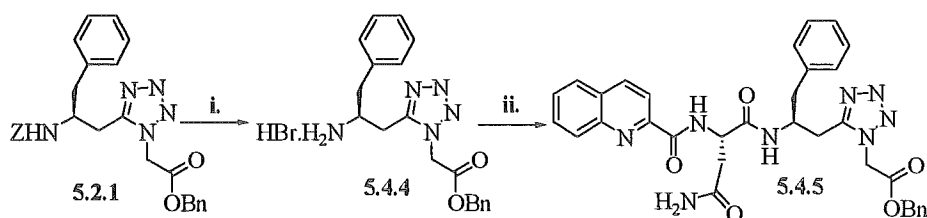
	P_3	P_2	P_1 - P_1'	P_2'	P_3'	P_4'
5.4.1.	QC	Asn		NHtBu		
5.4.2.	QC	Asn		Ile	OCH ₃	
5.4.3.	QC	Asn		Ile	Val	OCH ₃

Table 5.4.2. α -Methylene tetrazole based inhibitors.

The *N*-Z-protection of the dipeptide mimic, **5.2.1**, was selectively removed in the presence of the benzyl ester *C*-terminal protection to give free amine, **5.4.4** (Scheme 5.4.1). Coupling of the *N*-terminal and subsequent *C*-terminal deprotection and elongation, gave the inhibitors, **5.4.1**, **5.4.2** and **5.4.3**. We have also investigated an alternative deprotection and coupling strategy, starting with deprotection and coupling of the *C*-terminal and subsequent elongation of the *N*-terminal.

The tetrazole, **5.2.1**, was deprotected by treatment with 50% hydrobromic acid/acetic acid to yield the amine hydrobromide, **5.4.4**, in 99% yield (Scheme 5.4.1). The free amine, **5.4.4**, was coupled to *N*-(2-quinolinylcarbonyl)-*L*-asparagine, **4.2.7**, with BOP reagent in the presence of triethylamine. The crude protected tripeptide was purified by flash column chromatography to give **5.4.5**, in 51% yield.



Scheme 5.4.1. Reagents and conditions; **i.** 50% HBr/acetic acid, rt, 30 min; **ii.** BOP, Et₃N, QC-L-Asn-OH (4.2.7), rt, 18 h.

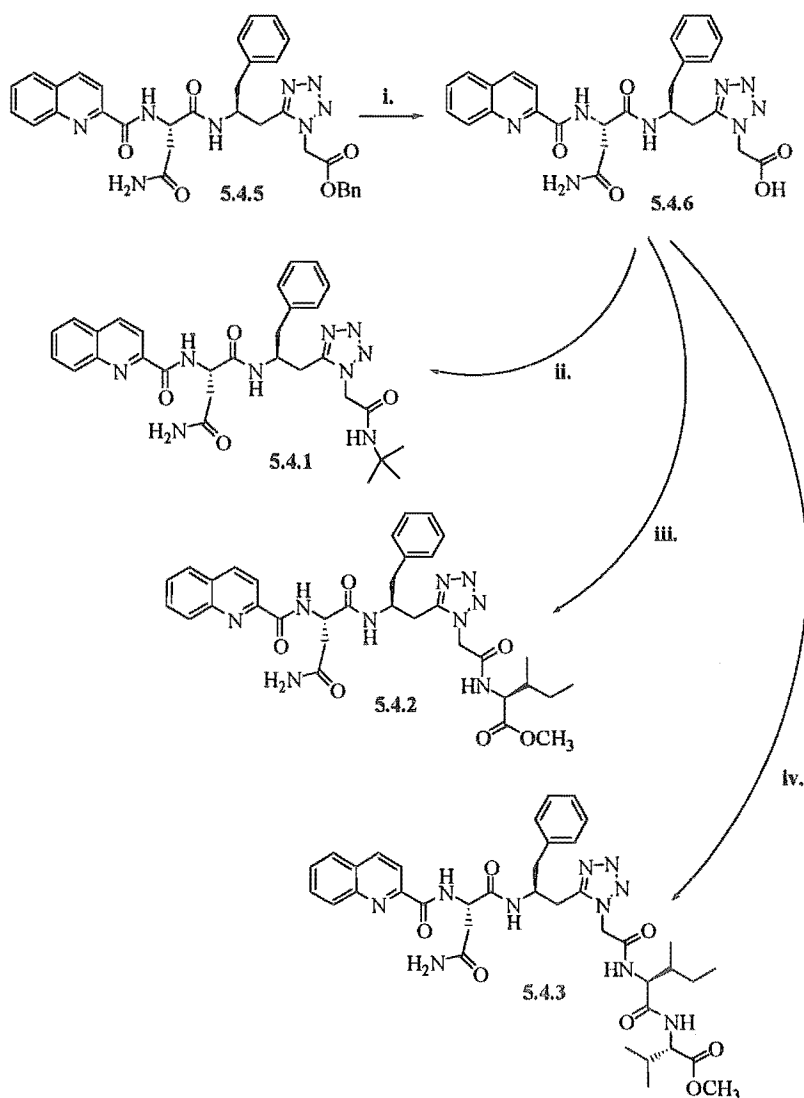
Catalytic hydrogenation of 5.4.5, with 10% palladium on carbon, gave the free acid, 5.4.6, in 70% yield (Scheme 5.4.2). Several coupling reagents were investigated to maximise coupling of the free acid, 5.4.6, to *tert*-butylamine to give the target inhibitor 5.4.1 (Scheme 5.4.2 ii). The coupling reagents BOP, *O*-benzotriazol-1-yl-*N,N,N',N'*-tetramethyluronium hexafluorophosphate (HBTU), and EDCI were trialed under appropriate conditions,⁸ and the reagents compared based on the yield and purity of 5.4.1 (Table 5.4.3). Under these criteria, EDCI, used in conjunction with the trapping agent *N*-hydroxybenzotriazole (HOBt), was used in subsequent coupling reactions of the free acid, 5.4.6.

Coupling Reagent	Yield
BOP, Et ₃ N	11%
EDCI, HOBt	17%
TBTU, DIPEA	5%

Table 5.4.3. The percentage yield of coupled product, 5.4.1, under various coupling conditions

Inhibitor 5.4.1 was synthesised in low yield (17%) by coupling the free acid, 5.4.6, to *tert*-butylamine with EDCI in the presence of HOBt (Scheme 5.4.2). The crude product was purified by flash column chromatography and reverse-phase high pressure liquid chromatography (HPLC). Coupling of the free acid, 5.4.6, to commercially available *L*-isoleucine methyl ester, using EDCI, gave inhibitor 5.4.2. The inhibitor was

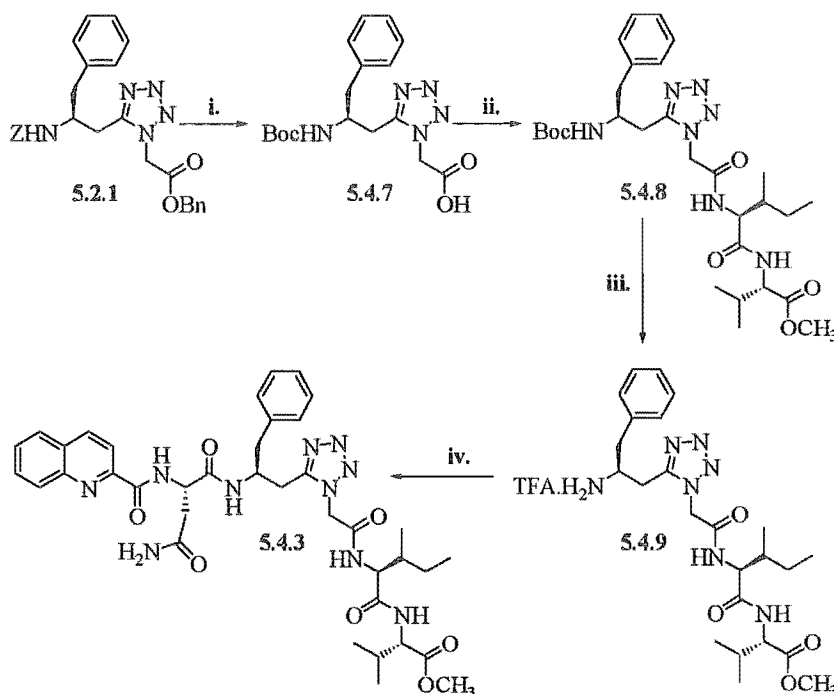
purified by flash column chromatography and HPLC and obtained in 18% yield. The commercially available dipeptide *N*-(*L*-isoleucine)-*L*-valine was methylated with 2,2-dimethoxypropane in the presence of aqueous hydrogen chloride according to the general procedure of Rachele.⁹ The resulting dipeptide methyl ester hydrochloride (*L*-Ile-*L*-Val-OCH₃) was coupled to **5.4.6** using EDCI in the presence of HOBT. The crude protected pentapeptide, **5.4.3**, was purified by flash column chromatography and reverse-phase HPLC, and finally precipitated from ether as a white solid, in 11% yield.



Scheme 5.4.2. Reagents and conditions; i. H₂, 10% Pd/C, 1 atm, rt, 24 h.
 ii. *t*-BuNH, EDCI, HOBT, rt, 18 h; iii. *L*-Ile-OCH₃, EDCI, HOBT, rt, 18 h;
 iv. *L*-Ile-*L*-Val-OCH₃, EDCI, HOBT, rt, 18 h.

We have also synthesised inhibitor 5.4.3 by an alternative deprotection and coupling strategy using the *N*-*tert*-butyloxycarbonyl (*N*-Boc) amine protecting group. The *N*-Boc protecting group is not a viable *N*-terminal protecting group for the synthesis of 1,5-disubstituted tetrazoles by the method of Zabrocki *et al.*,³ where formation of the tetrazole heterocycle is favoured by aromatic *N*-terminal protection (see Chapter 4.2). However, we have transformed the dipeptide mimic, 5.2.1, to the *N*-Boc protected free acid, 5.4.7, which allowed coupling of the *C*-terminal prior to extension of the *N*-terminal (Scheme 5.4.3). This strategy is more in keeping with established peptide synthesis procedures where the peptide is elongated from the *N*-terminal. The transformation was made possible by the procedure of Ohfuné *et al.*¹⁰ whereby the *N*-*Z*-protected tetrazole, 5.2.1, underwent a simultaneous deprotection of both the *C*-terminal benzyl ester and the amine *N*-*Z*-protection, with an *in situ* conversion to the *N*-Boc-protected amine. A palladium catalysed hydrogenation of 5.2.1 at atmospheric pressure was carried out in the presence of di-*tert*-butyl dicarbonate (Boc₂O) (Scheme 5.4.3). After 5 h at room temperature, the palladium catalyst was removed by filtration and the free acid, 5.4.7, was obtained as a white solid, in 76% yield.

The free acid, 5.4.7, was elongated via the *C*-terminal by EDCI coupling to *N*-(*L*-isoleucine)-*L*-valine methyl ester hydrochloride, in the presence of HOBt and Hunigs base (DIPEA, *N,N*-diisopropylethylamine). The *N*-Boc-protected tetrapeptide, 5.4.8, was obtained as a white solid in 75% yield following flash column chromatography. Deprotection of the *N*-Boc protecting group was achieved by treatment of 5.4.8 with 95% aqueous trifluoroacetic acid (TFA) for 30 min, at room temperature. After drying over potassium hydroxide *in vacuo* for 24 hours the amine trifluoroacetate, 5.4.9, was obtained quantitatively and used without further purification. This was then coupled to *N*-(2-quinolinylcarbonyl)-*L*-asparagine, 4.2.7, with EDCI, HOBt and DIPEA and the crude product was purified by plate layer chromatography, to give 5.4.3 in 40% yield.



Scheme 5.4.3. Reagents and conditions: i. H₂, 10% Pd/C 1 atm, Boc₂O, rt, 5 h; ii. EDCI, HOBt, DIPEA, *L*-Ile-*L*-Val-OCH₃, rt, 18 h; iii. 95% TFA/water, rt, 30 min; iv. EDCI, HOBt, DIPEA, QC-*L*-Asn-OH (4.2.7), rt, 18 h.

This later deprotection and coupling strategy (Scheme 5.4.3) represents an improvement in yield over the former strategy (Scheme 5.4.2). The overall yield of inhibitor 5.4.3 by the *N*-Boc amine protecting group strategy was 23% from the tetrazole dipeptide mimic, 5.2.1. This can be compared with an overall yield of 3% of inhibitor 5.4.3 via the former method, which required initial elongation of the *N*-terminal and subsequent substitution of the *C*-terminal.

5.5. BIOLOGICAL ACTIVITY OF THE α -METHYLENE TETRAZOLE-BASED INHIBITORS

The α -methylene tetrazole based inhibitors, 5.4.1, 5.4.2 and 5.4.3 were tested for *in vitro* activity against HIVp.¹¹ The activity of the inhibitors is expressed as an IC₅₀ value, where the lower the IC₅₀ value the more potent the inhibitor. The assay was run at

pH 5.6 in 0.2 M aqueous sodium chloride and 0.1 M MES buffer at 37 °C. The results are detailed in Table 5.5.1, along side the activity of the α -hydroxymethylene, and α -methylene tetrazole based inhibitors, 4.1.1a and 4.1.2a, reported by Foulds *et al.*²

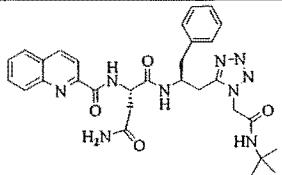
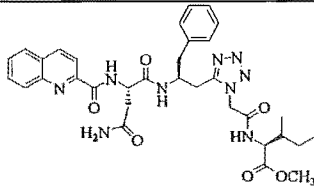
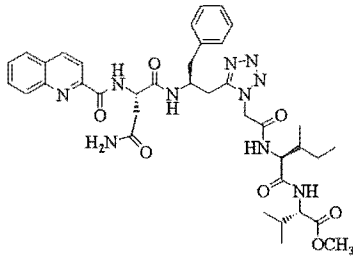
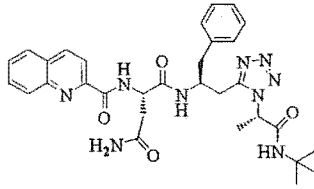
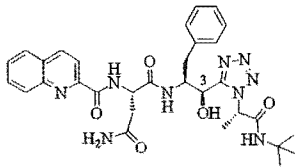
	Inhibitor	IC ₅₀ (μ M)
5.4.1		94(\pm 50)
5.4.2		47(\pm 20)
5.4.3		18(\pm 10)
4.1.1a		170(\pm 20)
4.1.2a (3S)		60(\pm 10)

Table 5.5.1. Inhibitor potency against HIVp.

The α -methylene tetrazole inhibitors have provided insight into the preferred C-terminal substituents and also the binding mode of the tetrazole-based inhibitors. We were interested in establishing trends in the activity of the tetrazole-based inhibitors with

increasing *C*-terminal substitution. The assay results show that inhibitor potency of 5.4.1, 5.4.2 and 5.4.3 increases as the *C*-terminal is elongated. We propose that the relative potency of inhibitor 5.4.3 ($IC_{50}=18 \mu\text{M}$) results from filling all the available subsites (S_3 - S_3') of the enzyme binding cleft with the corresponding P_3 - P_4' residues of the inhibitor. A decrease in potency is seen when the S_3' subsite is left unfilled by inhibitor 5.4.2 ($IC_{50}=47 \mu\text{M}$). This result suggests that for maximum binding interaction to occur between the tetrazole-based inhibitor and the enzyme binding cleft, all available subsites of the binding cleft should be accommodated by inhibitor residues.

The inhibitors show reasonable activity with IC_{50} values in the low micromolar (μM) range. The most active HIVp inhibitors are significantly more potent with IC_{50} values in the low nanomolar (nM) range. The HIVp inhibitor, JG-365 (1.2.4.3), upon which the design of the tetrazole dipeptide mimic was based exhibits an IC_{50} of 6.0 nM. The most potent inhibitor of the α -methylene tetrazole series, 5.4.3 ($IC_{50}=18 \mu\text{M}$), is approximately 3000 fold less potent than JG-365.[†] This is to be expected, as the core dipeptide isostere, 5.2.1, lacks specific functionality required for potent activity, namely a central hydroxyl and a large S_1' residue.

Comparison of the activity of inhibitor 5.4.2 ($IC_{50}=47 \mu\text{M}$) and 5.4.1 ($IC_{50}=94 \mu\text{M}$) suggests that the binding mode of the latter inhibitor is unfavourably influenced by the *tert*-butylamine *C*-terminal substitution (see Chapter 5.1). The solid state structure of inhibitor-HIVp complexes where the inhibitor has the *tert*-butyl *C*-terminal shows the *tert*-butyl group fills the S_2' subsite and in doing so, orientates the ligand backbone into a pseudo *trans*- conformation about the central isostere.[†] We have designed the tetrazole dipeptide isosteres as mimics of the alternative *cis*- binding mode seen in the bound conformation of JG-365 (1.2.4.3), where the ligand backbone adopts an extended conformation. The above results suggest that the *C*-terminal *tert*-butyl group of inhibitor 5.4.1 is incompatible with the *cis*- conformation of the tetrazole-based mimic. We propose that the *tert*-butyl P_2' residue of inhibitor 5.4.1 twists the ligand backbone so as to maximise interaction with the S_2' subsite. The backbone twist that occurs would be conformationally at odds with the tetrazole-based *cis*- mimic. In contrast, the isoleucine

[†] IC_{50} values of 1.2.4.3 and 5.4.3 were obtained under different assay conditions.

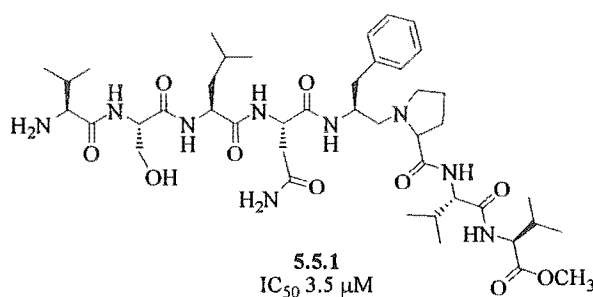
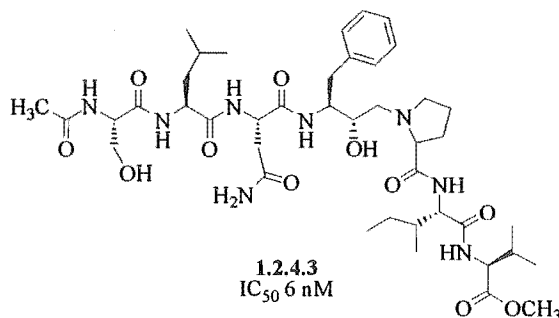
residue of inhibitor 5.4.2 can fill the S_2' subsite, with the ligand backbone still remaining in an extended conformation that is compatible with the *cis*- conformation of the tetrazole-based isostere. This would give an inhibitor-enzyme complex [5.4.2-HIVp] of lower energy, relative to the 5.4.1-HIVp complex.

The inhibitors 5.4.1 ($IC_{50}=94 \mu M$) and 4.1.1a ($IC_{50}=170 \mu M$),² show similar activity against HIVp, suggesting that the P_1' glycine residue of 5.4.1 is tolerated.[‡] This is supported by literature observations,¹² which have shown that there is only a moderate increase in activity by replacing a glycine residue at P_1' with an alanine residue. Real gains in potency are only seen when large aromatic residues are placed in the S_1' binding subsite.

A suprising result from this work was the potency of the α -methylene tetrazole-based dipeptide inhibitor, 5.4.3 ($IC_{50}=18 \mu M$), relative to the α -hydroxymethylene tetrazole-based inhibitor, 4.1.2a ($IC_{50}=60 \mu M$). It has been well established that inhibitors containing the central hydroxyl functionality are more potent than analogous inhibitors with the α -methylene isostere.¹³ Hydroxyethylamine, and α -hydroxy isosteres (eg 4.1.2) give rise to potent HIVp inhibitors, due to the favourable interaction of the central hydroxyl with the catalytic aspartate residues of HIVp. In the absence of any α -hydroxy functionality in our tetrazole-based inhibitors we would not expect potent HIVp inhibition, due to the lack of α -functionality which prohibits this favourable binding interaction. The increased potency of 5.4.3 relative to 4.1.2a must in part be due to the complimentarity between the tetrazole-based isostere (2.5.1) and the *C*-terminal substituents of 5.4.3, and that the inhibitor spans all available subsites of the enzyme binding cleft. The dipeptide mimic, 5.2.1, is similar in structure to the reduced amide isostere, [CH₂NH], which also lacks an α -hydroxy functionality. The reduced amide isostere has been incorporated into the HIVp inhibitor 5.5.1,¹⁴ an analogue of the potent inhibitor JG-365 (1.2.4.3). Inhibitor 5.5.1 ($IC_{50}=3.5 \mu M$) was shown to be less potent than JG-365 ($IC_{50}=6 nM$), due to the lack of the central hydroxyl functionality. Subsequent studies that compared various isosteres with identical flanking peptide residues, indicated that the reduced amide isostere is the least effective of the isosteric

[‡] IC_{50} values of 5.4.1 and 4.1.1a were obtained under different assay conditions.

replacements specifically due to a lack of α -functionality.¹⁵ Therefore, we would expect the potency of inhibitor 5.4.3 would increase dramatically with the addition of the central α -hydroxy functionality.



Incorporation of the 1,5-disubstituted tetrazole ring as a *cis*-amide bond mimic into biologically active peptide substrates often results in reduced activity with respect to the parent peptide (see Introduction 3.0). This has been attributed, in part, to the increased steric bulk of the tetrazole heterocycle, which may cause undue steric congestion within the active site and hence reduce ligand-receptor interactions. Additionally, the tetrazole ring lacks the adjacent hydrogen-donor, hydrogen-acceptor arrangement of the amide bond. This may preclude the tight binding of tetrazole containing peptidomimetics, due to the lack of specific hydrogen-bonding interactions between the central tetrazole isostere and the receptor site. The modest potency of the α -methylene tetrazole-based inhibitors, 5.4.1-5.4.3, may also be attributed to these structural factors, which would limit interactions between the tetrazole-based inhibitors and the active site of HIVp.

5.6. CONCLUSION

We have synthesised tetrazole-based dipeptide mimic, 5.2.1, which incorporated the α -methylene tetrazole isostere [CH₂CN₄] 2.5.1. The solid state structure of the dipeptide mimic, 5.2.1, closely resembles the bioactive conformation of the non-hydrolysable isostere of the potent inhibitor JG-365, which was the design basis of the tetrazole-based isostere.

Elongation of the tetrazole-based dipeptide mimic, 5.2.1, via the *C*-terminal has been used to establish trends in activity against HIVp with increasing ligand-enzyme interactions. This has shown that HIVp activity can be greatly improved by incorporating the tetrazole-based dipeptide mimic into HIVp substrates that span the S₃-S₄' subsites.

The investigation has also enabled us to account for the reduced activity of the *C*-terminal *tert*-butyl tetrazole-based inhibitors, 4.1.1, and 4.1.2. We propose that the reduced activity is due to the non-complimentarity of the *tert*-butyl substitution, and the tetrazole-based *cis*- amide mimic.

5.7. REFERENCES

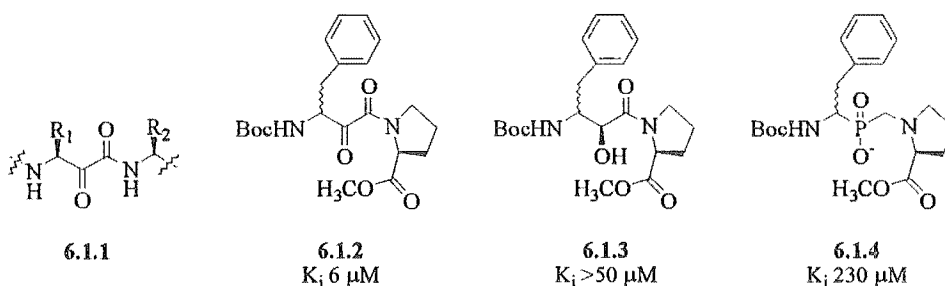
- ¹ Rich, D. H.; Sun, C-Q.; Prasad, J. N. V. N.; Pathiasseril, A.; Toth, M. V.; Marshall, G. R.; Clare, M.; Mueller, R. A.; Houseman, K. *J. Med. Chem.* **1991**, *34*, 1225. Krohn, A.; Redshaw, S.; Ritchie, J. C.; Graves, B. J.; Hatada, M. H. *J. Med. Chem.* **1991**, *34*, 3340.
- ² Foulds, G. J. *Biologically Active Peptide Analogues* Ph.D. thesis, University of Canterbury **1996**. Abell, A. D.; Foulds, G. J. *Chem. Soc. Perkin I* **1997**, 2475.
- ³ Zabrocki, J.; Dunbar, J. B.; Marshall, K. W.; Toth, M. V.; Marshall, G. R. *J. Org. Chem.* **1992**, *57*, 202.
- ⁴ Seebach, D.; Overhand, M.; Kuhnle, F. N. M.; Martinoni, B. *Helv. Chim. Acta.* **1996**, *79*, 913. Bastiaans, H. M. M.; Alewijnse, A. E.; van der Baan, J. L.; Ottenheijm, H. C. J. *Tetrahedron Lett.* **1994**, *41*, 7659.
- ⁵ Marshall, G. R.; Humblet, C.; van Opdenbosch, N.; Zabrocki, J. In, *Peptides, Structure-Synthesis-Function*, Eds. Rich, D. H.; Gross, E. Pierce: Rockford Illinois **1981**.
- ⁶ Roberts N. A.; Martin, J. A.; Kinchington, D.; Broadhurst, A. V.; Craig, J. C.; Duncan, I. B.; Galpin, S. A.; Handa, B. K.; Kay, J.; Krohn, A.; Lambert, R. W.; Merrett, J. H.; Mills, J. S.; Parkes, K. E. B.; Redshaw, S.; Ritchie, A. J.; Taylor, D. L.; Thomas, G. J.; Machin, P. J. *Science* **1990**, 358.
- ⁷ Dreyer, G. B.; Metcalf, B. W.; Tomaszek, T. A.; Carr, T. J.; Chandler, A. C. *Proc. Natl. Acad. Sci. USA* **1989**, *86*, 9752.
- ⁸ Bodansky, M.; Bodansky, A. In, *The Practice of Peptide Synthesis*. Springer-Verlag: Berlin **1984**.
- ⁹ Rachele, J. R. *J. Org. Chem.* **1963**, *28*, 2898.
- ¹⁰ Salaitani, M.; Hori, K.; Ohfuné, Y. *Tetrahedron Lett.* **1988**, *29*, 2983.
- ¹¹ HIVp inhibition was determined by Zachery Beck, Scripps Research Institute, La Jolla, California, to whom we are indebted.
- ¹² Dreyer, G. B.; Lambert, M. B.; Meek, T. D.; Carr, T. J.; Tomaszek, T. A. *Biochemistry* **1992**, *31*, 6646.

- ¹³ Wlodawer, A.; Erickson, J. W. *Annu. Rev. Biochem.* **1993**, *62*, 543.
- ¹⁴ Tomasseli, A. G.; Olsen, M. K.; Hui, J. O.; Staples, D. J.; Sawyer, T. K.; Heinrekson, R. L.; Tomich, C-S. C. *Biochemistry* **1990**, *29*, 264.
- ¹⁵ Urban, J.; Konvalinka, J.; Stehlikova, J.; Gregorova, E.; Majer, P. *FEBS Lett.* **1992**, *298*, 9.

CHAPTER SIX
SYNTHESIS OF THE α -KETO
TETRAZOLE ISOSTERE

6.1. INTRODUCTION

The α -keto amide functionality (eg. 6.1.1) has found widespread application as an isosteric replacement in reversible inhibitors of the proteinase family of enzymes. Amino acid derived α -keto amides have been incorporated into inhibitors of α -chymotrypsin,¹ calpain,² cathepsin B,³ and the aspartyl proteinase, pepsin.⁴ The α -keto amide isostere, 6.1.1, has been incorporated into potent inhibitors of HIVp.⁵ A comparison of the biological activity of HIVp inhibitors which were based on the α -keto amide (6.1.2), the hydroxyethylamine,⁶ (6.1.3), and phosphinic acid⁷ (6.1.4) isosteres, has shown that the α -keto amide isostere is the most potent of the isosteric replacements used in this series of inhibitors.⁵



It is proposed that the α -keto amide isostere inhibits protease enzymes via the formation of a stabilised tetrahedral adduct between the electrophilic carbonyl of the isostere and catalytic residues of the proteolytic enzyme.⁸ For example, it is proposed that the α -keto amide based inhibitors of HIVp (eg. 6.1.2) are hydrated within the active site to form a stabilised hydrate (Figure 6.1.1), which is a good mimic of the tetrahedral intermediate formed during normal amide bond hydrolysis (Figure 2.2.2).

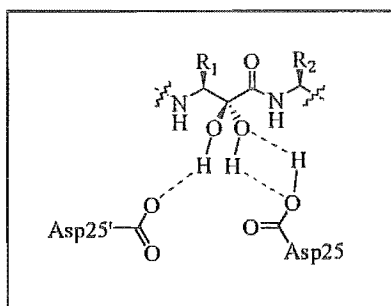
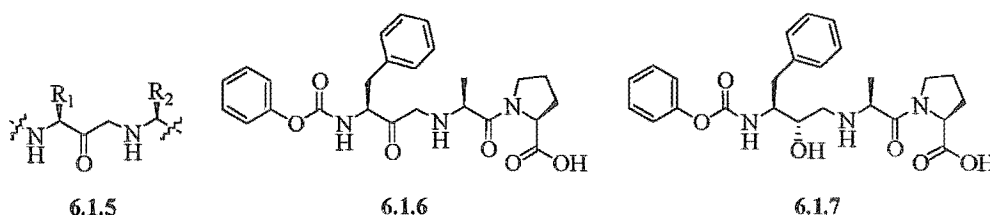
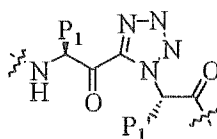


Figure 6.1.1. The proposed stabilised hydrate of the α -keto amide isostere, 6.1.1, in the active site of HIVp.

A related isostere, the aminoketone [COCH₂NH] (6.1.5), has been incorporated into an ACE inhibitor, 6.1.6,⁹ and shown to be more potent than the hydroxyethylamine based analogue, 6.1.7. The ketomethylene isostere [COCH₂] is found in the naturally occurring aminopeptidase inhibitor arphmenine and has been incorporated into aminopeptidase,¹⁰ renin,¹¹ and calpain inhibitors.¹² The mode of action of the aminoketone isostere is thought to be similar to α -keto amide isostere, where nucleophilic attack on the ketone within the active site leads to a hemi-ketal, a mimic of the tetrahedral intermediate (Figure 6.1.1).



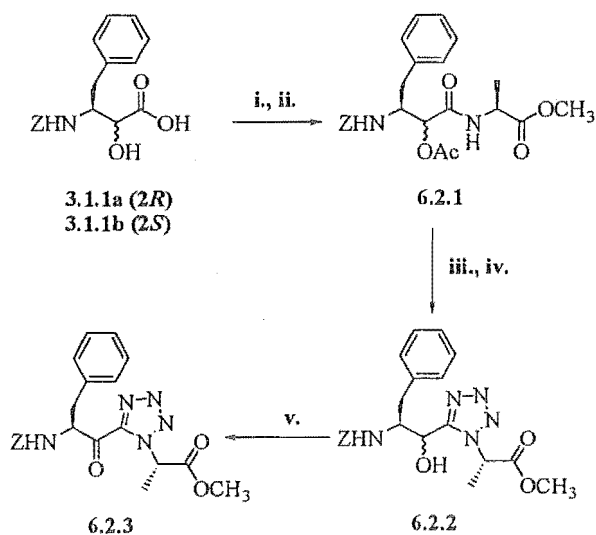
We have designed the α -keto tetrazole isostere [COCN₄], 2.5.3 as part of the novel tetrazole-based isosteric replacements. The α -keto tetrazole isostere (2.5.3) combines structural elements of a non-hydrolysable α -keto methylene isostere, with the conformational restriction of the 1,5-disubstituted tetrazole. This novel class of isosteric replacement is an important addition to the structural analogues available to peptidomimetic chemists for incorporation into enzyme inhibitors and conformational probes. We have been interested in developing synthetic routes to the α -keto tetrazole isostere.



2.5.3

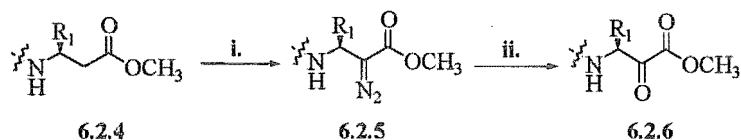
6.2. FUNCTIONALISATION OF TETRAZOLE-BASED DIPEPTIDE MIMICS

By far the most common route to the α -keto amide isostere, **6.1.1**, has been by oxidation of *N*-protected β -amino- α -hydroxy amides (eg **3.1.1** Scheme 6.2.1) prepared by elaboration of the *N*-protected α -amino acids. Foulds *et al.*¹³ synthesised the tetrazole-based dipeptide mimic, **6.2.3** (Scheme 6.2.1), containing the α -keto tetrazole isostere by this strategy. The synthesis of the dipeptide mimic, **6.2.3** (Scheme 6.2.1), required the synthesis of the α -hydroxy acid, *N*-Z-*L*-AHPBA **3.1.1** (see Chapter 2.0), incorporation of the protected acid into the dipeptide, **6.2.1**, and conversion of the dipeptide to the corresponding tetrazole, **6.2.2**. The synthesis was completed by a Dess-Martin periodinane¹⁴ oxidation of the α -hydroxymethylene tetrazole, **6.2.2**, to the α -keto tetrazole, **6.2.3**. The ten step synthetic sequence was low yielding, giving a 2% overall yield from commercially available *N*-Z-*L*-phenylalanine. We have been interested in developing a more expedient route to the α -keto tetrazole isostere, **2.5.3**, from that used by Foulds *et al.*¹³



Scheme 6.2.1. Reagents and conditions; **i**. *L*-Ala-OCH₃.HCl, DCC, HOBT, Et₃N, rt; **ii**. Ac₂O, pyridine, rt; **iii**. PCl₅, quinoline, HN₃, rt; **iv**. K₂CO₃, rt; **v**. Dess-Martin periodinane, rt, 18 h.

Darkins *et al.*¹⁵ have developed a synthetic route to α -keto esters by direct introduction of the α -ketone functionality to homologated amino acid esters (Scheme 6.2.2). A homologated amino acid ester, 6.2.4, was prepared via Wolff rearrangement of the corresponding α -diazoketone in the presence of methanol (see Chapter 4.2). A diazo group was introduced at the α -position of 6.2.4 by acylation with 2,2,2-trifluoroethyl trifluoroacetate, prior to azide transfer from mesityl azide (MsN_3), in the presence of triethylamine, according to the method of Dansheiser *et al.*¹⁶ To complete the synthesis, the diazo function of 6.2.5 was oxidatively cleaved by exposure to dimethyldioxirane (DMD),¹⁷ which furnished the α -keto esters, 6.2.6, in high yield. No detectable epimerisation was observed by ^{13}C NMR in the preparation of diastereomeric α -keto esters by this method.



Scheme 6.2.2. Reagents and conditions: i. $\text{CF}_3\text{CO}_2\text{CH}_2\text{CF}_3$, LiHMDS, -78°C 10 min, then MsN_3 , Et_3N , rt, 2.5 h; ii. DMD.

We considered that the α -keto functionality of the α -keto tetrazole isostere, 2.5.3, could be introduced directly to the tetrazole dipeptide, according to the method developed by Darkins *et al.*¹⁵ for the synthesis of the α -keto esters, 6.2.6. A retrosynthetic analysis

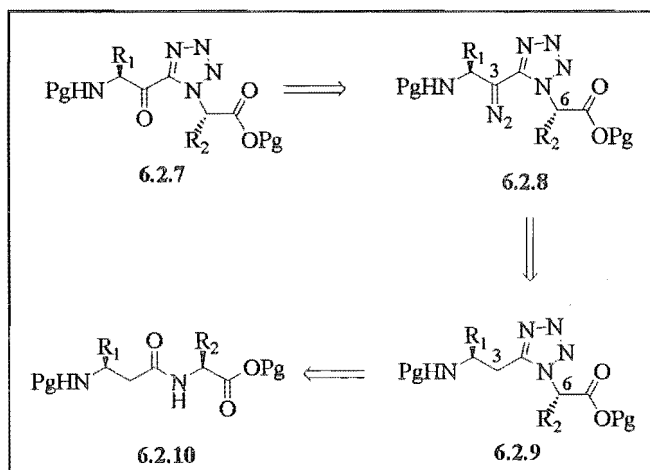


Figure 6.2.1. Retrosynthetic analysis of the α -keto tetrazole dipeptide mimic, 6.1.8, via direct introduction of the α -keto functionality.

of the proposed method is outlined in Figure 6.2.1.

The proposed synthesis required an α -methylene tetrazole dipeptide, 6.2.9, to which the α -keto functionality could be introduced, to give the desired α -keto tetrazole-based dipeptide mimic, 6.2.7. We have had experience in the synthesis of dipeptide mimics containing the α -methylene tetrazole isostere [CH_2CN_4] such as 6.2.9 (see Chapters 4.2, 5.2). The key step in the transformation of the α -methylene tetrazole isostere, 6.2.9, to the α -keto tetrazole isostere, 6.2.7, is the formation of the α -diazio intermediate, 6.2.8, by alkylation of the α -carbon of 6.2.9 in the presence of lithium hexamethyldisilazide (LiHMDS). We have established that the carbon centres adjacent to the tetrazole ring (C3 and C6), are susceptible to base catalysed epimerisation. The α -protons adjacent to the tetrazole ring are removed under the basic conditions of peptide coupling leading to the observed epimerisation of these carbon centres (see Chapter 4.3). Alkylation of a tetrazole dipeptide (eg. 6.2.9) to give the key diazo intermediate could occur at either of the carbon centres (C3 or C6) adjacent to the tetrazole heterocycle (broad arrows, Figure 6.2.2). We have undertaken a study on the alkylation of tetrazole-based dipeptides and have shown that there is a preferential addition of electrophiles to the tetrazole dipeptides.

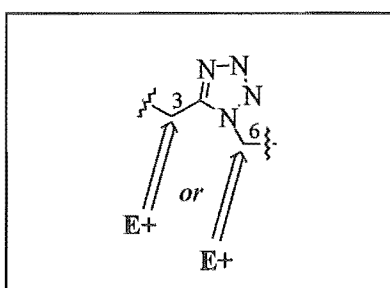
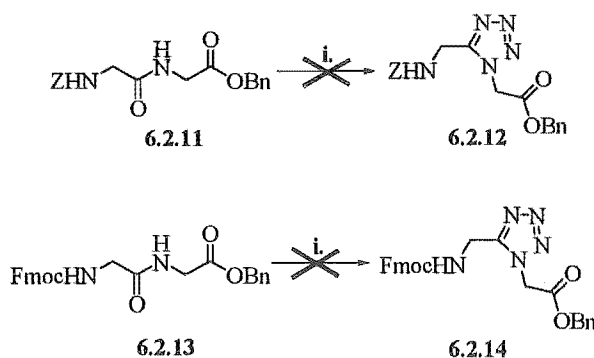


Figure 6.2.2. Possible electrophilic addition to the tetrazole dipeptide at either the C3, or C6 carbon centres.

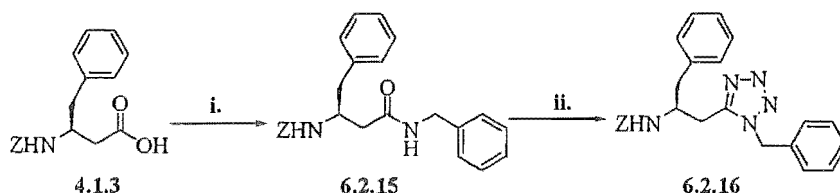
We considered that a simple protected glycine-[CN₄]-glycine tetrazole-based dipeptide (eg. 6.2.11 or 6.2.13 Scheme 6.2.3) would be an ideal substrate with which to study alkylation of the unsubstituted C3 and C6 carbon centres (Figure 6.2.2). The dipeptides, 6.2.11 and 6.2.13 (Scheme 6.2.3), were synthesised by coupling the appropriate *N*-protected glycine, to glycine benzyl ester with EDCI. The *N*-Z-protected dipeptide, 6.2.11, was obtained in 96% yield, and the *N*-Fmoc-protected dipeptide, 6.2.13, was obtained in 85% yield. We attempted to convert the dipeptides, 6.2.11 and 6.2.13, to the corresponding tetrazole-based dipeptides, 6.2.12 and 6.2.14, however both reactions returned unreacted starting dipeptide. The reason for the lack of reactivity of the *N*-protected glycine-glycine dipeptides is unknown. Yu and Johnson¹⁸ have observed that conversion of dipeptides to 1,5-disubstituted tetrazoles is unfavoured with a glycine residue at the *N*-terminal.



Scheme 6.2.3. Reagents and conditions: i. PCl₃, quinoline, HN₃, rt, 48 h

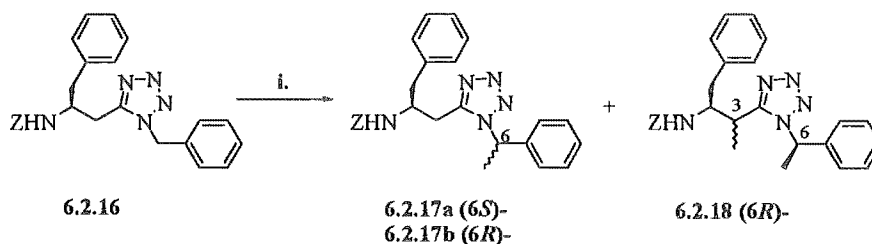
As an alternative to the glycine-[CN₄]-glycine tetrazole-based dipeptides, we have investigated the alkylation of a simplified tetrazole system, 6.2.16. We have synthesised the model tetrazole from the corresponding amide, 6.2.15, according to the method of Zabrocki *et al.*¹⁹ *N*-Z-*L*-Homophenylalanine, 4.1.3, was prepared by a silver (I) catalysed Wolff rearrangement of the corresponding *N*-Z-protected α -diazoketone (see Chapter 4.2). The homologated amino acid, 4.1.3, was coupled to benzyl amine with the coupling reagent EDCI, in the presence of DIPEA. The crude product was purified by flash column chromatography to give the amide, 6.2.15, in 91% yield. The amide was converted to the tetrazole, 6.2.16, by treatment with phosphorous pentachloride in the

presence of quinoline, followed by an *in situ* reaction of the imidoyl chloride with hydrazoic acid.¹⁹ The crude product was purified by flash column chromatography and the tetrazole, **6.2.16**, was obtained in 71% yield, as a white crystalline solid.



Scheme 6.2.4. Reagents and conditions: i. BnNH₂, EDCI, HOBT, DIPEA, rt, 18 h; ii. PCl₅, quinoline, HN₃, rt, 48 h.

To investigate alkylation of the tetrazole, **6.2.16**, we deprotonated with the LiHMDS, and then methylated with methyl iodide (MeI) (Scheme 6.2.4). A solution of tetrazole, **6.2.16**, was added dropwise to a solution of LiHMDS at $-78\text{ }^{\circ}\text{C}$. After 30 min a solution of methyl iodide was added dropwise and the reaction was stirred at $-78\text{ }^{\circ}\text{C}$ for 30 minutes. The reaction was then allowed to slowly warm the room temperature over a period of 30 minutes. The crude reaction mixture was purified by plate layer chromatography to give two fractions, one containing the mono-methylated products, **6.2.17a** and **6.2.17b**, (86%) and the other fraction containing the di-methylated product, **6.2.18** (14%) (Scheme 6.2.4). The mono-methylated products, which resulted from alkylation of the C6 carbon, were obtained as an epimeric mixture of **6.2.17a** and **6.2.17b** (1:1 by ¹H NMR). The di-methylated product, **6.2.18**, resulted from alkylation at both the C6 and C3 carbon centres in the presence of excess methyl iodide and was obtained as a single C6 epimer. The configuration of the C6 stereocentre of **6.2.18** was assigned on the basis of trends observed during the stereochemical assignment of the tetrazole-based inhibitors, **4.1.1a** and **4.1.1b** (see Chapter 4.3). This investigation established that tetrazole-based dipeptides with the (6*R*)-configuration (**4.1.1b**) gave Ala- β -H₃ ¹H resonances downfield of the corresponding (6*S*)- epimer (**4.1.1a**). On this basis we propose that the C6 stereocentre of **6.2.17** has a (6*R*)- configuration.

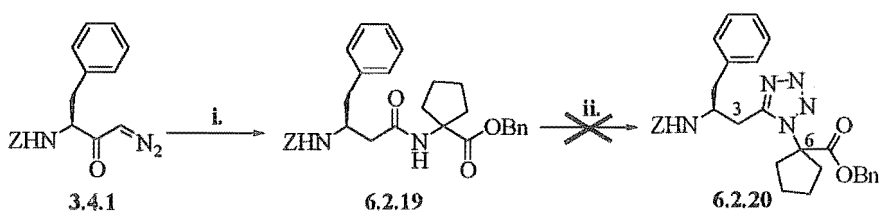


Scheme 6.2.5. Reagents and conditions: i. LiHMDS, -78°C , 30 min, then MeI - 78°C , 30 min, rt.

The relative yields of the methylated products, 6.2.17 (86%), and 6.2.18 (14%) indicated that the C6 carbon is more acidic than the C3 centre, leading to the predominance of the mono-methylated products, 6.2.17a and 6.2.17b. The observed alkylation of the C3 carbon to give the di-methylated product, 6.2.18, suggested that the C3 carbon could be functionalised. The problem was the relative reactivity of the C6 and C3 centres. For the introduction of the α -keto functionality to the C3 centre exclusively we required a tetrazole substrate that was block at the C6 carbon centre. It was thought that in blocking the C6 centre we would direct the functionalisation to the C3 carbon.

The α -methylene tetrazole-based dipeptide mimic, 6.2.20 (Scheme 6.2.5), was designed with a disubstituted amino acid incorporated at the C-terminal to direct functionalisation to the C3 carbon. The dipeptide, 6.2.19 (Scheme 6.2.5), was synthesised from 2-amino-2-cyclopentane carboxylic acid benzyl ester ($\text{H}_2\text{NCpCOOBn}$) and the α -diazoketone, 3.4.1. The cyclopentane benzyl ester was prepared by refluxing the corresponding acid in benzyl alcohol, in the presence of *para*-toluenesulphonic acid, in a Dean-Stark apparatus for 4 hours. The addition of 4 Å molecular sieves to the collector of the Dean-Stark apparatus greatly improved the yield of the cyclopentane benzyl ester over previously published methods.²⁰ The crude product was triturated with pre-cooled ether and the cyclopentane benzyl ester was removed by filtration as a white solid (50% yield). A mixture of the α -diazoketone, 3.4.1, and the cyclopentane benzyl ester were reacted photochemically in the presence of triethylamine, according to the established

procedure (see Chapter 4.2).²¹ The crude product was purified by flash column chromatography to give the dipeptide, **6.2.19**, as a white solid, in 25% yield.



Scheme 6.2.5. Reagents and conditions: **i**, *p*TsOH.H₂NCpCOOBn, 300 nm, Et₃N, rt, 18 h; **ii**, PCl₅, quinoline, HN₃, rt, 48 h.

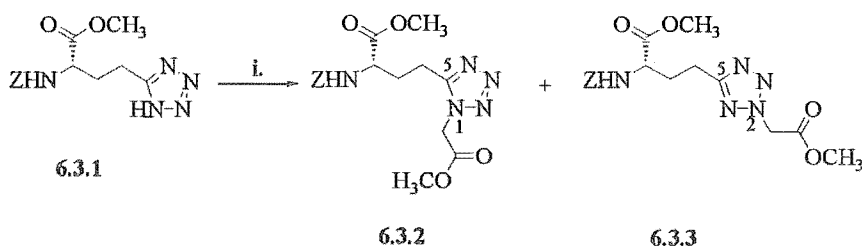
The dipeptide, **6.2.19**, was treated with phosphorous pentachloride and a solution of hydrazoic acid, according to the modified procedure of Hruby *et al.*²² These modifications to the original procedure of Zabrocki *et al.*¹⁹ were found to be necessary for the conversion of the sterically constrained *N*-Z-*L*-tryptophan-*L*-norleucine dipeptide (see Chapter 1.3 1.3.11), to the corresponding tetrazole-based dipeptide (see Chapter 1.3 1.3.12). The procedure employs longer reaction times and additional phosphorous pentachloride to ensure formation of the imidoyl chloride prior to the addition of hydrazoic acid. Analysis of the crude reaction product, by ¹H NMR, showed the presence of unreacted started dipeptide, **6.2.19**, following reaction of the dipeptide, according to the procedure of Hruby *et al.*²² An increase in the reaction time prior to the addition of hydrazoic acid (up to 4 hours) and an increase in the amount of phosphorous pentachloride, did not yield the desired tetrazole, **6.2.20**. We propose that the steric bulk of the cyclopentane *C*-terminal substituent limits formation of the tetrazole ring, due to unfavourable steric interaction in the tetrazole intermediates.

The attempted functionalisation of the tetrazole dipeptides provided some insight into the relative reactivity of the C3 and C6 centres, as well as highlighting the difficulty in synthesising sterically congested tetrazole-based dipeptides by the method of Zabrocki *et al.*¹⁹ An alternative synthesis of the α -keto tetrazole isostere was pursued, via direct alkylation of the tetrazole heterocycle.

6.3. SYNTHESIS OF THE α -KETO TETRAZOLE ISOSTERE BY DIRECT ALKYLATION OF THE TETRAZOLE HETEROCYCLE

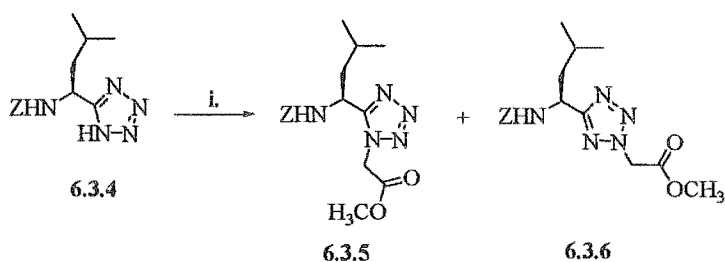
We have synthesised the α -methylene tetrazole isostere [CH_2CN_4] (2.5.1) by a functional group interconversion of the amide bond of a protected dipeptide (eg 6.2.15), to a tetrazole heterocycle (eg 6.2.16), according to the modified method of Zabrocki *et al.*¹⁹ This method has several drawbacks: i. The synthesis of the tetrazole-based dipeptides often suffers from low yields, (eg. see Chapter 4.2 4.1.5); ii. The reaction conditions place rigid requirements for aromatic *N*- and *C*-terminal protecting groups of the dipeptide substrate (eg. see Chapter 4.2); iii. Some amino acid residues (eg. glycine) limit formation of the tetrazole (eg. see Chapter 6.2 6.2.11); iv. It is difficult to transform sterically demanding dipeptides into the corresponding tetrazoles (eg. see Chapter 6.2 6.2.20); v. The reaction can be highly variable, with repeatability often being a problem. With this in mind, we have investigated an alternative synthesis of tetrazole-based dipeptide mimics and used this approach to synthesise the α -keto tetrazole isostere [COCN_4], 2.5.3.

It is possible to directly alkylate (1*H*)-tetrazoles (eg 6.3.1 Scheme 6.3.1) to yield 1,5-disubstituted and 2,5-disubstituted tetrazoles. This approach has been used by Bavetsias *et al.*²³ for the synthesis of thymidylate synthase (TS) inhibitors that incorporated a 1,5-disubstituted tetrazole (Scheme 6.3.1). Alkylation of the known (1*H*)-tetrazole, 6.3.1,²⁴ with methyl bromoacetate in the presence of triethylamine, gave a mixture of regiomeric tetrazoles, 6.3.2, and 6.3.3. The 1,5-disubstituted tetrazole (6.3.2), and 2,5-disubstituted tetrazole (6.3.3), obtained in a 5:3 ratio (by ¹H NMR), were separated by flash column chromatography and subsequently elongated via the *N*-terminal to give the desired TS inhibitors.



Scheme 6.3.1. Reagents and conditions: i. Et_3N , $\text{BrCH}_2\text{CO}_2\text{CH}_3$, rt 3h.

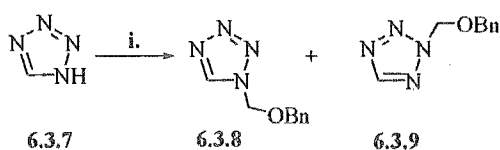
Using a similar approach, Valle *et al.*²⁵ prepared a conformationally restricted tripeptide analogue which incorporated a 1,5-disubstituted tetrazole ring, 6.3.5. Alkylation of the known tetrazole, 6.3.4,²⁶ with methyl bromoacetate in the presence of triethylamine gave a mixture of 1- and 2-tetrazoylacetic acid methyl esters, 6.3.5, and 6.3.6, in a 1:1 ratio (by ¹H NMR) (Scheme 6.3.2).



Scheme 6.3.2. Reagents and conditions: i. Et₃N, BrCH₂CO₂CH₃, rt, 3h.

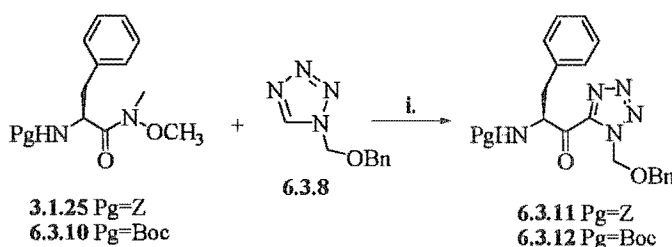
In consideration of the above examples, we postulated that direct alkylation of a suitable (1*H*)-tetrazole could be used for the preparation of the α -keto tetrazole isostere, 2.5.3. For the proposed synthesis we required a suitable (1*H*)-tetrazole substrate to which the *C*-terminal residue could be added by direct alkylation. We have used the procedure of Satoh *et al.*²⁷ for the synthesis of an α -hydroxy (1*H*)-tetrazole, 6.3.13 (Scheme 6.3.5) to which the *C*-terminal residue was added by direct alkylation of the tetrazole ring.

The requisite protected tetrazole, 6.3.8, was prepared by condensation of commercially available (1*H*)-tetrazole, 6.3.7, with benzyl chloromethylether (Scheme 6.3.3). The regiomer products, 6.3.8 and 6.3.9, were separated by flash column chromatography. The desired tetrazole, 6.3.8, eluted first and was obtained in 20% yield as a clear oil. Further elution gave the N-2 regiomer, 6.3.9.



Scheme 6.3.3. Reagents and conditions: i. NaHMDS, BnOCH₂Cl, 0 °C, 30 min, rt, 2 h.

Lithiation of **6.3.8** was successfully effected by treatment with *n*-butyl lithium at $-78\text{ }^{\circ}\text{C}$, to yield a deep purple solution typical of the 5-lithiotetrazoles. An *in situ* electrophilic condensation of the 5-lithiotetrazole with an *N*-protected Weinreb amide, **3.1.25** or **6.3.10**, gave the corresponding *N*-protected 1,5-disubstituted tetrazoles, **6.3.11** and **6.3.12**. Flash column chromatography of the crude reaction products gave the *N*-Z-protected tetrazole, **6.3.11**, or the *N*-Boc-protected tetrazole, **6.3.12**, both in 60% yield (Scheme 6.3.4).

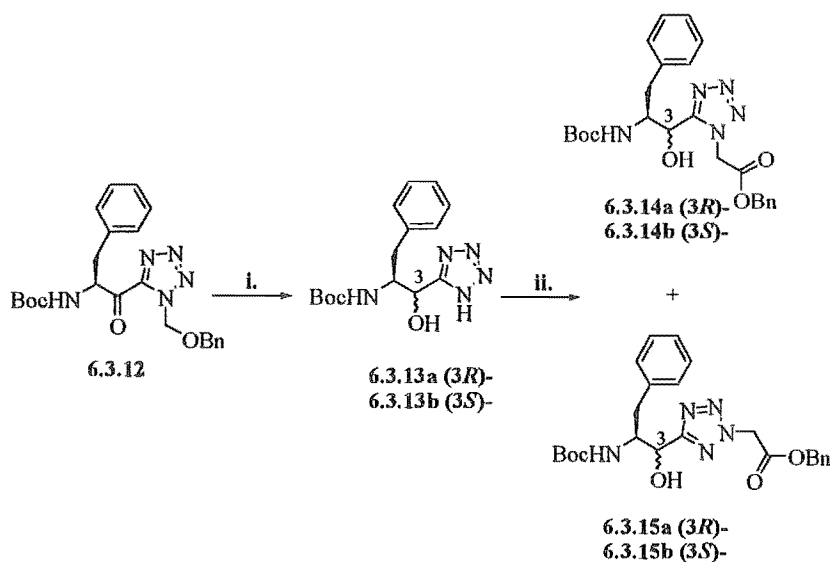


Scheme 6.3.4. Reagents and conditions: i. *n*-BuLi, $-78\text{ }^{\circ}\text{C}$, 5 min, $-78\text{ }^{\circ}\text{C}$ - $25\text{ }^{\circ}\text{C}$ over 30 min.

Removal of the *N*-1 benzyl methylether tetrazole protection can be achieved either under acidic conditions (6 M HCl/dioxane), or by hydrogenation in the presence of 10% palladium on carbon, following established procedures.²⁷ However, the success of the deprotection step was found to be dependant on the *N*-terminal protection of the 1,5-disubstituted tetrazole. A catalytic hydrogenation of the *N*-Z-protected tetrazole, **6.3.11**, resulted in comittant *N*-Z-deprotection and removal of the benzyl methylether tetrazole protecting group. Similarly, under acidic conditions the *N*-Z-protection of **6.3.11** was removed along with the benzyl methylether tetrazole protection. A catalytic hydrogenation of the *N*-Boc-protected tetrazole, **6.3.12**, resulted in removal of the tetrazole protecting group, as expected, but also a reduction of the α -ketone to the α -hydroxy (Scheme 6.3.5). Upon work-up, the reaction gave the epimeric α -hydroxy (1*H*)-tetrazoles, **6.3.13a** and **6.3.13b**, in 90% yield, which were used without further purification.

Having synthesised the desired (1*H*)-tetrazole substrate we turned our attention to alkylation of the tetrazole heterocycle (Scheme 6.3.5). Alkylation of the α -hydroxy (1*H*)-

tetrazoles, **6.3.13a** and **6.3.13b**, with benzyl bromoacetate in the presence of triethylamine gave the 1,5-disubstituted tetrazole products, **6.3.14a** and **6.3.14b**, and also the 2,5-disubstituted tetrazole products, **6.3.15a** and **6.3.15b**. The products were purified, but not separated, by flash column chromatography to give the regiomer tetrazoles, **6.3.14** and **6.3.15**, as a mixture in 60% yield. The alkylation was also carried out using DIPEA as the base, which gave an improved yield (75%) over the use of triethylamine.

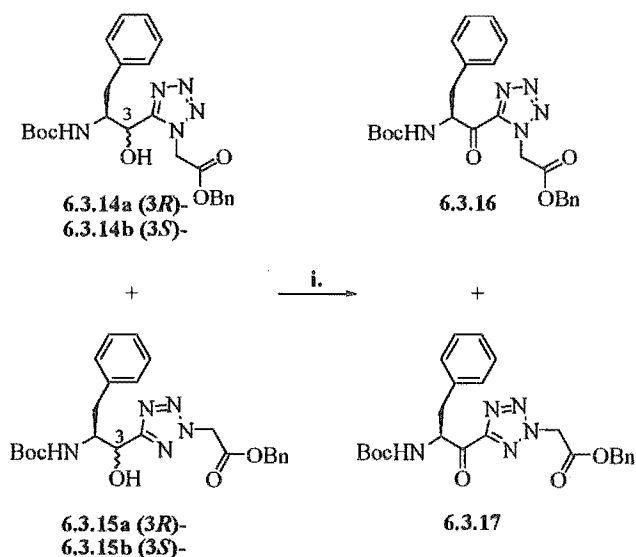


Scheme 6.3.5. Reagents and conditions: **i.** H_2 , 10% Pd/C, 1 atm, rt, 24 h; **ii.** DIPEA, $BrCH_2CO_2Bn$, rt, 24 h.

The α -hydroxy tetrazoles, **6.3.14** and **6.3.15** were oxidised, as a mixture, with a solution of TEMPO,²⁸ to give a mixture of the regiomer tetrazoles **6.3.16** and **6.3.17** (3:4 by 1H NMR) (Scheme 6.3.6).

The regiomer tetrazoles, **6.3.16** and **6.3.17**, were separated by flash column chromatography, the less polar 1,5-disubstituted tetrazole, **6.3.16**, eluted prior to the 2,5-disubstituted tetrazole, **6.3.17**. The tetrazoles were obtained in 30% and 40% yield, respectively. The structures of the regiomer tetrazoles were assigned on the basis of 1H and ^{13}C NMR, and an X-ray structure determination of **6.3.17**. In previous 1H NMR studies of regiomer tetrazoles,²⁹ it has been shown that the Gly- α - H_2 1H resonance for the 1,5-disubstituted tetrazole appears further upfield than the Gly- α - H_2 signal of the 2,5-disubstituted tetrazole. ^{13}C NMR studies of 1- and 2-methyltetrazoles have shown that the

methyl and CN_4 carbon atoms of the 1,5-disubstituted tetrazole are more shielded than the corresponding carbon atoms of the 2,5-disubstituted tetrazoles.³⁰ Based on the above observations the tetrazole that was eluted first was designated the 1,5-disubstituted tetrazole, **6.3.16**, since it showed a Gly- α - H_2 1H resonance at δ 5.47, and Gly- α - CH_2 and CN_4 ^{13}C resonances at δ 50.11 and δ 148.09, respectively. The more polar tetrazole, **6.3.17**, had a Gly- α - H_2 1H resonance at δ 5.53, and Gly- α - CH_2 and CN_4 ^{13}C resonances at δ 53.76, and δ 161.15, respectively. The 1H NMR and ^{13}C NMR spectra of the regiomer tetrazoles, **6.3.16** and **6.3.17**, are compared in Figures 6.3.1 and 6.3.2, where the diagnostic shift differences between the regiomer tetrazoles are annotated by a broad arrow.



Scheme 6.3.6. Reagents and conditions: **i.** TEMPO, KBr, sodium hypochlorite, 0 °C, 10 min.

More evidence for the stereochemical assignment of the tetrazole regiomers, **6.3.16** and **6.3.17**, was obtained by a heteronuclear multiple bond correlation (HMBC) experiment. The HMBC NMR experiment shows connectivity between carbon and hydrogen atoms at a two to three bond distance. The observed HMBC correlations for the tetrazole, **6.3.16** and **6.3.17**, are shown in Figure 6.3.3. Both compounds show similar HMBC correlations, however only the 1,5-disubstituted tetrazole, **6.3.16**, shows a correlation between the Gly- α - H_2 protons and the CN_4 carbon centre (indicated by a

broad arrow, Figure 6.3.3). The ring substitution of **6.3.16** places the CN_4 carbon centre three bonds from the Gly- α - H_2 protons, such that a weak correlation is observed. This correlation is not seen in the HMBC spectrum of **6.3.17**, as the Gly- α - H_2 protons and CN_4 carbon are separated by four bonds, and as such, are out of range for an observable HMBC correlation.

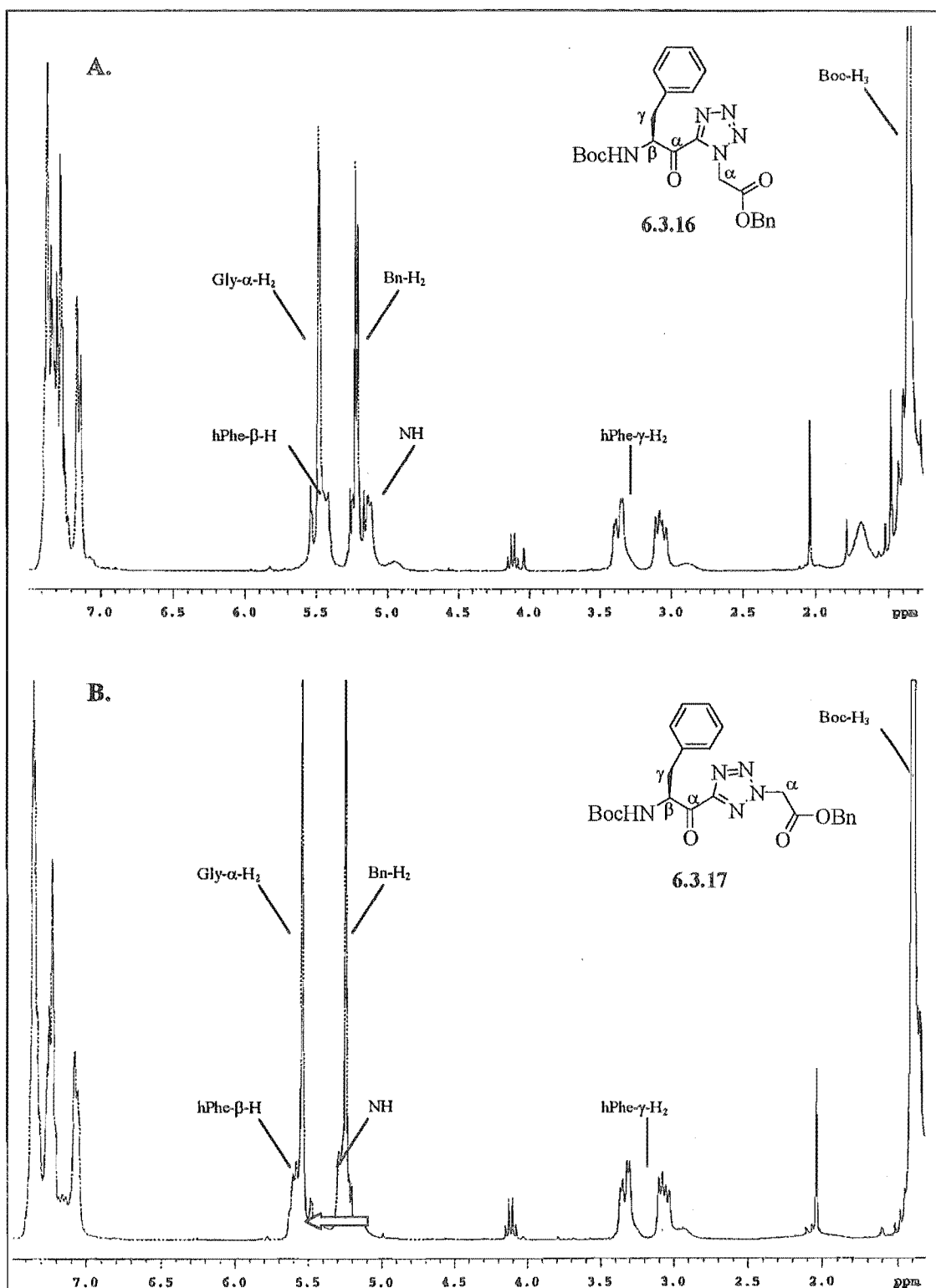
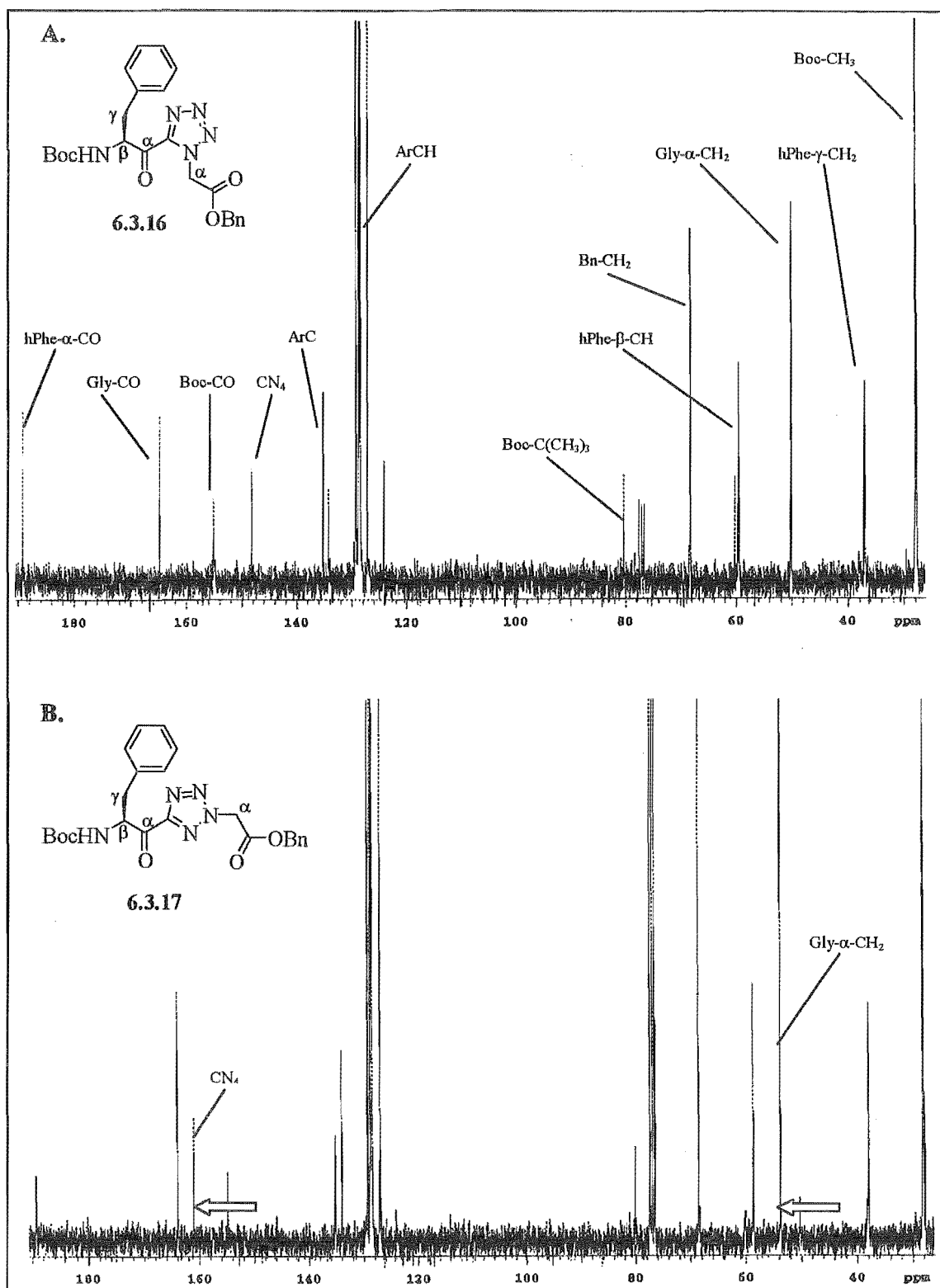


Figure 6.3.1 A. ^1H NMR spectrum of the 1,5-disubstituted tetrazole, **6.3.16**; B. ^1H NMR spectrum of the 2,5-disubstituted tetrazole, **6.3.17**.



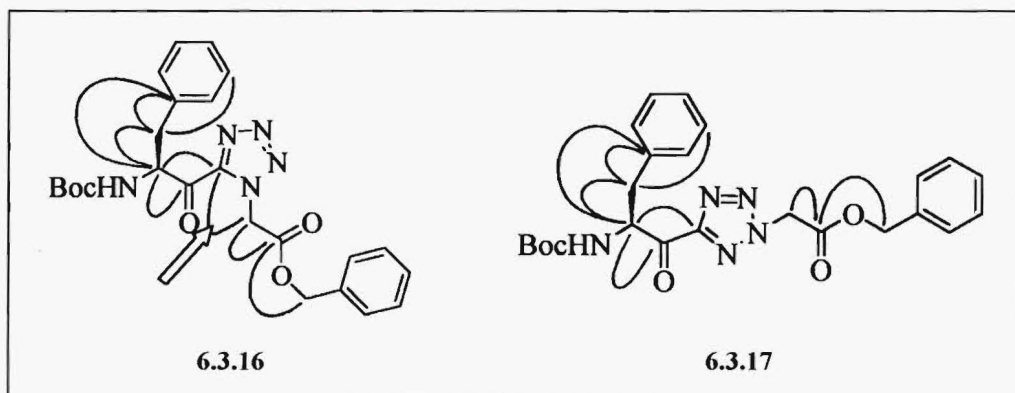


Figure 6.3.3. Observed HMBC correlations of the 1,5- and 2,5-disubstituted tetrazoles.

Single crystals of the 2,5-disubstituted tetrazole, **6.3.17**, were grown from methanol by slow evaporation. The structure of **6.3.17** was confirmed by an X-ray structure determination at 173(2) K and was satisfactorily refined (Figure 6.3.4) For a detailed discussion of the crystal structure of **6.3.17** see Chapter 7.3.

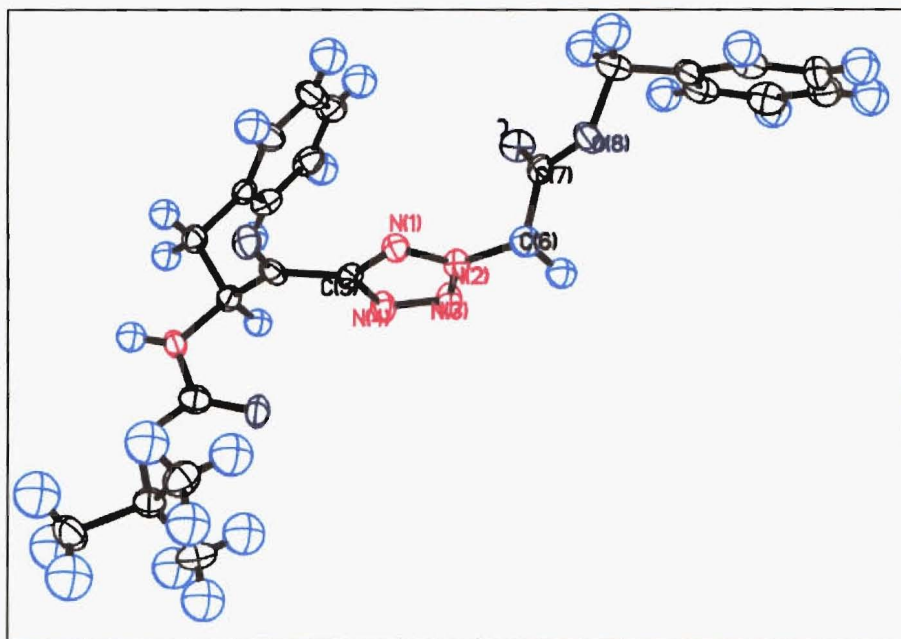


Figure 6.3.4. The solid state structure of the 2,5-disubstituted tetrazole, **6.3.17**.

6.4. CONCLUSION

Although our investigation into the direct functionalisation of tetrazole-based dipeptides could not be used as a synthetic route to the α -keto tetrazole isostere (see Discussion 6.2), the work gave some insight into the relative reactivity of the C3 and C6 carbon centres adjacent to the tetrazole. We have established that alkylation of the tetrazole-based dipeptides will occur at the more acidic C6 carbon centre in preference to the C3 centre. This preliminary investigation into the synthesis of the α -keto tetrazole isostere also highlighted deficiencies in the synthesis of tetrazole-based dipeptides by the method of Zabrocki *et al.*¹⁹

An alternative synthesis of tetrazole-based dipeptides has been investigated and this method has been used as a novel route to the α -keto tetrazole isostere, 2.5.3. A direct alkylation of the α -hydroxy (1*H*)-tetrazole, 6.3.13, was used to introduce the C-terminal P₁' glycine residue and gave a mixture of readily separable regioisomers. The method developed here is more succinct than the method employed by Foulds *et al.*¹³ involving only five synthetic steps from *N*-protected *L*-phenylalanine, to yield the desired isostere, 2.5.3, in 10% overall yield.

The synthetic method than we have investigated would also provide an expedient route to the α -hydroxy tetrazole isostere, 2.5.2, through reduction of the α -keto tetrazole isostere, 2.5.3. This new method has more scope than the previous method employed,¹³ as it allows for the introduction of a variety of P₁ and P₁' residues into the tetrazole-based dipeptide mimic. This increases the utility of the α -keto tetrazole isostere for incorporation into substrate sequences as potential inhibitors or conformational probes.

6.5. REFERENCES

- ¹ Angelastro, M. R.; Mehdi, S.; Burkhart, J. P.; Peet, N. P.; Bey, P. *J. Med. Chem.* **1990**, *33*, 13.
- ² Chetterjee, S.; Dunn, D. D.; Tao, M.; Wells, G.; Gu, Z-Q.; Bihovsky, R.; Ator, M. A.; Siman, R.; Mallamo, J. P. *Bioorg. Med. Chem. Lett.* **1999**, *9*, 2371.
- ³ Peet, N. P.; Burkhart, J. P.; Angelastro, M. R.; Giroux, E. L.; Mehdi, S.; Bey, P.; Kolb, M.; Neises, B.; Schirlin, D. *J. Med. Chem.* **1990**, *33*, 394.
- ⁴ Hori, H.; Tasutake, A.; Minematsu, Y.; Powers, J. C. In, *Peptides, Structure and Function*. Eds. Deber, C. M.; Hruby, V. J.; Kopple, K. D. Pierce: Rockford, Illinois **1985**, 819.
- ⁵ Slee, D. H.; Laslo, K. L.; Elder, J. H.; Ollman, I. R.; Gustchina, A.; Kervinen, J.; Zdanov, A.; Wlodawer, A.; Wong, C-H. *J. Am. Chem. Soc.* **1995**, *117*, 11867.
- ⁶ Rich, D. H.; Sun, C-Q.; Prasad, J. V. N. V.; Patheriasseril, A.; Toth, M. V.; Marshall, G. R.; Clare, M.; Mueller, R. A.; Houseman, K. *J. Med. Chem.* **1991**, *34*, 1225.
- ⁷ Ikeda, S.; Ashley, J. A.; Wirshing, P.; Janda, K. D. *J. Am. Chem. Soc.* **1992**, *114*, 7604.
- ⁸ Angelastro, M. R.; Peet, N. P.; Bey, P. *J. Org. Chem.* **1989**, *54*, 3913.
- ⁹ Gordon, E. M.; Godfrey, J. D.; Pluscec, J.; Von Langen, D.; Natarajan, S. *Biochem. Biophys. Res. Commun.* **1985**, *126*, 419.
- ¹⁰ Harbeson, S. L.; Rich, D. H. *J. Med. Chem.* **1989**, *32*, 1378.
- ¹¹ Kaltenbronn, J. S.; Hudspeth, J. P.; Lunney, E. A.; Michnikewicz, B. M.; Nicholaides, E. D.; Repine, J. T.; Roark, W. H.; Stier, M. A.; Tinney, F. J.; Woo, P. D. W.; Essenburg, A. D. *J. Med. Chem.* **1990**, *33*, 838.
- ¹² Angelastro, M. R.; Marquart, A. L.; Mehdi, S.; Koehl, J. R.; Bey, P.; Vaz, J. R.; Peet, N. P. *Bioorg. Med. Chem. Lett.* **1999**, *9*, 139.
- ¹³ Abell, A. D.; Foulds, G. *J. Chem. Soc. Perkin 1* **1997**, 2475. Foulds G. J. *Biologically Active Peptide Analogues*. Ph.D. thesis, University of Canterbury **1996**.

- ¹⁴ Dess, D. B.; Martin, J. C. *J. Org. Chem.* **1983**, *48*, 4155.
- ¹⁵ Darkins, P.; McCarthy, N.; McKervey, M. A.; O'Donnell, K.; Ye, T.; Walker, B. *Tetrahedron:Asymmetry* **1994**, *5*, 195.
- ¹⁶ Danheiser, R. L.; Miller, R. F.; Brisbois, R. G.; Park, S. Z. *J. Org. Chem.* **1990**, *55*, 1959.
- ¹⁷ Darkins, P.; McCarthy, N.; McKervey, M. A.; Ye, T. *J. Chem. Soc. Chem. Commun.* **1993**, 1223.
- ¹⁸ Yu, K-L.; Johnson, R. L. *J. Org. Chem.* **1987**, *52*, 2051.
- ¹⁹ Zabrocki, J.; Dunbar, J. B.; Marshall, K. W.; Toth, M. V.; Marshall, G. R. *J. Org. Chem.* **1992**, *57*, 202.
- ²⁰ Huang, Z.; Probstel, A.; Spencer, J. R.; Yamazaki, T.; Goodman, M. *Int. J. Peptide Protein Res.* **1993**, 352.
- ²¹ Seebach, D.; Overhand, M.; Kuhnle, F. N. M.; Martinoni, B. *Helv. Chim. Acta.* **1996**, *79*, 913. Bastiaans, H. M. M.; Alewijnse, A. E.; van der Baan, J. L.; Ottenheijm, H. C. J. *Tetrahedron Lett.* **1994**, *41*, 7659.
- ²² Hruby, V. J.; Boteju, L. W. *Tetrahedron Lett.* **1993**, *34*, 1757.
- ²³ Bavetsias, V.; Bisset, G. M. F.; Kimbell, R.; Boyle, F. T.; Jackman, A. L. *Tetrahedron* **1997**, *53*, 13383.
- ²⁴ Boyle, F. T.; Crook, J. W.; Matusiak, Z. S. UK Pat. GB2272217A1 **1994** (*Chem. Abstr.* **1995**, *122*, 160665).
- ²⁵ Valle, G.; Crisma, M.; Yu, K-L.; Toniolo, C.; Mishra, R. K.; Johnson, R. L. *Coll. Czech. Chem. Commun.* **1988**, *53*, 2863.
- ²⁶ Grzonka, Z.; Liberek, B. *Rocz. Chem.* **1971**, *45*, 967.
- ²⁷ Satoh, Y.; Moliterni, J. *Synlett* **1998**, 528.
- ²⁸ Harbeson, S. L.; Abelleira, S. M.; Akiyama, A.; Barrett, R.; Carroll, R. M.; Straub, J. A.; Tkacz, J. N.; Wu, C.; Musso, G. F. *J. Med. Chem.* **1994**, *37*, 2918.
- ²⁹ Raap, R.; Howard, J. *Can. J. Chem.* **1969**, *47*, 813. Einberg, F. *J. Org. Chem.* **1970**, *35*, 3978.
- ³⁰ Elguero, J.; Marzin, C.; Roberts, J. D. *J. Org. Chem.* **1974**, *39*, 357. Butler, R. N. *Adv. Heterocycl. Chem.* **1977**, *21*, 323.

CHAPTER SEVEN
SOLID STATE STRUCTURES OF
TETRAZOLE-BASED DIPEPTIDE MIMICS

7.1. INTRODUCTION

During the course of this investigation into the synthesis of tetrazole-based isosteres we have been able to determine the solid structures of three tetrazole-based dipeptide mimics. What follows is a brief discussion of some of the features of the solid state structures of the tetrazole-based dipeptide mimics.

7.2. SOLID STATE STRUCTURES OF 1,5-DISUBSTITUTED TETRAZOLE-BASED DIPEPTIDE MIMICS

The solid state structures of three 1,5-disubstituted tetrazole-based dipeptide mimics have been presented in the literature to date (Figure 7.2.1 1.3.5-1.3.7). The structures all show a remarkable resemblance to the *cis*-amide bond, in their orientation of the peptide backbone and adjacent amino acid side chains (see Chapter 1.3). The tetrazole ring and its 1,5-substituents adopt an essentially planar arrangement, such that the torsion angle, ω , approximates zero in all three examples presented to date (1.3.5¹ $\omega=7.2^\circ$, 1.3.6² $\omega=4.8^\circ$, 1.3.7³ $\omega=2.9^\circ$). The tetrazole ring represents a good geometrical mimic, with bond angles and lengths reasonably close to the *cis*-amide conformer.²

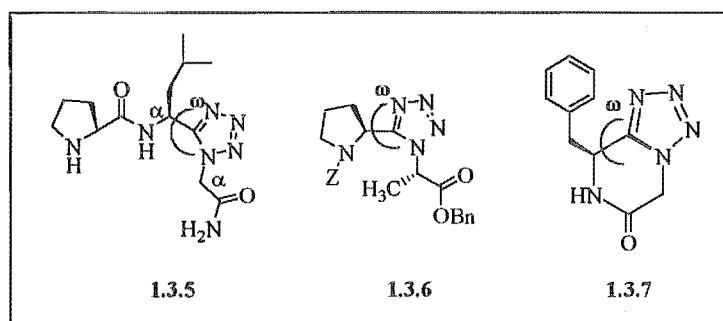
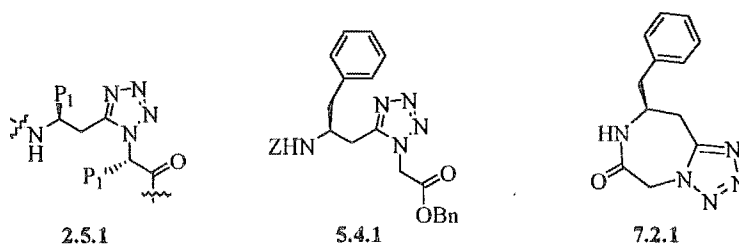


Figure 7.2.1. Tetrazole-based peptides of which the solid state structure is known.

We have observed the solid state structures of two tetrazole-based dipeptide mimics, 5.4.1 and 7.2.1, where the tetrazole heterocycle has been incorporated to lock the non-hydrolysable isostere of the ligand into a *cis*-conformation. We have designed and

synthesised an α -methylene tetrazole isostere, **2.5.1**, and incorporated this into a tetrazole-based dipeptide mimic, *N-Z-L*-homophenylalanine-[CN₄]-glycine benzyl ester, **5.4.1** (see Chapter 5.2 for a comparison of the solid state structure of the α -methylene tetrazole isostere, **2.5.1** and JG-365, 1.2.4.3). Single crystals of the tetrazole-based dipeptide, **5.4.1** were obtained by slow evaporation from methanol and the structure confirmed by an X-ray structure determination (Table 7.2.1, Figure 7.2.2)



The structural data obtained for the tetrazole heterocycle of **5.4.1** compares well with other reported 1,5-disubstituted tetrazoyl groups.⁴ The tetrazole ring was found to be essentially planar with the torsion angles C3-N2-N3-N4, N2-N3-N4-N5, N4-N5-C3-N2, N3-N2-C3-N5, C3-N5-N4-N3, being 0.04 (0.40)°, -0.02 (0.41)°, 0.03 (0.40)°, -0.04 (0.41)°, -0.01 (0.42)°, respectively and the ring atoms show a mean deviation from the plane of 0.00 Å. Bond lengths of the tetrazole heterocycle are all similar, with the bonds C3-N5, N5-N4, N4-N3, N3-N2, N2-C3 being, 1.317 (5) Å, 1.364 (5) Å, 1.302 (5) Å, 1.356 (4) Å, 1.334 (5) Å, respectively. The C3-N5 and N4-N3 bonds are slightly shorter than the other ring bonds, indicative of their double bond character. The N5-N4-N3 endocyclic bond angle, 110.5 (3)°, is wider than the C3-N5-N4 and N4-N3-N2 bond angles, 106.1 (3)° and 105.9 (3)°. The dipeptide mimic is folded at the homophenylalanine-[CN₄]-glycine sequence with the torsion angles, C3-C2-C1-N1, N2-C3-C2-C1, C3-N2-C4-C5, and N2-C4-C5-O4, being, 66.26 (0.36)°, -97.14 (0.40)°, 98.23 (0.43)°, and -172.34 (0.24)° respectively. The ω torsion angle at the homophenylalanine-glycine junction, C2-C3-N2-C4, is forced by the tetrazole heterocycle into a *cis*-conformation, where ω =13.05 (0.59)°. The phenyl ring of the homophenylalanine side chain is disordered in the crystal structure (Figure 7.2.1). The ring can be seen in two conformations, related by rotation about the C₂ axis.

Data collection device	CCD	
Empirical formula	C ₂₇ H ₂₇ N ₅ O ₄	
Formula weight	485.54	
Temperature	160(2) K	
Crystal system	Triclinic	
Space group	P1	
Unit cell dimensions	a = 5.0379(3) Å	α = 83.577(2)°
	b = 10.1066(7) Å	β = 81.897(2)°
	c = 12.7865(9) Å	γ = 76.475(2)°
Volume	624.55(7) Å ³	
Z	1	
Density (calculated)	1.291 Mg/m ³	
Absorption coefficient	0.089 mm ⁻¹	
F(000)	256	
Crystal size	0.8 x 0.4 x 0.02 mm ³	
Theta range for data collection	3.23 to 25.61°	
Index ranges	-1 ≤ h ≤ 5, -10 ≤ k ≤ 11, -12 ≤ l ≤ 15	
Reflections collected	2198	
Independent reflections	1867 [R(int) = 0.1010]	
Data / restraints / parameters	1867 / 3 / 365	
Goodness-of-fit on F ²	1.064	
Final R indices [I > 2σ(I)]	R1 = 0.0359, wR2 = 0.0898	
R indices (all data)	R1 = 0.0427, wR2 = 0.0957	

Table 7.2.1. Crystal data and X-ray experimental details for **5.4.1**.

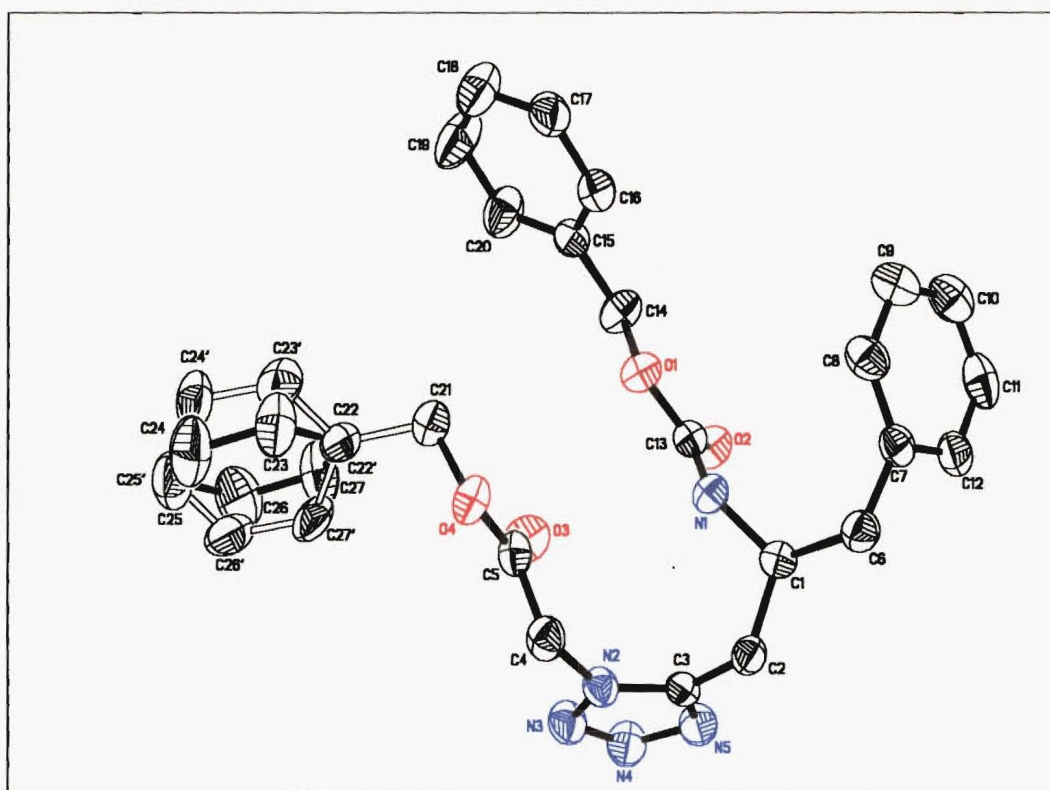
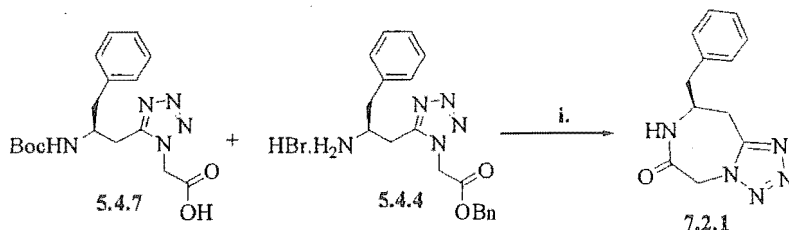


Figure 7.2.2. The solid state structure of *N-Z-L*-homophenylalanine-[CN₄]-glycine benzyl ester, **5.4.1**.

We have also been able to determine the solid state structure of the cyclic tetrazole-based dipeptide mimic, *cyclo*-{*L*-homophenylalanine-[CN₄]-glycine} 7.2.1, a seven-membered ring analogue of 1.3.7 (Figure 7.2.1). Compound 7.2.1 is a tetrazolodiazepines derivative of which very few exist in the literature.⁵ A great deal of synthetic work has been presented in the literature describing the preparation of nitrogen-containing five membered rings fused to the diazepine nucleus. Pyrrolodiazepines, imidazodiazepines, and triazolodiazepines are of great interest due to their interesting pharmacological activity on the central nervous system. The tetrazolodiazepine, 7.2.1, was formed during the attempted EDCI mediated coupling of the *N*-Boc-protected tetrazole-based dipeptide, 5.4.7, to amine hydrobromide, 5.4.4 (Scheme 7.2.1). The attempted coupling in the presence of DIPEA gave the cyclic product 7.2.1, in 93% yield.* The target coupled tetrapeptide was not observed by ¹H NMR or mass spectrometry. Single crystals of 7.2.1 were obtained by slow evaporation from methanol. The structure of 7.2.1 was solved at 163 (2) K, and was satisfactorily refined (see Figure 7.2.3).



Scheme 7.2.1. Reagents and conditions: i. EDCI, HOBt, DIPEA, rt, 18h.

The solid state structure of the cyclic tetrazole-based peptide mimic, 7.2.1 (Table 7.2.2, Figure 7.2.3), shows the tetrazole ring as essentially planar with a mean deviation from the plane of 0.003 Å. The ring torsion angles, N2-C5-N5-N4, C5-N5-N4-N3, N5-N4-N3-N2, N4-N3-N2-C5, and N3-N2-C5-N5 being -0.55 (15)°, 0.17 (16)°, 0.27 (16)°, -0.62 (15)° and 0.74 (15)°, respectively. The N3-N4 bond [1.2887 (18) Å] possesses the most double bond character of the heterocyclic bonds. The N2-N3 and N4-N5 bonds are the longest being 1.3537 (16) Å and 1.3650 (18) Å, respectively. The N2-C5 bond

* Yield based on starting benzyl ester, 5.4.4.

[1.3455 (18) Å] is shorter than the amide bond, N1-C2 [1.3508 (19) Å]. The diazepine ring is puckered with a deviation from the plane of 0.317 Å. The phenylalanine ring is essentially planar and adopts a flagpole orientation over the diazepine ring. The ω torsion angle at the homophenylalanine-glycine junction is forced to adopt a planar *cis*-conformation, where $\omega=3.3$ (2)°. This torsion angle is more than that observed for the six-membered analogue, 1.3.7 ($\omega=2.2^\circ$), possibly due to the increased flexibility of the seven-membered ring of 7.2.1, compared to the six-membered ring of 1.3.7.

Data collection device	CCD	
Empirical formula	C12 H13 N5 O	
Formula weight	243.27	
Temperature	163(2) K	
Crystal system	Orthorhombic	
Space group	P2(1)2(1)2(1)	
Unit cell dimensions	a = 6.374(2) Å	a = 90°.
	b = 8.621(3) Å	b = 90°.
	c = 20.890(7) Å	c = 90°.
Volume	1147.8(7) Å ³	
Z	4	
Density (calculated)	1.408 Mg/m ³	
Absorption coefficient	0.096 mm ⁻¹	
F(000)	512	
Crystal size	0.63 x 0.24 x 0.21 mm ³	
Theta range for data collection	2.56 to 26.42°.	
Index ranges	-4 ≤ h ≤ 7, -10 ≤ k ≤ 10, -26 ≤ l ≤ 25	
Reflections collected	14344	
Independent reflections	2338 [R(int) = 0.0271]	
Completeness to theta = 26.42°	99.4 %	
Absorption correction	Semi-empirical from equivalents	
Max. and min. transmission	0.9800 and 0.9418	
Refinement method	Full-matrix least-squares on F ²	
Data / restraints / parameters	2338 / 0 / 163	
Goodness-of-fit on F ²	1.036	
Final R indices [I > 2σ(I)]	R1 = 0.0323, wR2 = 0.0827	
R indices (all data)	R1 = 0.0374, wR2 = 0.0853	

Table 7.2.1. Crystal data and X-ray experimental details for 7.2.1.

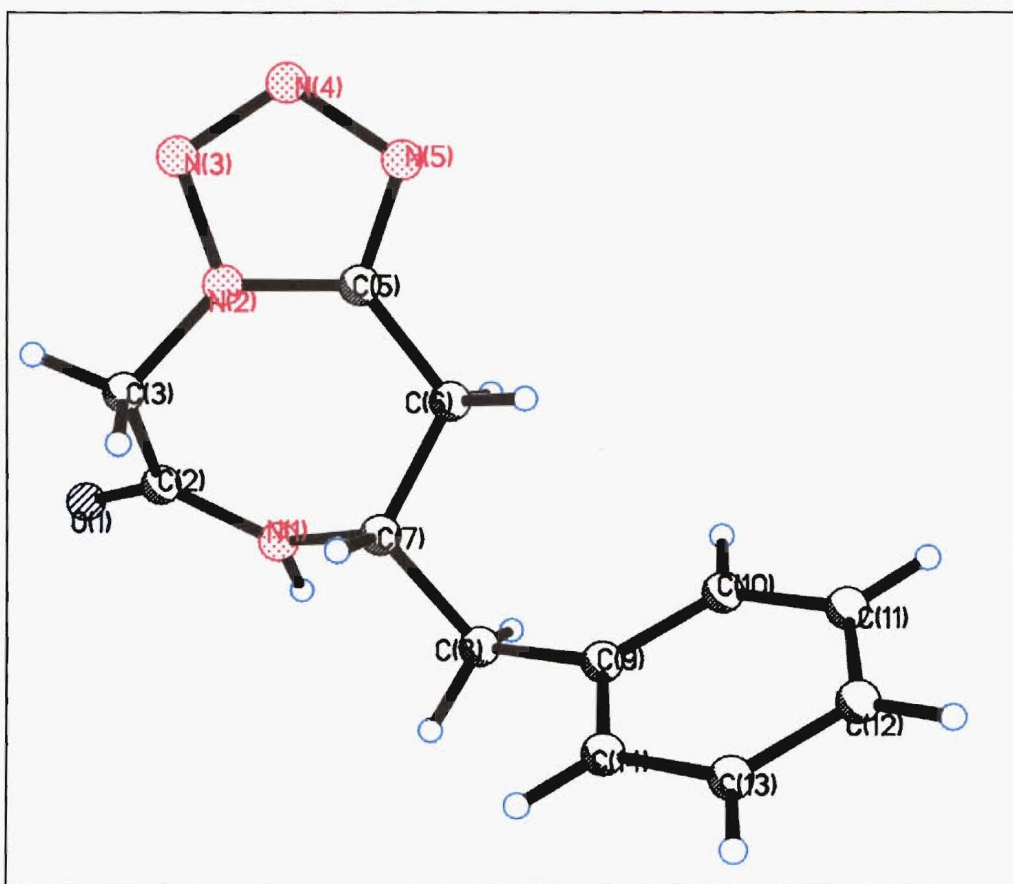


Figure 7.2.3. The solid state structure of *cyclo*-[homophenylalanine-[CN₄]-glycine], 7.2.1.

Figure 7.2.4 compares the geometric properties of the *cis*- amide bond obtained from a statistical analysis of published peptide X-ray diffraction structures,⁶ with geometric properties of the tetrazole-based dipeptides, 5.4.1 and 7.2.1. The tetrazole-based dipeptide, 7.2.1, is an excellent candidate for comparison with known structures of cyclic dipeptides in which the amide bonds must assume a *cis*- conformation to allow ring closure. In the tetrazole-based dipeptides, 5.4.1 and 7.2.1, the critical C^α---C^α separation (Figure 7.2.4) between adjacent amino acid residues is only 0.3 angstrom greater than that typical of a *cis*- amide bond. The C^α---C^α separation is shorter in the cyclic tetrazole-based dipeptide, 7.2.1 (3.190 Å), than its linear analogue, 5.4.1 (3.229 Å) and the former cyclic dipeptide makes a closer approximation to the C^α---C^α distance in the *cis*- amide bond (2.9 Å). The small variation between the tetrazole-based dipeptide mimics, 5.4.1 and 7.2.1, and the *cis*- amide bond is mainly due to the wider bond angles

at the C^α -C=N bond of the tetrazole (see Figure 7.2.4), as a consequence of the increased steric bulk of the tetrazole moiety.

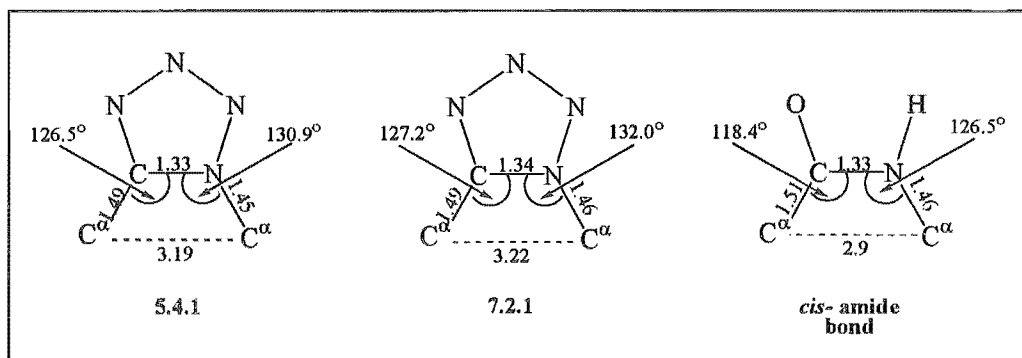
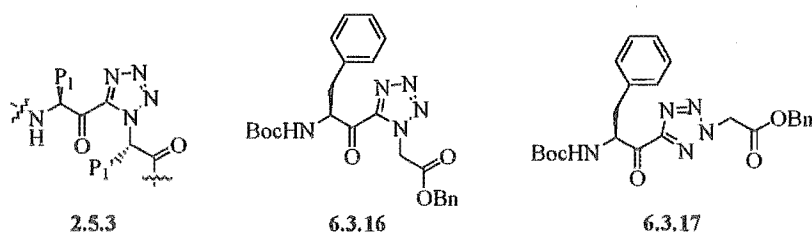


Figure 7.2.4. A comparison of the bond lengths (Å), angles and C^α --- C^α distances of the tetrazole-based amide bond surrogates, 5.4.1 and 7.2.1, and a generic *cis*-amide bond

The results of these structural determinations illustrate the rigidity of the tetrazole ring when it is incorporated into a peptide backbone. In addition, these results confirm the high degree of geometric similarity with linear peptides containing the *cis*-amide bond.

7.3. SOLID STATE STRUCTURE OF 2,5-*N*-Z-*L*-PHENYLALANINE-[COCN₄]-GLYCINE BENZYL ESTER

We have synthesised the α -keto tetrazole isostere [COCN₄] 2.5.3, and incorporated this into 1,5-disubstituted tetrazole-based dipeptide, 6.3.16, and 2,5-disubstituted tetrazole-based dipeptide, 6.3.17 (see Chapter 6.3). The solid state structure of 2,5-disubstituted, 6.3.17, was solved by a single crystal X-ray determination at 173 (2) K and was satisfactorily refined (Table 7.3.1). The solid state structure of 6.3.17 (Figure 7.3.1) was used to confirm the structural assignment of the regiomer tetrazoles, 6.3.16 and 6.3.17 (see Chapter 6.3) and this unique structure represents the first α -keto tetrazole-based dipeptide mimic to be reported.



The tetrazole ring of **6.3.17** is essentially planar with the ring torsion angles, C5-N1-N2-N3, N1-N2-N3-N4, N2-N3-N4-C5, N3-N4-C5-N1, N4-C5-N1-N2 being -0.3 (4) $^\circ$, 0.0 (4) $^\circ$, 0.3 (4) $^\circ$, -0.6 (4) $^\circ$ and 0.5 (4), respectively. The tetrazole ring of **6.3.17** showed a mean deviation from the plane of 0.002 Å. This indicates that the 2,5-tetrazole ring has similar planarity to the 1,5-tetrazole rings of **5.4.1**, and **7.2.1** (see Chapter 7.2) where the mean deviations from the plane were 0.00 Å, and 0.003 Å, respectively. The bond lengths of the tetrazole ring are all similar, with the C5-N1, N1-N2, N2-N3, N3-N4, N4-C5, being, 1.345 (4) Å, 1.325 (4) Å, 1.351 (3) Å, 1.327 (3) Å, and 1.352 (4) Å, respectively. The α -keto carbonyl bond sits in the same plane as the tetrazole ring, with the O18-C17-C5-N4, and O18-C17-C5-N4 torsion angles being -178.1 (3) $^\circ$ and -0.1 (5) $^\circ$, respectively. The core isostere [C17---C6] is essentially planar, with a mean deviation from the plane of 0.013 Å. The C17-C5 and N2-C6 bonds are offset by -10° . The phenylalanine ring is essentially planar and sits in a flagpole position over the tetrazole heterocycle.

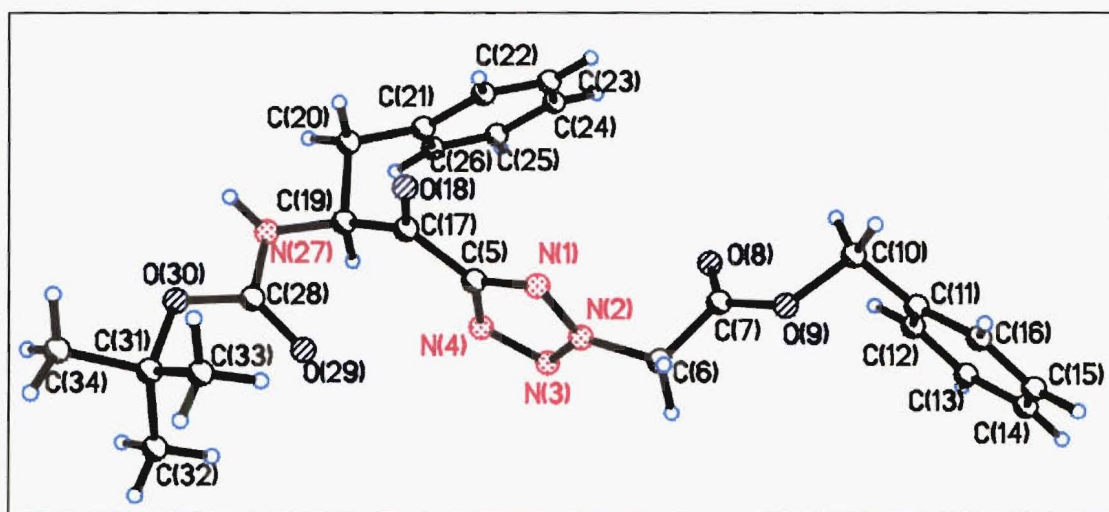


Figure 7.3.1. The solid state structure of the 2,5-disubstituted tetrazole-based dipeptide mimic, **6.3.17**.

Data collection device	CCD	
Empirical formula	C ₂₄ H ₂₇ N ₅ O ₅	
Formula weight	465.51	
Temperature	173(2) K	
Crystal system	Orthorhombic	
Space group	P2(1)2(1)2(1)	
Unit cell dimensions	a = 6.140(3) Å	a = 90°
	b = 16.264(7) Å	b = 90°
	c = 23.523(10) Å	g = 90°
Volume	2349.0(17) Å ³	
Z	4	
Density (calculated)	1.316 Mg/m ³	
Absorption coefficient	0.094 mm ⁻¹	
F(000)	984	
Crystal size	0.55 x 0.26 x 0.02 mm ³	
Theta range for data collection	2.14 to 26.45°	
Index ranges	-7<=h<=7, -20<=k<=18, -29<=l<=29	
Reflections collected	30663	
Independent reflections	4837 [R(int) = 0.1593]	
Completeness to theta = 26.45°	99.7 %	
Absorption correction	Semi-empirical from equivalents	
Max. and min. transmission	1.0000 and 0.8407	
Refinement method	Full-matrix least-squares on F ²	
Data / restraints / parameters	4837 / 0 / 307	
Goodness-of-fit on F ²	0.794	
Final R indices [I>2sigma(I)]	R1 = 0.0448, wR2 = 0.0714	
R indices (all data)	R1 = 0.1525, wR2 = 0.0904	

Table 7.3.1. Craystal data and X-ray experimental details for 6.3.17.

7.4. CONCLUSION

The solid state structures of the α -methylene tetrazole isostere [CH₂CN₄] 2.5.1, incorporated into the tetrazole-based dipeptide mimics, 5.4.1 and 7.2.1, have provided a useful insight into the structural properties of the tetrazole-based isostere. The tetrazole ring was shown to be essentially planar and compared well to the published structural data of known tetrazole-based dipeptides. We have used the tetrazole heterocycle as a *cis*-amide bond mimic to conformationally constrain ligands into the *cis*-conformation. The solid state structures of 5.4.1 and 7.2.1 illustrate the conformational restriction imparted by the tetrazole heterocycle forcing a pronounced 'kink' in the tetrazole-based dipeptide mimics. The solid state structure of the α -methylene tetrazole isostere, 2.5.1, is an

invaluable resource for the rational-based design of inhibitors and conformational probes that contain this tetrazole-based isosteres.

The cyclic tetrazole-based dipeptide, **7.2.1**, is part of a rare class of medicinally important compounds the tetrazolodiazepines. To date no solid state structure of a tetrazolodiazepine has been reported in the literature.

The solid state structure of the α -keto tetrazole-based dipeptide mimic, **6.3.17**, is unique in the literature and has aided in the unequivocal assignment of the regiomer α -keto tetrazoles, **6.3.16** and **6.3.17**.

7.5. REFERENCES

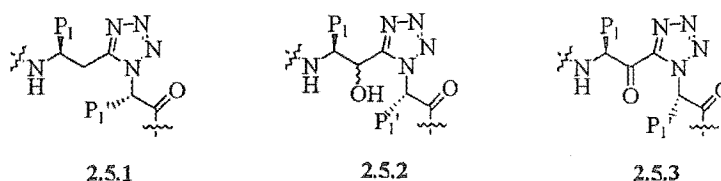
- ¹ Valle, G.; Crisma, M.; Yu, K-L.; Toniolo, C.; Misha, R. K.; Johnson, R. L. *Coll. Czech. Chem. Commun.* **1988**, *53*, 2863.
- ² Smith, G. D.; Zabrocki, J.; Flak, T. A.; Marshall, G. R. *Int. J. Peptide Protein Res.* **1991**, *37*, 191.
- ³ Zabrocki, J.; Smith, G. D.; Dunbar, J. B.; Iijima, H.; Marshall, G. R. *J. Am. Chem. Soc.* **1988**, *110*, 5875.
- ⁴ Dauter, Z.; Chawdhuri, S. A.; Hamid, M. A.; *Cryst. Struct. Commun.* **1982**, *11*, 999.
- ⁵ Peet, N. P.; Sunder, S. *J. Heterocycl. Chem.* **1977**, *14*, 561. Shishoo, C. J.; Devani, M. B.; Ullas, G. V.; Ananthan, S.; Bhadti, V. S. *J. Heterocycl. Chem.* **1988**, *25*, 615.
- ⁶ Liberek, B.; Kasprzykowska, R. *Int. J. Peptide Protein Res.* **1987**, *30*, 522.

CHAPTER EIGHT

FUTURE WORK

8.1. HIVP INHIBITORS

We have developed synthetic routes to the α -methylene tetrazole (2.5.1), α -hydroxymethylene tetrazole (2.5.2), and α -keto tetrazole (2.5.3) isosteres. The potent HIVp inhibitor JG-365 (1.2.4.3) formed the design basis of the tetrazole-based isosteres, 2.5.1-2.5.3, and of these the α -methylene tetrazole isostere (2.5.1) was incorporated into the modestly potent HIVp inhibitors, 5.4.1-5.4.3 (see Chapter 5.4). Computationally based studies should be undertaken to compare the bioactive conformation of JG-365 (1.2.4.3) and the more potent of the α -methylene tetrazole-based inhibitors, compound 5.4.3. It is thought that computational studies may support the effectiveness of the tetrazole-based isostere in its ability to orient the inhibitor backbone and side chain residue of the inhibitor, 5.4.3, into an equivalent conformation to that seen in the bioactive conformation of JG-365.



Future work directed at the inhibition of HIVp should also focus on the incorporation of the α -hydroxymethylene tetrazole (2.5.2) and α -keto tetrazole (2.5.3) isosteres into substrate sequences of HIVp which span the S_3 - S_3' subsites. We propose, based on the observed potency of α -hydroxy and α -keto based isosteric replacements, that the tetrazole-based equivalents, 2.5.2 and 2.5.3, could be used to generate HIVp inhibitors of improved potency over the α -methylene tetrazole-based inhibitors (5.4.1-5.4.3 Chapter 5.4) presented in this current work. Additionally, research should be directed at incorporating larger P_1' substituents into the tetrazole-based HIVp inhibitors 5.4.1-5.4.3.

8.2. TARGETING MEDICINALLY IMPORTANT RECEPTORS

The Brookhaven Protein Database (PDB) should be screened *in compuo* to identify target enzymes or receptors that bind ligands with a *cis*- conformation, as identified though the conformation of bound ligands in available receptor-ligand complexes. Having identified target receptors in this manner, ligands could be designed making use of the tetrazole-based isosteres to mimic the *cis*- conformation observed in these solid-state structures of ligand-receptor complexes. For this, the structural and electronic features of the α -methylene tetrazole isostere (2.5.1) obtained from the solid state structures of the tetrazole-based dipeptide mimics, 5.4.1 and 7.2.1 (Chapter 7.2) should be utilised in the rational design of tetrazole-based peptidomimetic ligands.

CHAPTER NINE

EXPERIMENTAL

9.1. GENERAL METHODS AND EXPERIMENTAL PROCEDURES

Nuclear Magnetic Resonance

Proton detected NMR spectra were obtained on a Varian Unity 300 spectrometer operating at 300 MHz. Carbon detected NMR spectra were obtained on a Varian XL 300 spectrometer operating at 75 MHz. Unless otherwise indicated, spectra were obtained at 23 °C. Other NMR experiments described in this thesis *viz*, reverse-detected HMQC, HSQC and HMBC were all obtained on the Unity 300 spectrometer at 300 MHz. At various stages this instrument was fitted with either a Nalorac Z.spec MID300 3 mm Indirect Detection Probe or a Pulsed Field Gradient MLD driver with a 5 mm Indirect Detection Probe. Chemical shifts are reported in parts per million (ppm), on the δ scale and are referenced to the appropriate solvent peaks; CDCl_3 referenced to $(\text{CH}_3)_4\text{Si}$ at $\delta_{\text{H}}=0$ ppm (^1H) and CDCl_3 at $\delta_{\text{C}}=77.0$ ppm (^{13}C); CD_3OD referenced to CHD_2OD at $\delta_{\text{H}}=3.30$ ppm (^1H) and CD_3OD at $\delta_{\text{C}}=49.3$ ppm (^{13}C); DMSO-d_6 referenced to $(\text{CD}_3)(\text{CHD}_2)\text{CO}$ at $\delta_{\text{H}}=2.17$ ppm (^1H) and $(\text{CD}_3)_2\text{CO}$ $\delta_{\text{C}}=29.2$ ppm (^{13}C). ^1H NMR spectra were obtained using an acquisition time (A_t) of 2 s. ^{13}C NMR were obtained with an A_t of 0.878 and typically at delay (D_1) of 0.5 s. HMQC experiments with the pulsed field gradient system were run with an A_t of 0.137 s, a D_1 of 1.0 s, and $^1J_{\text{CH}}=140$ Hz. HMBC experiments were obtained with an A_t of 0.21 s (0.137 s with the pulsed field gradient system), a relaxation delay of 0.3 s, $^1J_{\text{CH}}=140$ Hz, and $^nJ_{\text{CH}}=8.3$ Hz, unless otherwise stated.

Mass Spectroscopy

Mass spectroscopy was performed on a Kratos MS80 Mass Spectrometer operating at 4 kV. Various ionisation techniques were used including Electron Impact (EI MS) at 70 eV and chemical ionisation (CI; C_4H_{10}). The softer ionisation technique of Fast Atom Bombardment (FAB MS) was used where necessary and was performed with an Ion Tech ZN11FN ion gun using Xe as the reagent gas, operating at 8 kV and 2 mA with either NOBA (*m*-nitrobenzyl alcohol), m-b (magic bullet, 50% dithioerythritol/dithiothreitol), or glycerol as the matrix. Alternatively, compounds were

analysed by Electrospray (ES MS) by a Micromass LCT probe at 150 °C, operating at 3200 V, with an acetonitrile/water (1:1) carrier, from a source at 80 °C.

Infra-Red Spectroscopy

Infra-red (IR) spectra were obtained using a Shimadzu 8201PC series FTIR interfaced with a Intel 486 PC running Shimadzu's HyperIR[®] software. Spectra were run in a solution of CHCl₃, or as KBr plates.

Melting Points

Melting points were taken on an Electrothermal apparatus, and are uncorrected.

Optical Rotations

Optical rotations were measured on a JASCO J-20C recording spectropolarimeter or a Perkin Elmer polarimeter Model 341, both with a 10 mm path length. The $[\alpha]_D^{20}$ values are given in units of 10^{-1} deg cm² g⁻¹, with the concentration given in gcm⁻³.

Reagents and Solvents

Unless otherwise indicated, all reactions were conducted in flame-dried glassware, under an atmosphere of dry N₂ or Ar. Solvents and reagents used in reactions were purified according to well established procedures.¹ Tetrahydrofuran (THF), ether and benzene were distilled from sodium benzophenone ketyl immediately prior to use. Dichloromethane (CH₂Cl₂), chloroform (CHCl₃) were distilled from calcium hydride. Triethylamine (Et₃N), Hunig's base (*N,N*-diisopropyl-*N*-ethylamine, DIPEA), were distilled fresh from potassium hydroxide. Methanol and ethanol were distilled from iodine-magnesium turnings and stored over 4 Å molecular sieves under N₂ or Ar. *N,N*-Dimethylformamide (DMF) and acetonitrile (CH₃CN), were dried over 4 Å molecular sieves under N₂ or Ar. Organolithium reagents were titrated before use by the method of Watson and Eastham.²

Chromatography

Analytical thin layer chromatography (TLC) was conducted on aluminium-backed Merck Kieselgel KG60F₂₅₄ silica plates. Visualisation was by short-wave ultraviolet light. Flash chromatography was performed on Merck Silica 60 following the guidelines of Still *et al.*³ Plate layer chromatography (PLC) was performed on aluminium-backed Merck Kieselgel KG60F₂₅₄ silica plates, visualised by short-wave ultraviolet light. Preparative high pressure liquid chromatography (HPLC) was performed on a Philips PU4100 HPLC, fitted with a PU4120 diode array detector. Injections were made to either a Rainin RP-C₁₈ analytical or RP-C₁₈ preparative column.

General Procedure A: Preparation of esters and amides via Wolf rearrangement⁴

To a solution of diazoketone (1.0 eq.) in dry THF (0.15 M), in a flame-dried flask under N₂, was added the appropriate nucleophile (eg. benzyl alcohol, or methanol) (1.3 eq.) at rt. A solution of silver benzoate (catalytic, 0.3 eq.) in triethylamine (6.6 eq.) was added dropwise to the stirred solution and the reaction was stirred for a further 2 h at rt. Volatiles were removed under reduced pressure and the resulting residue was taken up in ethyl acetate, washed with 10% aqueous HCl (2 x 10 mL), saturated aqueous NaHCO₃ (2 x 10 mL), saturated aqueous NaCl (2 x 10 mL), dried (MgSO₄), filtered and evaporated. See experimental for details.

General Procedure B: Amino acid homologation with comittant peptide coupling⁵

A solution of amino acid ester hydrochloride or *para*-toluenesulphonate salt (1.5 eq.) and triethylamine (2.0 eq.) in dry acetonitrile (0.07 M) was prepared in a flame-dried quartz reaction vessel (100 mL capacity) under N₂. A solution of α -diazoketone (1.0 eq.) in dry acetonitrile (0.15 M) was prepared in a flame-dried flask under N₂ and then transferred, via syringe, to the quartz reaction vessel. The reaction vessel was irradiated at 300 nm under N₂ for 24 h or until the evolution of N₂ had ceased. Solvent was removed to 1/4 of the original volume, diluted with ethyl acetate and washed with 1 M aqueous citric acid (2 x 100 mL), saturated aqueous NaCl (2 x 100 mL), dried (MgSO₄), filtered and evaporated. See experimental for details.

General Procedure C: Tetrazole formation^{6,7}

A solution of phosphorous pentachloride (1.2 eq.) in dry CHCl_3 (0.12 M) was prepared in a flame-dried flask under N_2 . Freshly distilled quinoline (2.4 eq.) was added dropwise to the stirred solution at rt. The white precipitate that formed was stirred for 20 min at rt, while a solution of dipeptide (1.0 eq.) in dry CHCl_3 (0.08 M) was prepared in a flame-dried flask under N_2 . The reaction was cooled in an ice-water bath, prior to the dropwise addition of the dipeptide over 30 min. After 30 min at $<10^\circ\text{C}$ the ice-water bath was removed and a further portion of phosphorous pentachloride (0.2 eq.) was added. The reaction was stirred at rt for 2.5 h then a dry (Na_2SO_4) CHCl_3 or benzene solution of hydrazoic acid (30-50 eq.) was added. The reaction was stirred at rt for 48 h, then evaporated and redissolved in ethyl acetate (20-50 mL). The organic phase was washed with aqueous 2 M HCl (2×50 mL), water (2×50 mL) and saturated aqueous NaCl (2×50 mL), dried (MgSO_4), filtered and evaporated. See experimental for detail.

General Procedure D: Acidic cleavage of *N*-benzyloxycarbonyl (Z) protecting group⁸

The peptide (1.0 eq.) was dissolved in concentrated acetic acid (2.0 M) and the solution treated with 50% hydrobromic acid/acetic acid (0.4 M). The reaction was stirred at rt for 30 min, then ether (45 mL), precooled at 0°C was added with vigorous stirring. Petroleum ether (20 mL) was added and the reaction stood at 0°C for 30 min. The solvent was decanted off and the brown residue washed with ether/petroleum ether (1:1, 3×30 mL). Solvent was removed under vacuum and the brown residue dried *in vacuo*, over KOH for 24 h. The hydromide salts were used without further purification. See experimental for detail.

General Procedure E: Catalytic hydrogenation of the benzyl ester (OBn) protecting group⁹

A stirred solution of the benzyl ester (1.0 eq.) and acetic acid (6.2 M) in ethyl acetate/ethanol (4:1, 50 mL) was hydrogenated at rt in the presence of 10% palladium on carbon (390 mgmmol^{-1}). The mixture was filtered through a plug of celite, evaporated and redissolved in aqueous 1 M NaHCO_3 . The aqueous phase was washed with ethyl

acetate (20 mL) and then acidified to pH=2 with solid sodium bisulphite. The free acid was extracted with ethyl acetate (4 × 50 mL), dried (MgSO₄), evaporated and the solid dried *in vacuo* over KOH for 24 h. The free acids were used without further purification. See experimental for detail.

General Procedure F: Acidic cleavage of *N*-*tert*-butyloxycarbonyl (Boc) protecting group¹⁰

The protected peptide (1.0 eq.) was dissolved in 95% aqueous trifluoroacetic acid (1-5 mL) and stirred slowly at rt for 30 min. Solvent was removed by rotary evaporation and the brown residue washed with petroleum ether (3 × 50 mL). The residue was dried *in vacuo* for 24 h over KOH and used without further purification.

General Procedure G: Peptide coupling with benzotriazo-1-ylxytris(dimethylamino)phosphonium hexafluorophosphate (BOP) reagent¹¹

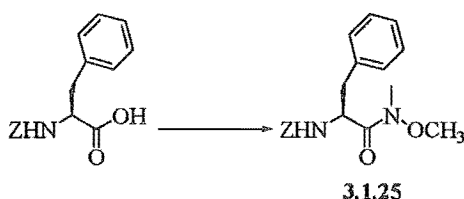
A solution of the amine hydrobromide or hydrochloride (1.0 eq.), carboxylic acid (1.1 eq.), BOP reagent (1.1 eq.) and dry DMF (100 μL), in dry CH₂Cl₂ (0.15 M) was prepared in a flame-dried flask under N₂. The solution was stirred at rt and triethylamine (3.0 eq.) was added dropwise. The reaction was stirred for 1 h, prior to the addition of a further portion of triethylamine (1.0 eq.). The reaction stirred at rt for 18 h and was quenched with saturated aqueous NaCl (5 mL). The reaction was diluted with ethyl acetate (100 mL), separated and washed with 2 M aqueous HCl (3 × 100 mL), 2 M aqueous NaHCO₃ (3 × 100 mL) and saturated aqueous NaCl (2 × 100 mL). The solution was dried (MgSO₄), filtered and evaporated. See experimental for detail.

General procedure H: Peptide coupling with 1-(3-dimethylaminopropyl)-3-ethylcarbodiimide hydrochloride (EDCI)¹²

To a solution of carboxylic acid (1.0 eq.) and HOBt (1.5 eq.) in dry DMF (0.2 M) in a flame-dried flask under N₂, was added amine hydrochloride or hydrobromide (1.1 eq.) as a solution in dry DMF (0.2 M). The reaction was cooled to 0 °C with stirring and EDCI (1.5 eq.), as a solution in dry DMF (0.5 M) was added dropwise. The reaction was stirred at 0 °C for 1 h, then for 24 h at rt. The reaction mixture was diluted with ethyl

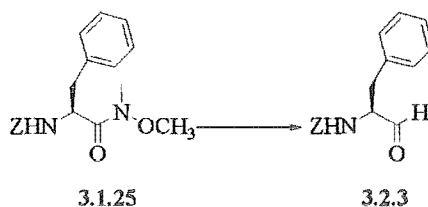
acetate (20 mL), and washed with saturated aqueous NaHCO_3 (3×20 mL), 1 M aqueous HCl (3×20 mL) and saturated aqueous NaCl (2×25 mL). The organic phase was dried (MgSO_4), filtered and evaporated. See experimental for detail.

9.2. SYNTHESIS OF 3-AMINO-2-HYDROXY-4-PHENYLBUTANOIC ACID

9.2.1. SYNTHESIS BY FUNCTIONALISATION OF *N-Z-L*-PHENYLALANINALSynthesis of *N-Z-L*-Phenylalaninal, 3.2.3, -Method APreparation of (2*S*)-*N*-(*N,O*-dimethylhydroxyl)-2-(*N*-benzyloxycarbonylamino)-3-phenylpropanamide, 3.1.25¹³

N-Z-L-Phenylalanine (500 mg, 1.6 mmol) was coupled to Weinreb amine hydrochloride¹⁴ (*N,O*-dimethylhydroxylamine hydrochloride, 180 mg, 1.84 mmol) with BOP reagent (739 mg, 1.67 mmol), in dry CH₂Cl₂ (5 mL), according to general procedure G. Purification of the crude reaction mixture by flash column chromatography (50% ethyl acetate/petroleum ether) gave amide, 3.1.25 (495 mg, 86%).

¹H NMR (300 MHz, CDCl₃) δ 2.91-3.08 (2H, m, Phe-β-H₂), 3.18 (3H, s, NCH₃), 3.68 (3H, s, OCH₃), 5.02 (1H, m, Phe-α-H), 5.06 (2H, AB system, δ_A=5.03, δ_B=5.09, d, J=12.2 Hz, Z-H₂), 5.41 (1H, d, J=7.8 Hz, NH), 7.15-7.37 (10H, m, ArH).

Preparation of (2*S*)-2-(*N*-benzyloxycarbonylamino)-3-phenylpropanal, 3.2.3¹³

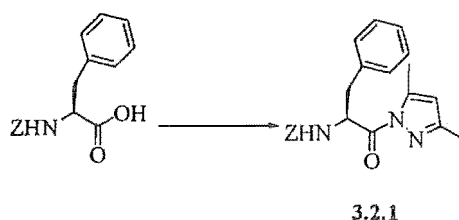
A solution of amide, 3.1.25 (760 mg, 2.23 mmol) in dry THF (15 mL) was added dropwise to a solution of lithium aluminum hydride (100 mg, 2.67 mmol) in dry THF (5 mL) at -50 °C, over 5 min. After stirring at -50 °C for 10 min the mixture was allowed to warm to 0 °C over 20 min, before recooling to -50 °C. Ethyl acetate (2 mL) was slowly

added to decompose remaining lithium aluminum hydride and the mixture was stirred at 0 °C for 20 min. The mixture was filtered and evaporated. The residue was re-dissolved in ethyl acetate (10 mL) washed with ice-cooled aqueous 1 M HCl (5 mL), aqueous 10% NaHCO₃ (5 mL) and water (5 mL), dried (MgSO₄), filtered and evaporated to give aldehyde, **3.2.3** (484 mg, 77%).

¹H NMR (300 MHz, CDCl₃) δ 3.14 (2H, d, J=6.4 Hz, Phe-β-H₂), 5.51 (1H, m, Phe-α-H), 5.11 (2H, s, Z-H₂), 5.33 (1H, d, J=6.3 Hz, NH), 7.14-7.37 (10H, m, ArH), 9.64 (1H, s, CHO).

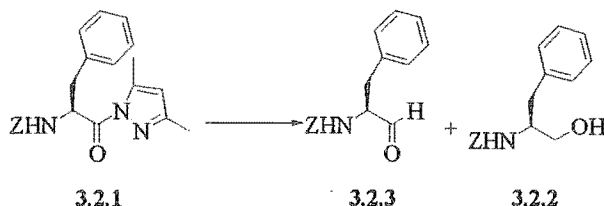
Synthesis of *N-Z-L*-Phenylalaninal, **3.2.3** -Method B

Preparation of (2*S*)-*N*-(3,5-dimethylpyrazole)-2-(*N*-benzyloxycarbonylamino)-3-phenylpropanamide, **3.2.1**¹⁵



To a solution of *N-Z-L*-phenylalanine (5.06 g, 16.9 mmol) and 3,5-dimethylpyrazole (1.93 g, 20.3 mmol) in CHCl₃ (250 mL) at -10 °C, was added dicyclohexylcarbodiimide (DCC, 3.59 g, 20.3 mmol) and the mixture was stirred for 1 h before warming to rt and stirring for a further 48 h. The insoluble urea was removed by filtration and solvent removed by evaporation. The residue was redissolved in ethyl acetate (50 mL), washed with aqueous 2 M HCl (10 mL) and water (10 mL), dried (MgSO₄), filtered and evaporated. A single recrystallisation from ethyl acetate/petroleum ether gave amide, **3.2.1**, as fine white needles (5.44 g, 85%).

¹H NMR (300 MHz, CDCl₃) δ 2.77 (3H, s, CH₃), 2.48 (3H, s, CH₃), 3.21 (2H, AB system, δ_A=3.09, δ_B=3.33, dd, J=7.1, 13.8 Hz, Phe-β-H₂), 5.07 (2H, AB system, δ_A=5.05, δ_B=5.10, d, J=12.2 Hz, Z-H₂), 5.47 (1H, d, J=8.8 Hz, NH), 5.99 (1H, s, Py-4-H), 7.06-7.33 (10H, m, ArH).

Preparation of (2*S*)-2-(*N*-benzyloxycarbonylamino)-3-phenylpropanal, 3.2.3, and (2*S*)-2-(*N*-benzyloxycarbonylamino)-3-phenylpropanol, 3.2.2¹⁵

A solution of amide, 3.2.1 (5.44 g, 14.4 mmol) in dry THF (150 mL) was added dropwise to a solution of lithium aluminum hydride (5.08 mg, 17.0 mmol) in dry THF (100 mL) at $-50\text{ }^{\circ}\text{C}$ over 5 min. After stirring at $-50\text{ }^{\circ}\text{C}$ for 10 min the mixture was allowed to warm to $0\text{ }^{\circ}\text{C}$ over 20 min, before recooling to $-50\text{ }^{\circ}\text{C}$. Ethyl acetate (80 mL) was slowly added to decompose remaining lithium aluminum hydride and the mixture was stirred at $0\text{ }^{\circ}\text{C}$ for 20 min. The mixture was filtered and evaporated. The residue was redissolved in ethyl acetate (150 mL), washed with ice-cooled aqueous 1 M HCl (150 mL), aqueous 10% NaHCO_3 (150 mL) and water (150 mL), dried (MgSO_4), filtered and evaporated. Purification of the crude reaction mixture by flash column chromatography (30% ethyl acetate/petroleum ether) gave aldehyde, 3.2.3 (1.99 g, 49%).

Spectral data for aldehyde, 3.2.3, was identical to that already reported (see Method A).

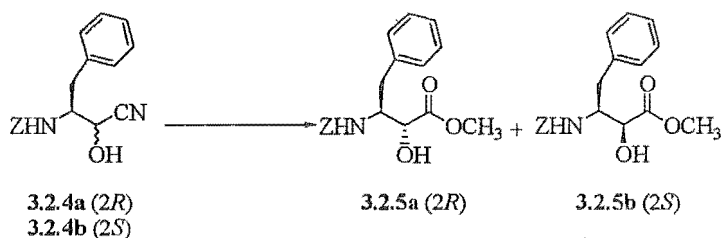
Further elution gave alcohol, 3.2.2 (1.19 g, 29%).

^1H NMR (300 MHz, CDCl_3) δ 2.86 (2H, d, $J=7.3$ Hz, Phe- γ - H_2), 3.63 (2H, AB system, $\delta_A=3.58$, $\delta_B=3.68$, dd, $J=4.9$, 11.2 Hz, Phe- α - H_2), 3.94 (1H, m, Phe- β -H), 5.00 (1H, d, $J=7.3$ Hz, NH), 5.07 (2H, s, Z- H_2), 7.18-7.93 (10H, m, ArH).

(2*R*,3*S*)-3.2.4a; ^1H NMR (300 MHz, CDCl_3) δ 2.85 (2H, d, $J=7.8$ Hz, hPhe- γ - H_2), 4.17 (1H, m, hPhe- β -H), 4.42 (1H, d, $J=3.0$ Hz, hPhe- α -H), 5.00 (2H, s, Z- H_2), 5.08 (1H, d, $J=8.8$ Hz, NH), 7.10-7.31 (10H, m, ArH).

(2*S*,3*S*)-3.2.4b; ^1H NMR (300 MHz, CDCl_3) δ 2.95 (2H, m, hPhe- γ - H_2), 3.96 (1H, m, hPhe- β -H), 4.49 (1H, d, $J=3.9$ Hz, hPhe- α -H), 5.01 (2H, s, Z- H_2), 5.18 (1H, d, $J=7.9$, NH), 7.10-7.31 (10H, m, ArH).

Preparation of (2*R*,3*S*) and (2*S*,3*S*)-3-(*N*-benzyloxycarbonylamino)-2-hydroxy-4-phenylbutanoic acid methyl esters [*N*-Z-(2*R*,3*S*)-AHPBA methyl ester, 3.2.5a and *N*-Z-(2*S*,3*S*)-AHPBA methyl ester, 3.2.5b]¹¹



The cyanohydrins, 3.2.4, as an epimeric mixture (3.2.4a and 3.2.4b 1:1 by ^1H NMR, 1.78 g, 5.7 mmol) were dissolved in pre-cooled (0°C) dry ether/methanol (3:1, 80 mL), previously saturated with gaseous HCl. The reaction was stirred at 5°C for 24 h, prior to the addition of ice-cooled water (15 mL), added at such a rate that the temperature was maintained below 10°C . The mixture was stirred at 5°C for a further 48 h. Solvent was removed to 1/3 of the volume and extracted with CH_2Cl_2 (3×10 mL). Combined organic extracts were washed with water (5 mL) and saturated aqueous NaCl (5 mL), dried (MgSO_4), filtered and evaporated. The crude reaction products were separated by flash column chromatography (30% ethyl acetate/petroleum ether) to give methyl esters, 3.2.5a and 3.2.5b.

N-Z-(2*R*,3*S*)-AHPBA methyl ester, 3.2.5a; (567 mg, 29%); mp $95\text{--}96^\circ\text{C}$ (lit.¹⁹ mp $94\text{--}95^\circ\text{C}$); $[\alpha]_{\text{D}}^{20}$ -68° ($c=0.0036$, methanol) (lit.¹⁹ $[\alpha]_{\text{D}}^{20}$ -82° $c=0.83$, methanol).

^1H NMR (300 MHz, CDCl_3) δ 2.93 (2H, m, hPhe- γ - H_2), 3.69 (3H, s, OCH_3), 4.08 (1H, bs, hPhe- α -H), 4.32, (1H, m, hPhe- β -H), 5.03 (2H, s, Z- H_2), 5.16 (1H, d, $J=9.9$ Hz, NH), 7.20-7.36 (10H, m, ArH).

^{13}C NMR (75 MHz, CDCl_3) δ 38.22 (hPhe- γ - CH_2), 52.83 (OCH_3), 54.69 (hPhe- β -CH), 66.72 (Z- CH_2), 70.09 (hPhe- α -CH), 126.69, 127.88, 128.03, 128.44, 128.58, 129.34 (ArCH), 136.34, 137.24 (ArC), 155.67 (Z-CO), 174.08 (COOCH_3).

TLC (analytical, 30% ethyl acetate/petroleum ether) $R_f=0.20$; IR (CDCl_3 , cm^{-1}) 3529, 3435, 3033, 2956, 2252, 1732, 1508, 1456, 1442, 1220; EI MS 254.1189 $\text{C}_{16}\text{H}_{16}\text{NO}_2$ ($\text{M}-\text{C}_3\text{H}_5\text{O}_3^+$) requires m/z 254.1181, 252.0879 $\text{C}_{12}\text{H}_{14}\text{NO}_5$ ($\text{M}-\text{C}_7\text{H}_7^+$) requires m/z 252.0872; EI MS (rel. intensity) 91(100), 108(70), 143(15), 203(20).

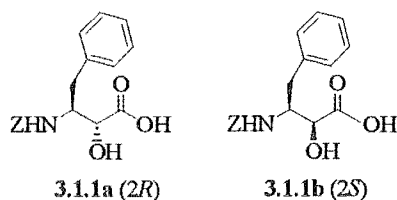
N-Z-(2S,3S)-AHPBA methyl ester, **3.2.5b**; (584 mg, 30%); mp 121-122 °C (lit.¹⁹ mp 121-122 °C); $[\alpha]_{\text{D}}^{20} -3^\circ$ ($c=0.013$, methanol) (lit.¹⁹ $[\alpha]_{\text{D}}^{20} -6^\circ$ $c=0.85$, methanol).

^1H NMR (300 MHz, CDCl_3) δ 2.80 (2H, m, hPhe- γ - H_2), 3.55 (3H, s, OCH_3), 4.34 (1H, bs, hPhe- α -H), 4.37 (1H, m, hPhe- β -H), 5.03 (2H, s, Z- H_2), 5.13 (1H, d, $J=9.0$ Hz, NH), 7.17-7.32 (10H, m, ArH).

^{13}C NMR (75 MHz, CDCl_3) δ 35.58 (hPhe- γ - CH_2), 52.54 (OCH_3), 54.61 (hPhe- β -CH), 66.76 (Z- CH_2), 72.17 (hPhe- α -CH), 126.64, 127.96, 128.04, 128.35, 128.43, 129.40 (ArCH), 136.27, 136.80 (ArC), 155.87 (Z-CO), 172.95 (COOCH_3).

TLC (analytical, 30% ethyl acetate/petroleum ether) $R_f=0.12$; IR (CDCl_3 , cm^{-1}) 3531, 3436, 3031, 2956, 2252, 1720, 1510, 1456, 1440, 1220; EI MS 254.1189 $\text{C}_{16}\text{H}_{16}\text{NO}_2$ ($\text{M}-\text{C}_3\text{H}_5\text{O}_3^+$) requires m/z 254.1181, 252.0876 $\text{C}_{12}\text{H}_{14}\text{NO}_5$ ($\text{M}-\text{C}_7\text{H}_7^+$) requires m/z 252.0872; EI MS m/z (rel. intensity) 91(100), 108(60), 143(5), 203(25).

9.2.2. PREPARATION OF (2*R*,3*S*) AND (2*S*,3*S*)-3-(*N*-BENZYLOXYCARBONYLAMINO)-2-HYDROXY-4-PHENYLBUTANOIC ACID [*N*-Z-(2*R*,3*S*)-AHPBA, 3.1.1A AND *N*-Z-(2*S*,3*S*)-AHPBA, 3.1.1B]¹¹



The methyl esters, (*N*-Z-(2*R*,3*S*)-AHPBA methyl ester 3.2.5a or *N*-Z-(2*S*,3*S*)-AHPBA methyl ester 3.2.5b (1.0 eq.) and sodium hydroxide (1.4 eq.) were dissolved in methanol/water (80%, 5 mL) and the mixture stirred at rt for 2 h. The methanol was evaporated under reduced pressure and the aqueous layer acidified to pH=2 with 2 M aqueous HCl. The white precipitate was extracted with ethyl acetate (3 × 10 mL), dried (MgSO₄), filtered and evaporated. The white solid was dried *in vacuo* over KOH for 24 h, to give acids, 3.1.1a or 3.1.1b.

N-Z-(2*R*,3*S*)-AHPBA, 3.1.1a (88%); ¹H NMR (300 MHz, DMSO-*d*₆) δ 2.92 (2H, m, hPhe-γ-H₂), 3.93 (1H, bs, hPhe-α-H), 4.08 (1H, m, hPhe-β-H), 4.95 (2H, AB system, δ_A=4.92, δ_B=4.98, d, J=12.6 Hz, Z-H₂), 7.12-7.36 (10H, m, ArH).

¹³C NMR (75 MHz, DMSO-*d*₆) δ 37.44 (hPhe-γ-CH₂), 55.44 (hPhe-β-CH), 65.17 (Z-CH₂), 70.74 (hPhe-α-CH), 126.31, 127.46, 127.75, 128.36, 128.41, 129.30 (ArCH), 137.26, 139.70 (ArC), 155.67 (Z-CO), 174.09 (hPhe-COOH).

EI MS 254.1182 C₁₆H₁₆NO₂ (M-C₂H₃O₃⁺) requires *m/z* 254.1181; EI MS *m/z* (rel. intensity) 143 (20), 108 (50), 91 (100), 51 (50).

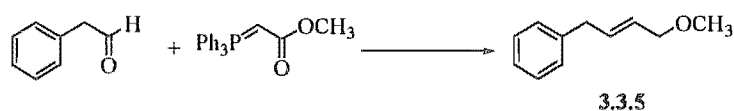
N-Z-(2*S*,3*S*)-AHPBA, 3.1.1b; (88%); ¹H NMR (300 MHz, DMSO-*d*₆) δ 2.68 (2H, m, hPhe-γ-H₂), 3.99 (1H, m, hPhe-β-H), 4.02 (1H, s, hPhe-α-H), 4.87 (2H, AB system, δ_A=4.88, δ_B=4.92, d, J=6.9 Hz, Z-H₂) 7.18-7.34 (10H, m, ArH).

¹³C NMR (DMSO-*d*₆) δ 38.75 (hPhe-γ-CH₂), 55.38 (hPhe-β-CH), 64.92 (Z-CH₂), 72.77 (hPhe-α-CH), 126.02, 127.35, 127.64, 128.12, 128.33, 129.13 (ArCH), 139.13 (d, ArCH), 155.63 (Z-CO), 174.05 (hPhe-COOH).

EI MS 254.1187 $C_{16}H_{16}NO_2$ ($M-C_2H_3O_3^+$) requires m/z 254.1181; EI MS m/z (rel. intensity) 143 (20), 108 (50), 91 (100), 51 (30).

9.2.3. SYNTHESIS BY AMINOHYDROXYLATION OF (*E*)-4-PHENYL-2-BUTENOIC ACID METHYL ESTER

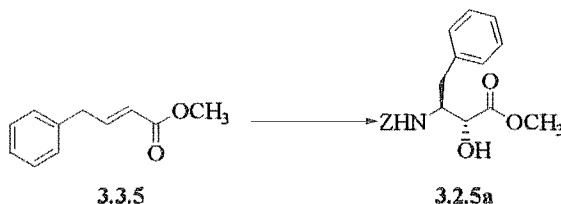
Preparation of (*E*)-4-phenyl-2-butenoic acid methyl ester, 3.3.5²⁰



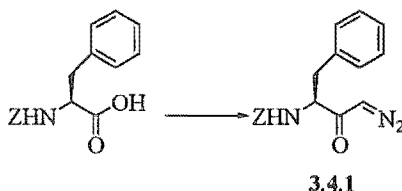
To a solution of methyl(triphenylphosphoranylidene)acetate (1.1 eq., 9.41 g, 28.2 mmol) in dry CH_2Cl_2 (50 mL), was added phenylacetaldehyde (3.08 g, 25.6 mmol, 3.0 mL) and the reaction stirred at rt for 16 h. The mixture was diluted with saturated aqueous NH_4Cl (50 mL) and the layers were separated. The organic layer was washed with saturated aqueous $NaCl$ (3 × 50 mL), dried ($MgSO_4$), filtered and evaporated. The resulting white solid was triturated with ether/petroleum ether (1:10, 10 mL) and filtered to remove the white solid. Solvent was removed from the filtrate to give crude methyl esters, *E*-3.3.5 and *Z*-3.3.5 (9:1). The methyl esters were separated by flash column chromatography (5% ethyl acetate/petroleum ether) to give the desired product, *E*-3.3.5, as a yellow oil (2.42 g, 54%).

1H NMR (300 MHz, $CDCl_3$) δ 3.51 (2H, AB system, $\delta_A=3.50$, $\delta_B=3.52$, d, $J=0.09$ Hz, γ -H₂), 3.71 (3H, s, OCH₃), 5.81 (1H, dt, $J=1.5$, 15.6 Hz, β -H), 7.11 (1H, dt, $J=6.9$, 15.6 Hz, α -H), 7.15-7.33 (5H, m, ArH).

TLC (analytical, 5% ethyl acetate/petroleum ether) $R_f=0.32$; EI MS 176.0837 (M^+) $C_{11}H_{12}O_2$ requires m/z 176.0837; EI MS m/z (rel. intensity) 176.1 (50), 144 (30), 117 (100), 91 (35).

Preparation of (2*R*,3*S*)-3-(*N*-benzyloxycarbonylamino)-2-hydroxy-4-phenylbutanoic acid methyl ester; [*N*-*Z*-(2*R*,3*S*)-AHPBA methyl ester, 3.2.5a]²¹

A solution of sodium hydroxide (122 mg, 3.05 mmol) in water (8.5 mL), was prepared in a single-necked round bottom flask. Potassium osmate dihydrate (14.7 mg, 0.04 mmol) was dissolved in a vial with a portion of the aqueous sodium hydroxide solution (0.5 mL). Benzyl carbamate (469 mg, 3.1 mmol) was dissolved in acetonitrile (4 mL) and cooled to 0 °C in an ice-bath. The fume hood was darkened and freshly prepared *tert*-butyl hypochlorite (346 μ L, 3.05 mmol) was added dropwise over 2 min. In another flask hydroquinidine 1,4-phthalazinediyl diether [(DHQ₂)(PHAL), 39 mg, 0.05 mmol], and aryl olefin, (*E*)-3.3.5 (190 mg, 1.0 mmol), were dissolved in acetonitrile (4.5 mL). This mixture was transferred to the aqueous sodium hydroxide solution. The pink osmate solution was transferred to the mixture and the reaction was stirred vigorously at rt for 2 h. The reaction was quenched with sodium sulphite (2.0 g) and the reaction mixture separated. The aqueous layer was extracted with ethyl acetate (3 \times 10 mL). The combined organic phases were washed with saturated aqueous NaCl (3 \times 25 mL), dried (MgSO₄), filtered and evaporated. Purification of the crude reaction mixture by flash column chromatography (30% ethyl acetate/petroleum ether) gave methyl ester 3.2.5a (<5%), contaminated with benzyl carbamate.

9.2.4. SYNTHESIS BY ENOLATE HYDROXYLATION OF *N-Z-L*-HOMOPHENYLALANINE METHYL ESTERPreparation of (3*S*)-3-(*N*-benzyloxycarbonylamino)-4-phenylbutane diazoketone, 3.4.1²²

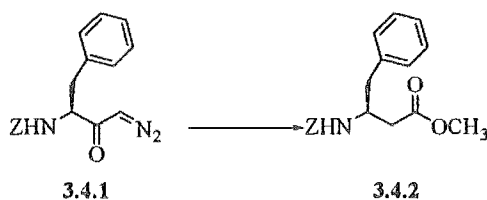
To a stirred solution of *N-Z-L*-phenylalanine (2.92 g, 9.7 mmol) in dry THF/ether (1:1, 50 mL) was added triethylamine (1.0 eq., 0.98 g, 9.7 mmol, 1.36 mL) and ethyl chloroformate (1.0 eq., 1.06 g, 9.7 mmol, 0.93 mL) at $-20\text{ }^{\circ}\text{C}$. After 15 min at $-20\text{ }^{\circ}\text{C}$ the mixed anhydride was added to a dried (Na_2SO_4) ethereal solution of diazomethane²³ (5.0 eq.). The mixture was stirred at $-15\text{ }^{\circ}\text{C}$ for 1 h, then left to stand at $5\text{ }^{\circ}\text{C}$ overnight. Excess diazomethane was destroyed by the dropwise addition of acetic acid [caution] until the evolution of N_2 ceased. The mixture was washed with saturated aqueous NaHCO_3 ($2 \times 30\text{ mL}$), saturated aqueous NaCl ($2 \times 30\text{ mL}$), dried (MgSO_4), filtered and evaporated. Flash column chromatography (30% ethyl acetate/petroleum ether) of the crude product and a single recrystallisation (ethyl acetate/petroleum ether) gave α -diazoketone, 3.4.1 (2.24 g, 71%). mp $85\text{--}86\text{ }^{\circ}\text{C}$ (lit.²² mp $84\text{--}85\text{ }^{\circ}\text{C}$); $[\alpha]_{\text{D}}^{20} -28^{\circ}$ ($c=0.005$, methanol).

^1H NMR (300 MHz, CDCl_3) δ 3.28 (2H, d, $J=6.9\text{ Hz}$, Phe- β - H_2), 4.48 (1H, m, Phe- α -H), 5.06 (1H, s, Z- H_2), 5.20 (1H, s, CHN_2), 5.47 (d, $J=7.5\text{ Hz}$, NH), 7.16-7.39 (10H, m, ArH).

^{13}C NMR (75 MHz, CDCl_3) δ 38.30 (Phe- β - CH_2), 54.53 (CHN_2), 58.76 (Phe- α -CH), 66.91 (Z- CH_2), 126.97, 127.93, 128.12, 128.44, 128.57, 129.21 (ArCH), 135.94, 136.05 (ArC), 155.66 (Z-CO), 192.78 (Phe-CO).

TLC (analytical, 30% ethyl acetate/petroleum ether) $R_f=0.44$; IR (CDCl_3 , cm^{-1}) 2124, 1730, 1635; FAB MS 324.1355 $\text{C}_{18}\text{H}_{17}\text{N}_3\text{O}_3$ (MH^+) requires m/z 324.1348.

Preparation of (3*S*)-3-(*N*-benzyloxycarbonylamino)-4-phenylbutanoic acid methyl ester, 3.4.2⁴



A solution of diazoketone, 3.4.1 (1.0 eq., 3.0 g, 9.6 mmol) was reacted with dry methanol (1.3 eq., 0.4 g, 13.0 mmol, 0.5 mL) in dry THF (100 mL) in the presence of silver benzoate (0.1 eq., 0.25 g, 1.0 mmol) and triethylamine (2.9 eq., 2.9 g, 29.0 mmol, 4.0 mL) according to general procedure A. The crude reaction mixture was purified by flash column chromatography (10% ethyl acetate/petroleum ether) and a single recrystallisation (ethyl acetate/petroleum ether) to give methyl ester, 3.4.2 as a pale solid (2.7 g, 84%), mp 54-55 °C (lit.⁴ mp, 56-57 °C).

¹H NMR (300 MHz, CDCl₃) δ 2.44 (2H, m, hPhe-γ-H₂), 2.83 (2H, m, hPhe-α-H₂), 3.60 (3H, s, OCH₃), 4.16 (1H, m, hPhe-β-H), 5.00 (2H, s, Z-H₂), 5.23 (1H, d, J=9.0, NH), 7.08-7.31 (10H, m, ArH).

¹³C NMR (75 MHz, CDCl₃) δ 37.29 (hPhe-α-CH₂), 40.19 (hPhe-γ-CH₂), 66.60 (Z-CH₂), 126.69, 127.99, 128.05, 128.47, 128.55, 129.30 (ArCH), 136.48, 137.48 (ArC), 155.58 (Z-CO), 171.92 (hPhe-COOCH₃).

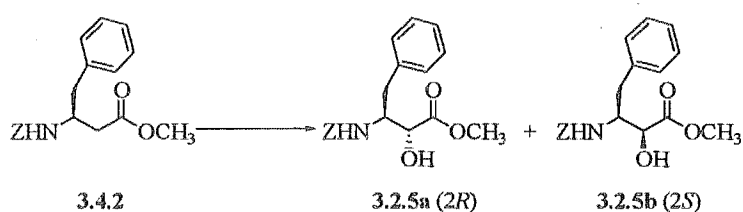
TLC (analytical, 40% ethyl acetate/petroleum ether) R_f=0.65; IR (CDCl₃, cm⁻¹) 3435, 2962, 2252, 1724, 1508, 1438, 1220; EI MS 296.1285 C₁₈H₁₈NO₃ (M-OCH₃⁺) requires *m/z* 296.1285, 236.0922 C₁₂H₁₄NO₄ (M-PhCH₂⁺) requires *m/z* 236.0926; EI MS *m/z* (rel. intensity) 176 (50), 145 (20), 117 (30) 91 (100).

Preparation of oxodiperoxymolybdenum(pyridine)(hexamethylphosphoric triamide) (MoOPH)²⁴

MoOPH was freshly prepared according to the procedure of Vedejs *et al.*²⁴ Molybdenum oxide (30 g, 0.2 mmol) and 30% aqueous hydrogen peroxide (150 mL) were stirred by a mechanical paddle in a 500 mL three-necked flask equipped with an internal thermometer. The mixture was heated in a 40 °C oil bath, until the internal

temperature reached 35 °C. At this time an exothermic reaction was initiated. The oil bath was removed and replaced with a water bath to maintain the internal temperature below 40 °C.²⁵ The mixture was then stirred at 40 °C for 3.5 h to give a yellow solution, with a small amount of white particulate. The solution was cooled to rt and filtered through a plug of celite. The resulting yellow filtrate was cooled in an ice bath to 10 °C and hexamethylphosphoric triamide (HMPA) (37.3 g, 0.21 mmol) was added dropwise to the stirred filtrate over 5 min. Stirring was continued for 15 min at 10 °C to give a yellow crystalline precipitate which was filtered and air dried using a vacuum aspirator for 30 min. The yellow solid was recrystallised from methanol and the resulting yellow needles were filtered and washed with cold methanol to give oxodiperoxymolybdenum(aqua)(hexamethylphosphoric triamide). The crystalline product was dried *in vacuo* over phosphorous pentoxide for 24 h to give oxodiperoxymolybdenum(hexamethylphosphoric triamide) as a hygroscopic yellow solid. A sample of this material, (36 g, 0.10 mol) was dissolved in dry THF (150 mL), and the solution filtered through a celite plug to remove any particulate. The filtrate, collected in a Buchner funnel equipped with a magnetic stirrer, was placed in a 20 °C water bath. Dry pyridine (8.0 g, 0.10 mol) was added portion-wise to the stirred solution over 10 min to give a yellow crystalline precipitate. The product was filtered off, washed with dry THF (25 mL), dry ether (200 mL) and finally dried *in vacuo*. Oxodiperoxymolybdenum(pyridine)(hexamethylphosphoric triamide) was thus obtained as a finely divided crystalline yellow solid (35 g); mp 111-112 °C (lit.²⁴ mp 103-105 °C).

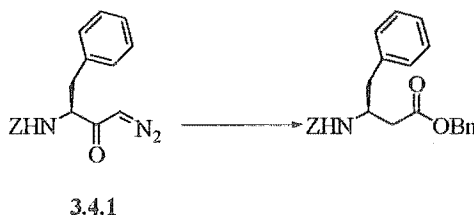
Preparation of (2*R*,3*S*) and (2*S*,3*S*)-3-(*N*-benzyloxycarbonylamino)-2-hydroxy-4-phenylbutanoic acid methyl esters [*N*-Z-(2*R*,3*S*)-AHPBA methyl ester, 3.2.5a and *N*-Z-(2*S*,3*S*)-AHPBA methyl ester, 3.2.5b]²⁶



A solution of KHMDS (6.0 eq., 0.5 M in toluene, 2.5 mmol, 5.2 mL) in dry THF (2 mL) was stirred and cooled to $-78\text{ }^{\circ}\text{C}$. A solution of methyl ester, **3.4.2** (140 mg, 0.43 mmol) in dry THF (4 mL) was prepared and added dropwise to the solution of KHMDS. The reaction mixture was warmed to $-25\text{ }^{\circ}\text{C}$, then cooled back down to $-78\text{ }^{\circ}\text{C}$ prior to the addition of MoOPH (1.5 eq., 360 mg, 0.64 mmol) as a single portion. The reaction mixture was warmed to $-60\text{ }^{\circ}\text{C}$ and stirred for 3 h. The reaction was quenched with saturated aqueous Na_2SO_3 (1 mL) and saturated aqueous NH_4Cl (1 mL), warmed to rt and stirred until dissolution of the white solids. The aqueous layer was extracted with THF (3 \times 10 mL) and the combined organic layers were washed with 10% aqueous HCl/saturated aqueous NaCl (1:1, 2 \times 10 mL), 2% aqueous Na_2CO_3 (2 \times 10 mL), saturated aqueous NaCl (2 \times 10 mL) and dried (MgSO_4). After filtration, solvent was removed under reduced pressure to give a yellow oil. The crude reaction mixture was purified by flash column chromatography (30% ethyl acetate/petroleum ether) to give unreacted starting material methyl ester, **3.4.2** (52 mg, 33%) and product methyl esters, *N*-Z-(2*R*,3*S*)-AHPBA methyl ester **3.2.5a** (34 mg, 35%) and *N*-Z-(2*S*,3*S*)-AHPBA methyl ester **3.2.5b** (32%, 31 mg).

Spectral data was identical to that already reported for these compounds.

Preparation of (3*S*)-3-(*N*-benzyloxycarbonylamino)-4-phenylbutanoic acid benzyl ester



Diazoketone **3.4.1** (100 mg, 0.31 mmol) in dry THF (2 mL) was reacted with benzyl alcohol (1.3 eq., 43 mg, 0.40 mmol, 42 μL) in the presence of silver benzoate (0.3 eq., 21 mg, 0.09 mmol) and triethylamine (6.6 eq., 206 mg, 2.04 mmol, 285 μL) according to general procedure A. The crude reaction mixture was purified by flash

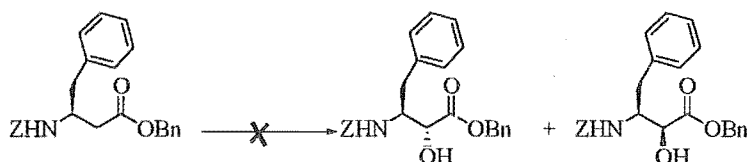
column chromatography (10% ethyl acetate/petroleum ether) and a single recrystallisation (ethyl acetate/petroleum ether) to give the benzyl ester as a pale solid (104 mg, 83%).

^1H NMR (300 MHz, CDCl_3) δ 2.55 (2H, m, hPhe- γ - H_2), 2.88 (2H, m, hPhe- α - H_2), 4.24 (1H, m, hPhe- β -H), 5.06 (2H, s, Z- H_2), 5.11 (2H, AB system, $\delta_{\text{A}}=5.08$, $\delta_{\text{B}}=5.14$, d, $J=12.3$ Hz, Bn- H_2), 5.29 (1H, d, $J=7.5$ NH), 7.10-7.35 (15H, m, ArH).

^{13}C NMR (75 MHz, CDCl_3) δ 37.50 (hPhe- α - CH_2), 40.15 (hPhe- γ - CH_2), 49.53 (hPhe- β -CH), 66.50 (Z- CH_2), 66.62 (Bn- CH_2), 126.69, 128.00, 128.07, 128.35, 128.37, 128.48, 128.55, 128.59, 129.31 (ArCH), 135.59, 136.48, 137.36 (ArC), 155.56 (Z-CO), 171.33 (hPhe-COObn).

IR (CDCl_3 , cm^{-1}) 3433, 3033, 2252, 1720, 1508, 1456, 1222; FAB MS 404.1872 $\text{C}_{25}\text{H}_{26}\text{NO}_4$ (MH^+) requires m/z 404.1861.

Attempted preparation of (2*R*,3*S*) and (2*S*,3*S*)-3-(*N*-benzyloxycarbonylamino)-2-hydroxy-4-phenylbutanoic acid benzyl esters [*N*-Z-(2*R*,3*S*)-AHPBA benzyl ester and *N*-Z-(2*S*,3*S*)-AHPBA benzyl ester]



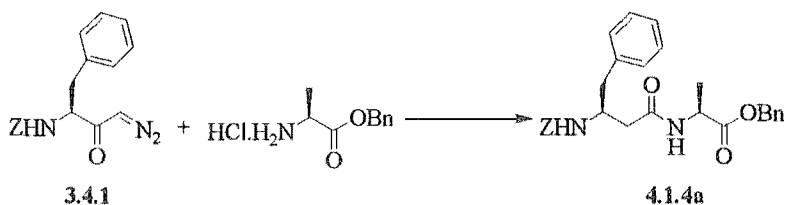
A solution of KHMDS (6.0 eq., 0.5 M in toluene, 0.21 mmol, 0.35 mL) in dry THF (0.3 mL) was stirred and cooled to -78 °C. A solution of the benzyl ester (14 mg, 0.03 mmol) in dry THF (0.02 mL) was prepared and added dropwise to the solution of KHMDS. The reaction mixture was warmed to -25 °C then cooled back down to -78 °C, prior to the addition of MoOPH (1.5 eq., 45 mg, 0.10 mmol) as a single portion. The reaction mixture was warmed to -60 °C and stirred for 3 h. The reaction was quenched with saturated aqueous Na_2SO_3 (1 mL) and saturated aqueous NH_4Cl (1 mL), warmed to rt and stirred until dissolution of the white solids. The aqueous layer was extracted with THF (3×10 mL) and the combined organic layers were washed with 10% aqueous HCl/saturated aqueous NaCl (1:1, 2×10 mL), 2% aqueous Na_2CO_3 (2×10 mL),

saturated aqueous NaCl ($2 \times 10\text{mL}$) and dried (MgSO_4). After filtration, the solvent was removed under reduced pressure to give a pale solid. The crude reaction mixture was purified by flash column chromatography (30% ethyl acetate/petroleum ether) to yield unreacted starting benzyl ester.

9.3. STEREOCHEMICAL ASSIGNMENT OF TETRAZOLE-BASED INHIBITORS

9.3.1. SYNTHESIS OF *L*-ALANINE DERIVATIVES

Preparation of (3*S*)-*N*-[3-(*N*-benzyloxycarbonylamino)-4-phenylbutanoic acid]-*L*-alanine benzyl ester, 4.1.4a¹¹



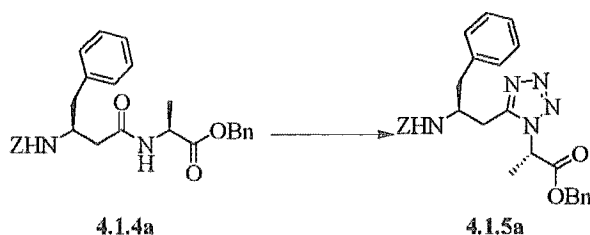
N-*Z*-*L*-Phenylalanine diazoketone, **3.4.1** (1.0 eq., 370 mg, 1.14 mmol) was reacted with *L*-alanine benzyl ester hydrochloride (1.2 eq., 372 mg, 1.72 mmol) in the presence of triethylamine (2.0 eq., 232 mg, 2.28 mmol, 0.4 mL) according to general procedure B. The crude reaction product was purified by flash column chromatography (30% ethyl acetate/petroleum ether) and a single recrystallisation (ethyl acetate/petroleum ether), to give dipeptide, **4.1.4a** (330 mg, 61%), as a white solid.

¹H NMR (300 MHz, CDCl₃) δ 1.36 (3H, d, J=7.2 Hz, Ala-β-H₃), 2.39 (2H, m, hPhe-γ-H₂), 2.88 (2H, m, hPhe-α-H₂), 4.14 (1H, m, hPhe-β-H), 4.59 (1H, q, J=7.2 Hz, Ala-α-H), 5.05 (2H, s, Z-H₂), 5.17 (2H, AB system, δ_A=5.14, δ_B=5.21, d, J=12.0 Hz, Bn-H₂), 5.79 (1H, d, J=7.5 Hz, NH), 6.21 (1H, d, J=6.3 Hz, NH), 7.17-7.34 (15H, m, ArH).

¹³C NMR (75 MHz, CDCl₃) δ 18.01 (Ala-β-CH₃), 38.51 (hPhe-α-CH₂), 40.13 (hPhe-γ-CH₂), 48.05 (Ala-α-CH), 50.10 (hPhe-β-CH), 66.44 (Z-CH₂), 67.12 (Bn-CH₂), 126.52, 127.85, 127.93, 128.12, 128.41, 128.51, 128.58, 129.27 (ArCH), 135.24, 136.54, 137.86 (ArC), 155.81 (Z-CO), 170.40 (Ala-CO), 172.57 (hPhe-CO).

TLC (analytical, 30% ethyl acetate/petroleum ether) R_f=0.25; FAB MS 475.2228 C₂₈H₃₁N₂O₅ (MH⁺) requires *m/z* 475.2233.

Preparation of (1*S*,2'*S*)-1-(benzyl 1-methyl-2-ethanoate)-5-[2-(*N*-benzyloxycarbonylamino)-3-phenylpropane]tetrazole, 4.1.5a¹¹



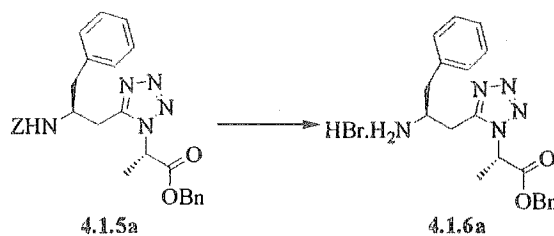
Dipeptide, 4.1.4a (100 mg, 0.21 mmol) was reacted according to general procedure C. Purification of the crude reaction mixture by radial chromatography (20%-50% ethyl acetate/petroleum ether) and HPLC (RP-C₁₈ preparative column, 30% H₂O/methanol, retention time 10.5 min) gave tetrazole, 4.1.5a (10 mg, 10%).

¹H NMR (300 MHz, CDCl₃) δ 1.87 (3H, d, J=6.9 Hz, Ala-β-H₃), 2.88 (2H, m, hPhe-γ-H₂), 2.89 (2H, d, J=6.0 Hz, hPhe-α-H₂), 4.25 (1H, m, hPhe-β-H), 5.00 (1H, q, J=6.9 Hz, Ala-α-H), 5.03 (2H, s, Z-H₂), 5.11 (2H, AB system δ_A=5.07, δ_B=5.14, d, J=12.3 Hz, Bn-H₂), 5.50 (1H, d, J=8.4 Hz, NH), 7.05-7.36 (15H, m, ArH).

¹³C NMR (75 MHz, CDCl₃) δ 16.80 (Ala-β-CH₃), 26.77 (hPhe-α-CH₂), 39.08 (hPhe-γ-CH₂), 55.92 (Ala-α-CH), 66.75 (Z-CH₂), 68.26 (Bn-CH₂), 126.84, 127.06, 127.33, 127.91, 128.14, 128.51, 128.70, 128.81, 129.30 (ArCH), 134.35, 136.16, 137.10 (ArC), 152.75 (CN₄), 155.78 (Z-CO), 167.59 (Ala-CO).

TLC (analytical, 50% ethyl acetate/petroleum ether) R_f=0.46; ES MS 500.2292 C₂₈H₃₀N₅O₄ (MH⁺) requires *m/z* 500.2298.

Preparation of (1*S*,2'*S*)-5-(2-amino-3-phenylpropane)-1-(benzyl 1-methyl-2-ethanoate)tetrazole hydrobromide, 4.1.6a¹¹

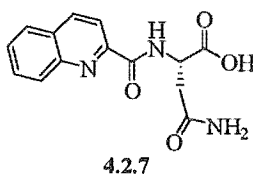


The tetrazole 4.1.5a (11 mg, 0.02 mmol) was deprotected according to general procedure D to give the amine hydrobromide salt 4.1.6a (8 mg, 90%), as a mixture of C-6 epimers (9:1 4.1.6a:4.1.6b).

^1H NMR (major product 4.1.6a, 300 MHz, CD_3OD) δ 1.89 (3H, d, $J=6.6$ Hz, Ala- β - H_3), 3.01-3.45 (4H, m, hPhe- α - H_2 & hPhe- γ - H_2), 4.10 (1H, m, hPhe- β -H), 5.13 (2H, s, Bn- H_2), 5.67 (1H, q, $J=6.6$ Hz, Ala- α -H), 7.21-7.34 (10H, m, ArH).

^{13}C NMR (major product 4.1.6a, 75 MHz, CD_3OD) δ 16.81 (Ala- CH_3), 27.14 (hPhe- α - CH_2), 39.55 (hPhe- γ - CH_2), 52.35 (hPhe- β -CH), 57.43 (Ala- α -CH), 69.50 (Bn- CH_2), 127.95, 128.97, 129.95, 129.80, 129.90, 129.94, 130.44, (ArCH), 136.59 (ArC), 154.17 (CN_4), 169.67 (Ala-CO).

Preparation of *N*-(2-quinolinylcarbonyl)-*L*-asparagine, 4.2.7²⁷



Quinaldic acid (1.0 eq., 2.0 g, 11.5 mmol) was dissolved in dry CH_2Cl_2 (60 mL) in a flame dried flask under N_2 . Thionyl chloride (2.0 eq., 1.75 mL, 23 mmol) was added and the white precipitate redissolved with the addition of triethylamine (1.0 eq., 1.6 mL, 11.5 mmol). The reaction was stirred at rt for 3 h then the solvent was removed under reduced pressure to give the acid chloride as a brown solid. A solution of *L*-asparagine (1.0 eq., 1.53 g, 11.5 mmol) and K_2CO_3 (1.0 eq., 3.45 g, 11.5 mmol) was prepared in water (20 mL) and the acid chloride, as a solution in toluene (80 mL) was added at rt. The reaction was stirred vigorously for 4 h, then the layers separated. The aqueous layer was acidified to pH=2 with 6 M aqueous HCl to precipitate a white solid. The solid product was filtered off and redissolved in ethanol, decolourised, filtered and evaporated *in vacuo*. The crude product was recrystallised from ethanol, to give acid, 4.2.7 (1.33 g, 40%).

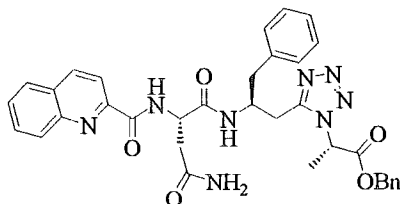
^1H NMR (300 MHz, $\text{DMSO}-d_6$) δ 2.79 (2H, AB system, $\delta_A=2.17$, $\delta_B=2.85$, dd, $J=4.8$, 16.2 Hz, Asn- β - H_2), 4.81 (1H, m, Asn- α -H), 7.73 (1H, t, $J=7.8$ Hz, QC-6-H), 7.88

(1H, t, J=7.8 Hz, QC-7-H), 8.08-8.19 (3H, m, QC-3-H & QC-5-H & QC-8-H), 8.59 (1H, d, J=8.4, QC-4-H), 9.16 (1H, d, J=8.7 Hz, QC-NH).

^{13}C NMR (75 MHz, DMSO- d_6) δ 36.48 (Asn- β -CH $_2$), 48.97 (Asn- α -CH), 118.65 (QC-3-CH), 128.25, 128.34, 129.04, 129.28, 130.79 (ArCH), 138.19 (QC-4-CH), 146.02 (QC-9-C), 149.53 (QC-2-C), 163.49 (QC-CO), 171.91 (Asn-CONH $_2$), 172.60 (Asn-COOH).

FAB MS 288.0983 C $_{14}$ H $_{14}$ N $_3$ O $_4$ (MH $^+$) requires m/z 288.0984.

Preparation of (1*S*,2'*S*)-1-(benzyl 1-methyl-2-ethanoate)-5-{2-[*N*-(2-quinolinylcarbonyl)-*L*-asparaginyl]amino]-3-phenylpropane}tetrazole, 4.1.7a¹¹



4.1.7a

The amine hydrobromide (1.0 eq., 8 mg, 0.02 mmol, as a mixture of C6 epimers 9:1 4.1.6a:4.1.6b) was coupled to *N*-(2-quinolinylcarbonyl)-*L*-asparagine 4.2.7 (2.5 eq., 17 mg, 0.05 mmol) according to general procedure G. The crude reaction product was purified by plate layer chromatography (ethyl acetate) to give protected tripeptide 4.1.7a (3 mg, 25%) as a mixture of C-6 epimers (7:3 4.1.7a:4.1.7b).

^1H NMR (major product 4.1.7a, 300 MHz, CDCl $_3$) δ 1.92 (3H, d, J=6.6 Hz, Ala- β -H $_3$), 2.72 (2H, m, Asn- β -H $_2$), 2.89-3.06 (4H, m, hPhe- α -H $_2$ & hPhe- γ -H $_2$), 4.49 (1H, m, hPhe- β -H), 4.91 (1H, m, Asn- α -H), 5.16 (2H, s, Bn-H $_2$), 5.21 (1H, q, J=7.5 Hz, Ala- α -H), 5.50 (1H, bs, NH), 5.98 (1H, bs, NH), 6.98-7.33 (10H, m, ArH), 7.63 (1H, t, J=6.3 Hz, QC-6-H), 7.77 (1H, t, J=7.8 Hz, QC-7-H), 7.87 (1H, d, J=6.0 Hz, QC-3-H), 8.19 (1H, q, J=9.3 Hz, QC-5-H), 8.29 (1H, t, J=11.7 Hz, QC-4-H), 9.25 (1H, d, J=8.1 Hz, NH).

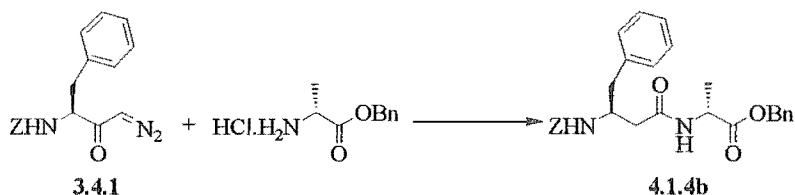
^{13}C NMR (major product 4.1.7a, 75 MHz, acetone) δ 16.25 (Ala- β -CH $_3$), 27.47 (hPhe- α -CH $_2$), 38.20 (Asn- β -CH $_2$), 39.65 (hPhe- γ -CH $_2$), 50.23 (hPhe- β -CH), 50.66 (Asn- α -CH), 55.49 (Ala- α -CH), 67.74 (Bn-CH $_2$), 118.64, 126.78, 127.58, 128.18, 128.32,

128.59, 128.72, 129.18, 129.38, 130.06, 130.14 (ArCH), 136.75, 137.46 (ArC), 146.56 (QC-9-C), 148.80 (QC-2-C), 155.94 (CN₄), 164.75 (QC-CO), 167.84 (Ala-CO), 170.65 (Asn-CO), 172.96 (Asn-CONH₂).

TLC (analytical, ethyl acetate) $R_f=0.24$; ES MS 635.2708 C₃₄H₃₅N₈O₅ (MH⁺) requires m/z 635.2730.

9.3.2. SYNTHESIS OF *D*-ALANINE DERIVATIVES

Preparation of (3*S*)-*N*-[3-(*N*-benzyloxycarbonylamino)-4-phenylbutanoic acid]-*D*-alanine benzyl ester, 4.1.4b



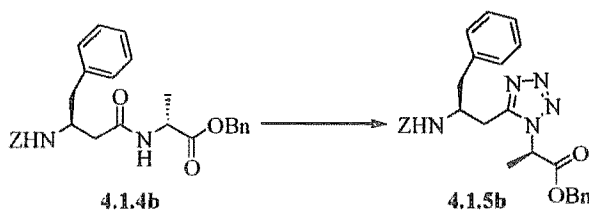
N-Z-*L*-Phenylalanine diazoketone, 3.4.1 (1.0 eq., 200 mg, 0.62 mmol) was reacted with *D*-alanine benzyl ester *para*-toluenesulphonate (2.4 eq., 525 mg, 1.48 mmol) in the presence of triethylamine (2.0 eq., 125 mg, 1.2 mmol, 0.2 mL) according to general procedure B. The crude reaction product was purified by flash column chromatography (30% ethyl acetate/petroleum ether) and a single recrystallisation (ethyl acetate/petroleum ether) to give dipeptide, 4.1.4b (200 mg, 65%), as a white solid. mp 149-150 °C.

¹H NMR (300 MHz, CDCl₃) δ 1.39 (3H, d, $J=7.5$ Hz, Ala-β-H₃), 2.39 (2H, m, hPhe-γ-H₂), 2.90 (2H, m, hPhe-α-H₂), 4.17 (1H, m, hPhe-β-H), 4.60 (1H, q, $J=7.5$ Hz, Ala-α-H), 5.06 (2H, s, Z-H₂), 5.16 (2H, AB system, $\delta_A=5.13$, $\delta_B=5.19$, d, $J=12.3$ Hz, Bn-H₂), 5.75 (1H, d, $J=7.8$ Hz, NH), 6.17 (1H, d, $J=6.9$ Hz, NH), 7.17-7.34 (15H, m, ArH).

¹³C NMR (75 MHz, CDCl₃) δ 18.15 (Ala-β-CH₃), 38.62 (hPhe-α-CH₂), 40.02 (hPhe-γ-CH₂), 48.09 (Ala-α-CH), 50.01 (hPhe-β-CH), 66.49 (Z-CH₂), 67.19 (Bn-CH₂), 126.57, 127.89, 127.96, 128.12, 128.43, 128.52, 128.59, 129.28 (ArCH), 135.22, 136.56, 137.84 (ArC), 155.84 (Z-CH₂), 170.36 (Ala-CO), 172.71 (hPhe-CO).

TLC (analytical, 30% ethyl acetate/petroleum ether) $R_f=0.12$; ES MS 475.2238 $C_{28}H_{31}N_2O_5$ (MH^+) requires m/z 475.2233.

Preparation of (1*R*,2'*S*)-1-(benzyl 1-methyl-2-ethanoate)-5-[2-(*N*-benzyloxycarbonylamino)-3-phenylpropane]tetrazole, 4.1.5b



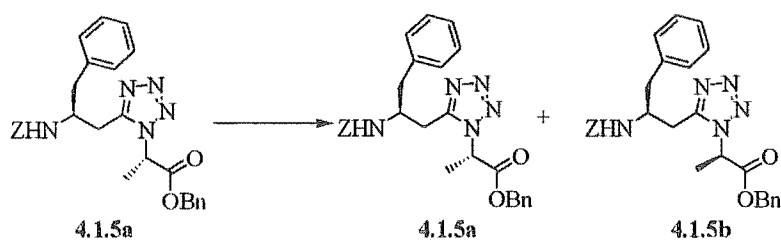
Dipeptide, 4.1.4b (100 mg, 0.21 mmol) was reacted according to general procedure C. Purification of the crude reaction mixture by radial chromatography (20%-50% ethyl acetate/petroleum ether) and HPLC (RP- C_{18} preparative column, 30% H_2O /methanol, retention time 10.8 min) gave tetrazole, 4.1.5b (15 mg, 15%).

1H NMR (300 MHz, $CDCl_3$) δ 1.87 (3H, d, $J=7.5$ Hz, Ala- β - H_3), 2.93 (2H, d, $J=6.9$ Hz, hPhe- γ - H_2), 3.02 (2H, d, $J=5.7$ Hz, hPhe- α - H_2), 4.22 (1H, m, hPhe- β -H), 5.00 (2H, s, Z- H_2), 5.13 (2H, s, Bn- H_2), 5.15 (1H, q, $J=7.5$ Hz, Ala- α -H), 5.30 (1H, d, $J=7.8$ Hz, NH), 7.14-7.33 (15H, m, ArH).

^{13}C NMR (75 MHz, $CDCl_3$) δ 16.66 (Ala- β - CH_3), 26.93 (hPhe- α - CH_2), 38.99 (hPhe- γ - CH_2), 50.36 (hPhe- β -CH), 55.53 (Ala- α -CH), 66.73 (Z- CH_2), 68.24 (Bn- CH_2), 126.91, 127.96, 128.16, 128.26, 128.51, 128.73, 129.05, 129.23 (ArCH), 134.36, 136.05, 136.81 (ArC), 152.48 (CN_4), 155.81 (Z-CO), 167.67 (Ala-CO).

TLC (analytical, 50% ethyl acetate/petroleum ether) $R_f=0.28$.

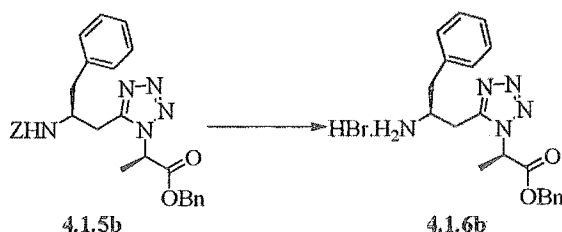
Preparation of (1*R*,2'*S*)-1-(benzyl 1-methyl-2-ethanoate)-5-[2-(*N*-benzyloxycarbonylamino)-3-phenylpropane]-tetrazole, 4.1.5b by racemisation of (1*S*,2'*S*)-1-(benzyl 1-methyl-2-ethanoate)-5-[2-(*N*-benzyloxycarbonylamino)-3-phenylpropane]tetrazole, 4.1.5a⁷



Protected tetrazole, 4.1.5a (40 mg, 0.08 mmol) was dissolved in 10% triethylamine/ CDCl_3 . Epimerisation was monitored by ^1H NMR (300 MHz, CDCl_3). After 48 h epimerisation of tetrazole, 4.1.5a had occurred to give a 1:1 mixture (by ^1H NMR) of tetrazoles, 4.1.5a and 4.1.5b. The tetrazoles were separated by plate layer chromatography (50% ethyl acetate/petroleum ether). Tetrazole 4.1.5a (7 mg, 17%) was collected from a higher R_f band ($R_f=0.46$), while tetrazole 4.1.5b (8 mg, 20%) ran as a lower R_f band ($R_f=0.28$).

Spectral data for both compounds, 4.1.5a and 4.1.5b, was identical to that already reported.

Preparation of (1*R*,2'*S*)-5-(2-amino-3-phenylpropane)-1-(benzyl 1-methyl-2-ethanoate)tetrazole hydrobromide, 4.1.6b

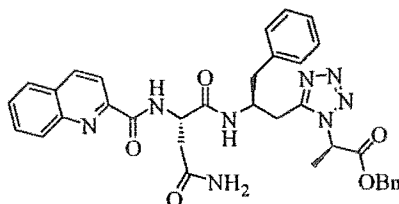


The tetrazole, 4.1.5b (13 mg, 0.03 mmol) was deprotected according to general procedure D to give the amine hydrobromide salt, 4.1.6b (9 mg, 89%), as a mixture of C-6 epimers (4:1 4.1.6b:4.1.6a).

^1H NMR (major product 4.1.6b, 300 MHz, CD_3OD) δ 1.91 (3H, d, $J=6.3$ Hz, Ala- β - H_3), 3.10 (2H, d, $J=6.9$ Hz, hPhe- γ - H_2), 3.36 (2H, m, hPhe- α - H_2), 4.11 (1H, m, hPhe- β -H), 5.19 (2H, s, Bn- H_2), 5.69 (1H, q, $J=6.3$ Hz, Ala- α -H), 7.21-7.40 (10H, m, ArH).

^{13}C NMR (major product 4.1.6b, 75 MHz, CD_3OD) δ 16.96 (Ala- CH_3), 27.26 (hPhe- α - CH_2), 39.49 (hPhe- γ - CH_2), 52.28 (hPhe- α -CH), 57.55 (Ala- α -CH), 69.57 (Bn- CH_2), 128.93, 129.16, 129.61, 129.88, 129.94, 130.38, 130.77, 130.84 (ArCH), 136.51 (ArC), 154.07 (CN_4), 169.81 (Ala-CO).

Preparation of (1*R*,2'*S*)-1-(benzyl 1-methyl-2-ethanoate)-5-{2-[*N*-(2-quinolinylcarbonyl)-*L*-asparaginyl]amino]-3-phenylpropane}tetrazole, 4.1.7b



4.1.7b

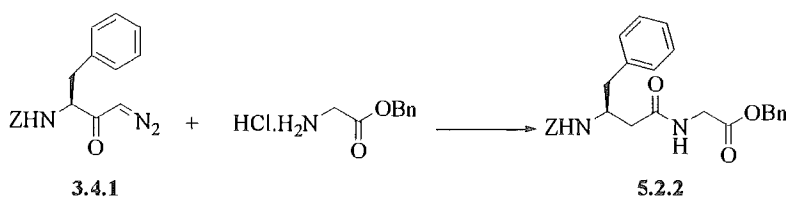
The amine hydrobromide, 4.1.6b (9 mg, 0.02 mmol, as a mixture of C6 epimers 4:1 4.1.6b:4.1.6a) was coupled to *N*-(2-quinolinylcarbonyl)-*L*-asparagine, 4.2.7 (17 mg, 0.05 mmol) according to general procedure G. The crude reaction product was purified by plate layer chromatography (ethyl acetate) to give protected tripeptide, 4.1.7b (3 mg, 23%) as a mixture of C-6 epimers (5.5:4.5 4.1.7b:4.1.7a).

^1H NMR (major product 4.1.7b, 300 MHz, CDCl_3) δ 1.97 (3H, d, $J=8.4$ Hz, Ala- β - H_3), 2.69 (2H, m, Asn- β - H_2), 2.89-3.06 (4H, m, hPhe- α - H_2 & hPhe- γ - H_2), 4.45 (1H, m, hPhe- β -H), 4.89 (1H, m, Asn- α -H), 5.14 (2H, s, Bn- H_2), 5.37 (1H, q, $J=8.4$ Hz, Ala- α -H), 5.87 (1H, bs, NH), 6.98-7.33 (10H, m, ArH), 7.63 (1H, t, $J=7.2$ Hz, QC-6-H), 7.77 (1H, t, $J=7.2$ Hz, QC-7-H), 7.88 (1H, d, $J=7.8$ Hz, QC-3-H), 8.18 (2H, t, $J=7.8$ Hz, QC-5-H & QC-8-H), 8.30 (1H, t, $J=8.1$ Hz, QC-4-H), 9.24 (1H, d, $J=6.3$ Hz, NH).

^{13}C NMR (major product 4.1.7b, 75 MHz, acetone) δ 16.33 (Ala- β - CH_3), 27.85 (hPhe- α - CH_2), 37.13 (Asn- β - CH_2), 39.18 (hPhe- γ - CH_2), 49.33 (hPhe- β -CH), 50.11 (Asn- α -CH), 55.54 (Ala- α -CH), 67.77 (Bn- CH_2), 118.88, 126.50, 128.52, 128.39, 128.50,

128.75, 129.52, 129.85, 130.60 (ArCH), 137.94, 138.16 (ArC), 146.74 (QC-9-C), 149.95 (QC-2-C), 152.32 (CN₄), 164.75 (QC-CO), 167.82 (Ala-CO), 170.83 (Asn-CO), 172.83 (Asn-CONH₂).

TLC (analytical, ethyl acetate) R_f=0.18; ES MS 635.2720 C₃₄H₃₅N₈O₅ (MH⁺) requires *m/z* 635.2730.

9.4. SYNTHESIS OF α -METHYLENE TETRAZOLE-BASED INHIBITORS**Preparation of (3*S*)-*N*-[3-(*N*-benzyloxycarbonylamino)-4-phenylbutanoic acid]-glycine benzyl ester, 5.2.2**

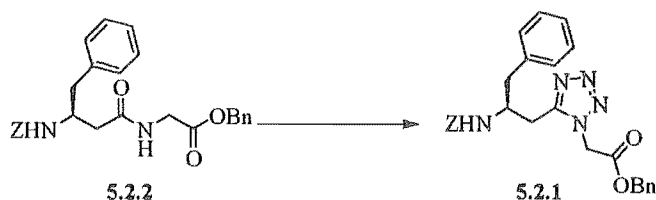
Glycine benzyl ester hydrochloride (1.0 eq., 1.12 g, 3.7 mmol), was reacted with α -diazoketone, 3.4.1 (1.5 eq., 1.20 g, 5.6 mmol) in the presence of triethylamine (2.0 eq., 0.75 g, 7.4 mmol, 1.05 mL) according to general procedure B. The crude reaction product was purified by flash column chromatography (30% ethyl acetate/CH₂Cl₂) and a single recrystallisation (ethyl acetate/petroleum ether) to give dipeptide, 5.2.2, as a white solid (2.19 g, 85%). mp 144-146 °C; $[\alpha]_D^{20}$ -2.8° (c=0.0043, methanol).

¹H NMR (300 MHz, CDCl₃) δ 2.43 (2H, m, hPhe- γ -H₂), 2.90 (2H, m, hPhe- α -H₂), 4.01 (2H, d, J=5.4 Hz, Gly- α -H₂), 4.16 (1H, m, hPhe- β -H), 5.04 (2H, s, Z-H₂), 5.16 (2H, s, Bn-H₂), 5.76 (1H, d, J=7.8 Hz, hPhe-NH), 6.24 (1H, bs, Gly-NH), 7.18-7.34 (15H, m, ArH).

¹³C NMR (75 MHz, CDCl₃) δ 38.56 (hPhe- α -CH₂), 40.06 (hPhe- γ -CH₂), 41.22 (Gly- α -CH₂), 50.08 (hPhe- β -CH), 66.47 (Z-CH₂), 67.22 (Bn-CH₂), 126.55, 127.88, 127.96, 128.36, 128.40, 128.51, 128.61, 129.29 (ArCH), 135.04, 136.55, 137.83 (ArC), 155.85 (Z-CO), 169.64 (Gly-CO), 171.07 (hPhe-CO).

TLC (analytical, 30% ethyl acetate/CH₂Cl₂) R_f=0.25; IR (CDCl₃, cm⁻¹), 3429, 3033, 2252, 1743, 1712, 1674, 1498; FAB MS 461.2088 C₂₆H₂₉N₂O₅ (MH⁺) requires *m/z* 461.2076.

Preparation of (2*S*)-1-(benzyl ethanoate)-5-[2-(*N*-benzyloxycarbonylamino)-3-phenylpropane]-tetrazole, 5.2.1



Dipeptide, 5.2.2 (502 mg, 1.0 mmol) was reacted according to general procedure C. The crude reaction product was purified by flash column chromatography (30% ethyl acetate/ CH_2Cl_2) and a single recrystallisation (ethyl acetate/petroleum ether) to give tetrazole, 5.2.1 (300 mg, 62%). mp 101-104 °C; $[\alpha]_{\text{D}}^{20}$ -14.6° ($c=0.0015$, methanol).

^1H NMR (300 MHz, CDCl_3) δ 2.89-3.04 (4H, m, hPhe- α - H_2 & hPhe- γ - H_2), 4.21 (1H, m, hPhe- β -H), 4.98 (2H, s, Z- H_2), 5.00 (2H, AB system, $\delta_{\text{A}}=4.93$, $\delta_{\text{B}}=5.04$, d, $J=18.1$ Hz, Gly- α - H_2) 5.16 (2H, AB system, $\delta_{\text{A}}=5.14$, $\delta_{\text{B}}=5.19$, d, $J=12.3$ Hz, Bn- H_2), 5.45 (1H, d, $J=15$ Hz, hPhe-NH), 7.11-7.35 (15H, m, ArH).

^{13}C NMR (75 MHz, CDCl_3) δ 26.67 (hPhe- α - CH_2), 39.07 (hPhe- γ - CH_2), 47.46 (Gly- α - CH_2), 50.64 (hPhe- β -CH), 66.48 (Z- CH_2), 68.16 (Bn- CH_2), 126.74, 127.97, 128.19, 128.26, 128.37, 128.46, 128.58, 128.75, 129.04, (ArCH), 134.11, 136.15, 136.95 (ArC), 153.25 (CN_4), 155.71 (Z-CO), 165.12 (Gly-CO).

TLC (analytical, 30 % ethyl acetate/ CH_2Cl_2), $R_{\text{f}}=0.40$; IR (CDCl_3 , cm^{-1}), 3315, 1749, 1693, 1535, 1452, 1272, 1257; FAB MS 486.2131 $\text{C}_{27}\text{H}_{28}\text{N}_5\text{O}_4$ (MH^+) requires m/z 486.2141.

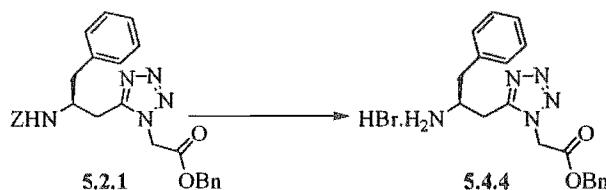
Crystallographic structure determination of (2*S*)-1-(benzyl ethanoate)-5-[2-(*N*-benzyloxycarbonylamino)-3-phenylpropane]-tetrazole, 5.2.1, by X-ray analysis

$\text{C}_{27}\text{H}_{27}\text{N}_5\text{O}_4$, M 485.54, mp 101-104 °C, crystal dimensions 0.8 \times 0.4 \times 0.02 mm, triclinic, a 5.0379 (3) Å, b 10.1066 (7) Å, c 12.7865 (9) Å, α 83.577 (2)°, β 81.897 (2)°, γ 76.475 (2)°, $V=624.55$ (7) Å³, spacegroup P1, $Z=1$, $F(000)=256$, $D_{\text{calc}}=1.291$ mg/m³, absorption coefficient 0.089 mm⁻¹, θ range for data collection 3.23 to 25.61, index ranges $-1 \leq h \leq 5$, $-10 \leq k \leq 11$, $-12 \leq l \leq 15$, data/restraints/parameters 1867/3/365, goodness of

fit on F^2 was 1.063, final R indices [$I > 2\sigma(I)$] $R_1=0.0359$, $wR_2=0.0898$, R indices (all data) $R_1=0.0427$, $wR_2=0.0957$, largest difference peak and hole 0.169 and $-0.151 \text{ e}\text{\AA}^{-3}$.

A unique data set was measured at 160(2) K within $2\theta_{\text{max}}=57^\circ$ limit (ω scans). Of the 2198 reflections obtained, 1867 were unique ($R_{\text{int}}=0.1010$) and were used in the full-matrix least-squares refinement.²⁸ The structure was solved by direct methods.²⁹ Hydrogen atoms were fixed in idealised positions. All non-hydrogen atoms were refined with anisotropic atomic displacement parameters. Neutral scattering factors and anomalous dispersion corrections for non-hydrogen atoms were taken from Ibers and Hamilton.³⁰

Preparation of (2*S*)-5-(2-amino-3-phenylpropane)-1-(benzyl ethanoate)tetrazole hydrobromide, 5.4.4



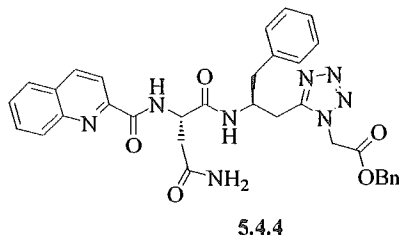
The tetrazole, 5.2.1 (840 mg, 1.73 mmol) was deprotected according to general procedure D. The hydromide, 5.4.4 (746 mg, 99%) was used without further purification.

^1H NMR (300 MHz, CD_3OD) δ 2.58 (2H, m, hPhe- γ -H₂), 2.75 (2H, m, hPhe- α -H₂), 3.59 (1H, m, hPhe- β -H), 4.73 (2H, s, Bn-H₂), 4.94 (2H, d, $J=3.0$ Hz, Gly- α -H₂), 6.77-6.89 (10H, m, ArH).

^{13}C NMR (75 MHz, CD_3OD) δ 26.90 (hPhe- α -CH₂), 39.81 (hPhe- γ -CH₂), 48.20 (Gly- α -CH₂), 52.30 (hPhe- β -CH₂), 69.63 (Bn-CH₂), 129.12, 129.88, 130.04, 130.08, 130.55, 130.77 (ArCH), 136.54, 136.60 (ArC), 154.50 (CN₄), 167.83 (Gly-CO).

FAB MS 352.1771 $\text{C}_{19}\text{H}_{22}\text{N}_5\text{O}_2$ (MH^+) requires m/z 352.1773.

Preparation of (2*S*)-1-(benzyl ethanoate)-5-{2-[*N*-((2-quinolinylcarbonyl)-*L*-asparaginy)amino]-3-phenylpropane} tetrazole, 5.4.5

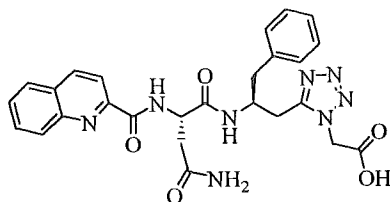


The hydrobromide salt, 5.4.4 (1.0 eq., 630 mg, 1.49 mmol), was coupled to *N*-(2-quinolinylcarbonyl)-*L*-asparagine, 4.2.7 (1.1 eq., 1.63 mmol, 469 mg), with BOP reagent (1.1eq., 723 mg, 1.63 mmol), according to general procedure G. The crude product was purified by flash column chromatography (ethyl acetate) and a single recrystallisation (methanol) to give protected tripeptide, 5.4.4 (470 mg, 51%). mp 187-189 °C; $[\alpha]_D^{20} +12^\circ$ (c=0.001, methanol).

$^1\text{H NMR}$ (300 MHz, CDCl_3) δ 2.78 (AB system, $\delta_A=2.67$, $\delta_B=2.89$, $J=7.2$, 15.6 Hz, Asn- β - H_2), 2.98 (2H, d, $J=7.5$ Hz, hPhe- γ - H_2), 3.06 (2H, d, $J=6.3$ Hz, hPhe- α - H_2), 4.45 (1H, m, hPhe- β -H), 4.89 (1H, m, Asn- α -H), 5.19 (2H, s, Bn- H_2), 5.21 (2H, s, Gly- α - H_2), 5.37 (1H, bs, NH), 5.80 (1H, bs, NH), 7.03-7.37 (10H, m, ArH), 7.64 (1H, t, $J=6.9$ Hz, QC-6-H), 7.79 (1H, t, $J=6.6$ Hz, QC-7-H), 7.89 (1H, d, $J=7.8$ Hz, QC-3-H), 8.17-8.22 (2H, m, QC-8-H & QC-5-H), 8.33 (1H, d, $J=8.1$ Hz, QC-4-H), 9.25 (1H, d, $J=8.1$ Hz, QC-NH).

$^{13}\text{C NMR}$ (300 MHz, $\text{CDCl}_3/\text{DMSO-}d_6$) δ 25.91 (hPhe- α - CH_2), 36.29 (Asn- β - CH_2), 38.88 (hPhe- γ - CH_2), 46.92 (Gly- α - CH_2), 48.80 (hPhe- β -CH), 49.07 (Asn- α -CH), 66.82 (Bn- CH_2), 117.65, 125.45, 126.80, 127.10, 127.38, 127.63, 128.19, 128.69, 129.23 (ArCH), 133.61, 136.42, 136.45 (ArC), 145.36 (QC-9-C), 148.23 (QC-2-C), 152.87 (CN_4), 163.05 (QC-CO), 165.02 (Gly-CO), 169.63 (Asn-CO), 171.49 (Asn-CONH $_2$).

TLC (analytical, ethyl acetate), $R_f=0.20$; IR (CDCl_3 , cm^{-1}), 3394, 3305, 3215, 1749, 1649, 1616, 1533, 1500, 1215; FAB MS (MH^+) 621.2583 $\text{C}_{33}\text{H}_{33}\text{N}_8\text{O}_5$ requires m/z 621.2573.

Preparation of (2S)-1-(ethanoic acid)-5-{2-[N-((2-quinolinylcarbonyl)-L-asparaginyl)amino]-3-phenylpropane} tetrazole, 5.4.6

5.4.6

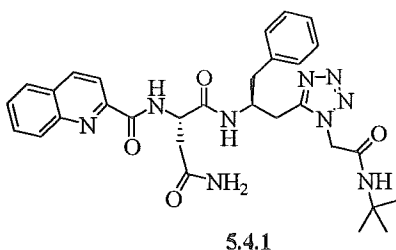
The benzyl ester, 5.4.5 (382 mg, 0.62 mmol), was hydrogenated according to general procedure E. The free acid was dried *in vacuo* over KOH to give the acid, 5.4.6 (312 mg, 70 %), as a white solid. mp 184-185 °C; $[\alpha]_D^{20}$ -36° ($c=0.0005$, methanol).

^1H NMR (300 MHz, CD_3OD) δ 2.72 (2H, d, $J=5.7$ Hz, Asn- β - H_2), 2.94 (2H, m, hPhe- γ - H_2), 3.12 (2H, d, $J=6.6$ Hz, hPhe- α - H_2), 4.52 (1H, m, hPhe- β -H), 4.83 (1H, m, Asn- α -H), 5.30 (2H, s, Gly- α - H_2), 6.95 (1H, t, $J=6.9$ Hz, Ph-4-H) 7.08 (2H, t, $J=7.8$ Hz, Ph-3- H_2), 7.20 (2H, d, $J=7.2$ Hz, Ph-2- H_2), 7.71 (1H, q, $J=7.8$ Hz, QC-6-H), 7.85 (1H, q, $J=7.2$ Hz, QC-7-H), 8.00 (1H, d, $J=8.1$ Hz, QC-3-H), 8.16 (2H, d, $J=8.7$ Hz, QC-8-H, & QC-5-H), 8.47 (1H, d, $J=8.7$ Hz, QC-4-H).

^{13}C NMR (75 MHz, DMSO-d_6) δ 27.17 (hPhe- α - CH_2), 30.57 (Asn- β - CH_2), 37.16 (hPhe- γ - CH_2), 47.90 (Gly- α - CH_2), 49.48 (hPhe- β -CH), 50.18 (Asn- α -CH), 118.78, 125.06, 126.30, 128.30, 128.39, 129.07, 129.26, 130.83 (ArCH), 138.14, 138.23 (ArC), 146.04 (QC-9-C), 149.59 (QC-2-C), 153.99 (CN_4), 163.59 (QC-CO), 167.99 (Asn-CO), 170.33 (Asn- CONH_2), 171.75 (Gly-COOH).

IR (KBr, cm^{-1}) 3421, 3315, 1747, 1718, 1647, 1529, 1498; EI MS 531.2099 $\text{C}_{26}\text{H}_{27}\text{N}_8\text{O}_5$ (MH^+) requires m/z 351.2100.

Preparation of (2*S*)-1-[*N*-(1,1-dimethylethyl)ethanamide]-5-{2-[*N*-((2-quinolinylcarbonyl)-*L*-asparaginyl)amino]-3-phenylpropane} tetrazole, 5.4.1



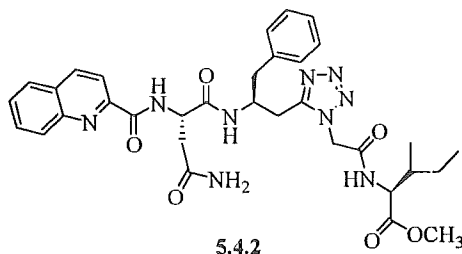
The free acid, 5.4.6 (1.0 eq., 10 mg, 0.02 mmol), was coupled to *tert*-butyl amine (2.0 eq., 3 mg, 0.04 mmol, 4 μ L) with EDCI (1.5 eq., 5 mg, 0.03 mmol) and HOBt (1.5 eq., 4 mg, 0.03 mmol) according to general procedure H. The crude protected tripeptide was purified by HPLC (RP-C₁₈ preparative column, 28% H₂O/methanol, retention time 14 min) to give the protected tripeptide, 5.4.1 (2 mg, 17%). $[\alpha]_D^{20} +12^\circ$ (c=0.001, methanol).

¹H NMR (300 MHz, CD₃OD) δ 1.30 (9H, s, C(CH₃)₃), 2.71 (2H, d, J=6.3 Hz, Asn- β -H₂), 2.94 (2H, m, hPhe- γ -H₂), 3.11 (2H, d, J=6.9 Hz, hPhe- α -H₂), 4.51 (1H, m, hPhe- β -H), 4.83 (1H, m, Asn- α -H₂), 5.08 (2H, AB system, $\delta_A=5.09$, $\delta_B=5.12$, d, J=17.1 Hz, Gly- α -H₂), 6.96 (1H, t, J=7.5 Hz, Ph-4-H), 7.08 (2H, t, J=7.8 Hz, Ph-3-H₂), 7.21 (2H, d, J=7.2 Hz, Ph-2-H₂), 7.69 (1H, t, J=6.9 Hz, QC-6-H), 7.84 (1H, t, J=7.2 Hz, QC-7-H), 8.01 (1H, d, J=7.8 Hz, QC-3-H), 8.16 (2H, d, J=8.7 Hz, QC-8-H & QC-5-H), 8.47 (1H, d, J=8.4 Hz, QC-4-H).

¹³C NMR (75 MHz, CD₃OD) δ 28.05 (hPhe- α -CH₂), 28.86 (C(CH₃)₃), 37.89 (Asn- β -CH₂), 40.96 (hPhe- γ -CH₂), 49.93 (Gly- α -CH₂), 51.12 (hPhe- β -CH), 51.93 (Asn- α -CH), 53.89 (C(CH₃)₃), 122.73, 127.89, 129.18, 129.67, 130.63, 131.12 (ArCH), 139.18, 139.02 (ArC), 148.05 (QC-9-C), 150.63 (QC-2-C), 155.79 (CN₄), 165.96 (Gly-CO), 168.70 (QC-CO), 172.89 (Asn-CO), 175.31 (Asn-CONH₂).

FAB MS 610.2878 C₃₀H₃₇N₉O₄Na (MHN⁺) requires m/z 610.2866.

Preparation of (2*S*)-1-[*N*-(*L*-isoleucine methyl ester)ethanamide]-5-{2-[*N*-(2-quinolinylcarbonyl)-*L*-asparaginyl)amino]-3-phenylpropane} tetrazole, 5.4.2

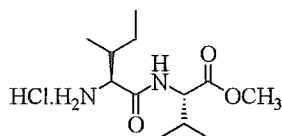


The free acid, 5.4.6 (1.0 eq., 58 mg, 0.11 mmol), was coupled to *L*-isoleucine methyl ester hydrochloride (1.1 eq., 22 mg, 0.12 mmol) with EDCI (1.5 eq., 31 mg, 0.16 mmol) and HOBT (1.5 eq., 25 mg, 0.16 mmol) according to general procedure H. The crude protected tetrapeptide was purified by HPLC (RP-C₁₈ preparative column, 25% H₂O/methanol, retention time 12 min), and precipitated from ether to give the protected tripeptide, 5.4.2 (13 mg, 18%). mp 105-107 °C; $[\alpha]_D^{20}$ -4° (c=0.0028, methanol).

¹H NMR (300 MHz, CD₃OD) δ 0.87 (3H, d, J=6.3 Hz, Ile- β -CH₃), 0.88 (3H, t, J=7.5 Hz, Ile- δ -H₃), 1.34 (2H, AB system, δ_A =1.24, δ_B =1.43, m, Ile- γ -H₂), 1.84 (1H, m, Ile- β -H), 2.70 (2H, m, Asn- β -H₂), 2.94 (2H, d, J=6.9 Hz, hPhe- γ -H₂), 3.11 (2H, d, J=6.9 Hz, hPhe- α -H₂), 3.67 (3H, s, OCH₃), 4.28 (1H, d, J=5.7 Hz, Ile- α -H), 4.53 (1H, m, hPhe- β -H), 4.83 (1H, t, J=6.6 Hz, Asn- α -H), 5.28 (2H, AB system, δ_A =5.24, δ_B =5.32, d, J=17.1 Hz, Gly- α -H₂), 6.96 (1H, t, J=7.2, Ph-4-H), 7.08 (2H, t, J=7.3 Hz, Ph-3-H₂), 7.21 (2H, d, J=7.5 Hz, Ph-2-H₂), 7.69 (1H, t, J=7.2 Hz, QC-6-H), 7.83 (1H, t, J=7.5 Hz, QC-7-H), 7.99 (1H, d, J=8.4 Hz, QC-3-H), 8.15 (2H, d, J=8.7 Hz, QC-5-H & QC-8-H), 8.46 (1H, d, J=8.7 Hz, QC-4-H).

¹³C NMR (75 MHz, CD₃OD) δ 12.08 (Ile- δ -CH₃), 16.24 (Ile- β -CH₃), 26.56 (Ile- γ -CH₂), 28.77 (hPhe- α -CH₂), 38.08 (Asn- β -CH₂), 38.62 (Ile- β -CH), 41.07 (hPhe- γ -CH₂), 49.93 (Gly- α -CH₂), 51.27 (hPhe- β -CH), 51.91 (Asn- α -CH), 52.91 (OCH₃), 58.91 (Ile- α -CH), 119.94 (QC-3-CH), 127.82, 129.32, 129.73, 130.66, 131.09, 131.83 (ArCH), 136.95, 139.20, 139.22 (ArC), 148.18 (QC-9-C), 150.63 (QC-2-C), 155.87 (CN₄), 166.55 (QC-CO), 167.43 (Gly-CO), 172.91 (Asn-CO), 173.66 (Ile-CO), 175.34 (Asn-CONH₂).

FAB MS 680.2933 C₃₃H₃₉N₉O₆Na (MHNa⁺) requires m/z 680.2921.

Preparation of *N*-(*L*-isoleucine)-*L*-valine methyl ester hydrochloride³¹

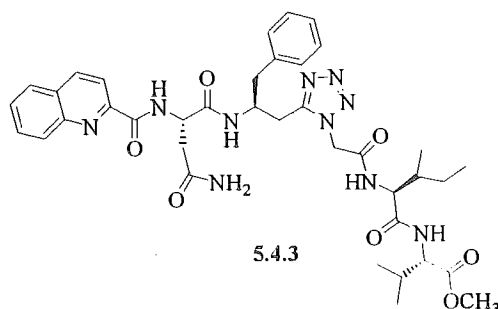
Commercially available *N*-(*L*-isoleucine)-*L*-valine (100 mg, 0.43 mmol) was suspended in 2,2-dimethoxypropane (4 mL). Concentrated HCl (400 μ L) was added dropwise to the stirred solution. The suspension cleared upon addition of the acid and the reaction was allowed to stand at rt for 18 h. Solvent was removed under reduced pressure at <50 $^{\circ}$ C to give a brown solid. A single recrystallisation (methanol/ethyl acetate/petroleum ether) gave the dipeptide methyl ester (111 mg, 92%) as a white crystalline solid, which was dried *in vacuo* over KOH. mp 176-178 $^{\circ}$ C; $[\alpha]_{\text{D}}^{20} +9^{\circ}$ ($c=0.0018$, methanol).

^1H NMR (300 MHz, CD_3OD) δ 0.97 (3H, t, $J=7.2$ Hz, Ile- δ - H_3), 0.98 (6H, d, $J=7.2$ Hz, Val- γ - H_3), 1.05 (3H, d, $J=6.6$ Hz, Ile- β - CH_3), 1.39 (2H, AB system, $\delta_{\text{A}}=1.22$, $\delta_{\text{B}}=1.57$, m, Ile- γ - H_2), 1.95 (1H, m, Ile- β -H), 2.18 (1H, m, Val- β -H), 3.71 (3H, s, OCH_3), 3.80 (1H, d, $J=5.4$ Hz, Ile- α -H), 4.35 (1H, d, $J=6.0$ Hz, Val- α -H).

^{13}C NMR (75 MHz, CD_3OD) δ 11.94 (Ile- δ - CH_3), 15.44 (Ile- β - CH_3), 18.87 (Val- δ - CH_3), 19.66 (Val- δ - CH_3), 25.38 (Ile- γ - CH_2), 31.81 (Val- β -CH), 38.54 (Ile- β -CH), 52.78 (OCH_3), 59.14 (Ile- α -CH), 59.89 (Val- α -CH), 166.34 (Ile-CO), 170.32 (Val-CO).

IR (KBr, cm^{-1}) 3215, 2968, 2879, 1747, 1668, 1548, 1492, 1467, 1205, 1155; FAB MS 245.1870 $\text{C}_{12}\text{H}_{25}\text{N}_2\text{O}_3$ (MH^+) requires m/z 245.1865.

Preparation of (2*S*)-1-[*N*-(*N*-(*L*-isoleucine)-*L*-valine methyl ester)ethanamide]-5-{2-[*N*-((2-quinolinylcarbonyl)-*L*-asparaginyl)amino]-3-phenylpropane} tetrazole, 5.4.3

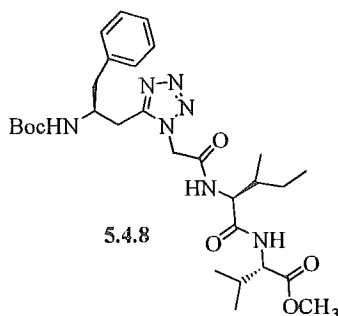


The free acid, 5.4.6 (1.0 eq., 50 mg, 0.09 mmol), was coupled to *N*-(*L*-isoleucine)-*L*-valine methyl ester hydrochloride (1.1 eq., 30 mg, 0.10 mmol), with EDCI (1.5 eq., 27 mg, 0.14 mmol) and HOBT (1.5 eq., 22 mg, 0.14 mmol) according to general procedure H. The crude protected pentapeptide was purified by HPLC (RP-C₁₈ preparative column, 28% H₂O/methanol, retention time 24 min), and precipitated from ether to give the protected tetrapeptide, 5.4.3 (7 mg, 11%). mp 238-240 °C; $[\alpha]_D^{20}$ -4° (c=0.0036, methanol).

¹H NMR (300 MHz, CD₃OD) δ 0.88 (6H, dd, J=2.4, 7.8 Hz, Val- γ -H₃), 0.90 (3H, t, J=8.1 Hz Ile- γ -H₃), 0.93 (3H, d, J=6.9 Hz, Ile- β -CH₃), 1.39 (2H, AB system, δ_A =1.21, δ_B =1.57, m, Ile- γ -H₂), 1.86 (1H, m, Ile- β -H), 2.09 (1H, m, Val- β -H), 2.69 (2H, d, J=6.0 Hz, Asn- β -H₂), 2.93 (2H, m, hPhe- γ -H₂), 3.13 (2H, d, J=6.3 Hz, hPhe- α -H₂), 3.68 (3H, s, OCH₃), 4.29 (1H, d, J=6.3 Hz, Val- α -H), 4.32 (1H, d, J=8.1 Hz, Ile- α -H), 4.53 (1H, m, hPhe- β -H), 5.27 (2H, AB system, δ_A =5.25, δ_B =5.30, d, J=8.7 Hz, Gly- α -H₂), 6.92 (1H, t, J=7.2 Hz, Ph-4-H), 7.06 (2H, t, J=7.8 Hz, Ph-3-H₂), 7.20 (2H, d, J=7.5 Hz, Ph-2-H₂), 7.69 (1H, t, J=7.5 Hz, QC-6-H), 7.84 (1H, t, J=7.2 Hz, QC-7-H), 8.01 (1H, d, J=7.8 Hz, QC-3-H), 8.14, 8.17 (2H, d, J=3.9 Hz, QC-5-H, & QC-8-H), 8.47 (1H, d, J=8.4 Hz, QC-4-H).

¹³C NMR (75 MHz, CD₃OD) δ 11.66 (Ile- δ -CH₃), 16.03 (Ile- β -CH₃), 18.95 (Val- γ -CH₃), 19.74 (Val- γ -CH₃), 26.20 (Ile- γ -CH₂), 28.85 (hPhe- α -CH₂), 31.94 (Val- β -CH), 38.15 (Asn- β -CH₂), 38.54 (Ile- β -CH), 41.01 (hPhe- γ -CH₂), 49.49 (Gly- α -CH₂), 51.27 (hPhe- β -CH), 51.95 (Asn- α -CH₂), 52.68 (OCH₃), 59.67 (Ile- α -CH & Val- α -CH), 119.98 (QC-3-CH), 127.87, 129.34, 129.73, 130.66, 131.09, 131.122, 131.87 (ArCH), 139.40,

Preparation of (2*S*)-1-[*N*-(*N*-(*L*-isoleucine)-*L*-valine methyl ester)ethanamide]-5-[2-(*N*-*tert*-butyloxycarbonylamino)-3-phenylpropane]tetrazole, 5.4.8

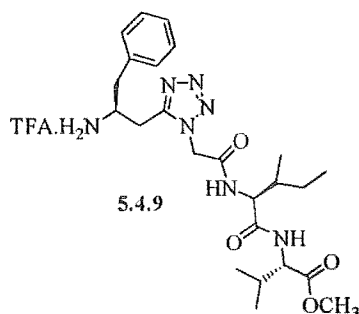


The tetrazole free acid, 5.4.7 (1.0 eq., 17 mg, 0.05 mmol) was coupled to *N*-(*L*-isoleucine)-*L*-valine methyl ester hydrochloride (1.1 eq., 14 mg, 0.05 mmol) with EDCI (1.5 eq., 13 mg, 0.07 mmol), HOBt (1.5 eq., 10 mg, 0.07 mmol) and DIPEA (1.1 eq., 7 mg, 0.05 mmol, 10 μ L) in dry DMF (5 mL), according to general procedure H. The crude product was purified by flash column chromatography to give tetrazole, 5.4.8 (22 mg, 75%) as a white solid. mp 158-160 $^{\circ}$ C.

^1H NMR (300 MHz, CD_3OD) δ 0.84 (3H, t, $J=6.3$ Hz, Ile- δ - H_3), 0.85 (6H, d, $J=5.7$ Hz, Val- γ - H_3), 1.27 (9H, s, Boc-(CH_3) $_3$), 1.37 (2H, AB system, $\delta_{\text{A}}=1.26$, $\delta_{\text{B}}=1.55$, m, Ile- γ - H_2), 1.84 (1H, m, Ile- β -H), 2.11 (1H, m, Val- β -H), 2.87 (1H, d, $J=6.6$ Hz, hPhe- γ - H_2), 3.02 (2H, d, $J=9.9$ Hz, hPhe- α - H_2), 3.68 (3H, s, OCH_3), 4.15 (1H, m, hPhe- β -H), 4.25 (1H, d, $J=7.8$ Hz, Ile- α -H), 4.33 (1H, d, $J=5.7$ Hz, Val- α -H), 5.13 (2H, AB system, $\delta_{\text{A}}=5.09$, $\delta_{\text{B}}=5.18$, d, $J=17.1$ Hz, Gly- α - H_2), 6.34 (1H, d, $J=8.1$ Hz, NH), 7.17-7.27 (5H, m, ArH).

^{13}C NMR (75 MHz, CD_3OD) δ 11.44 (Ile- δ - CH_3), 15.86 (Ile- β - CH_3), 18.66 (Val- γ - CH_3), 19.60 (Val- γ - CH_3), 25.74 (Ile- γ - CH_2), 28.82 (Boc-(CH_3) $_3$), 29.20 (hPhe- α - CH_2), 31.51 (Val- β -CH), 37.75 (Ile- β -CH), 41.15 (hPhe- γ - CH_2), 49.74 (Gly- α - CH_2), 51.36 (hPhe- β -CH), 52.67 (OCH_3), 58.92 (Val- α -CH), 59.29 (Ile- α -CH), 80.38 (Boc-C(CH_3) $_3$), 127.57, 129.42, 130.15 (ArCH), 138.70 (ArC), 155.34 (CN_4), 157.21 (Boc-CO), 166.21 (Gly-CO), 173.14 (Val-CO), 173.28 (Ile-CO).

ES MS 588.3512 $\text{C}_{29}\text{H}_{46}\text{N}_7\text{O}_6$ (MH^+) requires m/z 588.3510.

Preparation of (2*S*)-5-[2-amino-3-phenylpropane]-1-[*N*-(*N*-(*L*-isoleucine)-*L*-valine methyl ester)ethanamide]tetrazole trifluoroacetate, 5.4.9

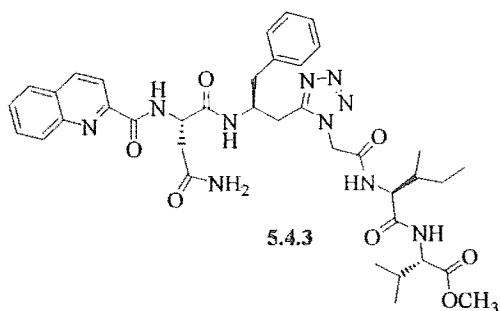
Protected tetrapeptide, 5.4.8 (22 mg, 0.04 mmol) was deprotected with 95% aqueous trifluoroacetic acid (5 mL) according to general procedure F to give trifluoroacetate, 5.4.9 (25 mg, quant.), which was used without further purification.

^1H NMR (300 MHz, CD_3OD) δ 0.87 (12H, m, Val- γ - H_3 , Ile- γ - H_3 , Ile- β - CH_3), 1.37 (2H, AB system, $\delta_{\text{A}}=1.22$, $\delta_{\text{B}}=1.52$, m, Ile- γ - H_2), 1.86 (1H, m, Ile- β -H), 2.07 (1H, m, Val- β -H), 3.12 (2H, m, hPhe- γ - H_2), 3.29 (2H, m, hPhe- α - H_2), 3.62 (3H, s, OCH_3), 4.10 (1H, m, hPhe- β -H), 4.24 (2H, m, Ile- α -H, Val- α -H), 5.31 (2H, bs, Gly- α - H_2), 7.23-7.29 (5H, m, ArH).

^{13}C NMR (75 MHz, CD_3OD) δ 11.54 (Ile- δ - CH_3), 15.80 (Ile- β - CH_3), 18.77 (Val- γ - CH_3), 19.43 (Val- γ - CH_3), 25.61 (Ile- γ - CH_2), 26.12 (hPhe- α - CH_2), 31.29 (Val- β -CH), 37.98 (Ile- β -CH), 39.17 (hPhe- γ - CH_2), 48.95 (Gly- α - CH_2), 52.10 (hPhe- β -CH), 52.45 (OCH_3), 59.11 (Val- α -CH), 59.43 (Ile- α -CH), 128.43, 129.91, 130.40 (ArCH), 136.21 (ArC), 154.21 (CN_4), 166.52 (Gly-CO), 173.14 (Val-CO), 173.25 (Ile-CO).

ES MS 488.2991 $\text{C}_{24}\text{H}_{38}\text{N}_7\text{O}_4$ (MH^+) requires m/z 488.2985.

Preparation of (2*S*)-1-[*N*-(*N*-(*L*-isoleucine)-*L*-valine methyl ester)ethanamide]-5-{2-[*N*-((2-quinolinylcarbonyl)-*L*-asparaginyloamino)]-3-phenylpropane} tetrazole, 5.4.3

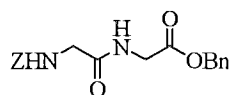


The tetrazole methyl ester trifluoroacetate, 5.4.9 (1.0 eq., 25 mg, 0.04 mmol) was coupled to *N*-(2-quinolinylcarbonyl)-*L*-asparagine, 4.2.7 (1.0 eq., 12 mg, 0.04 mmol) with EDCI (1.5 eq., 12 mg, 0.06 mmol), HOBt (1.5 eq., 9 mg, 0.06 mmol) and DIPEA (1.0 eq., 5 mg, 0.04 mmol, 7 μ L) in dry DMF (5 mL) according to general procedure H. The crude coupled product was purified by plate layer chromatography (ethyl acetate), to give the protected pentapeptide, 5.4.3 (12 mg, 40%) as a white solid.

Spectral data was identical to that previously recorded for this compound.

9.5. SYNTHESIS OF α -KETO THE TETRAZOLE ISOSTERE

9.5.1. FUNCTIONALISATION OF TETRAZOLE-BASED DIPEPTIDE MIMICS

Preparation of *N*-[(*N*-benzyloxycarbonyl)glycine]glycine benzyl ester, 6.2.11

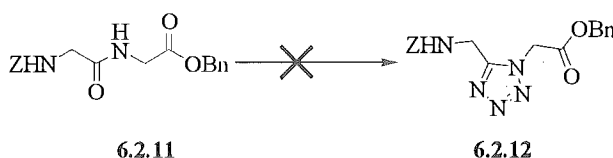
6.2.11

N-Z-Glycine (1.0 g, 4.8 mmol) was coupled to glycine benzyl ester *para*-toluenesulphonate (1.0 eq., 1.6 g, 4.8 mmol) with BOP reagent (1.1 eq., 2.3 g, 5.3 mmol) in the presence of triethylamine (3.0 eq., 1.4 g, 14.3 mmol) according to general procedure G. A single recrystallisation (ethyl acetate/petroleum ether) of the crude reaction product gave dipeptide, 6.2.11 (1.65 g, 96%). mp 103-105 °C.

^1H NMR (300 MHz, CDCl_3) δ 3.89 (2H, d, $J=5.1$ Hz, Gly- α -H $_2$), 4.03 (2H, d, $J=5.4$ Hz, Gly- α -H $_2$), 5.09 (2H, s, Z-H $_2$), 5.14 (2H, s, Bn-H $_2$), 5.72 (1H, bs, NH), 6.84 (1H, bs, NH), 7.31-7.33 (10H, m, ArH).

^{13}C NMR (75 MHz, CDCl_3) δ 41.16 (Gly- α -CH $_2$), 44.29 (Gly- α -CH $_2$), 67.15 (Z-CH $_2$), 67.20 (Bn-CH $_2$), 128.00, 128.17, 128.28, 128.47, 128.58 (ArCH), 135.01, 136.03 (ArC), 156.63 (Z-CO), 169.48 (Gly-CO), 169.60 (Gly-CO).

IR (KBr, cm^{-1}) 3379, 3062, 3035, 2962, 1708, 1651, 1454, 1411, 1253, 1199, 975, 948, 752, 725; FAB MS 357.1456 $\text{C}_{19}\text{H}_{21}\text{N}_2\text{O}_5$ (MH^+) requires m/z 357.1450.

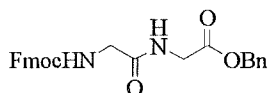
Attempted preparation of 5-[1-(*N*-benzyloxycarbonylamino)methane]-1-(benzyl ethanoate)tetrazole, 6.2.12

6.2.11

6.2.12

The dipeptide, **6.2.11** (50 mg, 0.14 mmol) was reacted according to general procedure C. ^1H NMR (300 MHz, CDCl_3) of the crude reaction mixture showed unreacted starting material, dipeptide **6.2.11**.

Preparation of *N*-[(*N*-((9*H*)-fluorenylmethyloxycarbonyl)glycine]glycine benzyl ester, **6.2.13**



6.2.13

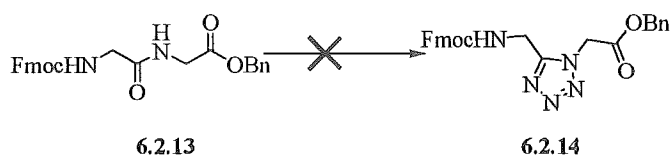
N-Fmoc-Glycine (1.0 eq., 1.0 g, 3.4 mmol) was coupled to glycine benzyl ester *para*-toluenesulphonate (1.1 eq., 1.2 g, 3.7 mmol) in the presence of HOBt (1.5 eq., 680 mg, 5.0 mmol), EDCI (1.5 eq., 970 mg, 5.0 mmol) and triethylamine (1.1 eq., 374 mg, 3.7 mmol) according to general procedure H. A single recrystallisation (ethyl acetate/petroleum ether) gave dipeptide, **6.2.13** (1.28 g, 85%), as a white solid. mp 125-126 °C.

^1H NMR (300 MHz, CDCl_3) δ 3.91 (2H, d, $J=5.4$ Hz, Gly- α -H₂), 4.07 (2H, d, $J=5.1$ Hz, Gly- α -H₂), 4.20 (1H, t, $J=6.9$ Hz, Fmoc- β -H), 4.42 (2H, d, $J=6.9$ Hz, Fmoc- α -H₂), 5.15 (2H, s, Bn-H₂), 5.56 (1H, bs, NH), 7.25-7.40 (8H, m, ArH), 7.57 (2H, d, $J=7.5$ Hz, ArH), 7.74 (2H, d, $J=7.2$ Hz, ArH).

^{13}C NMR (75 MHz, CDCl_3) δ 41.25 (Gly- α -CH₂), 47.07 (Gly- α -CH₂), 67.30 (Bn-CH₂), 119.69, 124.89, 127.06, 127.71, 128.29, 128.36, 128.57, 128.62 (ArCH), 135.00, 141.26, 143.67 (ArC), 156.60 (Fmoc-CO), 169.21 (Gly-CO), 169.49 (Gly-CO).

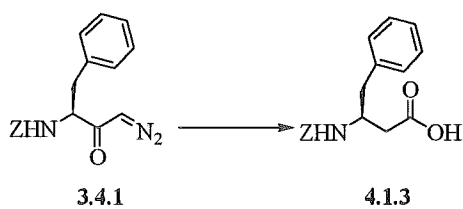
IR (KBr, cm^{-1}) 3332, 1732, 1651, 1535, 1442, 1245, 1203, 1110, 991, 952, 756, 736; FAB MS 445.1769 $\text{C}_{26}\text{H}_{25}\text{N}_2\text{O}_5$ (MH^+) requires m/z 445.1763.

Attempted preparation of 1-(benzyl ethanoate)-5-{1-[N-(9H)-fluorenylmethyloxycarbonylamino)methane]tetrazole, 6.2.14



The dipeptide, 6.2.13 (50 mg, 0.11 mmol) was reacted according to general procedure C. ^1H NMR (300 MHz, CDCl_3) of the crude reaction mixture showed unreacted starting material, dipeptide 6.2.13.

Preparation of (3*S*)-3-(*N*-benzyloxycarbonylamino)-4-phenylbutanoic acid, 4.1.3²²



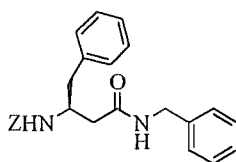
A solution of silver (I) oxide (360 mg, 1.5 mmol), sodium carbonate (75 mg, 0.71 mmol), $\text{Na}_2\text{S}_2\text{O}_3 \cdot 5\text{H}_2\text{O}$ (160 mg, 0.64 mmol) in water (5 mL), was heated to 80 °C in a two-necked flask fitted with a condenser. A solution of diazoketone, 3.4.1 (506 mg, 1.5 mmol) in dioxane (5 mL), was added dropwise over 1.5 h to the stirred solution.³³ Then a further portion of silver (I) oxide (180 mg) was added in two portions. Stirring was continued until the evolution of N_2 had ceased. The cooled reaction was filtered, diluted with water (20 mL) and extracted with ether (3×50 mL). The aqueous layer was acidified to pH=1 with 1 M aqueous HCl and extracted with ethyl acetate (3×30 mL). The pooled organic washes were dried (MgSO_4), filtered and evaporated. The free acid was dried *in vacuo* over KOH for 24 h to yield acid, 4.1.3 (322 mg, 68%) as a white solid. mp 119-120 °C (lit.²² 118-119 °C).

^1H NMR (300 MHz, CD_3OD) δ 2.47 (2H, d, $J=6.3$ Hz, hPhe- γ - H_2), 2.80 (2H, m, hPhe- α - H_2), 4.18 (1H, m, hPhe- β -H), 4.99 (2H, AB system, $\delta_A=4.96$, $\delta_B=5.01$, d, $J=13.2$ Hz, Z- H_2), 7.17-7.32 (10H, m, ArH).

^{13}C NMR (75 MHz, CD_3OD) δ 40.04 (hPhe- α - CH_2), 41.85 (hPhe- γ - CH_2), 51.50 (hPhe- β -CH), 67.44 (Z- CH_2), 127.74, 128.85, 129.11, 129.67, 130.72 (ArCH), 138.69, 139.83 (ArC), 158.33 (Z-CO), 175.14 (hPhe-COOH).

IR (KBr, cm^{-1}) 3328, 3031, 2920, 1685, 1535, 1450, 1286, 1218, 1053748, 698; EI MS 222.0763 $\text{C}_{11}\text{H}_{12}\text{NO}_4$ ($\text{M}-\text{C}_7\text{H}_7^+$) requires m/z 222.0766; EI MS m/z (rel. intensity) 108 (25), 91 (100), 79 (25), 65 (20).

Preparation of (3*S*)-*N*-[3-(*N*-benzyloxycarbonylamino)-4-phenylbutanoic acid]benzyl amine, 6.2.15



6.2.15

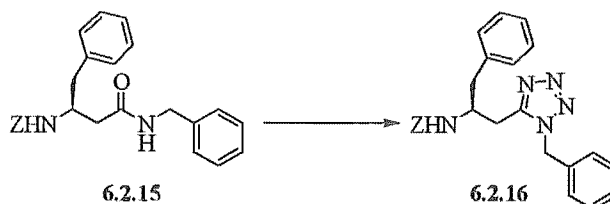
N-*Z*-*L*-Homophenylalanine, 4.1.3 (500 mg, 1.59 mmol) was coupled to benzyl amine (1.2 eq., 170 mg, 1.91 mmol) in the presence of EDCI (1.3 eq., 400 mg, 2.07 mmol), HOBT (1.5 eq., 323 mg, 2.39 mmol), and DIPEA (1.2 eq., 247 mg, 1.91 mmol) according to general procedure H. Recrystallisation of the crude reaction product gave amide, 6.2.15 (581 mg, 91%) as a white solid. mp 181-182 °C.

^1H NMR (300 MHz, CDCl_3) δ 2.40 (2H, m, hPhe- α - H_2), 2.93 (2H, m, hPhe- γ - H_2), 4.16 (1H, m, hPhe- β -H), 4.40 (2H, AB system, $\delta_{\text{A}}=4.34$, $\delta_{\text{B}}=4.45$, dd, $J=5.7$, 14.7 Hz, Bn- α - H_2), 5.05 (2H, s, Z- H_2), 5.82 (1H, bs, NH), 5.98 (1H, bs, NH), 7.13-7.35 (15H, m, ArH).

^{13}C NMR (75 MHz, CDCl_3) δ 38.79 (hPhe- α - CH_2), 40.19 (hPhe- γ - CH_2), 43.54 (Bn- α - CH_2), 50.14 (hPhe- β -CH), 66.52 (Z- CH_2), 126.60, 127.62, 127.82, 127.90, 128.01, 128.46, 128.55, 128.74, 129.24 (ArCH), 137.86, 137.88 (ArC), 155.68 (Z-CO), 165.35 (hPhe-CO).

TLC (analytical, 25% ethyl acetate/petroleum ether) $R_f=0.66$; IR (KBr, cm^{-1}) 3305, 3028, 1693, 1639, 1527, 1265, 1056, 748, 698; ES MS 425.1860 $\text{C}_{25}\text{H}_{26}\text{N}_2\text{O}_3\text{Na}$ (MNa^+) requires m/z 425.1841.

Preparation of (2*S*)-1-benzyl-5-[2-(*N*-benzyloxycarbonylamino)-3-phenylpropane]-tetrazole, 6.2.16



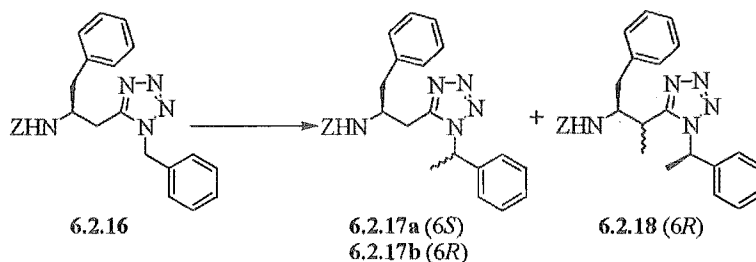
The amide, 6.2.15 (340 mg, 0.84 mmol) was reacted according to general procedure C. Flash column chromatography (5% ethyl acetate/ether) of the crude product gave tetrazole, 6.2.16 (256 mg, 71%). mp 116-118 °C.

^1H NMR (300 MHz, CDCl_3) δ 2.80-3.03 (4H, m, hPhe- α - H_2 & hPhe- γ - H_2), 4.24 (1H, m, hPhe- β -H), 5.03 (2H, s, Z- H_2), 5.32 (2H, AB system, $\delta_{\text{A}}=5.29$, $\delta_{\text{B}}=5.36$, d, $J=15.6$ Hz, Bn- H_2), 5.37 (1H, d, $J=8.4$ Hz, NH), 7.07-7.37 (15H, m, ArH).

^{13}C NMR (75 MHz, CDCl_3) δ 26.77 (hPhe- α - CH_2), 39.27 (hPhe- γ - CH_2), 50.46 (hPhe- β -CH), 50.66 (Z- CH_2), 126.89, 127.52, 127.95, 128.13, 128.49, 128.74, 128.84, 129.08, 129.14 (ArCH), 133.07, 136.23, 136.97 (ArC), 152.19 (CN_4), 155.75 (Z-CO).

TLC (analytical, 25% ethyl acetate/petroleum ether) $R_f=0.81$; IR (KBr, cm^{-1}) 3394, 3024, 1701, 1519, 1450, 1242, 1060, 732, 702; ES MS 428.2090 $\text{C}_{25}\text{H}_{26}\text{N}_5\text{O}_2$ (MH^+) requires m/z 428.2087.

Preparation of (2*S*,2'*RS*)-5-[2-(*N*-benzyloxycarbonylamino)-3-phenylpropane]-1-(2-phenylethane)tetrazole, 6.2.17a and 6.2.17b, and (1*RS*,2*S*,2'*R*)-5-[2-(*N*-benzyloxycarbonylamino)-1-methyl-3-phenylpropane]-1-(2-phenylethane)tetrazole, 6.2.18



A solution of LiHMDS (3.0 eq., 140 μ L, 1.0 M in THF) in dry THF (2 mL), was prepared in a flame-dried flask under N_2 . The solution was cooled to -78 $^{\circ}C$ prior to the dropwise addition of a solution of tetrazole, **6.2.16** (20 mg, 0.05 mmol) in dry THF (2 mL) over 15 min. The reaction was stirred at -78 $^{\circ}C$ for 30 min. A solution of iodomethane (1.1 eq., 7.3 mg, 0.05 mmol) in dry THF (2 mL) was added to the reaction dropwise over 10 min. The reaction was stirred at -78 $^{\circ}C$ for a further 30 min, then allowed to warm to rt. The reaction was quenched with saturated aqueous Na_2SO_3 (5 mL) and the aqueous phase extracted with ethyl acetate (3×20 mL). The pooled organics were washed with 10% aqueous citric acid (3×25 mL), 0.5 M aqueous $NaHCO_3$ (3×25 mL) and saturated aqueous $NaCl$ (3×25 mL), dried ($MgSO_4$), filtered and evaporated. The crude reaction products were purified by plate layer chromatography (10% ethyl acetate/ CH_2Cl_2) to give;

6.2.17a and **6.2.17b** (1:1 by 1H NMR, 15 mg, 86%).

1H NMR (300 MHz, $CDCl_3$) δ 1.87 (3H, d, $J=7.5$ Hz, Bn- β - H_3), 2.65-2.94 (4H, m, hPhe- α - H_2 & hPhe- γ - H_2), 4.13 (1H, m, hPhe- β -H), 4.92, 4.95 (2H, s, Z- H_2), 5.28 (1H, q, $J=6.9$ Hz, (6*S*)-Bn- α -H), 5.35 (1H, d, $J=8.4$ Hz, NH), 5.37 (1H, q, $J=6.6$ Hz, (6*R*)-Bn- α -H), 5.56 (1H, d, $J=7.8$ Hz, NH), 6.91-7.28 (15H, m, ArH).

^{13}C NMR (75 MHz, $CDCl_3$) δ 21.94, 22.21 (Bn- β - CH_3), 26.87, 27.05 (hPhe- α - CH_2), 38.92, 39.51 (hPhe- γ - CH_2), 50.39 (hPhe- β -CH), 58.11 ((6*S*)-Bn- α -CH), 58.27 ((6*R*)-Bn- α -CH), 66.65 (Z- CH_2), 125.97, 126.08, 126.74, 126.85, 127.89, 128.06, 128.44, 128.55, 128.58, 128.63, 128.68, 129.04, 129.11 (ArCH), 136.22, 136.34, 136.96, 137.06, 139.01 (ArC), 151.84, 151.94 (CN_4), 155.69, 155.78 (Z-CO).

TLC (analytical, 10% ethyl acetate/petroleum ether) $R_f=0.50$; ES MS 442.2256 $C_{26}H_{28}N_5O_2$ (MH^+) requires m/z 442.2243.

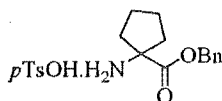
6.2.18 (4 mg, 14%).

1H NMR (300 MHz, $CDCl_3$) δ 1.27 (3H, d, $J=7.2$ Hz, hPhe- δ - H_3), 1.92 (3H, d, $J=6.9$ Hz, Bn- β - H_3), 2.35 (2H, AB system, $\delta_A=2.22$, $\delta_B=2.48$, dd, $J=6.9$, 14.4 Hz, hPhe- γ - H_2), 3.18 (1H, m, hPhe- α -H), 4.11 (1H, m, hPhe- β -H), 4.98 (2H, s, Z- H_2), 5.47 (1H, q, $J=6.9$ Hz, (6*R*)-Bn- α -H), 6.13 (1H, d, $J=9.0$ Hz, NH), 6.56-7.28 (15H, m, ArH).

^{13}C NMR (75 MHz, CDCl_3) δ 16.70 (hPhe- δ - CH_3), 23.04 (Bn- β - CH_3), 31.74 (hPhe- α -CH), 38.83 (hPhe- γ - CH_3), 55.46 (hPhe- β -CH), 58.16 ((6*R*)-Bn- α -CH), 66.58 (Z- CH_2), 126.41, 127.77, 127.97, 128.45, 128.66, 128.74, 129.24 (ArCH), 136.41, 137.14, 139.19 (ArC), 155.91 (CN_4), 156.40 (Z-CO).

TLC (analytical, 10% ethyl acetate/petroleum ether) $R_f=0.43$; ES MS (MH^+) 468.2636 $\text{C}_{27}\text{H}_{30}\text{N}_5\text{O}_2$ (MH^+) requires m/z 468.2632.

Preparation of benzyl 2-amino-2-cyclopentane carboxylate *para*-toluenesulphonate³⁴



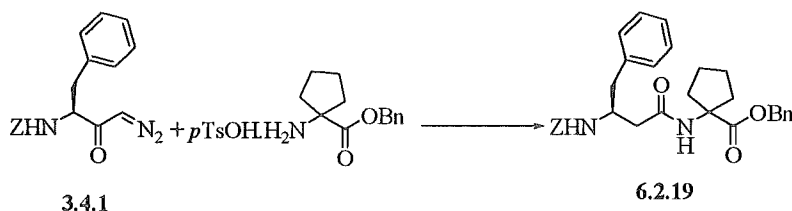
2-Amino-2-cyclopentane carboxylic acid (500 mg, 3.87 mmol), and *para*-toluenesulphonic acid (1.02 eq., 751 mg, 3.95 mmol) were refluxed in benzyl alcohol in a Dean-Stark apparatus with the receiver packed with 4 Å molecular sieves. The mixture was refluxed for 4 h, after which time any solid particulate had dissolved. The reaction was allowed to cool. The excess benzyl alcohol was removed to one quarter the original volume by vacuum distillation. Pre-cooled ether (20 mL) was added and the mixture left to stand at 5 °C for 16 h. The white precipitate that formed was filtered off and dried *in vacuo* over KOH for 24 h to give the benzyl ester (699 mg, 50%).

^1H NMR (300 MHz, CD_3OD) δ 1.88 (8H, m, Cp- β - H_2 & Cp- γ - H_2), 2.35 (3H, s, *p*TsOH- H_3), 5.27 (2H, s, Bn- H_2), 7.22 (2H, d, $J=7.8$ Hz, Ph-3- H_2), 7.38 (5H, m, ArH), 7.70 (2H, d, $J=8.4$ Hz, Ph-2- H_2).

^{13}C NMR (75 MHz, CD_3OD) δ 21.60 (*p*TsOH- CH_3), 26.80 (Cp- γ - CH_2), 37.94 (Cp- β - CH_2), 66.44 (Cp- α -C), 69.57 (Bn- CH_2), 127.25, 129.91, 130.05, 130.11, 130.53 (ArCH), 136.76, 141.93, 143.86 (ArC), 173.45 (Cp-CO).

IR (KBr, cm^{-1}) 3413, 2360, 1739, 1616, 1188, 1122, 1010, 682; ES MS 220.1330 $\text{C}_{13}\text{H}_{18}\text{NO}_2$ (MH^+) requires m/z 220.1338.

Preparation of (3*S*)-*N*-[3-(*N*-benzyloxycarbonylamino)-4-phenylbutanoic acid]-2-amino-2-cyclopentane carboxylic acid benzyl ester, 6.2.19



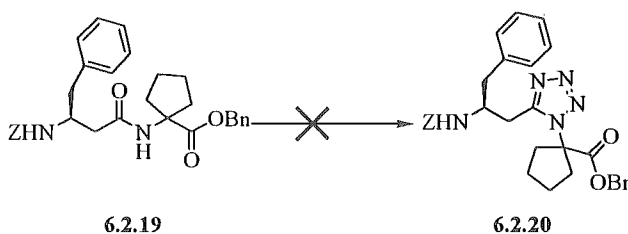
The diazoketone, 3.4.1 (1.0 eq., 572 mg, 1.76 mmol) was reacted with 2-amino-2-cyclopentane carboxylic acid benzyl ester (1.1 eq., 699 mg, 1.94 mmol) in the presence of triethylamine (1.1 eq., 196 mg, 1.94 mmol) according to general procedure B. Flash column chromatography (30% ethyl acetate/petroleum ether) of the crude reaction product gave amide, 6.2.19 (224 mg, 25%) as a white solid. mp 134-135 °C

$^1\text{H NMR}$ (300 MHz, CDCl_3) δ 1.66-1.94 (8H, m, Cp- β - H_2 & Cp- γ - H_2), 2.23-2.38 (2H, m, hPhe- γ - H_2), 2.83 (2H, m, hPhe- α - H_2), 4.09 (1H, m, hPhe- β -H), 5.05 (2H, s, Z- H_2), 5.15 (2H, s, Bn- H_2), 5.75 (1H, d, $J=7.2$ Hz, NH), 5.98 (1H, s, NH), 7.16-7.31 (15H, m, ArH).

$^{13}\text{C NMR}$ (75 MHz, CDCl_3) δ 24.54 (Cp- γ - CH_2), 37.24 (Cp- β - CH_2), 37.27 (Cp- β - CH_2), 38.26 (hPhe- α - CH_2), 39.89 (hPhe- γ - H_2), 50.13 (hPhe- β -CH), 65.98 (Cp- α -C), 66.41 (Z- CH_2), 67.08 (Bn- CH_2), 126.47, 126.96, 127.84, 127.94, 128.16, 128.19, 128.39, 128.46, 129.25 (ArCH), 135.70, 136.55, 138.01 (ArC), 155.88 (Z-CO), 170.72 (hPhe-CO), 173.69 (Cp-COOBn).

IR (KBr, cm^{-1}) 3363, 3328, 2962, 1708, 1670, 1527, 1454, 1315, 1249, 1211, 1076, 1018, 702; ES MS 515.2568 $\text{C}_{31}\text{H}_{35}\text{N}_2\text{O}_5$ (MH^+) requires m/z 515.2546.

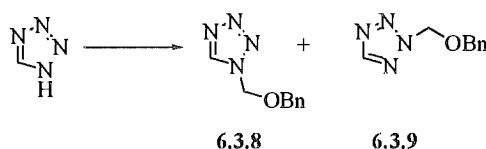
Attempted preparation of (2*S*)-5-[2-(*N*-benzyloxycarbonylamino)-3-phenylpropane]-1-(2-cyclopentane carboxylic acid benzyl ester)tetrazole, 6.2.20



Amide, **6.2.19** (50 mg, 0.1 mmol) was reacted according to general procedure C. Flash column chromatography of the crude reaction product gave starting amide, **6.2.19**.

9.5.2. SYNTHESIS OF THE α -KETO TETRAZOLE ISOSTERE BY DIRECT ALKYLATION OF THE TETRAZOLE HETEROCYCLE

Preparation of 1-(benzyloxymethyl)-1*H*-tetrazole, **6.3.8**³⁵



Sodium hexamethyldisilazide (NaHMDS, 1.0 eq., 28.5 mL of a 1.0 M solution in THF, 28.5 mmol) was added dropwise to a stirred solution of 1*H*-tetrazole (2.0 g, 28.5 mmol) in dry THF (100 mL) in a flame-dried flask under Ar, over 30 min at 0 °C. After a further 30 min at 0 °C freshly distilled benzyl chloromethylether (1.0 eq., 4.47 g, 28.5 mmol, 4.0 mL) was added and the white mixture stirred at rt for 2 h. The reaction mixture was partitioned between ethyl acetate (50 mL) and water (50 mL). The organic layer was separated and the aqueous phase extracted with ethyl acetate (2 × 50 mL). The pooled organic phases were washed with saturated aqueous NaCl (2 × 50 mL), dried (MgSO₄), filtered and dried *in vacuo*. The desired N-1 regioisomer **6.3.8** (0.9 g, 20%) was isolated from the oily residue by flash column chromatography (20% ether/petroleum ether), as a clear oil.

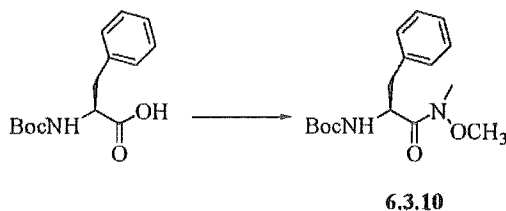
¹H NMR (300 MHz, CDCl₃) δ 4.65 (2H, s, Bn-H₂), 5.95 (2H, s, CN₄- α -H₂), 7.34 (5H, m, ArH), 8.59 (1H, s, CN₄-H).

¹³C NMR (75 MHz, CDCl₃) δ 72.20 (Bn-CH₂), 79.66 (CN₄- α -CH₂), 128.49, 128.68, 128.85 (ArCH), 135.83 (ArC), 153.62 (CN₄).

TLC (analytical, 30% ethyl acetate/petroleum ether) R_f=0.51; ES MS 191.0931 C₉H₁₁N₄O (MH⁺) requires *m/z* 191.0933.

Further elution gave the undesired N-2 regioisomer, **6.3.9**.

Preparation of (2*S*)-*N*-(*N*,*O*-dimethylhydroxyl)-2-(*N*-*tert*-butyloxycarbonylamino)-3-phenylpropanamide, 6.3.10¹³

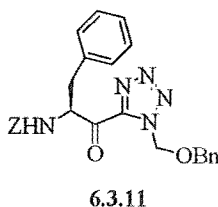


N-Boc-*L*-Phenylalanine (1.0 g, 3.8 mmol) was coupled to Weinreb amine hydrochloride¹⁴ (*N*,*O*-dimethylhydroxylamine hydrochloride, 1.1 eq., 0.41 g, 4.2 mmol) with BOP reagent (1.0 eq., 1.7 g, 3.8 mmol) in the presence of triethylamine (2.1 eq., 0.80 g, 8.0 mmol, 1.05 mL) in dry CH₂Cl₂ (40 mL), according to general procedure G. Purification of the crude reaction mixture by flash column chromatography (50% ethyl acetate/petroleum ether) gave amide, 6.3.10 (0.96 g, 82%) as a viscous oil.

¹H NMR (300 MHz, CDCl₃) δ 1.38 (9H, s, Boc-(CH₃)₃), 2.96 (2H, AB system, $\delta_A=2.87$, $\delta_B=3.05$, dd, $J=7.2$, 12.9 Hz, Phe- β -H₂), 3.16 (3H, s, NCH₃), 3.65 (3H, s, NOCH₃), 4.95 (1H, m, Phe- α -H), 5.19 (1H, d, $J=7.8$ Hz, NH), 7.16-7.30 (5H, m, ArH).

TLC (analytical, 30% ethyl acetate/petroleum ether) $R_f=0.33$; ES MS 309.1806 C₁₆H₂₅N₂O₄(MH⁺) requires m/z 309.1814.

Preparation of (2*S*)-1-(benzyloxymethyl)-5-[2-(*N*-benzyloxycarbonylamino)-1-oxo-3-phenylpropane]-tetrazole, 6.3.11³⁵



To a solution of tetrazole, 6.3.8 (3.0 eq., 170 mg, 0.89 mmol) in dry THF (2 mL) was prepared in a flame-dried flask under Ar and cooled to -78 °C. *n*-Butyllithium (3.0 eq., 640 μ L of a 1.4 M in *n*-hexanes) was added dropwise to the stirred solution to give a deep purple colour. After 5 min Weinreb amide, 3.1.25 (1.0 eq., 100 mg, 0.30 mmol), as a solution in dry THF (2 mL), was added dropwise and the reaction was stirred at -78 °C

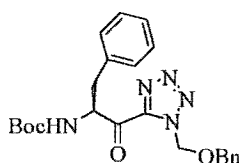
for 15 min. The reaction was allowed to slowly warm to rt over a period of 30 min, before quenching with saturated aqueous NH_4Cl (5 mL). The reaction mixture was extracted with ethyl acetate (3×10 mL) and the pooled organics washed with saturated aqueous NaCl (20 mL), dried (MgSO_4), filtered and dried *in vacuo*. The crude reaction product was purified by flash column chromatography (30% ethyl acetate/petroleum ether) and gave 1,5-disubstituted tetrazole, **6.3.11** (83 mg, 60%) as a clear oil.

^1H NMR (300 MHz, CDCl_3) δ 3.24 (2H, AB system, $\delta_A=3.12$, $\delta_B=3.35$, dd, $J=6.9$, 14.1 Hz, hPhe- γ - H_2), 4.70 (2H, s, Bn- H_2), 5.07 (2H, s, Z- H_2), 5.53 (1H, d, $J=7.8$ Hz, NH), 5.68 (1H, m, hPhe- β -H), 5.99 (2H, s, CN_4 - α - H_2), 7.05-7.34 (15H, m, ArH).

^{13}C NMR (75 MHz, CDCl_3) δ 38.87 (hPhe- γ - CH_2), 58.64 (hPhe- β -CH), 66.45 (Z- CH_2), 72.47 (Bn- CH_2), 80.35 (CN_4 - α - CH_2), 127.04, 127.32, 128.18, 128.54, 128.59, 128.63, 128.93, 129.34 (ArCH), 135.11, 135.28, 137.82 (ArC), 155.02 (CN_4), 156.87 (Z-CO), 189.76 (hPhe- α -CO).

TLC (analytical, 30% ethyl acetate/petroleum ether) $R_f=0.28$; ES MS 472.1989 $\text{C}_{26}\text{H}_{26}\text{N}_5\text{O}_4$ (MH^+) requires m/z 472.1985.

Preparation of (2*S*)-1-(benzyloxymethyl)-5-[2-(*N*-*tert*-butyloxycarbonylamino)-1-oxo-3-phenylpropane]-tetrazole, **6.3.12**



6.3.12

To a solution of tetrazole, **6.3.8** (3.0 eq., 170 mg, 0.89 mmol) in dry THF (2 mL) was prepared in a flame-dried flask under Ar and cooled to -78 °C. *n*-Butyllithium (3.0 eq., 640 μL of a 1.4 M in *n*-hexanes) was added dropwise to the stirred solution to give a deep purple colour. After 5 min Weinreb amide, **6.3.10** (1.0 eq., 90 mg, 0.30 mmol) as a solution in dry THF (2 mL) was added dropwise and the reaction was stirred at -78 °C for 15 min. The reaction was allowed to slowly warm to rt over a period of 30 min, before quenching with saturated aqueous NH_4Cl (5 mL). The reaction mixture was extracted with ethyl acetate (3×10 mL) and the pooled organics washed with saturated

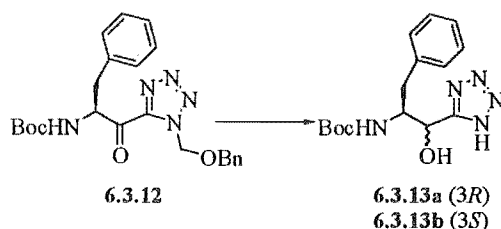
aqueous NaCl (20 mL), dried (MgSO_4), filtered and dried *in vacuo*. The crude reaction product was purified by flash column chromatography (20% ethyl acetate/petroleum ether) to give 1,5-disubstituted tetrazole, **6.3.12** (77 mg, 60%) as a white solid. mp 96-97 °C.

^1H NMR (300 MHz, CDCl_3) δ 1.40 (9H, s, Boc-(CH_3)₃), 3.20 (2H, AB system, $\delta_A=3.08$, $\delta_B=3.33$, dd, $J=6.9$, 13.5 Hz, hPhe-hPhe- H_2), 4.70 (2H, s, Bn- H_2), 5.27 (1H, d, $J=7.5$ Hz, NH), 5.62 (1H, m, hPhe- β -H), 6.00 (2H, s, CN_4 - α - H_2), 7.10-7.39 (10H, m, ArH).

^{13}C NMR (75 MHz, CDCl_3) δ 28.18 (Boc-(CH_3)₃), 38.03 (hPhe- γ - CH_2), 58.64 (hPhe- β -CH), 72.47 (Bn- CH_2), 80.11 (Boc-C(CH_3)₃), 80.36 (CN_4 - α - CH_2), 127.04, 128.18, 128.54, 128.63, 129.34 (ArCH), 135.11, 135.28 (ArC), 155.02 (CN_4), 161.20 (Boc-CO), 189.76 (hPhe- α -CO).

TLC (analytical, 20% ethyl acetate/petroleum ether) $R_f=0.18$; ES MS 438.2142 $\text{C}_{23}\text{H}_{28}\text{N}_5\text{O}_4$ (MH^+) requires m/z 438.2141.

Preparation of (1*RS*,2*S*)-5-[2-(*N*-*tert*-butyloxycarbonylamino)-1-hydroxyl-3-phenylpropane]-1*H*-tetrazole, **6.3.13a** and **6.3.13b**



The 1,5-disubstituted tetrazole, **6.3.12** (220 mg, 0.5 mmol) in methanol (15 mL), was catalytically hydrogenated in the presence of 10% palladium on carbon (220 mg) for 24 h according to general procedure E. Upon work-up the reaction gave α -hydroxy tetrazoles, **6.3.13a** and **6.3.13b**, in 90% yield, as a mixture of C2 epimers, which were not separated.

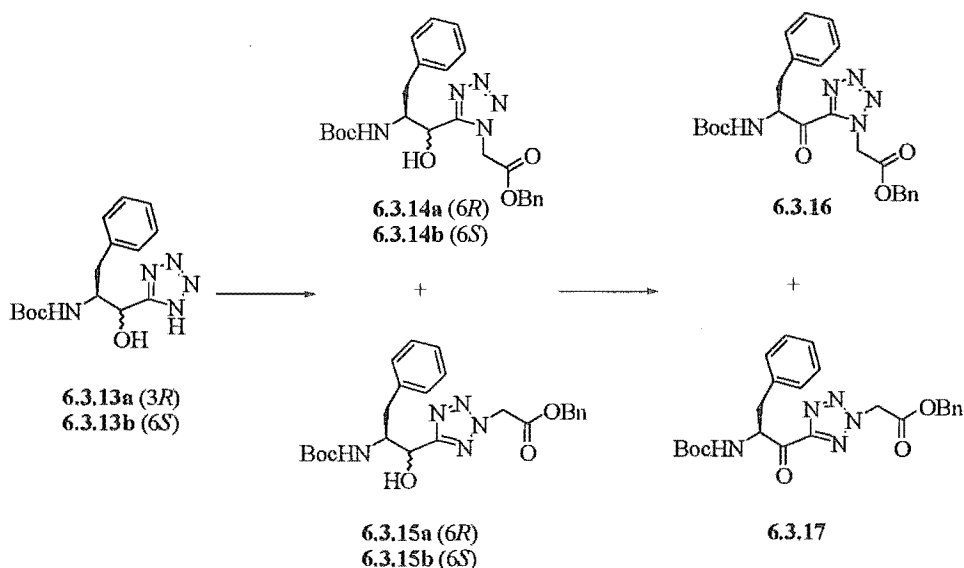
^1H NMR (300 MHz, CD_3OD , for the mixture) δ 1.23, 1.26 (9H, s, Boc-(CH_3)₃), 2.90 (2H, AB system, $\delta_A=2.76$, $\delta_B=3.03$, dd, $J=6.9$, 13.2 Hz, hPhe- γ - H_2), 4.07, 4.12 (1H,

m, hPhe- β -H), 5.01 (1H, d, $J=6.6$ Hz, NH), 5.08, 5.13 (1H, bs, hPhe- α -H), 7.17-7.28 (5H, m, ArH).

^{13}C NMR (75 MHz, CD_3OD , for the mixture) δ 28.36, 28.82 ($\text{Boc}-(\text{CH}_3)_3$), 38.37, 39.52 (hPhe- γ - CH_2), 57.77, 59.42 (hPhe- β -CH), 67.22, 69.01 (hPhe- α -CH), 80.50, 80.55 ($\text{Boc}-\text{C}(\text{CH}_3)_3$), 127.46, 127.67, 129.43, 129.63, 130.50 (ArCH), 139.38, 139.39 (ArC), 157.51 (CN_4), 159.99, 160.02 ($\text{Boc}-\text{CO}$).

ES MS 320.1721 $\text{C}_{15}\text{H}_{22}\text{N}_5\text{O}_3$ (MH^+) requires m/z 320.1723.

Preparation of (2*S*)-1-(benzyl ethanoate)-5-[2-(*N*-*tert*-butyloxycarbonylamino)-1-oxo-3-phenylpropane]-tetrazole, 6.3.16, and (2*S*)-2-(benzyl ethanoate)-5-[2-(*N*-*tert*-butyloxycarbonylamino)-1-oxo-3-phenylpropane]-tetrazole, 6.3.17



A solution of 1*H*-tetrazole as a mixture of **6.3.13a** and **6.3.13b** (1.0 eq., 110 mg, 0.35 mmol) in dry CH_2Cl_2 (5 mL) was prepared in a flame-dried flask under Ar. DIPEA (3.0 eq., 130 mg, 1.04 mmol, 175 μL) was added dropwise to the stirred solution at rt. After 5 min benzyl bromoacetate (2.0 eq., 160 mg, 0.70 mmol, 110 μL) was added dropwise and the reaction was stirred for 24 h. The reaction was diluted with ethyl acetate (20 mL), washed with 10% aqueous HCl (2×10 mL), 1 M aqueous NaOH (2×10 mL), saturated aqueous NaCl (10 mL), dried (MgSO_4), filtered and evaporated. The crude reaction product was purified by flash column chromatography (40% ethyl

acetate/petroleum ether) to give α -hydroxy tetrazoles, **6.3.14a**, **6.3.14b**, **6.3.15a** and **6.3.15b** (127 mg, 77%), which were not separated.

^1H NMR (300 MHz, CDCl_3 , for the mixture) δ 1.32 (9H, bs, Boc-(CH_3)₃), 3.04 (2H, m, hPhe- γ -H₂), 4.20 (1H, m, hPhe- β -H), 4.96 (1H, d, $J=6.6$ Hz, NH), 5.06 (1H, d, $J=3.0$ Hz, hPhe- α -H), 5.14 (1H, d, $J=5.1$ Hz, hPhe- α -H), 5.20 (2H, bs, Bn-H₂), 5.41 (2H, bs, Gly- α -H₂), 7.17-7.36 (10H, m, ArH).

TLC (analytical, 40% ethyl acetate/petroleum ether) $R_f=0.17$.

The mixture of α -hydroxy tetrazoles, **6.3.14** and **6.3.15** (127 mg, 0.3 mmol), as a solution in CH_2Cl_2 (6 mL) was added to a solution of TEMPO³⁶ (4 mg, 0.03 mmol) and potassium bromide (3 mg, 0.03 mmol) in water (ca. 120 μL) at 0 °C. A 5.25% aqueous sodium hypochlorite solution (4.5 mL) was added dropwise over 5 min with vigorous stirring. After 30 min at 0 °C the reaction was diluted with ethyl acetate (20 mL) and 10% aqueous HCl (20 mL). The organic layer was separated and the aqueous layer extracted with ethyl acetate (2 \times 20 mL). The combined organic phases were dried (MgSO_4), filtered and evaporated. The regiomeric α -keto tetrazole products were separated by flash column chromatography (30% ethyl acetate/petroleum ether). The less polar 1,5-disubstituted tetrazole, **6.3.16** (41 mg, 30%), eluted first as a clear oil.

^1H NMR (300 MHz, CDCl_3) δ 1.35 (9H, s, Boc-(CH_3)₃), 3.22 (2H, AB system, $\delta_A=3.07$, $\delta_B=3.37$, dd, $J=8.1$, 14.1 Hz, hPhe- γ -H₂), 5.12 (1H, d, $J=6.6$ Hz, NH), 5.21 (2H, d, $J=4.8$ Hz, Bn-H₂), 5.42 (1H, m, hPhe- β -H), 5.47 (2H, d, $J=3.0$ Hz, Gly- α -H₂), 7.13-7.38 (10H, m, ArH).

^{13}C NMR (75 MHz, CDCl_3) δ 27.97 (Boc-(CH_3)₃), 37.02 (hPhe- γ -CH₂), 50.11 (Gly- α -CH₂), 59.48 (hPhe- β -CH) 68.14 (Bn-CH₂), 80.25 (Boc-C(CH_3)₃), 124.03, 127.06, 128.38, 128.55, 128.68, 129.18 (ArCH), 134.14, 135.13 (ArC), 148.09 (CN₄), 154.00 (Boc-CO), 164.71 (Gly-CO), 189.05 (hPhe- α -CO).

TLC (analytical, 30% ethyl acetate/petroleum ether) $R_f=0.39$; IR (CDCl_3 , cm^{-1}), 3392, 3324, 3215, 1756, 1632, 1603, 1528, 1497, 1230; ES MS 466.2097 $\text{C}_{24}\text{H}_{28}\text{N}_5\text{O}_5$ (MH^+) requires m/z 466.2090.

Further elution gave the 2,5-regioisomer, 6.3.17 (65 mg, 48%), as a white solid. mp 120-121 °C; $[\alpha]_D^{20}$ -18.3 ($c=0.00010$, methanol).

^1H NMR (300 MHz, CDCl_3) δ 1.39 (9H, s, Boc-(CH_3)₃), 3.19 (2H, AB system, $\delta_A=3.06$, $\delta_B=3.33$, dd, $J=6.9$, 13.8 Hz, hPhe- γ -H₂), 5.24 (1H, d, $J=6.4$ Hz, NH), 5.29 (2H, s, Bn-H₂), 5.53 (2H, s, Gly- α -H₂), 5.58 (1H, m, hPhe- β -H), 7.05-7.34 (10H, m, ArH).

^{13}C NMR (75 MHz, CDCl_3) δ 28.18 (Boc-(CH_3)₃), 37.93 (hPhe- γ -CH₂), 53.76 (Gly- α -CH₂), 58.70 (hPhe- β -CH), 58.57 (Bn-CH₂), 80.11 (Boc-C(CH_3)₃), 127.05, 128.52, 128.60, 128.74, 128.95, 129.34 (ArCH), 134.01, 135.24 (ArC), 155.00 (Boc-CO), 161.15 (CN₄), 164.03 (Gly-CO), 189.32 (hPhe- α -CO).

TLC (analytical, 30% ethyl acetate/petroleum ether) $R_f=0.29$; IR (CDCl_3 , cm^{-1}), 3395, 3307, 3215, 1756, 1649, 1610, 1533, 1500; ES MS 466.2096 $\text{C}_{24}\text{H}_{28}\text{N}_5\text{O}_5$ (MH^+) requires m/z 466.2090.

Crystallographic determination of (2*S*)-2-(benzyl ethanoate)-5-[2-(*N*-tert-butylloxycarbonylamino)-1-oxo-3-phenylpropane]-tetrazole, 6.3.17, by X-ray analysis

$\text{C}_{24}\text{H}_{27}\text{N}_5\text{O}_5$, M 465.51, mp 120-121 °C, crystal dimensions 0.55 \times 0.26 \times 0.02 mm, orthorhombic, a 6.140 (3) Å, b 16.264 (7) Å, c 23.523 (10) Å, α 90 (2)°, β 90 (2)°, γ 90 (2)°, $V=2349.0$ (17) Å³, spacegroup P2(1)2(1)2(1), $Z=4$, $F(000)=984$, $D_{\text{calc}}=1.316$ mg/m³, absorption coefficient 0.096 mm⁻¹, θ range for data collection 2.14 to 26.45, index ranges $-7 \leq h \leq 7$, $-20 \leq k \leq 18$, $-29 \leq l \leq 29$, data/restraints/parameters 4837/0/307, goodness of fit on F^2 was 0.794, final R indices [$I > 2\sigma(I)$] $R_1=0.0448$, $wR_2=0.0714$, R indices (all data) $R_1=0.1525$, $wR_2=0.0904$, largest difference peak and hole 0.174 and -0.355 eÅ⁻³.

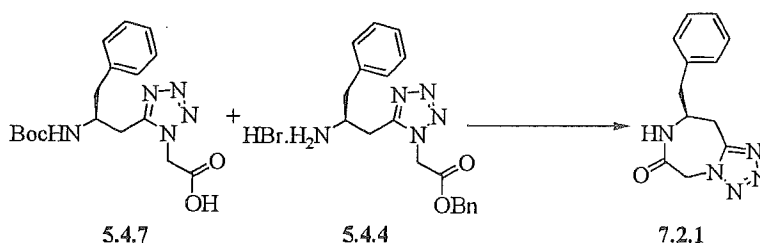
A unique data set was measured at 173(2) K within $2\theta_{\text{max}}=57^\circ$ limit (ϖ scans). Of the 30663 reflections obtained, 4837 were unique ($R_{\text{int}}=0.1593$) and were used in the full-matrix least-squares refinement.²⁸ The structure was solved by direct methods.²⁹ Hydrogen atoms were fixed in idealised positions. All non-hydrogen atoms were refined with anisotropic atomic displacement parameters. Neutral scattering factors and

anomalous dispersion corrections for non-hydrogen atoms were taken from Ibers and Hamilton.³⁰

9.6. SOLID-STATE STRUCTURES OF TETRAZOLE-BASED DIPEPTIDE MIMICS

Preparation of (2*S*)-1-(benzyl ethanoate)-5-[2-(*N*-benzyloxycarbonylamino)-3-phenylpropane]-tetrazole, 5.2.1, see Chapter 9.3.

Preparation of *cyclo*-{[(2*S*)-5-(2-amino-3-phenylpropane)-1-ethanamide]tetrazole}, 7.2.1



A solution of benzyl ester hydrobromide, 5.4.4 (1.1 eq., 80 mg, 0.19 mmol) and triethylamine (1.1 eq., 19 mg, 0.19 mmol) in dry DMF (2 mL) was added to a solution of dipeptide acid, 5.4.7 (1.0 eq., 55 mg, 0.15 mmol), EDCI (1.5 eq., 43 mg, 0.22 mmol) and HOBt (1.5 eq., 30 mg, 0.22 mmol) in dry DMF (2 mL). The reaction was stirred at rt for 24 h. The reaction was diluted with water (20 mL) and extracted with ethyl acetate (3 × 20 mL). The pooled organics were washed with 1 M aqueous HCl (2 × 25 mL), saturated aqueous NaHCO₃ (2 × 25 mL) and saturated aqueous NaCl (2 × 25 mL), dried (MgSO₄), filtered and evaporated. The crude reaction product was purified by flash column chromatography (50% ethyl acetate/CH₂Cl₂). The major product, cyclic tetrazole peptidomimetic, 7.2.1 (43 mg, 93% of starting benzyl ester) was recrystallised from methanol. mp 198- 200°C; [α]_D²⁰ -10.7° (c=0.0005, methanol).

¹H NMR (300 MHz, CDCl₃) δ 2.91-3.43 (4H, m, hPhe- α -H₂ & hPhe- γ -H₂), 4.26 (1H, m, hPhe- β -H), 5.28 (2H, s, Gly- α -H₂), 7.27-7.41 (5H, m, ArH).

¹³C NMR (75 MHz, CDCl₃/CD₃OD) δ 30.36 (hPhe- α -CH₂), 39.92 (hPhe- γ -CH₂), 50.00 (hPhe- β -CH), 51.35 (Gly- α -CH₂), 127.26, 128.77 (ArCH), 135.40 (ArC), 151.97 (CN₄), 166.04 (Gly-CO).

TLC (analytical, 50% ethyl acetate/CH₂Cl₂) R_f=0.30; IR (KBr, cm⁻¹) 3548, 3471, 3406, 1697, 1639, 1438, 1411, 1091, 705, 644, 601; ES MS 244.1196 C₁₂H₁₄N₅O (MH⁺) requires *m/z* 244.1198.

Crystallographic determination of *cyclo*-{(2*S*)-5-(2-amino-3-phenylpropane)-1-ethanamide}tetrazole, 7.2.1, by X-ray analysis

C₁₂H₁₃N₅O, M 243.27, mp 198-200 °C, crystal dimensions 0.63 × 0.24 × 0.21 mm, orthorhombic, *a* 56.374 (2) Å, *b* 8.621 (3) Å, *c* 120.890 (7) Å, α 90 (2)°, β 90 (2)°, γ 90 (2)°, *V*=1147.8 (7) Å³, spacegroup P2(1)2(1)2(1), *Z*=4, F(000)=512, D_{calc}=1.408 mg/m³, absorption coefficient 0.096 mm⁻¹, θ range for data collection 2.56 to 26.42, index ranges $-4 \leq h \leq 7$, $-10 \leq k \leq 10$, $-26 \leq l \leq 25$, data/restraints/parameters 2338/0/163, goodness of fit on F² was 1.063, final *R* indices [*I*>2 σ (*I*)] *R*₁=0.0323, w*R*₂=0.0827, *R* indices (all data) *R*₁=0.0374, w*R*₂=0.0853, largest difference peak and hole 0.148 and -0.191 eÅ⁻³.

A unique data set was measured at 163(2) K within 2 θ_{\max} =57° limit (ω scans). Of the 14344 reflections obtained, 2338 were unique (*R*_{int}=0.0271) and were used in the full-matrix least-squares refinement.²⁸ The structure was solved by direct methods.²⁹ Hydrogen atoms were fixed in idealised positions. All non-hydrogen atoms were refined with anisotropic atomic displacement parameters. Neutral scattering factors and anomalous dispersion corrections for non-hydrogen atoms were taken from Ibers and Hamilton.³⁰

Preparation of (2*S*)-2-(benzyl ethanoate)-5-[2-(*N*-*tert*-butyloxycarbonylamino)-1-oxo-3-phenylpropane]-tetrazole, 6.3.17, see Chapter 9.52

9.7. REFERENCES

- ¹ Perrin, D. D.; Armarego, W. L. F.; Perrin, D. R. *Purification of Laboratory Chemicals*. Pergamon Press, 1986, 2nd Edition. (b) Furniss, B. S.; Hannaford, A. J.; Smith, N. P G.; Tatchell, A. R. Eds. *Vogel's Textbook of Practical Organic Chemistry*. Longman: London, 1989, 5th Edn.
- ² Watson, S. C.; Eastham, J. F. *J. Organomet. Chem.* 1967, 9, 165.
- ³ Still, W. C.; Khan, M.; Mitra A. J. *J. Org. Chem.* 1978, 43, 2923.
- ⁴ Podlech, J.; Seebach, D. *Liebigs Ann.* 1995, 1217.
- ⁵ Bastiaans, H. M. M.; Alewijnse, A. E.; van der Baan, J. L.; Ottenheijm, H. C. J. *Tetrahedron Lett.* 1994, 35, 7659.
- ⁶ Boteju, L. W.; Hruby, V. J. *Tetrahedron Lett.* 1993, 34, 1757.
- ⁷ Zabrochi, J.; Dunbar, J. B.; Marshall, K. W.; Toth, M. V.; Marshall, G. R. *J. Org. Chem.* 1992, 57, 202.
- ⁸ Bodansky, M.; Bodansky, A. In, *The Practice of Peptide Synthesis*. Springer-Verlag: Berlin 1984, pp 165.
- ⁹ Bodansky, M.; Bodansky, A. In, *The Practice of Peptide Synthesis*. Springer-Verlag: Berlin 1984, pp 153.
- ¹⁰ Bodansky, M.; Bodansky, A. In, *The Practice of Peptide Synthesis*. Springer-Verlag: Berlin 1984, pp 170.
- ¹¹ Foulds G. J. *Biologically Active Peptide Analogues*. Ph.D. thesis, University of Canterbury, 1996.
- ¹² Tian, Z-Q.; Brown, B. B.; Mack, D. P.; Hutton, C. A.; Bartlett, P. A. *J. Org. Chem.* 1997, 62, 514.
- ¹³ Fehrentz, J-A.; Castro, B. *Synthesis* 1983, 676.
- ¹⁴ Goel, O. P.; Krolla, U. *Org. Syn.* 1987, 19, 75.
- ¹⁵ Nishizawa, R.; Saino, T. *J. Med. Chem.* 1977, 20, 510.
- ¹⁶ Dess D. B.; Martin, J. C. *J. Org. Chem.* 1983, 48, 4155.
- ¹⁷ Ireland, R. E.; Liu, L. *J. Org. Chem.* 1993, 58, 2899.

- 18 Yuan, W.; Munoz, B.; Wong, C-H.; Haeggstrom, J. Z.; Wetterholm, A.; Samuelsson, B. *J. Med. Chem.* **1993**, *36*, 211.
- 19 Herranz, R.; Castro-Pichel, J.; Vinuesa, S.; Garcia-Lopez, M. T. *J. Org. Chem.* **1990**, *55*, 2232.
- 20 Hout, D. A. *The Design and Synthesis of Conformationally Restricted and Epoxide Based Peptidomimetics*. Ph.D. thesis, University of Canterbury, **1997**.
- 21 Li, G.; Sharpless, K. B. *Acta Chem. Scand.* **1996**, *50*, 649. Li, G.; Angert, H.; Sharpless, K. B. *Chem. Int. Ed. Eng.* **1996**, *35*, 2813.
- 22 Plucinska, K.; Liberek, B. *Tetrahedron* **1987**, *43*, 3509.
- 23 Hudlicky, M. *J. Org. Chem.* **1980**, *45*, 5377.
- 24 Vedejs, E.; Larsen, S. *Org. Syn.* **1984**, *64*, 127.
- 25 Failure to maintain the internal temperature below 40 °C resulted in the formation of amorphous, insoluble products.
- 26 May, B. C. H.; Abell, A. D. *Syn. Commun.* **1999**, *29*, 2515.
- 27 Camp, N. P.; Perry, D. A.; Kichington, D.; Hawkins, P. C. D.; Gani, D. *Bioorg. Med. Chem. Lett.* **1995**, *3*, 297.
- 28 Sheldrick, G. M.; SHELXL 93 *J. Appl. Crystallogr.*, in press.
- 29 Sheldrick, G. M.; *Acta Crystallogr. Sect. A.* **1990**, *46*, 467.
- 30 Ibers, J. A.; Hamilton, W. C. Eds. *International Tables for Crystallography*. Kynoch Press: Birmingham **1992**, Vol C.
- 31 Rachele, J. R. *J. Org. Chem.* **1963**, *28*, 2898.
- 32 Sakaitani, M.; Hori, K.; Ohfuné, Y. *Tetrahedron Lett.* **1988**, *29*, 2983.
- 33 Care was taken to maintain the temperature between 80-85 °C.
- 34 Huang, Z.; Probstl, A.; Spencer, J. R.; Yamazaki, T.; Goodman, M. *Int. J. Peptide Protein Res.* **1993**, *42*, 352.
- 35 Satoh, Y.; Moliterni, J. *Synlett* **1997**, 528.
- 36 Harbeson, S. L.; Abelleira, S. M.; Akiyama, A.; Barrett, R.; Carroll, R. M.; Straub, J. A.; Tkacz, J. N.; Wu, C.; Musso, G. F. *J. Med. Chem.* **1994**, *37*, 2918.